DÉBORA RODRIGUES SOBREIRA

"ESTUDOS SOBRE OS GENES DA FAMÍLIA *DAPPER*: ORIGEM, EVOLUÇÃO E ANÁLISE DA EXPRESSÃO DURANTE A ONTOGÊNESE DOS MEMBROS DE GALINHA"

"STUDIES ON THE DAPPER GENE FAMILY: ORIGIN, EVOLUTION AND EXPRESSION ANALYSIS DURING CHICKEN LIMB DEVELOPMENT"

Campinas, 2013

UNIVERSIDADE ESTADUAL DE CAMPINAS

INSTITUTO DE BIOLOGIA

DÉBORA RODRIGUES SOBREIRA

"ESTUDOS SOBRE OS GENES DA FAMÍLIA *DAPPER*: ORIGEM, EVOLUÇÃO E ANÁLISE DA EXPRESSÃO DURANTE A ONTOGÊNESE DOS MEMBROS DE GALINHA"

Orientadora: Profa. Dra. Lúcia Elvira Alvares
Coorientador: Prof. Dr. José Xavier-Neto

"STUDIES ON THE DAPPER GENE FAMILY: ORIGIN, EVOLUTION AND EXPRESSION ANALYSIS DURING CHICKEN LIMB DEVELOPMENT"

Tese de Doutorado apresentada ao Programa de Pós-Graduação em Biologia Celular e Estrutural do Instituto de Biologia da Universidade Estadual de Campinas para obtenção do Título de Doutora em Biologia Celular e Estrutural, na área de Biologia Tecidual.

Doctorate thesis presented to the Cellular and Structural Biology Postgraduation Programme of the Institute of Biology of the University of Campinas to obtain the Ph.D. grade in Tecidual Biology.

Este exemplar corresponde à versão final da tese defendida pela aluna *Débora Rodrigues Sobreira* e orientada pela Profa. Dra. Lúcia Elvira Alvares.

Assinatura da Orientadora

Campinas, 2013

Ficha catalográfica
Universidade Estadual de Campinas
Biblioteca do Instituto de Biologia
Mara Janaina de Oliveira - CRB 8/6972

So12e

Sobreira, Débora Rodrigues, 1981-
Estudos sobre os genes da família Dapper : origem, evolução e análise da expressão durante a ontogênese dos membros de galinha / Débora Rodrigues Sobreira. – Campinas, SP : [s.n.], 2013.

Orientador: Lúcia Elvira Alvares.
Coorientador: José Xavier Neto.
Tese (doutorado) – Universidade Estadual de Campinas, Instituto de Biologia.

1. Genes Dapper. 2. Evolução. 3. Via de sinalização Wnt. 4. Fator de crescimento transformador beta. I. Alvares, Lúcia Elvira,1968-. II. Xavier-Neto, José. III. Universidade Estadual de Campinas. Instituto de Biologia. IV. Título.

Informações para Biblioteca Digital

Título em outro idioma: Studies on the Dapper gene family : origin, evolution and expression analysis during chicken limb development
Palavras-chave em inglês:
Genes Dapper
Evolution
Wnt signaling pathway
Transforming growth factor beta
Área de concentração: Biologia Tecidual
Titulação: Doutora em Biologia Celular e Estrutural
Banca examinadora:
Lúcia Elvira Alvares [Orientador]
Luis Antonio Violin Dias Pereira
Erika Cristina Jorge
Allyson Coelho Sampaio
Carla Cristina Judice Maria
Data de defesa: 11-07-2013
Programa de Pós-Graduação: Biologia Celular e Estrutural

Campinas, 11 de julho de 2013.

BANCA EXAMINADORA

Profa. Dra. Lúcia Elvira Alvares (Orientadora)

Assinatura

Prof. Dr. Luís Antônio Violin Dias Pereira

Assinatura

Profa. Dra. Erika Cristina Jorge

Assinatura

Prof. Dr. Allysson Coelho Sampaio

Assinatura

Profa. Dra. Catarina Raposo Dias Carneiro

Assinatura

Profa. Dra. Carla Cristina Judice Maria

Assinatura

Prof. Dr. Mário Henrique Bengtson

Assinatura

Prof. Dr. Paulo Sergio Lopes De Oliveira

Assinatura

RESUMO

Os genes da família *Dapper* (*Dpr*) codificam proteínas adaptadoras capazes de ligar-se fisicamente a diferentes moléculas e modular as vias de sinalização Wnt e TGF-β. Diferentes análises funcionais revelaram que os *Dpr* atuam na especificação do eixo corporal e do tecido neural, nos movimentos morfogenéticos, no desenvolvimento do olho, na indução da cardiogênese, adipogênse e cicatrização. Diversos estudos foram realizados a fim de compreender o papel desempenhado pelos Dpr durante a embriogenêse dos vertebrados e na homeostase de tecidos adultos. Contudo, muitas questões ainda necessitam ser elucidadas. Este projeto de Doutorado teve como objetivo (1) descrever os sítios de expressão da família gênica *Dpr* durante a ontogênese dos membros de galinha, associando-a as vias de sinalização Wnt e TGF-β e (2) investigar a origem e a evolução desses genes durante a filogenia dos metazoários. Nossos resultados confirmaram que os genes *Dpr* são dinamicamente expressos durante o desenvolvimento dos membros de galinha, provavelmente, modulando os sinais Wnt e TGF-β. Os genes *Dpr* são encontrados no mesênquima indiferenciado dos membros em formação e em células progenitoras de condrócitos, pericôndrio e tendões. Esses resultados sugerem as moléculas Dpr como um novo grupo de marcadores do desenvolvimento dos membros em galinha. Já nossas análises filogenéticas revelaram que os *Dprs* surgiram durante a evolução dos organismos deuterostômios e um novo ortólogo dessa família de proteínas, denominado *Dpr4,* foi descrito. Acreditamos que o nosso trabalho irá fornecer bases para estudos moleculares com o intuito de estabelecer a função individual de cada membro da família Dpr, bem como auxiliar no entendimento sobre como estas proteínas podem interagir e cooperar entre si para modular diferentes vias de sinalização molecular em diferentes contextos celulares.

ABSTRACT

The Dapper (*Dpr*) genes form a small gene family of adaptor proteins important to several processes of vertebrates development, such as the specification of the body axis and neural tissue, morphogenetic movements, eye development, induction of cardiogenesis, adipogenesis and wound healing, by modulating the Wnt and TGF-β signaling pathways using specific conserved domains/motifs. Three *Dpr* genes have been identified in human and mouse, two in chicken, one in frog and two in zebrafish genome. Since the discovery of Dpr proteins, several assays have been performed in order to understand the role of this family during embryogenesis, although many questions still need to be elucidated. Thus, this PhD project aimed to (1) describe the possible role of *Dpr* genes during ontogeny of chicken regarding the regulation of Wnt and TGF-β signaling pathways and (2) investigate the origin and evolution of *Dpr* family over the course of metazoan evolution. Our results demonstrated that *Dpr* genes are involved in chicken limb development, probably, by modulating Wnt and TGF-β signals. Dpr genes were found in the undifferentiated limb mesenchyme, progenitor of chondrocytes, perichondrium and tendons. These results suggest that *Dpr* genes are good candidates to a new set of markers in chicken limb development. Furthermore, our phylogenetic analysis revealed that the *Dprs* arose late during the deuterostomes evolution and allowed the identification of a new *Dpr* paralog (*Dpr4*), meaning that a repertoire of four Dact genes is found in vertebrates. Thus, our work will provide the basis for molecular studies in order to establish the role of each individual member of this family as well as how the set of Dpr proteins can interact and cooperate to modulate different molecular signaling pathways in different cellular contexts.

SUMÁRIO

Este Trabalho foi realizado no Laboratório de Biologia do Desenvolvimento do Instituto de Biologia da Universidade Estadual de Campinas, pelo Programa de Pós-Graduação em Biologia Celular e Estrutural, com auxílio financeiro da Fundação de Amparo à pesquisa do Estado de São Paulo (FAPESP), bolsa de Doutorado, processo número 2009/01683-9 e da Coordenação de Aperfeiçoamento de Pessoal de Nível Superior (CAPES), Programa de Estágio no Exterior, processo número 6867-10-3.

Aos meus pais que por uma vida de dedicação, amor, coragem e trabalho sempre possibilitaram a seus filhos a oportunidade de realizar sonhos e conquistas.

AGRADECIMENTOS

"Se as coisas são inatingíveis... Ora, não é motivo para não querê-las... que tristes os caminhos que não fora a presença distante das estrelas...".

Mário Quintana

Aos meus pais, que sempre me incentivaram e estiveram ao meu lado. Mesmo não entendendo ao certo o que eu fazia, nunca deixaram de acreditar em mim e me ensinaram a perseguir meus ideais com dedicação e coragem. Vocês são os maiores e melhores exemplos que tenho na vida.

Aos meus irmãos, o meu infinito agradecimento por toda amizade e compreensão dedicados a mim. Smepre com carinho e bom humor, vocês me deram conselhos valiosos que me ajudaram a enfrentar os desafios. Amo e tenho muito orgulho de vocês dois.

À minha orientadora, Dra. Lúcia Elvira Alvares, por sempre contar com o seu entusiasmo contagiante, com a sua alegria e com sua palavra amiga de reconhecimento e de incentivo. O apoio, a disponibilidade manifestada e a confiança depositada contribuíram decisivamente para que este trabalho tenha chegado até aqui.

Ao meu co-orientador, Dr. José Xavier-Neto, pela oportunidade de trabalhar ao seu lado e por ser um grande exemplo de persistência, determinação e competência.

Aos meus professores, Dr. Luis Antônio Violin Dias Pereira e Dr. Paulo Pinto Joazeiro, pela amizade, comprometimento e orientação ao longo desses 10 anos de Unicamp. Agradeço ainda por sempre acreditarem em mim e me encorajarem a seguir os meus sonhos. Vocês contribuíram de forma significativa para o meu crescimento pessoal e profissional. Mais que professores, vocês são inspirações para mim.

To Susanne Dietrich and Frank R Shubert for their guidance, scholarly inputs and consistent encouragement I received throughout the research work in UK.

Aos meus companheiros de projeto, Angelica V. Pedrosa, Ricardo Janousek e Lucimara Ap. Sensiate, obrigada por cada momento no DHE, principalmente, pela nossa grande conquista em conjunto.

A Daniel Arantes, não só pela ajuda técnica, mas principalmente pelo companheirismo, paciência e dedicação durante os últimos meses do meu doutorado.

Aos meus amigos de sempre, Ayana, Gu, Kiki, Paty, Buja e Maria, por só quererem o meu bem e me valorizarem pelo que sou. Sei que não é uma tarefa fácil serem meus amigos, mas vocês sempre desempenharam esse papel com maestria. Muito obrigada por sempre estarem presentes e dispostos a me ajudar, escutar, compartilhar, sonhar... Enfim, obrigada pela amizade incondicional! E que venham mais 10 anos pela frente.

Às minhas fiéis escudeiras, Bianca, Letícia e Carol, obrigada por fazerem do laboratório um lugar mais feliz. Vocês fazem parte dos momentos mais lindos e divertidos do meu doutorado. Agradeço pela disposição, atenção e generosidade. Vocês são demais! Contem sempre comigo. "Vem ni mim, vem ni nim".

Às eternas companheiras de salinha, Nara e Marilia, pelo apoio permanente e incondicional e pela amizade sempre demonstrada. Obrigada por cada risada, abraço, ideia e sugestão. Vocês moram em meu coração.

À Hozana e Sylvia não só pela amizade, carinho e auxílio técnico, mas, principalmente, pelo sorriso e bom humor constantes.

My friends in UK were sources of laughter, joy, and support. Special thanks go to Maria Papanicolau, thank you for all the support and encouragement you give me, and the patience and unwavering faith you have in me. You believe in me even when I don't believe in myself. For that I am eternally grateful.

À amiga-funcionária, Natália Roberta, pela ajuda constante e incansável. Agradeço pela dedicação, competência e objetividade com que desempenha o seu trabalho.

A todos os alunos do DHE pela ajuda e amizade sempre presente.

À Liliam Panagio, secretária de pós-graduação do programa de Biologia Celular e Estrutural, pela atenção sempre a mim dispensada, assim como sua eterna disponibilidade.

À Universidade Estadual de Campinas, meu lar por 10 anos, e ao Programa de Pós-graduação em Biologia Celular e Estrutural por terem oferecido diversas oportunidades possibilitando meu crescimento profissional e pessoal. Serei eternamente grata por tudo que fizeram por mim.

Aos órgãos de fomento à pesquisa, FAPESP, CNPq, CAPES e FAEPEX, cujo apoio financeiro possibilitou a realização deste trabalho.

LISTA DE FIGURAS

Capítulo 1

Capítulo 2

LISTA DE TABELAS

Capítulo 1

Capítulo 2

LISTA DE ABREVIATURAS E SIGLAS

Aa Aminoácido

ActrRIA/B Receptor de Activina do tipo IA/B, do inglês *Activin receptor type IA/B*

AER Crista ectodérmica apical, do inglês *Apical Ectodermal Ridge*

AKT Proteína quinase Serina/Treonina, do inglês *Serine/Threonine-Protein Kinases*. Também conhecida como proteína quinase B (do inglês *protein kinase B*)

Alk4 e Alk5 Receptores Serina-quinases, do inglês *Receptor Serine Kinases*

AP Eixo ântero-posterior

APC Gene humano supressor de tumor, do inglês *Adenomatus polyposis coli*

BMP Proteínas morfogenéticas ósseas, do inglês *Bone Morphogenetic Proteins*

BMPR1A/B Receptor de proteína morfogenética óssea do tipo 1A/B, do inglês *bone morphogenetic protein receptor, type IA/B*

Ca_2^+ Íon Cálcio

CAMKII Proteína quinase dependente de Cálcio/Calmodulina do tipo II, do inglês *Calmodulin-Dependent Protein Kinase II*

cAMP Adenosina 3',5'-monofosfato cíclico, AMP cíclico, do inglês *3'-5'-cyclic adenosine monophosphate, Cyclic adenosine monophosphate*

CBP Proteína ligadora ao CREB, do inglês *Creb Binding Protein*

Celsr1 Receptor G do tipo 1 de caderinas, do inglês C*adherin EGF Lag seven-pass G-Type Receptor 1*

CKI Caseína-quinase I, do inglês *Casein Kinase I*

CKIα Caseína-quinase Iα, do inglês *Casein Kinase Iα*

CKIγ Caseína-quinase Iγ, do inglês *Casein Kinase Iγ*

CKIδ Caseína-quinase Iδ, do inglês *Casein Kinase I*δ

CKIε Caseína-quinase Iε, do inglês *Casein Kinase I*ε

CREB Elementos responsivos a AMP cíclico, do inglês, *cAMP Response Elements*

c-Ski Proto-oncoproteínas, do inglês *V-SKI Avian Sarcoma Viral Oncogene Homolog*

c-SnoN Proto-oncoproteínas relacionada a c-Ski, do inglês *Ski-Related Novel Protein N*

C-terminal Região carboxi-terminal

DAAM1 Ativador da morfogênese associado a Dishevelled, do inglês, *Dishevelled Associated Activator Of Morphogenesis*

DAB 3,3'-diaminobenzidina, do inglês *3,3'-Diaminobenzidine*

DAG 1,2-diacilglicerol

DNA Ácido desoxirribonucléico, do inglês *Deoxyribonucleic Acid*

Dpr Dapper, antagonista de Dsh associado a β-catenina, do inglês *Dishevelled-associated antagonist of β-catenin*

Dpr1 Dapper 1, antagonista de Dsh associado a β-catenina homologo 1, do inglês *Dishevelled-associated antagonist of β-catenin* homolog 1

Dpr2 Dapper 2, antagonista de Dsh associado a β-catenina homologo 2, do inglês *Dishevelled-associated antagonist of β-catenin* homolog 2

Dpr3 Dapper 3, antagonista de Dsh associado a β-catenina homologo 3, do inglês *Dishevelled-associated antagonist of β-catenin* homolog 3

Dpr4 Dapper 4, antagonista de Dsh associado a β-catenina homologo 4, do inglês *Dishevelled-associated antagonist of β-catenin* homolog 4

Dsh Dishevelled

Dsh1 Dishevelled 1

Dsh2 Dishevelled 2

DV Eixo dorso-ventral

Dvl Dishevelled

E Dias do desenvolvimento de camundongo

EC	Extensão convergente
ECM	Matriz extra-celular, do inglês *Extracellular Matrix*
EvoDevo	Biologia Evolutiva do Desenvolvimento
FGF	Fator de crescimento de fibroblasto, do inglês *Fibroblast Growth Factors*
Frd	Frodo - Ortólogo de *Dpr* no genoma de *Xenopus, do inglês Functional Regulator of Disheveled in Ontogenesis*
Fz	Frizzled
Fz3	Frizzled 3
Fz6	Frizzled 6
GDF	Fator de diferenciação e crescimento, do inglês *Growth Differentiation Factor*
Gr	Grupo, do inglês *Group*
GSK3	Glicogênio sintase quinase 3, do inglês *Glycogen synthase kinase 3*
GTPase	Proteína que degrada moléculas de GTP
HDAC	Histona deacetilase, do ingles *Histone deacetylase*
HDCA1	Histona deacetilase I, do ingles *Histone deacetylase I*
HEK293T	Células embionárias de rim humano 293T, do inglês *Human Embryonic Kidney 293T*
Hfp	Horas pós-fertilização, do inglês *Hours Post Fertilisation*
Hg	Hedgehog
HH	Estádios de embriões de galinha, do inglês *Hamburger–Hamilton Stages*
HIS	Hibridação *in situ*
HIV	Vírus da imunodeficiência humana, do inglês *Human Immunodeficiency Virus*
HMG	Grupo de alta mobilidade, do inglês *High Mobility Group*
IP3	Inositol 1,4,5-trifosfato, do inglês *Inositol- 1, 4,5-trisphosphate*
ISH	Hibridação *in situ*, do inglês *In Situ Hybridization*

JNK Quinase Jun N-terminal, do inglês *Jun N-terminal kinase*

LEF Fator potencializador de ligação linfóide, do inglês *Lymphoid Enhancer-binding Factor*

LEF1 Fator potencializador de ligação linfóide do tipo 1, do inglês *Lymphoid Enhancer-binding Factor 1*

LMB Leptomicina B, do inglês *Leptomycin B*

LRP5/6 Co-receptor das glicoproteínas secretadas na via de sinalização Wnt, do inglês *Low density lipoprotein Receptor-related Protein 5/6*

MA Membro Anterior

MAPK Proteína quinase ativadora de mitose, do inglês *Mitogen-activated Protein Kinase*

Min Minutos

MIS Substância inibidora Mulleriana

mL Mililitro

MP Membro Posterior

N-cam Molécula de adesão celular neuronal, do inglês *Neural Cell Adhesion Molecule*

NES Sinal de exportação nuclear, do inglês *Nuclear Export Signal*

NFAT Fator nuclear de céluas T ativadas, do ingles *Nuclear Factor Of Activated T Cells*

NFKβ NF-kappaB

NKL Um tipo de proteína quinase, do inglês *Nemo Like Kinase*

NLS Sinal de localização nuclear, do inglês *Nuclear Localization Signal*

n-terminal Região amino-terminal

P120 ctn p120-catenina, do inglês *p120-catenin*

PBS Tampão fosfato-salino, do inglês *Phosphate Buffered Saline*

PCP Via de polaridade celular planar, do inglês *Planar Cell Polarity*

PD Eixo próximo-distal

PDZ Domínio central da proteína Dishevelled, do inglês *Post synaptic density-95/Discs large/Zonula occludens-1*

PDZ-B Domínio de ligação para PDZ, do inglês *Post synaptic density-95/Discs large/Zonula occludens-1*

PhyMl Método de máxima verossimilhança, do inglês *Maximum Likelihood Method*

PI3K Fosfatidilinositol-3-quinase, do inglês *Phosphatidylinositol 3'-Kinase*

PIP2 Fosfatidilinositol 4,5-bifosfato, do inglês *Phosphatidylinositol 4,5-bisphosphate*

PKA Proteína quinase A, do inglês *Protein Kinase A*

PKC Preoteína quinase C, do inglês *Protein Kinase C*

PLC Fosfolipase C, do inglês *Phospholipase C*

PMC Programação de Morte Celular

PP2A Proteína fosfatase do tipo 2, do inglês *Protein Phosphatase 2*

PMS Mesoderme paraxial, do inglês *Presomitic Mesoderm*

pSmad Molécula Smad fosforilada

PTU Fenil-Tiouréia, do inglês *Phenylthiourea*

PZ Zona de progresso, do inglês *Progress Zone*

R Ciclo de duplicação do genoma dos vertebrados, do inglês, *Rounds Of Vertebrate Genome Duplications*

RAC1 Proteína relacionada à RAS, do inglês *Ras-Related C3 Botulinum Toxin Substrate 1*

RE Retículo Endoplasmático

Rho Família gênica homóloga à Ras, do inglês *Ras Homolog Gene Family*

RhoA Família gênica homóloga à RAS, do inglês *Ras homolog gene family, member A*

RNAm Ácido ribonucléico mensageiro, do inglês *Ribonucleic Acid*

ROCK Rho-quinase, do inglês *Rho-Associated Protein Kinase*

Ror1/2 Receptor de Tirosina quinase do tipoI/II, do inglês *Receptor Tyrosine Kinase*

RT Temperatura ambiente, do inglês *Room Temperature*

S Esqueleto, do inglês *Scaffold*

SHH Sonic Hedgehog

SNC Sistema Nervoso Central

S-rich Região rica em Serina, do inglês *Serine rich*

TAK1 Proteína quinase do tipo I, do inglês *Activated Kinase-1*

TBS Tampão salina tris, do inglês *Tris Buffered Saline*

TCF Fatores de transcrição celular, do inglês *Transcription Cell Factor*

TGF-β Fator de transformação do crescimento β, do inglês *Transforming Growth* Factor *β*

TGF-β2 Fator de transformação do crescimento β2, do inglês *Transforming Growth* Factor *β2*

TN Tubo Neural

TOPflash Plasmídeo repórter, do inglês *TCF Reporter Plasmid*

TTBS Tampão salina tris com tween, do inglês *Tris Buffered Saline with tween*

Vangl1/2 Van Gogh like 1/2

Wg Via de sinalização Wnt em drosófilas, do inglês *Wingless*

Wnt Via de sinalização, combinação dos nomes em inglês *Wg* e *Int,* do inglês *Wingless Related*

Wnt/ Ca_2^+ Via de sinalização Wnt dependente de do íon cálcio

Wnt/ PCP Via de sinalização Wnt polaridade celular planar, do inglês

Wnt/ β-cat Via de sinalização Wnt beta-catenina (via canônica), do inglês *Wnt β-catenin signaling pathway*

ZL Zíper de Leucina, do inglês *Leucin Ziper*

ZPA Zona de atividade polarizadora, do inglês *Zone of Polarizing Activity*

β-cat Beta-catenina

Mg Micro-grama

Mm Micrômetro

Dbf-4 Proteína reguladora do ciclo celular, do inglês *Dumbbell Former 4*

GSK-3β Glicogênio-sintase-quinase-3β, do inglês *Glycogen Synthase Kinase 3*

Int-1 Proto-oncogene Int-1 conhecido como Wnt1, do inglês *Wingless-Type Mmtv Integration Site Family, Member 1*

Frd 1 Frodo 1

2R Segundo ciclo de duplicação do genoma dos vertebrados, do inglês, *Two Rounds Of Vertebrate Genome Duplications*

3R Terceiro ciclo de duplicação do genoma dos vertebrados, do inglês, *Three Rounds Of Vertebrate Genome Duplications*

Introdução Geral

1 – Introdução Geral

A Biologia do Desenvolvimento é o campo da ciência que aborda os mecanismos envolvidos na formação progressiva dos seres vivos desde o momento de sua concepção até o seu envelhecimento (Stern, 2005; Gilbert, 2003). O desafio permanente daqueles que atuam nessa área de pesquisa é desvendar como tecidos multicelulares, órgãos e até mesmo animais inteiros são formados a partir de uma única célula (Fortini, 2009). Ao mesmo tempo, buscam entender de que maneira pequenas perturbações nesse sistema podem causar malformações severas, rompendo a estrutura de organismos altamente organizados (Fortini, 2009; Polakis, 2000).

Certamente, durante as fases iniciais do desenvolvimento embrionário, os organismos passam por transformações mais abruptas e complexas, pois a partir de uma única célula fecundada surge um indivíduo multicelular sofisticado dotado de diversos sistemas e estruturas interconectadas, responsáveis pelo desenvolvimento e manutenção desse organismo completo e autônomo (Cayuso & Marti, 2005; Bejsovec, 2005). Sabe-se que a maior parte dessas modificações é controlada por diferentes mecanismos de expressão gênica, que interferem de modo direto ou indireto no crescimento, diferenciação, comunicação e migração celular (Pires-da Silva & Sommer, 2003). Uma das descobertas mais surpreendentes acerca das vias de sinalização reside no fato de que todos esses processos são controlados por poucas famílias de moléculas sinalizadoras que atuam durante o desenvolvimento embrionário — BMP (*Bone Morphogenetic Proteins*), FGF (*Fibroblast Growth Factors*), Hedgehog, MAPK (*Mitogen-activated Protein Kinase*), Notch, TGF-β (*Transforming Growth* Factor *β*) e Wnt (Fortini, 2009; Cayuso &

Marti, 2005; Bejsovec, 2005; Pires-da Silva & Sommer, 2003). Essas famílias gênicas são conservadas em todo o reino animal e cooperam para o desenvolvimento, formação e organização de um conjunto diversificado de tecidos e órgãos que comporão quase todas as espécies de metazoários conhecidos (Fortini, 2009, Stern, 2005; Gilbert, 2003).

Dentre as famílias de proteínas sinalizadoras envolvidas na embriogênese, podemos destacar as famílias Wnt e TGF-β. Ambas controlam um conjunto diversificado de processos celulares, incluindo apoptose; especificação de destinos celulares; proliferação e diferenciação celular, desde espécies menos derivadas, como moscas e vermes, até as mais derivadas, como mamíferos e aves (Clevers 2006; Shi & Massagué 2003; ten Dijke *et al*., 2002; Polakis 2000; Patterson & Padgett 2000; Massagué *et al*., 2000; Wodarz & Nusse, 1998). Devido ao importante papel desempenhado por essas duas vias de sinalização, vários trabalhos têm sido realizados buscando identificar moléculas capazes de modular tanto sinais da via Wnt quanto TGF-β. Em 2002, o grupo do Dr. Moon e Dr. Sokol, das Universidades da Califórnia e Harvard, respectivamente, identificaram a molécula Dapper (Dpr) como uma possível reguladora da via de sinalização Wnt (Cheyette *et al*., 2002 e Gloy *et al*., 2002). Dois anos mais tarde, o grupo do Dr. Meng, da Universidade de Tsinghua, caracterizou as proteínas Dprs também como moduladoras dos sinais TGF-β através da sinalização Nodal (Zhang *et al*., 2004).

Atualmente, sabe-se que as moléculas Dprs atuam de diferentes maneiras na via de sinalização Wnt, ora assumindo papel de moduladoras negativas, ora de positivas (Brott & Sokoll, 2005a). Por exemplo, a proteína Dapper1 (Dpr1) é capaz de se ligar fisicamente à Dishevelled (Dsh), molécula chave da via de sinalização Wnt, encaminhado-a para a via de

degradação lisossômica/proteossômica (Zhang *et al*., 2006). Em tal processo, Dpr assume o papel de modulador negativo tanto da via de sinalização Wnt canônica quanto da não-canônica (Zhang *et al*., 2006; Yau *et al.,* 2004; Cheyette *et al*., 2002). Além disso, estudos em *Xenopus* e peixe-zebra demonstraram a proteína Dpr como moduladora positiva dos sinais Wnt/β-catenina (Gloy *et al*., 2002; Waxman *et al*., 2004). Nesse caso, a molécula Dpr se associa à proteína Dsh e juntas interagem com diferentes quinases ativando genes-alvo dessa via (Waxman *et al*., 2004). Já no que concerne a via de sinalização TGF-β, a proteína Dapper2 (Dpr2) foi caracterizada como potente moduladora negativa desta via, degradando os receptores de membrana Alk4 e Alk5 através do mecanismo lisossômico (Zhang *et al*., 2004).

Ademais, diversos estudos demonstraram que as proteínas Dpr estão relacionadas a diferentes processos biológicos — gastrulação, morfogênese cefálica e ocular, cardiogênese, adipogênese, desenvolvimento de sinapses excitatórias na região do hipocampo, cicatrização, desenvolvimento da uretra e câncer (Cheyette *et al.*, 2002; Gloy *et al.*, 2002; Waxman *et al.*, 2004; Yau *et al.*, 2004; Zhang *et al.*, 2006; Jiang *et al*., 2008; Lagathu *et al*., 2009; Suriben *et* al., 2009; Okerlund *et al*., 2012). A grande variedade de funções exercidas por essas proteínas é conferida pela habilidade de interagir com diferentes parceiros moleculares (Waxman *et al*., 2004; Zhang *et al*., 2004; Brott & Sokol, 2005a). Essas interações são mediadas por diferentes domínios de ligação que as moléculas Dprs apresentam em sua estrutura peptídica (Waxman *et al*., 2004; Zhang *et al*., 2004; Brott & Sokol, 2005a). Dessa forma, as Dprs formam uma família de proteínas adaptadoras que desempenham distintas funções dependendo do seu parceiro molecular e do contexto celular no qual estão inseridas (Brott & Sokol, 2005a).

Buscar entender o funcionamento das moléculas envolvidas nos processos de desenvolvimento — em particular a ativação e inativação dessas vias de sinalização moleculares — bem como a caracterização de possíveis agentes moduladores de sua atividade têm uma grande importância para as pesquisas básica e aplicada no campo da Biologia do Desenvolvimento.

Desde a descoberta dos genes *Dpr*, muitos estudos têm sido realizados a fim de compreender as funções desses genes durante o desenvolvimento embrionário dos vertebrados, em particular aspectos destes genes relacionados à sua capacidade de modular diversas vias de sinalizações, sua relação com doenças humanas, bem como o seu papel para a manutenção da homeostase do tecido adulto. Porém, ainda restam diversas questões que necessitam ser elucidadas.

Este projeto de Doutorado buscou: (1) investigar o possível papel dos genes *Dpr* durante o desenvolvimento dos membros de galinha, sobretudo na regulação das vias de sinalização Wnt e TGF-β. Para tanto, os padrões de expressão de *Dpr1* e *Dpr2* foram determinados durante o desenvolvimento inicial e padronização dos brotos dos membros, bem como nas fases mais tardias de formação dos membros, onde ocorre a diferenciação tecidual. Alem disso, esses padrões de expressão foram comparados aos sítios de expressão de marcadores teciduais/estruturais específicos. Nossos resultados demonstraram que os *Dprs* possuem um padrão de expressão bastante dinâmico e possivelmente estão envolvidos durante a formação do esqueleto apendicular e dos tendões e também no controle do crescimento dos dígitos. O segundo objetivo desse projeto foi (2) desvendar a origem e a evolução dos genes *Dpr*

utilizando análises de *bioinformática* e ensaios de hibridação *in situ.* Os resultados obtidos revelaram que os primeiros genes *Dpr* surgiram na linhagem dos animais deuterostômios e que, no genoma de anfioxo, existe um ortólogo *Dpr*. Ademais, nossas análises identificaram novos parálogos, *Dapper 3a, Dapper 3b,* bem como um novo ortólogo, *Dapper 4,* no genoma do peixe-zebra. Tais resultados estão de acordo com a hipótese de que esses organismos sofreram dois episódios de duplicação gênica durante a sua evolução. O presente estudo também caracterizou o *loci* genômico e os motivos proteicos que cada gene *Dpr* codifica. Por fim, ensaios de hibridação *in situ* utilizando embriões de peixe-zebra e galinha validaram nossos resultados *in silico.*

Para apresentar os dados obtidos durante o desenvolvimento desse projeto, esta tese de doutorado foi estruturada em dois capítulos: **Capítulo 1: "Padrão de expressão dos genes Dpr durante o desenvolvimento dos membros de galinha (*Gallus gallus*)**", o qual apresenta uma breve introdução sobre a ontogenia dos membros dos vertebrados, bem como os resultados expostos no manuscrito "*Dact genes expression profiles suggest a role of this gene family in integrating Wnt and TGF-β signaling during chicken limb development*", aceito para publicação na revista *Developmntal Dynamics*; e **Capítulo 2: "Origem e evolução dos genes da família Dpr"**, que traz uma pequena introdução sobre a área da Biologia Evolutiva do Desenvolvimento, cujos resultados serão apresentados por meio do manuscrito "*Dact genes are chordate specific regulators at the intersection of Wnt and Tgf beta pathways*". Ao final da tese, serão apresentadas discussões gerais e conclusões derivadas do desenvolvimento deste trabalho. Ainda, haverá um apêndice no qual constará o artigo científico: *Elastic fiber assembly in the*

adult mouse pubic symphysis during pregnancy and postpartum, fruto de uma colaboração realizada durante o doutorado.

Revisão Bibliográfica

2 – Revisão Bibliográfica

2.1 Vias de Sinalização

O adequado desenvolvimento embrionário é possível graças à capacidade das células se comunicarem (Berridge *et al*., 2012; Logan & Nusse, 2006; Gilbert, 2003). Através de complexas vias de sinalização compostas por várias proteínas de membrana e intracelulares rigorosamente controladas, a comunicação célula-célula ou célula-matriz torna-se viável, formando um embrião complexo e padronizado (Berridge *et al*., 2012; Logan & Nusse, 2006; Gilbert, 2003). Estudos genéticos e bioquímicos revelaram que um número pequeno de diferentes vias é suficiente para gerar uma grande variedade de células, tecidos e morfologias (Berridge *et al*., 2012; Pires-da Silva & Sommer, 2003). *Hedgehog* (Hh), *Wingless Related* (Wnt), Fatores de crescimento e transformação β (TGF-β), Notch e Fatores de Crescimento Fibroblásticos (FGF) são vias de sinalização utilizadas diversas vezes ao longo do desenvolvimento dos indivíduos e também na evolução dos metazoários (Fortini, 2009; Cayuso & Marti, 2005; Bejsovec, 2005; Pires-da Silva & Sommer, 2003). Nas últimas décadas, elas foram caracterizadas e seus mecanismos de atuação parcialmente elucidados. Tais estudos revelaram que todas possuem em comum a ativação de genes-alvo específicos pela regulação dos fatores de transcrição sinal-dependente (Berridge *et al*., 2012; Pires-da Silva & Sommer, 2003).

As moléculas da família Dpr são proteínas intracelulares capazes de se ligarem tanto a moléculas citoplasmáticas quanto nucleares e através dessas interações podem modular diferentes vias de sinalização (Li *et al*., 2013). Dados da literatura relacionam os genes *Dpr*, em

especial, às vias de sinalização Wnt e TGF-β. Assim, aspectos relevantes de ambas serão destacados a seguir.

2.2 Via de Sinalização Wnt e seus ligantes

As proteínas Wnt formam uma grande família de glicoproteínas sinalizadoras que possuem suas funções bem estabelecidas durante a regulação da padronização embrionária, proliferação e determinação celular (Angers & Moon, 2009; Bartscherer & Boutros, 2008). São classificadas como morfógenos e possuem a capacidade de transmitir informações entre células de diferentes tecidos (Berridge, 2012; Bartscherer & Boutros, 2008).

O primeiro gene *Wnt* foi identificado em drosófila (*Drosophila melanogaster*) através de uma mutação, que causa ausência das asas e dos halteres nesse organismo (Sharma & Chopra, 1976). Assim, em concordância com o fenótipo apresentado pelo mutante, o novo gene foi nomeado como *Wg (Wingless)* — "sem asas" (Sharma & Chopra, 1976). Anos mais tarde, identificou-se no genoma de camundongo uma sequência gênica capaz de induzir tumores mamários, que foi denominada *Int-1* (*proto-oncogene Int-1*) (Nusse *et al*., 1984). Após estudos filogenéticos, concluiu-se que *Wg* e *Int-1* eram homólogos e, então, os genes passaram a ser chamados de *Wnt*, junção dos dois nomes anteriores (Antara De, 2011). Hoje, temos descritas um total de 24 proteínas Wnt conhecidas no genoma de vertebrados, das quais 19 foram identificadas em humanos e camundongos, sete em drosófilas e cinco em *C.elegans* (Logan & Nusse, 2004; Patapoutian & Reichardt 2000). As glicoproteínas Wnt são capazes de interagir com a porção amino-terminal (N-terminal), rica em cisteínas, dos receptores transmembranares da família *Frizzled* (Fz) (Bartscherer & Boutros, 2008; Clevers, 2006). A ligação dos Wnt com os

receptores Fz ativa pelo menos dois eventos de sinalização intracelulares: um, que controla transcrição gênica que influencia proliferação, destino e sobrevivência celular, e outro, que controla o fluxo de Cálcio (Ca^{2+}), em geral envolvido nas mudanças de movimentos e de comportamentos celulares (Bartscherer & Boutros, 2008; Moon *et al.*, 2004; Patapoutian & Reichardt 2000).

Os membros da família Wnt são definidos pela sequência de aminoácidos (aa) que possuem (Gordon & Nusse, 2006). Essa é composta por uma porção sinalizadora seguida de uma região contendo 23 resíduos de cisteínas altamente conservados e responsáveis pelo dobramento da molécula por meio de pontes dissulfeto (Bartscherer & Boutros, 2008; Nusse, 2008; Mikels & Nusse, 2006; Wodarz & Nusse, 1998). Além disso, as moléculas Wnt são palmitoiladas e compostas por aa hidrofóbicos, tornando as proteínas pouco solúveis (Berridge, 2012; Bartscherer & Boutros, 2008).

A via de sinalização *Wnt* está presente em diversos processos do desenvolvimento embrionário tais como segmentação, gastrulação e formação do sistema nervoso em vertebrados (Berridge, 2012; Bartscherer & Boutros, 2008). Os sinais Wnt são pleiotrópicos, desempenhando um papel crucial no controle da proliferação, diferenciação, destino celular e apoptose (Berridge, 2012; Wordaz & Nusse, 1998). Durante a vida adulta, a sinalização Wnt atua na manutenção da homeostase tecidual e sua desregulação pode ocasionar diversas doenças, em particular, o câncer (Nusse, 2008; Mikels & Nusse, 2006; Patapoutian & Reichardt 2000; Wordaz & Nusse, 1998).

Existem três principais vias de sinalização Wnt. A via de sinalização canônica *Wnt/β-catenina*, que possui como principal função a ativação da transcrição gênica, controlando tanto processos envolvidos durante a embriogênese como na vida adulta dos organismos. As outras duas são conhecidas como vias de sinalização não canônicas: a *via polaridade celular planar*, envolvida na organização do citoesqueleto através da atuação das proteínas GTP ligantes, e a *via de sinalização Wnt/Ca^{2+}*, que medeia a padronização dorso-ventral de embriões de vertebrados, além de inibir a via Wnt/β-catenina (Berridge, 2012; Niehrs, 2012; Angers & Moon, 2009; Nusse, 2008; Moon *et al*., 2004; Wordaz & Nusse, 1998).

2.2.1 Sinalização Wnt canônica (via Wnt/β-catenina)

Dentre as vias de sinalização Wnt, a canônica é a que dispõe do maior número de dados na literatura e sua principal característica é a utilização da proteína β-catenina (β-cat) (Berridge, 2012; Angers & Moon, 2009; Clevers, 2006). Também conhecida como via Wnt/β-catenina (Wnt/β-cat) (Figura 1), ela atua durante o desenvolvimento embrionário, regeneração, determinação e proliferação celular, e também contribui para a homeostase de tecidos adultos (Angers & Moon 2009; Clevers, 2006). Todavia, seu desbalanceamento pode acarretar o surgimento de doenças como o câncer além de processos degenerativos (Angers & Moon 2009).

A proteína multifuncional β-cat é a molécula responsável pela regulação da transcrição dos genes-alvo da sinalização Wnt (Berridge, 2012). Em células livres de sinais Wnt, a concentração de β-cat no citoplasma é mantida em níveis baixos, uma vez que toda a β-cat solúvel é constantemente degrada (Berridge, 2012; Niehrs, 2012; Angers & Moon 2009; Mikels & Nusse, 2006). Esse processo ocorre por meio do complexo de degradação de β-cat, que

consiste em um complexo proteico formado pelas seguintes moléculas: Axina, Repressora tumoral APC (*Adenomatus polyposis coli*), Fosfatase PP2A, Caseína-quinase Iα (CKIα) e Glicogênio-sintase-quinase-3β (GSK-3β) (Berridge, 2012; Angers & Moon, 2009; Nusse, 2008; Clevers, 2006; Moon *et al*., 2004; Wordaz & Nusse, 1998). Dentro desse complexo multiproteico, a molécula β-cat é duplamente fosforilada pelas proteínas CKIα e GSK-3β em sítios amino-terminais (Berridge, 2012; Clevers, 2006). Em seguida, a β-cat fosforilada é reconhecida pelo complexo de ubiquitinação (F-box/β-TrCP/ubiquitina ligase) e encaminhada para degradação via proteossomo (Angers & Moon, 2009; Nusse, 2008; Moon *et al*., 2004). Na ausência de β-cat, os genes-alvo da sinalização Wnt se mantêm inativos, pois o complexo proteico nuclear formado pelo Grupo de Alta Mobilidade (HMG), Fator Celular T (TCF) e Fator Ativador Linfóide (LEF-1), mantêm-se fisicamente ligado ao DNA impedindo que os genes regulados pelos sinais *Wnt* sejam transcritos (Berridge, 2012; Clevers, 2006; Gordon & Nusse, 2006; Moon *et al*., 2004). Em adição ao complexo protéico nuclear, Histonas Deacetilases (HDAC) contribuem para o bloqueio da transcrição dos genes-alvo *Wnt* (Figura 1A) (Niehrs, 2012; Gordon & Nusse, 2006; Moon *et al*., 2004).

O desencadeamento da via de sinalização Wnt/β-cat ocorre à medida que as glicoproteínas Wnt secretadas no meio extracelular se ligam aos receptores transmembranares Fz e aos correceptores LRP5 e LRP6 (LRP5/6), membros da superfamília de receptores lipoprotéicos de baixa densidade (Berridge, 2012; Clevers, 2006, Moon *et al*., 2004). Em seguida, o correceptor LRP5/6 é fosforilado pela Caseína-quinase Iγ (CKIγ), presente na membrana plasmática, e liga-se fisicamente à proteína Axina do complexo de degradação da β-cat

(Berridge, 2012; Clevers, 2006, Moon *et al*., 2004; Logan & Nusse, 2004). Essa interação leva à hiperfosforilação da proteína citoplasmática *Dishevelled* (Dsh) que, por sua vez, se liga à molécula Axina, desestabilizando o complexo de degradação da β-cat (Berridge, 2012; Clevers, 2006, Moon *et al*., 2004; Logan & Nusse, 2004). Uma vez que esse complexo está neutralizado, a proteína β-cat é estabilizada, acumulada no citoplasma e encaminhada para o núcleo (Berridge, 2012; Clevers, 2006, Moon *et al*., 2004; Logan & Nusse, 2004). No núcleo, a molécula de β-cat liga-se aos fatores LEF-1 e TCF reduzindo a capacidade de inibição desses (Clevers, 2006). Assim, a transcrição dos genes-alvo da via de sinalização Wnt é iniciada, resultando na ativação da diferenciação e proliferação celular (Figura 1B) (Berridge, 2012; Clevers, 2006, Moon *et al*., 2004). Os sinais Wnt também podem ativar genes da própria via Wnt, e dessa forma, através de *feedback* positivo, controlam a transcrição de seus sinais (Berridge, 2012; Niehrs, 2012; Clevers, 2006, Moon *et al*., 2004; Logan & Nusse, 2004).

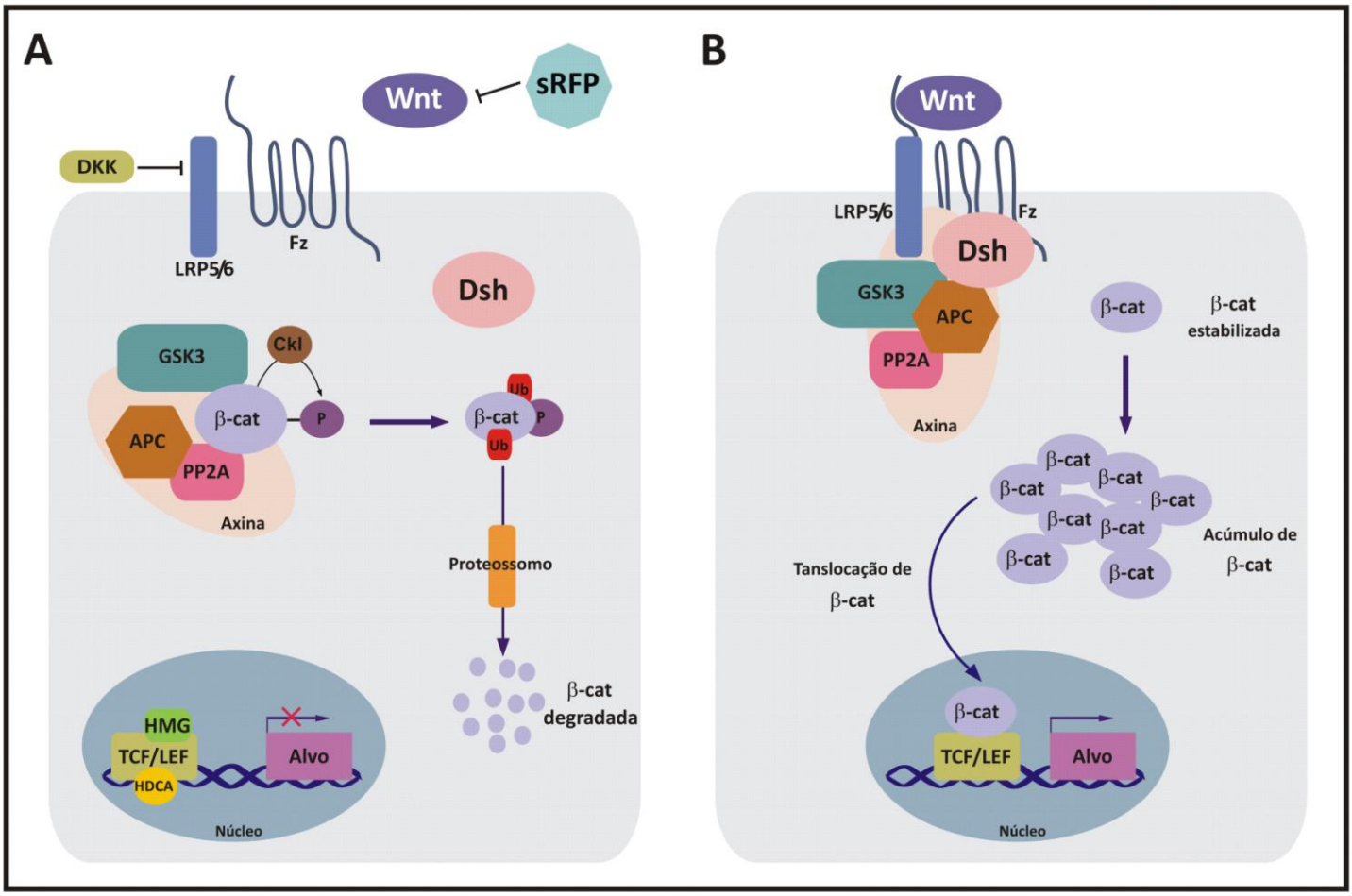

Figura 1. Via de Sinalização Wnt canônica. Em (A) temos a representação de uma célula na ausência dos sinais Wnt, na qual os genes-alvo da proteína multifuncional β-catenina (β-cat) estão repremidos. Nela, Dishevelled (Dsh) encontra-se desfosforilado e é incaz de interagir com o complexo de degradação da β-cat, composto pelas moléculas: APC (proteína repressora de câncer), fosfate PP2A, glicogênio-sintase-quinase-3β (GSK3) e caseína-quinase Iα (CKI). Nesse contexto, a β-cat é fosforilada pelo complexo, ubiquitinada (Ub) e encaminha da para via de degradação proteossômica. (B) Quando sinais Wnt se ligam aos receptores Frizzled (Fz) e aos correceptores LRP5 e LRP6 (LRP5/6), o complexo de degradação de β-cat é desestabilizado permitindo que ocorra acúmulo e translocação de β-cat para o núcleo, onde ativará genes-alvo dessa sinalização. Dkk (Dickkopf); HDCA (histonas deacetilases); HMG (grupo de alta mobilidade); P (grupo fosfato); sRFP (antagonista Frizzled); TCF/LEF (fator celular T/Fator ativador linfoide). Adaptado de Niehrs, 2012.

2.2.2 Sinalização Wnt não canônica – via Wnt/Polaridade Celular Planar

A via Wnt/Polaridade Celular Planar (PCP) fornece informações direcionais para que as células orientem-se e ocupem corretas posições espaciais em relação às células vizinhas, bem como ao contexto global do eixo corpóreo (Berridge, 2012; Gao *et al*., 2011; Tada & Kai, 2009; Wang & Nathans, 2007).

Através da remodelação do citoesqueleto e estabelecimento de localização assimétrica de outros componentes citoplasmáticos e de membrana, a via PCP regula a polaridade e os movimentos celulares durante o desenvolvimento embrionário (Niehrs, 2012; Gao *et al*., 2011; Moon & Shah, 2002). Para tanto, são ativadas as vias de sinalização envolvendo as moléculas GTPases RhoA e RAC1, Rho-quinase (ROCK) e N-teminal Jun-quinase (JNK) (Figura 2) (Niehrs, 2012; Gao *et al*., 2011; Wang & Nathans, 2007; Moon & Shah, 2002). Moléculas envolvidas na via de sinalização PCP são comumente classificadas em três categorias: (1) fatores responsáveis pela coordenação da polaridade planar em todo o tecido; (2) fatores que fornecem sinais de polarização intrínsecos dentro de células individuais através de sua localização subcelular assimétrica; e (3) fatores tecido-específicos que são necessários para o aparecimento da polarização (Niehrs, 2012; Gao *et al*., 2011; Wang & Nathans, 2007).

A via PCP tem sido bastante estudada em embriões de drosófilas*,* nos quais os primeiros genes que controlam essa via foram identificados (Berridge, 2012; Tada & Kai, 2009). Dentre os membros evolutivamente conservados que controlam a via PCP em drosófila temos as proteínas *Frizzled*, *Strabismus/Van Gogh, Flamingo e Dishevlled,* responsáveis pela orientação da

polaridade dos pêlos e cerdas, que cobrem a superfície do corpo, bem como das células fotorreceptoras encontradas nos olhos (Gao *et al*., 2011; Tada & Kai, 2009; Park & Moon, 2001).

Em vertebrados, a definição do que constitui os processos de PCP não é inteiramente clara (Wang & Nathans, 2007). Contudo, moléculas homólogas aos principais membros da via PCP de drosófila foram identificadas no genoma dos vertebrados: *Frizzled 3* e *Frizzled 6* (Fz3 e Fz6); *Van Gogh like 1 e Van Gogh like 2* (Vangl1 e Vangl2); *Celsr1* e *Dishevelled 1* e *Dishevelled 2* (Dsh1 e Dsh2) (Gao *et al*., 2011; Tada & Kai, 2009; Wang & Nathans, 2007). Estudos recentes demonstram que esses homólogos estão envolvidos em diferentes processos, tais como fechamento do tubo neural, orientação dos folículos capilares e estereocílios, além de regularem os movimentos de extensão convergentes (EC), presentes durante toda a fase de gastrulação (Berridge, 2012; Tada & Kai, 2009; Clevers, 2006, Moon *et al*., 2004).

Apesar das funções da via de sinalização PCP serem de extrema importância para o adequado desenvolvimento dos vertebrados, pouco se sabe sobre os mecanismos reguladores dessa via através dos sinais Wnt (Gao *et al*., 2011). No entanto, sabe-se que alguns membros da família Wnt, como Wnt5, transduzem seus sinais para o citoplasma independentemente da molécula β-cat e ineragem com a proteína Vangl2 (Gao *et al*., 2011; Suriben et al., 2009). Ademais, diversos estudos demonstraram que Wnt5 é capaz de sinalizar através da molécula Ror2, proteína transmembrana unipasso que apresenta o domínio quinase-tirosina, responsável pela ligação entre essas moléculas (Gao *et al*., 2011). É sabido que a molécula Ror2 mediada por Wnt5 está envolvida na inativação da via Wnt/β-cat e na ativação da proteína JNK (Gao *et al*.,

2011; Mikels & Nusse, 2006). Assim, a molécula Wnt5 tem sido investigada e frequentemente apontada como um dos principais membros Wnt que regula a via PCP (Gao *et al*., 2011).

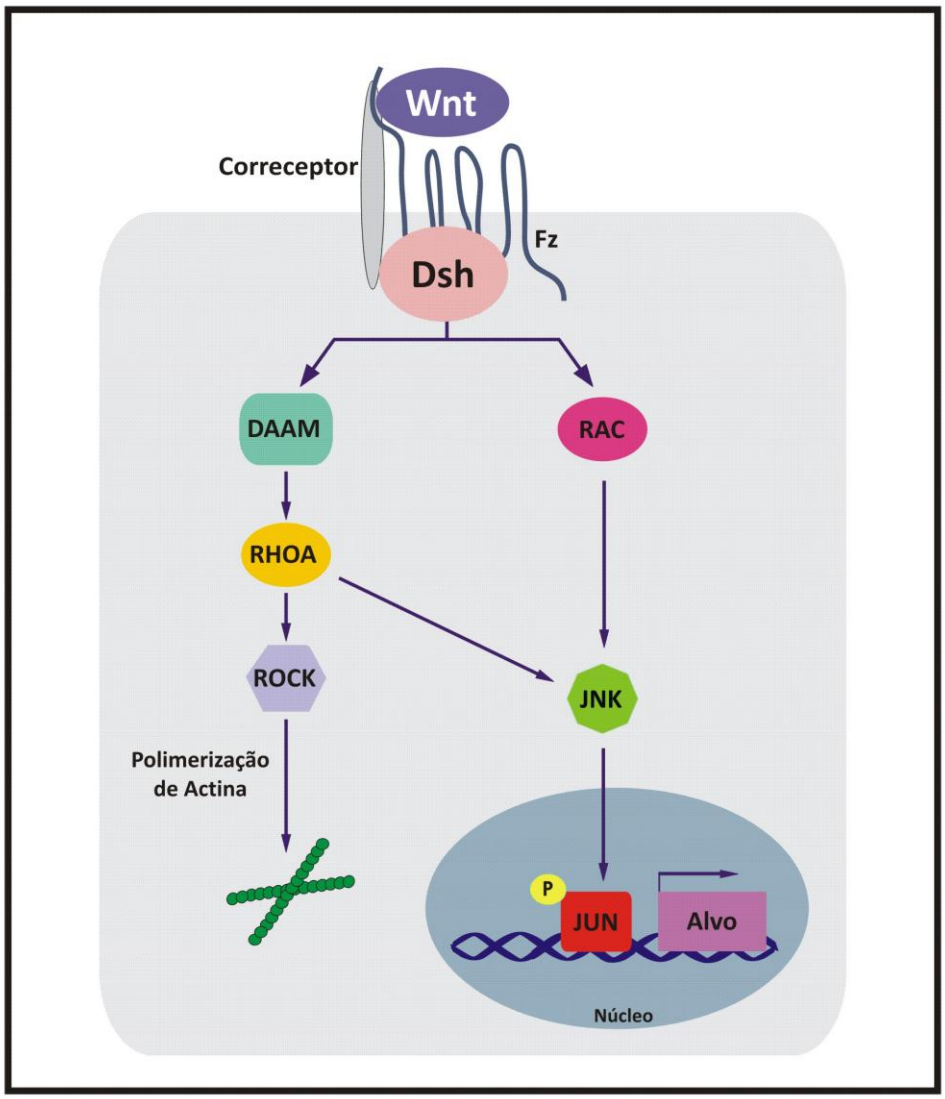

Figura 2. Via de sinalização Wnt polaridade celular planar (PCP). A via Wnt/PCP ativa as pequenas GTPases RhoA e RAC, a Rho-quinase (ROCK) e N-teminal Jun-quinase (JNK), permitindo a polimerização da actina e dos microtúbulos, regulando a mobilidade e a polaridade celular, bem como os movimentos morfogenéticos. DAAM (Ativador da morfogênese associado a Dsh); Dsh (Dishevelled); Fz *(Frizzled)*; Jun (gene alvo da JNK); P (grupo fosfato). Adaptado de Niehrs, 2012 e Moon *et al*., 2004.

2.2.3 Sinalização Wnt não canônica – via Wnt/Ca2+

Há pouco meno de duas décadas, os íons Ca^{2+} foram descritos como importantes moléculas mensageiras das vias de sinalização Wnt não canônica (Kuhl *et al*., 2000). Anos mais tarde, experimentos demonstraram que a sinalização mediada pelos íons Ca^{2+} (Wnt/Ca^{2+}) estava envolvida na regulação de diversos processos relacionados ao desenvolvimento embrionário (Antara De, 2011; Kohn & Moon, 2005; Kuhl *et al*., 2000).

A ativação da via de sinalização Wnt/Ca^{2+} se dá pelo aumento dos níveis dos íons Ca^{2+} no citoplasma. Para tanto, sinais Wnt extracelulares devem ligar-se ao receptor de membrana Fz, acoplado à proteína heterotrimétrica G, e ao correceptor Ror1/2 (Antara De, 2011; Kohn & Moon, 2005; Saneyoshi *et al*., 2002; Kuhl *et al*., 2000). A interação dos sinais Wnt com o receptor Fz leva ao aumento temporário de determinadas moléculas de sinalização intracelulares, tais como Inositol 1,4,5-trifosfato (IP3), 1,2-Diacilglicerol (DAG) e íons Ca^{2+}, causando rápidas alterações nas funções celulares (Antara De, 2011; Kohn & Moon, 2005; Saneyoshi *et al*., 2002). As moléculas IP3 e DAG são derivadas do fosfolipídio Fosfatidilinositol 4,5-bifosfato (PIP2) pela ação da Fosfolipase C (PLC) localizada na membrana celular, que é ativada pela interação do ligante Wnt ao receptor Fz (Antara De, 2011; Saneyoshi *et al*., 2002). Após a sua síntese, IP3 e DAG são difundidas pelo citoplasma e interagem com canais de Ca^{2+} presentes na membrana do retículo endoplasmático (RE), resultando na liberação desses íons para o citoplasma (Saneyoshi *et al*., 2002). Os íons Ca^{2+} liberados pela ação de IP3 serão responsáveis pela ativação da Proteína Quinase dependente de cálcio/calmodulina (CAMKII); já os liberados pela DAG irão ativar a Proteína Quinase C (PKC) (Antara De, 2011; Saneyoshi *et al*.,

2002). Por sua vez, CAMKII e PKC irão promover a expressão de alguns fatores transcricionais, tais como NFkB e CREB, que serão encaminhados para o núcleo e ativarão os genes-alvo dessa via (Figura 3) (Antara De, 2011; Saneyoshi *et al*., 2002). Através de experimentos envolvendo embriões de *Xenopus* e peixa-zebra, demonstrou-se que essa ativação estava envolvida na ventralização dos embriões nas fases iniciais do desenvolvimento, bem como nos movimentos de extensão durante a gastrulação desses organismos (Freisinger *et al*., 2010; Lin *et al*, 2010; Kuhl *et al*., 2000). Ademais, constatou-se que as moléculas CAMKII e PKC inibiam a via canônica Wnt/β-cat através da fosforilação das proteínas Dsh e LEF (Lin *et al*, 2010;). Em 2004, Yoshida e colaboradores bloquearam a via de sinalização Wnt/Ca^{2+} em embriões de *Xenopus* e os resultados obtidos a partir desse experimento revelaram uma série de anormalidades durante a organogênese do coração, rim, fígado e intestino e na formação dos somitos (Yoshida *et al*., 2004). Apesar dos mecanismos bioquímicos e genéticos da via Wnt/Ca^{2+} ainda não estarem totalmente elucidados, esta via já foi apontada, inúmeras vezes, como reguladora da mobilidade celular durante o processo metastático de diferentes tipos de câncer — próstata, tireóide, cólon, esôfago e pele (Antara De, 2011; Konh & Moon, 2005; Kuhl *et al*., 2000).

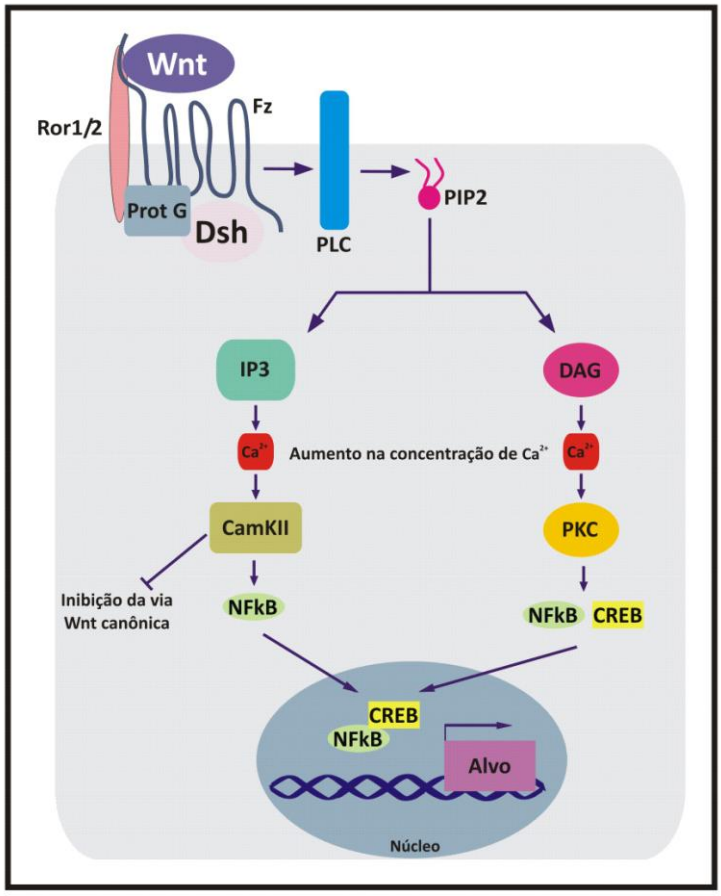

Figura 3. Via de sinalização Wnt/Ca2^{+}. Sinais Wnt se ligam ao receptor Fz *(Frizzled)* e ao correceptor Ror1/2 que irão ativar a proteína de membrana PLC (Fosfolipase C) que formará, com auxilio da PIP2 (Fosfatidilinositol 4,5-bifosfato), as proteínas IP3 (Inositol 1,4,5-trifosfato) e DAG (1,2-Diacilglicerol) responsáveis pelo aumento da concentração dos íons Ca^{2+} no citoplasma. A liberação de Ca^{2+} irá ativar as moléculas quinase dependente de cálcio/calmodulina (CAMKII) e Proteína quinase C (PKC) que irão promover a expressão de fatores transcricionais, NFkB e CREB, e ativarão genes-alvo dessa via. Adaptado de Niehrs, 2012 e Antara, 2011.

2.2.4 Via de sinalização Wnt: considerações finais

Vale destacar que as diferentes vias de sinalização Wnt não são autônomas nem se consegue limitá-las rigorosamente, uma vez que há um grau elevado de sobreposições entre elas (Antara De, 2011; Miller *et al*., 2009; Konh & Moon, 2005). A comunicação entre essas vias já foi demonstrada em diversos experimentos genéticos e bioquímicos, contudo estudos

buscando entender essas relações ainda se fazem necessários (Antara De, 2011; Miller *et al*., 2009; Konh & Moon, 2005).

2.3 Via de Sinalização TGF-β

A superfamília de proteínas sinalizadoras TGF-β (Fator de transformação de crescimento β) controla diversos mecanismos envolvidos no desenvolvimento embrionário e na homeostase dos tecidos adultos (Shen, 2007; Shi & Massague, 2003). Dentre os mecanismos regulados por essa via, podemos destacar a proliferação, diferenciação, reconhecimento celular, apoptose e especificação de destinos celulares (Shi & Massague, 2003; Wells, 2000). Além disso, linhagens de células imunes, incluindo linfócitos B, células T, células dendríticas e macrófagos utilizam a via TGF-β para regular negativamente sua proliferação, diferenciação e ativação (Moustakas *et al*., 2002). Dessa forma, os sinais TGF-β são importantes imunossupressores e quaisquer perturbações nessa via de sinalização podem desencadear doenças autoimunes, inflamações e câncer (Moustakas *et al*., 2002).

As proteínas ligantes que fazem parte da superfamília TGF-β são citocinas que apresentam seis resíduos conservados de cisteína e são codificadas por 42 quadros de leitura (*open reading frames*) em humanos, nove em moscas e seis em nematelmintos (Shi & Massague, 2003). Essas citocinas são subdivididas em dois grupos, de acordo com a identidade de sequência que apresentam e as vias de sinalização que ativam — (1) Ativina/Inibina; (2) BMP (Proteína Morfogenética Óssea); (3) GDF (Fator de Diferenciação e Crescimento); (4) Subfamília TGF-β/Nodal e família de fatores neurotróficos derivados da glia (GDNF) (Shen, 2007; Shi & Massague, 2003). Apesar de cada ligante induzir uma resposta celular específica, todas as vias

de sinalização ativadas por eles possuem um conjunto de características estruturais e sequenciais em comum (Shen, 2007; Shi & Massague, 2003; Wells, 2000). Em geral, a sinalização é iniciada quando citocinas extracelulares se ligam aos receptores transmembranais Serina/treonina quinase do tipo I (ALK4; ActrRIB) e do tipo II (ActRIIA), induzindo a oligomerização desses (Shen, 2007; Shi & Massague, 2003; Schier, 2003; Wells, 2000). Quando ocorre a interação dos receptores ALK4-ActrIIA, esses se tornam ativos e fosforilam a porção carboxi-terminal (c-terminal) das moléculas mediadoras citoplasmáticas conhecidas como Smads (Shen, 2007; Shi & Massague, 2003; Schier, 2003; Wells, 2000). Na via de sinalização desencadeada pelos ligantes TGF-β/Activinas/Nodal, as Smad2 e Smad3 são fosforiladas; já a via desencadeada por BMP/MIS/GDF fosforila as Smad1/5/8 (Schier, 2003; Wells, 2000). Uma vez fosforiladas, as Smads (2, 3 ou 1/5/8) irão interagir com proteínas também fosforiladas, Smad4, presentes no citoplasma, formando um complexo hetero-oligomérico (pSmad/pSmad4) (Shen, 2007; Shi & Massague, 2003; Wells, 2000). O complexo pSmad/pSmad4 é translocado para o núcleo, onde irá ativar fatores de transcrição na região promotora dos genes-alvo (Shen, 2007). Em adição, o complexo interage com coativadores e correpressores transcricionais, tais como p300 e CBP (Proteína ligadora ao CREB), regulando a transcrição de diferentes genes (Figura 4) (Shen, 2007; Shi & Massague, 2003; Wells, 2000).

A via de sinalização TFG-β também induz sinais independentes das proteínas Smads, denominada via não canônica (Zhang, 2009). Geralmente, essa via é ativada diretamente pela ligação das citocinas aos seus receptores transmembranais específicos que reforçam, atenuam ou modulam de outra forma os sinais celulares à jusante (*downstream*) (Zhang, 2009). A via não

canônica inclui ativação das Quinases ativadas por mitógenos (MAPK), Rho-GTPase e Fosfatidilinositol-3-quinase/AKT (PI3K/AKT) (Zhang, 2009).

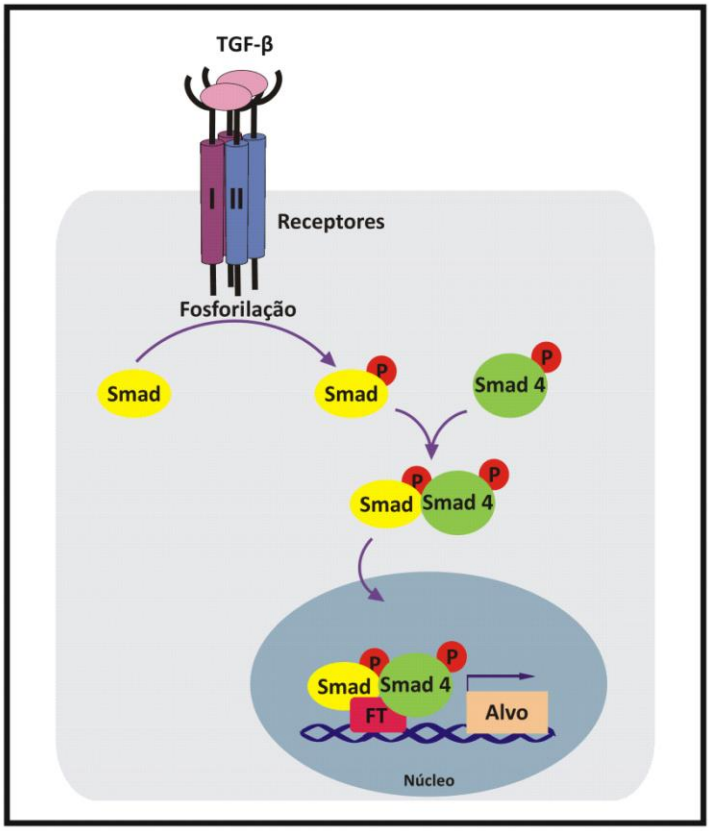

Figura 4. Diagrama simplificado da via de sinalização TGF-β. Sinais TGF-β se ligam aos receptores de membrana do tipo I e II (Alk4/5 e ActrRII) que irão interagir e fosforilar a proteína Smad (Smad 2/3 ou 1/5/8). Uma vez fosforilada (P), a Smad se liga a Smad4, também fosforilada e juntamente são translocadas para o núcleo, onde irão ativar genes-alvo dessa via por meio da interação com fatores de transcrição (FT). Adaptado de Shen, 2007.

Devido a seu papel crítico na determinação dos destinos celulares, a sinalização TFG-β está sujeita a vários níveis de regulação, positiva e negativa, tendo como alvo tanto os receptores quanto os mediadores intracelulares (Stroschein *et al*., 1999). Entre os reguladores negativos da função Smad, podemos destacar as proto-oncoproteínas c-Ski e c-SnoN, que

interagem diretamente com o complexo pSmad/Smad4 impedindo a transcrição dos genes-alvo da via de sinalização TFG-β (Stroschein *et al*., 1999).

Uma vez que as proteínas da superfamília TGF-β estão envolvidas em uma grande variedade de processos fisiológicos — secreção hormonal, resposta imunitária, hematopoiese, angiogênese, morfogênese e regeneração de tecidos — pode-se concluir que as proteínas TFG-β são as mais pleiotrópicas dentre os morfógenos existentes (Wu & Hill, 2009; Tian & Meng, 2006; Schier, 2003; Huo *et al*., 2002; Wu *et al*., 2002; Imai *et al*., 2001; Li *et al*., 1998). Ademais, trabalhos associam os sinais TFG-β a processos de inibição de tumores, manutenção da estabilidade genômica, indução da senescência, supressão da atividade da enzima telomerase, prevenção de angiogênese inapropriada e regulação da síndrome causada pelo Vírus da Imunodeficiência Humana (HIV) (Huo *et al*., 2002; Wu *et al*., 2002; Imai *et al*., 2001; Li *et al*., 1998).

2.4. Família gênica Dapper

2.4.1 Descoberta da família gênica Dapper (Dpr)

Em 2002, o grupo de pesquisa do Dr. Moon da Universidade da Califórnia (UCFS), realizando ensaios de duplo-híbrido em levedura que buscavam identificar novos parceiros moleculares da proteína Dishevelled (Dsh) no organismo peixe-zebra (*Danio rerio*), descobriu o primeiro membro da família gênica *Dpr*, denominado *Dpr1* (Cheyette *et al.,* 2002). Em paralelo, na Universidade de Harvard, o grupo do Dr. Sokol descrevia a proteína Frodo (Frd), altamente relacionada à Dpr1, também isolada por sua habilidade em interagir com Dsh em embriões de *Xenopus* (*Xenopus laevis*) (Gloy *et al*., 2002). Após análises filogenéticas, concluiu-se que no

genoma do anfíbio as duas proteínas estavam presentes, tanto *Dpr1* quanto *Frd*, geradas provavelmente por um processo recente de duplicação gênica no genoma desse organismo (Brott & Sokol, 2005a). A descoberta do segundo membro da família *Dpr*, *Dpr2* ocorreu inicialmente pela busca por sequências relacionadas às proteínas Frd e Dpr1 de *Xenopus* em banco de dados (Zhang *et al.,* 2004). Ainda no mesmo ano, Dr. Waxman e colaboradores isolaram a proteína Dpr2 de peixe-zebra e descreveram seu padrão de expressão (Gillhouse *et al.,* 2004; Waxman *et al.,* 2004; Zhang *et al.,* 2004). Por fim, em 2006, o terceiro membro da família *Dpr,* denominado *Dapper3* (*Dpr3*), foi identificado no genoma de camundongo (*Mus musculus*) por Fisher e colaboradores (Fisher *et al*, 2006).

Hoje em dia, sabemos que os Dpr*,* também conhecidos como Dact, Frodo ou ThyEx3 (Brott e Sokol, 2005a) fazem parte de uma família gênica constituída por três genes (*Dpr1*, *Dpr2* e *Dpr3*) em mamíferos, dois genes (*Dpr1* e *Dpr2)* em galinha e peixe-zebra e por apenas um gene *(Dpr1/Frodo)* em *Xenopus* (Waxman *et al.*, 2005; Waxman *et al.*, 2004). Até o momento, nenhum órtologo do gene *Dpr* foi descrito no genoma de invertebrados.

2.4.2 Estrutura gênica e proteica da família Dpr

O gene *Dpr1* de humanos está localizado no cromossomo 14, 14q22.3, (posição nucleotídica 59100685-59115039, orientação direta) e é composto por quatro exons que codificam um RNA mensageiro (RNAm) (NM_001079520) de 3766 pb e uma proteína (NP_001072988) de 799 aa (Katoh & Katoh, 2003). O gene *Dpr2* de humano localiza-se no cromossomo 6, 6q27, (posição nucleotídica, 168693512-168720434, orientação indireta) e também apresenta quatro exons que codificam um RNAm (NM_214462) de 2942 pb e uma

proteína (NP_999627.2) de 744 aa (Katoh & Katoh, 2003). Dpr3 é encontrado no cromossomo 19, 19q13.32, (posição nucleotídica 47150869-47164395, orientação reversa). Assim como *Dpr1* e *Dpr2*, *Dpr3* também possui quatro exons que codificam um RNAm (NM_145056) de 2834 pb e proteína (NP_659493.2) de 629 aa (Fisher *et al*., 2006).

As proteínas codificadas pelos diferentes genes da família *Dpr* apresentam, próximo à região N-terminal, o domínio de interação do tipo Zíper de Leucina (ZL), cujas sequências adjacentes foram sugeridas como sendo fracamente homólogas aos domínios presentes nas distrofinas (Gloy *et al*., 2002; Gillhouse *et al.*, 2004; Brott & Sokol, 2005a). A extremidade final da região C-terminal das proteínas Dprs possui o domínio de ligação PDZ-B *(Post synaptic density-95/Discs large/Zonula occludens-1)* o qual é responsável pela ligação das Dprs à molécula Dsh, proteína chave na via de sinalização Wnt/βcat e Wnt-PCP (Fisher *et al.*, 2006; Cheyette *et al.*, 2002). Ademais, o alinhamento entre as sequências peptídicas de Dpr1, Dpr2 e Dpr3 revelou a presença de regiões conservadas, dentre as quais podemos destacar os já mencionados domínios ZL e PDZ-B e uma região rica em serinas (Figura 5) (Fisher *et al.,* 2006; Waxman *et al.*, 2004).

Quando comparados os três parálogos de *Dpr* em camundongo, nota-se que Dpr1 é aproximadamente 26% semelhante a Dpr2 e 27% semelhante a Dpr3 e este 27% semelhante a Dpr2 (Fisher *et al.,* 2006; Waxman *et al*., 2004). Curiosamente, Dpr1 e Dpr2 são mais similares na região do domínio ZL, enquanto Dpr1 e Dpr3 são mais semelhantes no domínio de ligação PDZ-B (Fisher *et al.,* 2006).

Estudos filogenéticos envolvendo as proteínas Dpr1 evidenciam a elevada conservação de sequência, apresentada por essas moléculas, ao longo da evolução — 47% de identidade de sequência entre homem e anfíbio (Gillhouse *et al.,* 2004). As proteínas Dpr2 mostram um menor nível de conservação entre os organismos — 25% de identidade de sequência entre homem e anfíbio (Gillhouse *et al.,* 2004). As proteínas Dpr3 são altamente conservadas, apresentando uma identidade de sequência de até 85%. Contudo, devemos ressaltar que essa alta identidade de sequência se deve ao fato de que só existem ortólogos para Dpr3 nos mamíferos, ou seja, organismos altamente relacionados e com pouca divergência genética (Fisher *et al.,* 2006).

2.4.3 Família Dpr e seus parceiros moleculares

Desde a sua descoberta, as proteínas *Dpr* têm sido associadas a uma lista crescente de parceiros moleculares envolvidos em importantes vias de sinalização, tais como Wnt/β-cat, Wnt/PCP e TGF-β (Kivimäe *et al*., 2011; Brott & Sokol, 2005a; Hikasa & Sokol, 2004; Waxman *et al*., 2004; Zhang *et al*., 2004; Cheyette *et al*., 2002; Gloy *et al*., 2002). Aos membros da família Dpr foram atribuídas as características de proteínas adaptadoras e moduladoras, uma vez que essas moléculas são capazes de interagir com diferentes parceiros moleculares regulando sua atividade e, por este motivo, desempenhando múltiplas funções ao longo do desenvolvimento embrionário e na homeostase de tecidos adultos (Brott & Sokol, 2005a). Essas interações são mediadas por domínios estruturais conservados entre os parálogos Dprs, dentre os quais apenas os domínios ZL e o motivo de ligação ao domínio PDZ eram conhecidos previamente (Figura 5) (Waxman *et al*, 2004; Zhang *et al*., 2004).

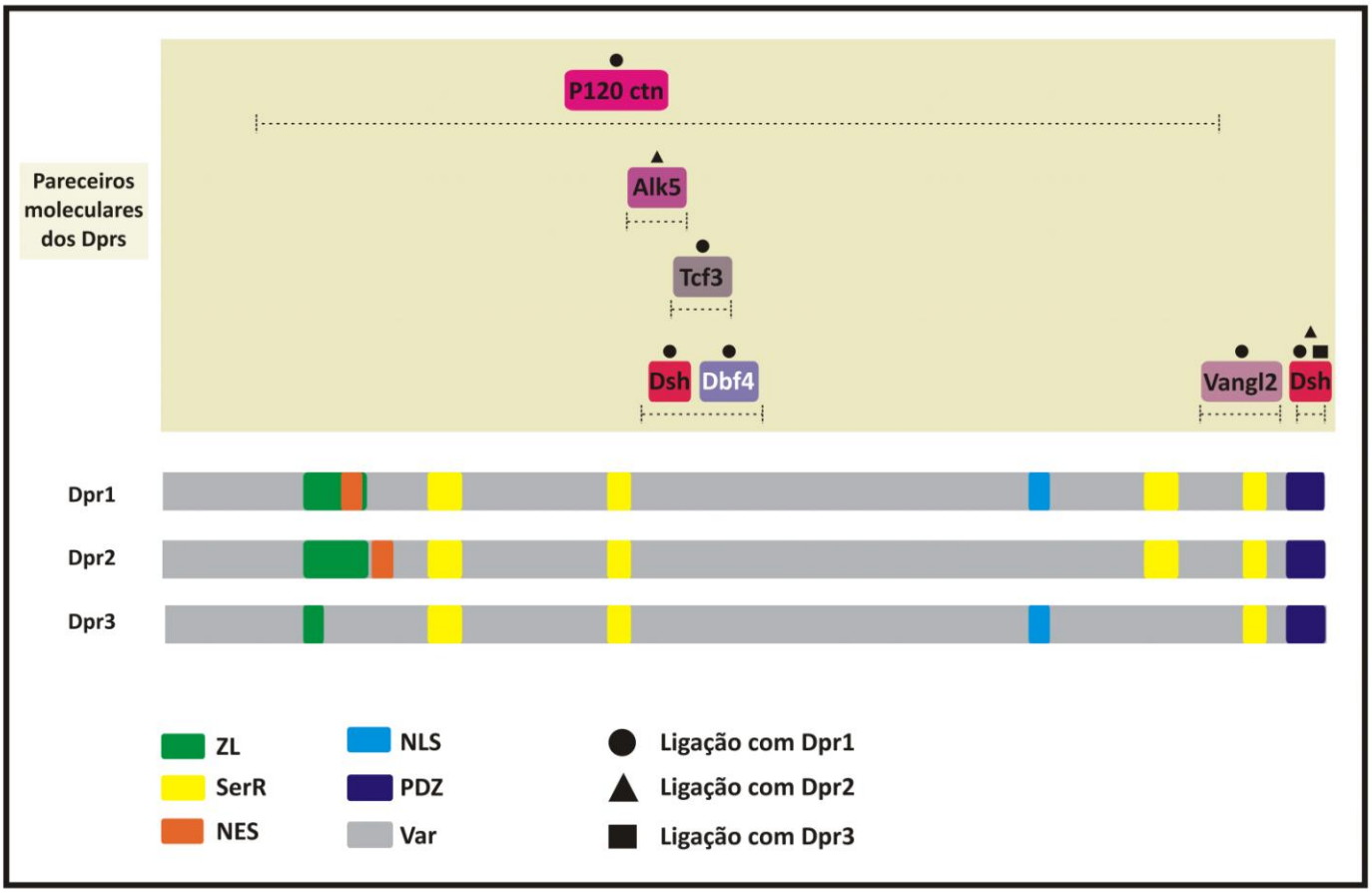

Figura 5. Diagrama ilustrando a característica modular das proteínas Dpr, juntamente com seus parceiros moleculares. A família das proteínas Dpr apresentam regiões conservadas filogeneticamente que provavelmente são importantes na interação de Dpr com seus diferentes parceiros moleculares. ZL (Zíper de Leucina); SerR (região rica em serinas); NES (Sinal de Exportação Nuclear); NLS (Sinal de Localização Nuclear); PDZ (domínio de ligação PDZ); P120 ctn (p120 catenina); Tcf3 (Fator de transcrição 3); Dsh (*Dishevelled*); Dbf4 (proteína do ciclo celular); Vangl2 (*Van Gogh like 2*); Var, regiões não conservadas entre os três membros da família Dpr. Círculo, triângulo e quadrado petros indicam interação com a moléluca Dpr1, Dpr2 e Dpr3, respectivamente.

A proteína Dsh, membro chave da via de sinalização Wnt canônica e PCP, foi o primeiro parceiro molecular das proteínas Dpr a ser identificado (Cheyette *et al*., 2002; Gloy *et al*., 2002). Dpr1, utilizando seu domínio de ligação PDZ, interage com a molécula Dsh − essa ligação foi demonstrada em ensaios de co-preciptação de Dsh com diferentes construções delecionais de

Dpr1, as quais continham diferentes domínios conservados dessa proteína (Cheyette *et al*., 2002; Gloy *et al*., 2002).

Com o objetivo de compreender os detalhes da interação Dpr1-Dsh, ensaios de ganho e perda de função foram realizados utilizando embriões de peixe-zebra e *Xenopus* (Cheyette *et al*., 2002; Gloy *et al*., 2002) Os resultados obtidos nesses ensaios revelaram que a proteína Dpr1 liga-se fisicamente à Dsh, no citoplasma, e induz a degradação dessa molécula através do mecanismo lisossômico e proteossômico, modulando negativamente a via de sinalização Wnt (Figura 6A) (Cheyette *et al*., 2002). Estudos subsequentes em hepatocarcinoma e em linhagens celulares de adipócitos humanos corroboraram a hipótese de que *Dpr1* atua como antagonista da via de sinalização Wnt, enquanto que outros estudos envolvendo *Xenopus* e peixe-zebra sustentavam a ideia contrária (Lagathu *et al*., 2009; Yau *et al*., 2004; Waxman *et al.*, 2005; Waxman *et al*., 2004; Gloy *et al*., 2002). Uma possível explicação para a contradição funcional mencionada anteriormente é que a modulação dos sinais Wnt através de Dpr1 possa estar relacionada com o estado de fosforilação da mesma (Chen *et al*., 2001; Teran *et al*., 2009).

Em adição, Hisaka e Sokol descobriram que, em embriões de *Xenopus,* Dpr1 (Frd1) é capaz de modular a via de sinalização Wnt/β-cat não apenas por intermédio da proteína Dsh, mas também por meio do complexo Fator Potencializador de Ligação Linfóide/Fator de Transcrição 3 (LEF/TCF-3) (Hisaka & Sokol, 2004). A interação Dpr1- LEF/TCF-3 se dá através da região N-terminal conservada, entre os aa 186 e 337, da proteína Dpr1 (Hisaka & Sokol, 2004). Posteriormente, Park e colaboradores também demonstraram que em *Xenopus,* Dpr1 ativava a via de sinalização Wnt dependente de p120-catenina (p120ctn) — mediadora das funções das

caderinhas e Rho GTPases — que atua paralelamente, mas independente, à via de sinalização Wnt/β-cat (Park *et al*., 2006).

Dois anos mais tarde, Gao e colaboradores descobriram que a proteína Dpr1 não era uma proteína exclusivamente citoplasmática. Eles a observaram no núcleo de células da linhagem HeLa quando tratadas com Leptomicina B (LMB), inibidor da exportação nuclear (Gao *et al*., 2008) No núcleo, Dpr1 interage e rompe com complexo formado pela β-actina e pelo Fator Potencializador de ligação linfoide (β-act/LEF1) atuando como modulador negativo dessa via (Gao *et al*., 2008).

Além de interagir com diversos componentes da via de sinalização Wnt canônica, Dpr1 também foi descrito como modulador da via Wnt não canônica PCP (Wen *et al*., 2010; Suriben *et al*., 2009). Dois experimentos independentes envolvendo inibição do gene *Dpr1* em camundongos revelaram que a eliminação desse gene interfere na via Wnt/PCP devido à capacidade de Dpr1 ligar-se e regular as proteínas Vangl2 e Dsh (Figura 6B) (Wen *et al*., 2010; Suriben *et al*., 2009). Estudos adicionais demonstraram que Dpr1 interage, em regiões ainda não bem definidas, com outras moléculas — pequenas GTPases, incluindo Rho e Rac; glicogênio-sintetase-quinase-3β (GSK3β); proteína 14-3-3β; histona deacetilase 1 (HDAC1); e proteína reguladora do ciclo celular Dbf-4 (Kivimäe *et al*., 2011; Chen *et al*., 2011; Okerlund *et al*., 2010; Wen *et al*., 2010; Gao *et al*., 2008; Park *et al*., 2006; Brott & Sokoll, 2005b; Cheyette *et al*., 2002)

Ensaios de superexpressão em embriões de peixe-zebra apontaram que os receptores da sinalização Nodal (Alk4/5) se ligam com a proteína Dpr2 na porção entre os aa 1 e 337 (Zhang *et al.,* 2004). Dpr2, ao interagir com os receptores Alk4/5, promove a marcação dos mesmos para serem degradados via lisossomal, modulando negativamente os sinais TGF-β (Figura 6C) (Zhang

et al., 2004). Esses dados foram reforçados por subsequentes estudos, nos quais o gene *Dpr2* foi inibido em camundongos e em linhagens celulares de mamíferos (Lee *et al*., 2010; Meng *et al.*, 2008; Su *et al*., 2007). Recentemente, Li e colaboradores demonstraram que Dpr2 pode atuar como inibidor da via de sinalização Wnt/β-cat através da interação com a o fator de transcrição PITX2 em células epiteliais de dentes de camundongo em desenvolvimento (Li *et al*., 2013).

No que concerne à proteína Dpr3, pouco se sabe sobre seus parceiros moleculares, contudo, dois estudos, um envolvendo câncer de cólon e outro ensaios de transfecção do vetor *TOPflash* em céluas *HEK293T*, revelaram que Dpr3 é capaz de interagir com a proteína Dsh (Zang *et al*., 2013; Kivimäe *et al*., 2011; Jiang *et al*., 2008). No contexto de câncer de cólon, Dpr3 e Dsh, juntas, regulam a estabilidade da proteína β-cat no citoplasma através da molécula GSK3 (Kivimäe *et al*., 2011; Jiang *et al*., 2008). Nos ensaios de *TOPflash*, Dpr3 se mostrou capaz de interagir fisicamente com Dsh, promovendo a degradação da mesma (Zang *et al*., 2013).

Mais recentemente, Kivimäe e colaboradores demonstraram que todos os membros da família Dpr são capazes de formar homodímeros ou heterodímeros entre si, utilizando o domínio ZL localizado na região N-terminal da molécula, que aparentemente, é necessário e suficiente para que essas interações sejam estabelecidas (Kivimäe *et al*., 2011).

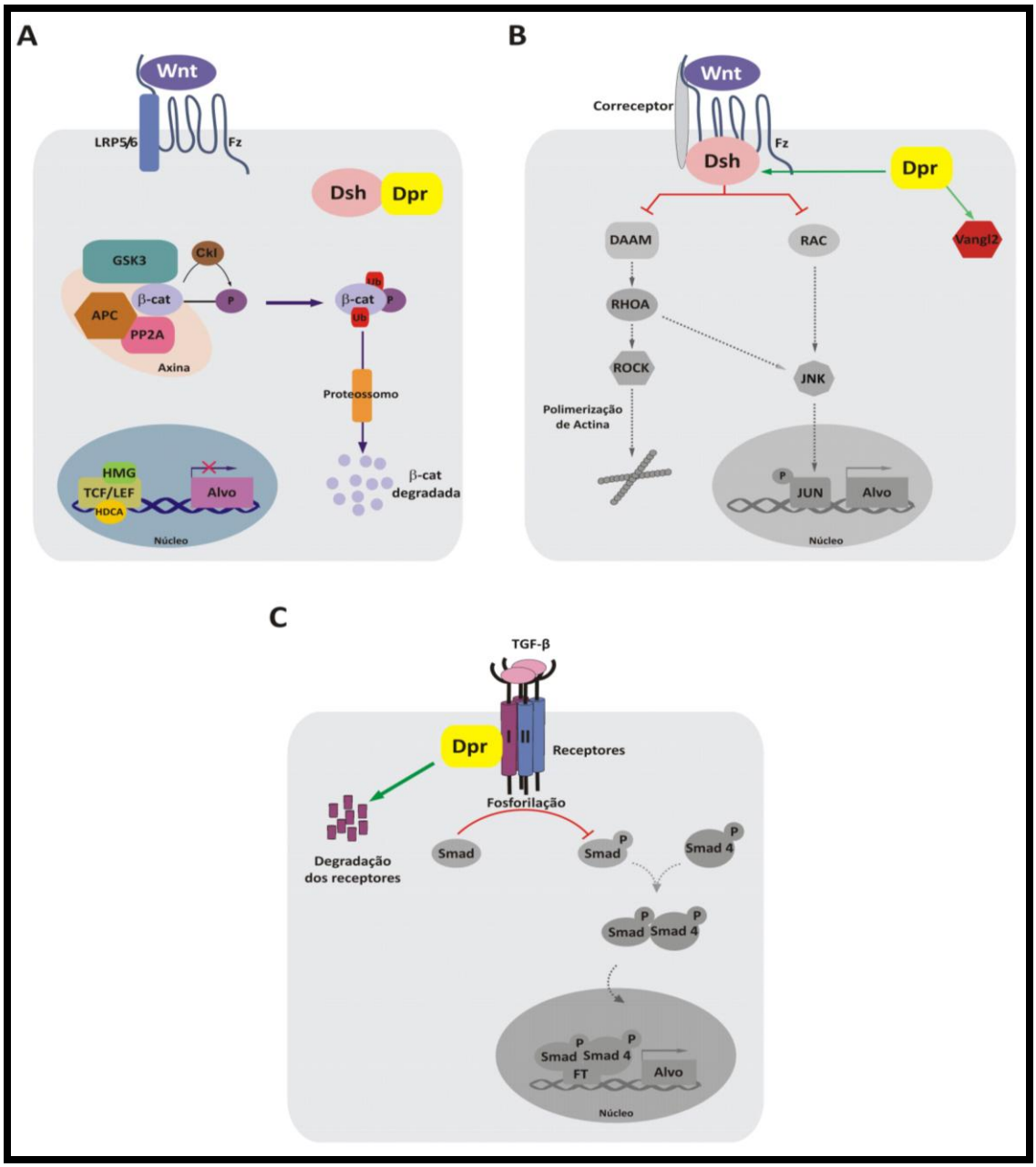

Figura 6. Moléculas Dprs são moduladoras de diferentes vias de sinalização durante o desenvolvimento embrionário. Em (A) a presença da proteína Dpr bloqueia a via de sinalização Wnt canônica. Dpr interage fisicamente com a molécula Dsh (*Dishevelled*) e a encaminha para degradação. Dessa forma, o complexo protéico formado pelas proteínas APC (proteína repressora de câncer), fosfate PP2A, glicogênio-sintase-quinase-3β (GSK3) e caseína-quinase Iα (CKI) captura a molécula β-catenina (β-cat) e a leva para a via de degradação impedindo assim a expressão dos genes-alvos da via Wnt; Em (B) a molécula Dpr atua como modulador negativo da via de sinalização Wnt/PCP. Nesse contexto Dpr interage fisicamente com a molécula Dsh e Vangl2 (*Van Gogh like 2*) bloqueando essa via. Em (C) Dpr bloqueia a sinalização TGF-β através da degradação via lisossomo dos receptores do tipo I e II.

2.4.4 Padrão de expressão dos genes Dpr durante o desenvolvimento embrionário e pós-natal

Os genes da família *Dpr* apresentam um padrão de expressão dinâmico ao longo do desenvolvimento embrionário. Por sua vez, cada membro da família apresenta um padrão de expressão distinto em relação ao local e estádio de desenvolvimento, sugerindo fortemente funções diferentes para cada parálogo (Fisher *et al*., 2006).

O padrão de expressão dos diferentes *Dprs* durante o desenvolvimento embrionário foi caracterizado em vários organismos. Esses padrões serão descritos abaixo, bem como o padrão obtido durante o período pós-natal.

Danio rerio

Em peixe-zebra, apenas dois parálogos dos genes *Dpr* foram identificados até o momento, *Dpr1* e *Dpr2* (Gillhouse *et al.,* 2004; Waxman *et al.,* 2004; Zhang *et al*., 2004). A expressão de ambos é bastante dinâmica e é encontrada já nos estádios iniciais do desenvolvimento deste organismo (Gillhouse *et al.,* 2004; Waxman *et al.,* 2004; Zhang *et al*., 2004).

Durante a fase de gástrula inicial (estádio de escudo), a expressão do gene *Dpr1* pode ser observada ao longo de todo o blastoderma, nas regiões que formarão o mesoderme e a endoderme, incluindo a região do organizador (Waxman *et al.,* 2004). Na gástrula média (80% de epibolia), os transcritos *Dpr1* são encontrados no mesoderma axial derivado do organizador e na região posterior da placa neural. Ainda durante a gástrula média, nenhuma expressão de *Dpr1* foi detectada na região ventral, na ectoderme não-neural, bem como na região anterior da neuro-ectoderme (Gillhouse *et al.,* 2004). Contudo, ao final da gastrulação (estádio de botão

caudal), a expressão de *Dpr1* é vista pela primeira vez na região anterior da placa neural (Gillhouse *et al.,* 2004). Durante o início da somitogênese (estádio de cinco somitos), a expressão de *Dpr1* é fortemente detectada na metade anterior do embrião e dois domínios adicionais de expressão são visíveis lateralmente na região, supostamente, responsável pela formação da região posterior do diencéfalo (mesoderma cefálico) (Gillhouse *et al.,* 2004). Mais adiante (estádio de onze somitos), a expressão na futura região do mesoderme é interrompida, no entanto uma forte expressão de *Dpr1* é encontrada na retina (Gillhouse *et al.,* 2004). No tronco dos embriões, *Dpr1* é fortemente expresso nos somitos e no mesoderme pré-somitico, bem como no mesoderme da placa lateral adjacente aos ductos pronéfricos (Gillhouse *et al.,* 2004). Nenhum transcrito de *Dpr1* é detectado no mesoderme axial nem na notocorda. Ao final da somitogênese, a expressão de *Dpr1* se torna intensa em diferentes domínios cerebrais, tais como telencéfalo, hipotálamo e retina. Mais adiante na embriogênese, a expressão de *Dpr1* é restrita ao botão caudal do embrião (Gillhouse *et al.,* 2004).

Ao contrário de *Dpr1*, o gene *Dpr2* possui uma expressão fraca e não tão bem definida durante o desenvolvimento do peixe-zebra. Os primeiros transcritos de *Dpr2* são encontrados na região dorsal do blastoderma (estádio de esfera), aproximadamente, quatro horas pós-fertilização (hfp) (Waxman *et al*., 2004). Durante a gástrula inicial (estádio de escudo), *Dpr2* é expresso ao longo de toda a região marginal do blastoderma dorsal, porém nenhum transcrito é detectado na região do organizador (Waxman *et al*., 2004). Durante a gastrulação, a expressão de *Dpr2* é restrita a todo o anel germinativo, onde as células precursoras do mesoderme estão localizadas (Waxman *et al*., 2004). Nesta fase, o maior nível de expressão observada é na região

do escudo embrionário. Quando o processo de segmentação se inicia, *Dpr2* é expresso no tubo neural, no mesoderme da placa lateral e no botão caudal. Durante a fase de somitogênese (estádio de três somitos), a expressão de *Dpr2* pode ser observada no limite entre o cérebro posterior e a medula espinhal anterior, adjacente ao rombômero 5 (Waxman *et al*., 2004). Na fase de doze somitos, transcritos de *Dpr2* estão mais concentrados nos somitos anteriores (mais maduros) e menos concentrado nos somitos posteriores (recém-formados) (Waxman *et al*., 2004). Com 24 hpf, transcritos de *Dpr2* estão restritos às regiões dos progenitores sanguíneos e do botão caudal (Gillhouse *et al.,* 2004).

Xenopus laevis

No anfíbio, dois parálogos altamente relacionados, *Dpr1* e *Frodo* (*Functional regulator of disheveled in ontogenesis*), foram identificados como membros da família gênica *Dpr* (Teran *et al*., 2009; Gao *et al*., 2008; Brott &Sokoll, 2005a; Gloy *et al*., 2002). Estudos mostram que *Frodo (Frd)* é, provavelmente, decorrente de uma duplicação gênica recente que ocorreu neste organismo (Teran *et al*., 2009; Brott &Sokoll, 2005a). As proteínas Dpr1 e Frd possuem 90% de identidade de sequência (Teran *et al*., 2009; Brott &Sokoll, 2005a).

Durante a fase de blástula tardia e gástrula inicial, transcritos de *Frd* são encontrados em todo o polo animal, incluindo a ectoderme neural presuntiva, além da região dorsal marginal do embrião (Hunter *et al*., 2006; Gloy *et al.*, 2002). Ainda nesta fase, pode-se observar fracamente tanto a expressão de *Frd,* quanto de *Dpr1,* no lábio dorsal do blastóporo, correspondente à região do mesoderme dorsal involutivo, local que coincide com o início dos movimentos morfogenéticos e marca o Organizador de *Spemann* (Hunter *et al*., 2006; Gloy *et al*., 2002).No

estádio 10,5, *Frd* é fortemente expresso no mesoderme posterior, apresentando baixos níveis de expressão na neuroecotderme e mesoderme ventral (Hunter *et al*., 2006). No início da fase de neururalação, o domínio de expressão de *Frd* e *Dpr1* na neuroectoderme se torna gradualmente restrita às regiões que originarão o diencéfalo posterior e à região da borda e linha média da placa neural (Hunter *et al*., 2006; Gilhouse *et al,.* 2002; Cheyette *et al.,* 2002; Gloy *et al*., 2002). Em nêurula tardia e estádio de botão caudal, transcritos *Frd* são fortemente expressos nas cristas neurais e região dos olhos (Hunter *et al*., 2006). Ainda nesta fase, a expressão de *Dpr1* pode ser observada nas dobras neurais dorsais, apresentando um alto nível de expressão nas células da crista neural (pré-migratórias e migratórias) e no botão caudal (Cheyette *et al*., 2002). Durante estádios tardios do desenvolvimento, *Frd* é encontrado nos placóides ectodérmicos, vesícula óptica, olhos e arcos branquiais (Hunter *et al*., 2006; Gloy *et al.*, 2002). Ainda nesta fase, o mesoderme pré-somítico, os somitos e a ponta da cauda, também são domínios importantes de expressão do gene *Frd* (Hunter *et al*., 2006). No girino, *Dpr1* é expresso em grande quantidade na região cefálica, incluindo o cérebro, a retina e os elementos cartilaginosos derivados dos arcos branquiais (Cheyette *et al*., 2002).

Gallus gallus

Em galinha, apenas dois genes parálogos para a família *Dpr* foram identificados até o momento, *Dpr1* e *Dpr2*, e ambos apresentam uma expressão dinâmica durante o desenvolvimento deste organismo (Brott & Sokoll, 2005a; Alvares *et al*., 2009). Em alguns tecidos, os genes *Dpr1* e *Dpr2* são coexpressos, em outros aparecem de forma sequencial ao

longo do desenvolvimento e em algumas regiões apresentam padrão de expressão complementar (Alvares *et al*., 2009).

Durante toda a fase de gastrulação (HH4-HH7), a expressão de *Dpr1* é detectada em células que deixam a região do epiblasto e migram para a formação da camada de mesoderme (Alvares *et al*., 2009). Também podemos observar *Dpr1* nas células que compõem o nódulo de *Hensen,* bem como nas células que irão formar o processo cefálico/notocorda (Alvares *et al*., 2009). Na região mais anterior do embrião, transcritos de *Dpr1* são detectados no mesoderme cardíaco (Alvares *et al*., 2009). Em HH8, a expressão de *Dpr1* na linha primitiva é diminuída, contudo um forte sinal é detectado no mesoderme cefálico, pré-somitico e lateral, incluindo as células que futuramente formarão o mesoderme cardíaco (Alvares *et al*., 2009). Mais adiante no desenvolvimento, em HH12, transcritos de *Dpr1* podem ser observados na ectoderme cefálica, mais precisamente no placoíde trigeminal (Alvares *et al*., 2009). Em HH14, a expressão de *Dpr1* no placóide trigeminal se torna mais proeminente na região maxilo-mandibular e na futura região que formará as vesículas ópticas (Alvares *et al*., 2009). Em HH18, *Dpr1* é encontrado nos placóides branquiais, e neurais, bem como no mesoderme esplâncnico que contribuirá para a formação das veias vitelínicas (Alvares *et al*., 2009). A expressão se estende ao longo do tronco, englobando o mesoderme esplânico, bem como no assoalho da aorta dorsal e no dermomiótomo dos somitos em formação (Alvares *et al*., 2009). Em HH20, a expressão de *Dpr1* foi observada nos placóides neurais e no mesênquima periocular. Ainda nesta fase, *Dpr1* apresenta uma expressão proeminente na região do sindétomo dos somitos, bem como nas células que revestem o miótomo, região que dará origem ao tecido muscular e ao tecido

conjuntivo dos tendões nos indivíduos adultos (Alvares *et al*., 2009). Ademais, a expressão de *Dpr1* foi observada em células que se acumulam na interface dermomiótomo/miótomo, ou seja, em células que darão origem a células tronco musculares que serão importantes para a formação tanto da musculatura embrionária como da adulta, bem como as células satélites no indivíduo adulto (Alvares *et al*., 2009). Finalmente, *Dpr1* é expresso na região da somatopleura que originará o mesoderme dos membros em formação (Alvares *et al*., 2009).

Semelhante a *Dpr1*, *Dpr2* também é proeminente durante a fase de gastrulação. Porém, a expressão de *Dpr2* em HH4 é fortemente observada na região anterior da linha primitiva e do nódulo de *Hensen*, abrangendo o epiblasto e o mesoderme emergente (Alvares *et al*., 2009). Durante os estádios HH5-HH6, a expressão de *Dpr2* se apresenta mais posteriormente na região da linha primitiva até desaparecer completamente dessa estrutura à medida que o desenvolvimento avança (Alvares *et al*., 2009). Nesses estádios, *Dpr2* é observado no mesoderme cefálico sobrejacente à placa neural. A expressão na placa neural é fraca na região da linha média, mas forte ao longo das pregas neurais (Alvares *et al*., 2009). Em HH7-HH8, o domínio de expressão mais anterior de *Dpr2* é no mesoderme pré-cordal e na endoderme do intestino anterior (Alvares *et al*., 2009). No mesoderme cefálico a diferença de expressão antero-posterior se torna bastante evidente, uma vez que a região anterior desta estrutura apresenta fraca expressão de *Dpr2* e gradualmente essa expressão se torna mais forte na região posterior desta estrutura. Marcação para *Dpr2* também foi encontrada em somitos em processo de epitelização, bem como naqueles já separados da placa segmentar (Alvares *et al*., 2009). Em HH9-HH10, os somitos passam a expressar *Dpr2*, logo que eles emergem do mesoderme pré-

somítico. No mesoderme cefálico, na endoderme do intestino anterior e na ectoderme da futura região oral também há expressão de *Dpr2*. No tubo neural, a expressão de *Dpr2* inicia-se na placa do teto, porém se torna mais proeminente na placa do assoalho (Alvares *et al*., 2009). Uma forte expressão de *Dpr2* é encontrada nas células da crista neural a partir do momento que elas deixam as pregas neurais. Essa expressão é mantida nas células que migram ventro-lateralmente, principalmente naquelas que circundam os olhos e nas que emergem da região do rombômero IV (Alvares *et al*., 2009). Entre os estádios HH12 e HH14, a expressão de *Dpr2* permanece associada às células de crista neural, ao mesoderme cefálico posterior, aos somitos epiteliais e à região lateral que flanqueia a placa segmentar (Alvares *et al*., 2009). Além disso, altos níveis de *Dpr2* são encontrados na futura região oral, abrangendo tanto a endoderme do intestino posterior, como a ectoderme oral (Alvares *et al*., 2009). Em HH14, a expressão de *Dpr2* surge na superfície ventral do gânglio trigeminal, ainda neste estádio, a parede dorso-medial da vesícula ótica também apresenta transcritos de *Dpr2* (Alvares *et al*., 2009). Em HH17, a expressão de *Dpr2* eleva-se na superfície da ectoderme dos arcos branquiais. Em adição, o mesoderme pré-somitico e o botão caudal passam a expressar *Drp2* (Alvares *et al*., 2009). Em HH20, surgem novos sítios de expressão de *Dpr2* — cristalino, porção dorsal da retina, mesoderme intermediário e região central do dermomiótomo (Alvares *et al*., 2009). Entre os estádios HH20 e HH21, transcritos de *Dpr2* são encontrados no mesênquima periocular e perinasal. Assim como *Dpr1*, *Dpr2* também está presente no mesênquima dos membros em formação, entretanto, diferentemente de *Dpr1*, a expressão de *Dpr2* é proeminente tanto na ectoderme proximal dorsal quanto na região ventral dos membros. Nos somitos, a expressão de *Dpr2* ainda é encontrada na porção central do dermomiótomo, marcando células tronco

musculares, as quais irão formar os músculos fetais e adultos, bem como as células satélites no indivíduo adulto (Alvares *et al*., 2009). Por fim, pode-se observar uma forte expressão de *Dpr2* nos botões pulmonares (Alvares *et al*., 2009).

Mus musculus

Durante o desenvolvimento de embriões de camundongo (*Mus musculus*), os genes que compõem a família *Dpr* possuem distintos padrões de expressão.

Nos primeiros dias de gestação, transcritos *Dpr* são observados apenas em tecidos maternos e extra-embrionários, porém a partir do sétimo dia de desenvolvimento, a expressão dos genes *Dpr* já pode ser observada em estruturas embrionárias (Hunter *et al*., 2005; Fisher *et al*., 2006).

A expressão do gene *Dpr1* é baixa nos primeiros dias do desenvolvimento, mas essa expressão é aumentada entre o dia 9,5 (E9,5) e E10,5 atingindo seu grau máximo de expressão entre E11,5 e E13,5, quando, então, diminui lentamente (Fisher *et al*., 2006). Em E7,5, quando os níveis de expressão para os genes *Dpr* ainda é baixa, pode-se observar transcritos de *Dpr1* no mesoderma e no neuroectoderma. Em E9,0, os níveis de expressão para *Dpr1* são altos no septo transverso, mesênquima cranial, mesoderma paraxial não segmentado (PSM) e nos somitos (Hunter *et al.*, 2005), bem como na aorta dorsal, no saco aórtico e artérias dos arcos branquiais (Fisher *et al*., 2006). *Dpr1* se apresenta formando um gradiente de expressão caudal-rostral, inversamente relacionado com a idade de desenvolvimento dos somitos. Dessa forma, pode-se esperar uma expressão mais elevada de *Dpr1* nos somitos recém-formados (caudal) e baixa expressão naqueles maduros (rostral) (Fisher *et al*., 2005). Durante E10, a expressão de *Dpr1*

permanece elevada na placa mesodérmica segmentar e nos somitos caudais, contudo uma fraca expressão pode ser observada no botão caudal (região do mesoderma ventral). Ainda nesse período, pode-se detectar transcritos de *Dpr1* nos brotos dos membros anteriores e posteriores, formando um gradiente de expressão do mesoderma proximal (baixa expressão) para o apical (alta expressão) (Fisher *et al.*, 2006). A expressão de *Dpr1* continua sendo forte no mesênquima que circunda o intestino anterior, bem como nos brônquios e esclerótomo derivado da região ventral dos somitos. No entanto, uma fraca expressão é detectada no mesênquima dos arcos braquiais. Nesse estádio, *Dpr1* passa a ser expresso nos neurônios pós-mitóticos estando evidente nos locais de diferenciação da medula espinhal. Após E10, a expressão de *Dpr1* se torna concentrada ao sistema nervoso central (SNC), no qual transcritos de *Dpr1* são abundantemente encontrados no cérebro e na medula espinhal (Fisher *et al*., 2006).

Diferentemente de *Dpr1*, que possui oscilações no nível de sua expressão ao longo do desenvolvimento, o gene *Dpr2* apresenta uma baixa expressão ao longo de toda a embriogênese (Fisher *et al.,* 2006). No estádio E9,0 transcritos de *Dpr2* são observados em baixos níveis de expressão, embora sejam amplamente distribuídos ao longo de todo embrião. Pode-se observar transcritos de *Dpr2* na retina, na vesícula óptica, no mesentério ventral do intestino anterior, nas veias umbilicais, no tubo neural dorsal, e formando um gradiente de expressão, similar a *Dpr1,* nos somitos (Fisher *et al*., 2006). Diferentemente de *Dpr1*, *Dpr2* não está presente no PMS neste estádio e sua expressão nos somitos assume uma posição dorsolateral enquanto que a expressão de *Dpr1* é ventromedial. Além disso, *Dpr2* se torna progressivamente restrito à região rostral do somito maduro, enquanto *Dpr1* possui expressão

caudal, assumindo os dois parálogos, dessa forma, uma distribuição complementar nos somitos maduros (Fisher *et al*., 2006). Em E10,5 a expressão de *Dpr2* é fracamente detectável e se torna mais restrita quando comparada ao estádio anterior, sendo a vesícula óptica e os somitos caudais os principais locais de expressão (Fisher *et al*., 2006). Após E10, podemos encontrar transcritos de *Dpr2* no SNC, porém a expressão mais significativa destas moléculas é observada em tecidos não neurais, como no desenvolvimento dos rins, glândulas salivares e timo (Fisher *et al*., 2006).

O último parálogo identificado em camundondo, *Dpr3,* possui níveis baixos de expressão durante os primeiros dias do desenvolvimento, atingindo o pico por volta do estádio E10,5, quando, então, sua expressão enfraquece novamente (Fisher *et al*., 2006). Em E9,0, transcritos de *Dpr3* são encontrados no mesênquima craniofacial e nos arcos branquiais, no septo transverso, no saco e arcos aórticos. Diferentemente de *Dpr1*, *Dpr3* não é expresso na PSM nem apresenta gradiente de expressão caudal-rostral ao longo dos somitos em desenvolvimento. Ao contrário, *Dpr3* é expresso no domínio ventral dos somitos maduros, localizado centralmente ao longo do eixo rostral-caudal. No E10,5 a expressão de *Dpr3* é bastante proeminente por todo o mesênquima dos arcos branquiais, no mesênquima dos brotos de membros e nos somitos em amadurecimento. A forte expressão de *Dpr3* nos arcos branquiais, no mesênquima facial e na região central dos somitos, sugere a importância deste gene na migração e diferenciação de células da crista neural e das células mesodérmicas derivadas do mesênquima. Após E10, a expressão de *Dpr3*, assim como a de *Dpr1*, se torna concentrada na região de formação do SNC (Fisher *et al.,* 2006).

Desenvolvimento pós-natal

Poucos são os trabalhos que descrevem o padrão de expressão dos genes da família *Dpr* durante o período pós-natal. No entanto, esses poucos trabalhos demonstraram que transcritos *Dprs* são detectados em diferentes tecidos/estruturas que compõem os mais variados sistemas dos indivíduos adultos (Kettunen *et al*, 2010; Suriben *et al*., 2009; Meng *et a.l*, 2008; Fisher *et al*, 2006).

Em 2006, Fisher e colaboradores descreveram brevemente o padrão de expressão dos três membros da família *Dpr* no sistema nervoso central (SNC) de camundongos adultos. Em nítido contraste com o período embrionário, *Dpr1* é o gene mais fracamente expresso no cérebro adulto (Fisher *et al.*, 2006). No entanto, RNAm de *Dpr1* foram encontrados em diversas populações de neurônios de diferentes subtipos (Fisher *et al.*, 2006). No cerebelo, *Dpr1* é expresso na camada celular granular, porém não está presente nas células de *Purkinje*. Este padrão de expressão é complementar ao padrão observado para os genes *Dpr2* e *Dpr3*, os quais são fortemente detectados nessas células (Fisher *et al.*, 2006). Além disso, todos os três membros *Dprs* são coexpressos no hipocampo (Fisher *et al.*, 2006). Na região dorsal do prosencéfalo, *Dpr1* e *Dpr3* estão presentes em todas as camadas do córtex cerebral, enquanto *Dpr2* é preferencialmente expresso nas camadas mais superficiais (Fisher *et al.*, 2006). Assim como no SNC, transcritos de *Dpr1* também foram encontrados no pulmão e no útero de camundongos adultos. Da mesma forma que *Dpr1*, *Dpr2* foi observado no útero, sendo também detectado nos rins, intestino, timo e testículos (Fisher *et al.*, 2006). Dentre os membros da

família *Dpr*, *Dpr3* é o que apresenta a expressão mais restrita em camundongos adultos, sendo detectado apenas no SNC e no útero (Fisher *et al.*, 2006).

Outra comparação do padrão de expressão dos três membros da família *Dpr* foi realizada durante o desenvolvimento dos dentes em camundongo (Li *et al*., 2013; Kettunen *et al*., 2010). Nesses estudos, os pesquisadores demonstraram que *Dpr1*, *Dpr2* e *Dpr3* apresentam padrão de expressão que podem ser distintos, complementares e algumas vezes similares nas estruturas que compõem o dente nos indivíduos adultos (Kettunen *et al*., 2010). *Dpr1* é expresso no folículo dental, na região cervical medial da papila dental e no epitélio dental. Por sua vez, *Dpr2* foi detectado apenas no epitélio dental e oral (Li *et al*., 2013; Kettunen *et al*., 2010). Contudo, RNAm de *Dpr3* foram encontrados em diversas estruturas, tais como polpa dental, epitélio dental, tecido muscular e especificamente na polpa dos dentes incisivos (Kettunen *et al*., 2010).

Por fim, Meng e colaboradores demonstraram que em ratos adultos, *Dpr2* é altamente expresso nos queratinócitos epidérmicos e folículos do pêlo (Meng *et al*., 2008).

2.4.5 Funções dos genes da família Dpr

Desde a descoberta dos genes *Dprs,* diferentes grupos de pesquisas utilizam diversas estratégias a fim de caracterizar funcionalmente essas moléculas. Ao longo desses anos, ensaios de ganho e perda de função (em *Xenopus* e Peixe-zebra) e camundongos mutantes foram utilizados com a finalidade de elucidar os possíveis papeis desempenhados por esses genes.

Em embriões de *Xenopus*, foi demonstrado através de ensaios de perda de função que *Dpr1(Frd1)* é necessário para a formação da notocorda, de estruturas cefálicas e oculares, bem como para o desenvolvimento do tubo neural (Gloy *et al*., 2002). Acredita-se que esses eventos

se devem à capacidade de Dpr1 recrutar e/ou estabilizar as moléculas GSK3 e Axina, através da interação com Dsh, durante a formação do complexo citoplasmático de degradação da β-cat (Cheyette *et al*., 2002). Em embriões de peixa-zebra, à molécula Dpr2 foi atribuída à capacidade de suprimir a indução mesodérmica através da via de sinalização Nodal, por promover a degradação dos receptores TGF-β, ALK4 e ALK5, utilizando o sistema lisossomal (Zhang *et al*., 2004b). Contudo, Waxman e colaboradores ao desenvolverem um *knock-down* de *Dpr2*, utilizando morfolinos em peixe-zebra, demonstraram que *Dpr2* está envolvido com os movimentos de extensão convergentes, modulando sinais da via de sinalização Wnt/PCP nesse organismo (Waxman *et al*., 2004).

Já experimentos com camundongos homozigotos negativos para o gene *Dpr1* (*Dpr1*-/-) morrem durantes os primeiros dias de vida (Wen *et al*., 2008; Suriben *et al*., 2009). Tais neonatos apresentam um grande número de malformações correspondentes à região posterior do corpo (Wen *et al*., 2010; Suriben *et al*., 2009). Análises estruturais desses animais revelaram uma série de malformações, dentre as quais podemos destacar: ausência do canal urinário, da bexiga, do ânus, e da genitália externa; presença de cólon com fundo cego; fusão dos ureteres com os ductos reprodutivos; e rins hidronefróticos (rins obstruídos) (Suriben *et al*., 2009). Ademais às malformações encontradas no trato gastrointestinal e genitourinário, a maioria dos animais *Dpr1*-/- possuía segmentação corporal truncada, podendo apresentar cauda encurtada, ou alterações na região sacral e lombar, sendo frequentemente acompanhadas de sirenomielia (Suriben *et al*., 2009). Em 2010, Meng e colaboradores descreveram um fenótipo de camundongos mutantes para *Dpr1* bastante similar ao encontrado por Suriben e colaboradores

no ano anterior (Meng *et al*., 2010; Wen *et al*, 2010). Porém, o novo estudo relatou que uma pequena parte dos neonatos (17%) também apresentavam malformações nos membros posteriores (Wen *et al*, 2010). Os autores acreditam que o espectro de malformações encontradas nos camundongos *Dpr1*-/- assemelha-se aos encontrados na síndrome de regressão caudal de humanos, uma vez que ambos os fenótipos apresentam defeitos congênitos dos sistemas urinário e genital, da espinha lombossacral e das extremidades inferiores do corpo do indivíduo (Wen *et al*, 2010). Diante das malformações descritas pelos dois grupos, sugeriu-se que distúrbios nos movimentos morfogenéticos e falha na migração celular da linha primitiva dos embriões, através de alterações na via Wnt/PCP, são os responsáveis pelo fenótipo encontrado (Suriben *et al*., 2009; Wen *et al*, 2010).

Ao contrário da alta mortalidade apresentada pelos camundongos neonatos *Dpr1*-/-, ratos homozigotos negativos para *Dpr2* (*Dpr2*-/-) apresentam desenvolvimento embrionário e pós-natal normais, alcançando a fase adulta sem desenvolver nenhum distúrbio morfológico ou comportamental evidente (Meng *et al*., 2010). A única alteração observada foi que os animais *Dpr2*-/- apresentavam acelerada reepitelização durante a recuperação de feridas cutâneas, pois a deficiência de *Dpr2* aumentava a resposta dos queratinócitos frente à estimulação da via de sinalização TGF- β, que promove migração dos queratinócitos e adesão de filamentos de fibronectina, através da regulação de genes específicos da integrina. (Meng *et al*., 2010). Dessa forma, a molécula de *Dpr2* atua como regulador negativo da reepitalização de feridas na pele de ratos adultos através da inibição da via de sinalização TGF- β, similar ao que ocorre em embriões de peixe-zebra (Su *et al*., 2007; Meng *et al*., 2010).

Dentre os três membros da família *Dpr, Dpr3* é o que possui menor quantidade de informações disponível na literatura. Até o momento, apenas dois trabalhos descrevem a atividade funcional dessa molécula. O primeiro estudo propõe que a proteína *Dpr3* atue como regulador negativo da via de sinalização Wnt canônica (Fisher *et al.*, 2006; Jiang *et al*., 2008; Wen *et al*., 2010, Kivimäe *et al*., 2011). Nesse trabalho, os autores sugerem que *Dpr3* exerce papel de supressor de tumores e dos efeitos pró-apoptóticos, sendo epigeneticamente silenciado por histonas modificadas durante o câncer de cólon (Wang *et al*., 2010; Kivimäe *et al*., 2011; Jiang *et al*., 2008). O segundo estudo, demonstrou que camundongos homozigotos negativos para o gene *Dpr3* (*Dpr3-/-*) apresentam normais taxas de sobrevivência pós-natal, desenvolvimento embrionário e capacidade de reprodução (Xue *et al,* 2013). Contudo, os indivíduos adultos *Dpr3-/-* apresentaram uma leve redução no peso corporal em comparação com seus irmãos de ninhada do tipo selvagem, sugerindo que *Dpr3* seja importante para o crescimento dos indivíduos no período pós-natal (Xue *et al,* 2013). Ainda nesse estudo, os pesquisadores demonstraram que os rins dos camundongos *Dpr3-/-*, após obstrução uretral unilateral, exibiam aumento na ativação dos miofibroblastos e na produção de matriz extra-celular (ECM) (Xue *et al,* 2013). Esses resultados foram acompanhados pelo aumento da expressão dos genes *Wnt* responsáveis pela formação de fibrose e pela regulação positiva dos genes *Dsh2* e *β-cat* (Xue *et al,* 2013).

Consistente com o papel de *Dpr3* na tumorigênese humana, tanto *Dpr1* quanto *Dpr2* também já haviam sido descritos como supressores de tumor (Gao *et al*., 2013; Zang *et al*., 2013; Wang *et al*., 2012; Yan *et al*., 2012; Wen *et al*., 2010; Yang *et al*., 2010; Yau *et al*., 2005). O

gene *Dpr1* foi associado pela primeira vez a tumorigênese em um trabalho publicado em 2005 por Yau e colaboradores. Neste trabalho, o gene *Dpr1* de humanos é apontado como supressor de hepatocarcinoma e apresenta-se silenciado, através de hipermetilação da região promotora, em 41% das linhagens celulares analisadas para esse tipo de tumor (Yau *et al*., 2005). Em 2010, Wang e colaboradores indicaram novamente o gene *Dpr1* como supressor de tumorigênese por promover apoptose e diminuição da proliferação celular através da inibição da via de sinalização NF-kβ (Wang *et al*., 2012). *Dpr1* apresentou-se silenciado em sete dos dez tipos de linhagens celulares de câncer gástrico e inativado em ratos que apresentavam carcinoma primário de estômago (Wang *et al*., 2012). Ainda neste trabalho, também foi demonstrado que o gene *Dpr1* é silenciado por meio de metilações de sua região promotora e essa metilação está associada diretamente com estágios avançados e agressividade do tumor (Wang *et al*., 2012). Ainda em 2010, *Dpr1* foi novamente apontado como supressor de processos de formação de tumores de pulmões (Yang *et al*., 2010). Yang e colaboradores identificaram que tanto RNAm quanto a proteína de *Dpr1* apresentavam-se em baixos níveis em tecidos tumorais quando comparado com tecidos correspondentes não tumorais (Yang *et al*., 2010). O silenciamento do gene *Dpr1* aumentou a habilidade de invasão das células tumorais, a qual está relacionada com a capacidade de interação/regulação da molécula *Dpr1* com a molécula p120cat (Yang *et al*., 2010). Dois anos mais tarde, Ji e colaboradores demonstraram que o gene *Dpr2* também é capaz de inibir a proliferação do câncer de pulmão através da supressão da via de sinalização Wnt (Jia *et al*., 2012; Yang *et al*., 2010). Assim como *Dpr1* no câncer gástrico, a hipermetilação da região promotora do gene *Dpr2* também está associada a estágios avançados do carcinoma pulmonar (Zang *et al*., 2013; Jia *et al*., 2012; Yang *et al*., 2010). De forma unânime, os trabalhos

que relacionam a família *Dpr* à tumorogênese acreditam que essas moléculas possam ser utilizadas no prognóstico de carcinomas, bem como empregadas em terapias gênicas para controle e combate dessa doença (Gao *et al*., 2013; Zang *et al*., 2013; Jia *et al*., 2012; Wang *et al*., 2012; Wen *et al*., 2010; Yang *et al*., 2010; Yau *et al*., 2005).

Por fim, a família *Dpr* foi associada ao processo de adipogênese (Lagathu *et al*., 2009). Nesse contexto, foi demonstrado através de ensaios de perda e ganho de função que o gene *Dpr1* atua como regulador positivo do processo de adipogênese, uma vez que sua presença é crucial para que pré-adipócitos se diferenciem em adipócitos maduros (Lagathu *et al*., 2009). Lagathu e colaboradores especulam que o gene *Dpr1* atue na maturação dos adipócitos regulando negativamente a via de sinalização Wnt canônica (Lagathu *et al*., 2009). Em adição, os autores acreditam que a modulação da molécula *Dpr1* apresenta potencial terapêutico para melhorar a eficiência metabólica do tecido adiposo, bem como para a prevenção da obesidade associada a complicações metabólicas (Lagathu *et al*., 2009).

Objetivos

3 – Objetivos

3.1 Objetivos gerais

Os objetivos gerais desse estudo foram investigar os possíveis papeis dos genes da família *Dpr* durante o desenvolvimento dos membros de galinha; e compreender a origem e a evolução dessa família gênica ao longo da história evolutiva dos metazoários.

3.2 Objetivos específicos — apresentados no capítulo 1

a) Determinação do padrão de expressão dos genes *Dpr1* e *Dpr2*, através de ensaios de HIS*,* durante o desenvolvimento dos membros de galinha;

b) Comparação do padrão de expressão dos genes *Dpr1* e *Dpr2* com o gene *Sox9*, em ensaios de HIS em embriões de galinha hemidissecados;

c) Comparação do padrão de expressão dos genes *Dpr1* e *Dpr2*, em membros nos estádios E7 e E8 do desenvolvimento de galinha, com o de marcadores para músculo esquelético (*MyoD* e *Pax7*); tecido conectivo muscular (*Tcf4*, *Sfrp2*); tendão (*Scx*); articulações (Wnt9a, *Gdf5*); mesênquima interdigital (*Zeb2*); cartilagem (*Sox9*); epífises (*Sfrp3*); cartilagem hipertrófica (*Ihh*) e osteoblastos (*Spp1*);

d) Obtenção de cortes em vibrátomo dos membros de galinha, para detalhamento dos padrões de expressão obtidos nas etapas anteriores;

e) Realização de HIS e imunohistoquímica em cortes histológicos longitudinais, a fim de se obter um detalhamento da região das articulações digitais.

3.3 Objetivos específicos — apresentados no capítulo 2

a) Identificar a maior quantidade possível dos ortólogos *Dprs* nas espécies que possuem o genoma disponível em bancos de dados;

b) Caracterizar os *loci* genômico e a sequência de proteína codificada pelos diferentes membros da família *Dpr* analisados no item anterior;

c) Construção de árvores filogenéticas, utilizando o método de máxima verossimilhança;

d) Identificação dos diferentes motivos protéicos conservados nos ortólogos *Dprs*;

e) Comparação dos *loci* genômico dos genes ortologos *Dprs*;

f) Validar em laboratório os dados obtidos nas análises de *Bioinformática* através de ensaios de HIS.

Materiais e Métodos

4 – Material e Métodos

4.1 Obtenção de embriões

Embriões de galinha foram obtidos a partir de ovos fertilizados provenientes da granja Yamaguishi (www.yamaguishi.com.br). Após incubação em atmosfera úmida a 38,5°C os embriões foram coletados nos estádios de interesse para a realização dos demais experimentos.

Os embriões de peixe-zebra (Biological Services Unit, King's College London) foram criados a temperatura de 28°C em aquário contendo água de peixe (0.3gL/L de sal marinho instântaneo, 1 mgL/L de azul de metileno; após 24hpf à água foi adicionado 0.2mM 1-phenyl-2-thiourea (PTU, Sigma) para prevenir pigmentação dos embriões). Os embriões foram coletados no estádio 36hpf de acordo com Kimmel e colaboradoes, (1995) e estocados para futuros experimentos.

4.2 Coleta dos embriões de galinha e peixe-zebra.

Embriões de galinha em diferentes estádios do desenvolvimento embrionário foram obtidos de ovos fertilizados após incubação dos mesmos a 38,5 °C até o estádio desejado. Após a incubação, os embriões foram rapidamente dissecados para remoção das membranas extra-embrionárias em solução salina fosfatada (PBS). Para tanto, o conteúdo do ovo foi colocado em uma placa de petri, mantendo o embrião voltado para a superfície. O albúmen que recobre o embrião foi retirado com lenço de papel e sobre o embrião, agora exposto, foi posicionada uma moldura de papel filtro que adere às membranas embrionárias e dessa forma possibilita a remoção do embrião do interior do ovo ao recortar as membranas ao redor. Os embriões foram coletados, lavados em PBS 1X, fixados em PFA 4% e mantidos a temperatura de 4°C.

Os embriões de peixe-zebra foram coletados em uma placa de petri contendo 100mL de água de peixe e a ela adicionados 3mL de Pronase para que ocorresse a remoção do córion. Após incubação por um min. os embriões foram gentilmente lavados por três vezes com água de peixe e mantidos a 28°C em placa de petri até o estádio desejado. Os embriões foram coletados e fixados em PFA 4% e mantidos a temperatura de 4°C.

4.3 Estadiamento dos embriões de galinha e peixe-zebra.

O estadiamento dos embriões de galinha foi feito segundo os critérios descritos por Hamburger & Hamilton (1951) (Tabela 1). Já os embriões de peixe-zebra foram estadiados de acordo com Kimmel e colaboradores (1995) (Tabela 2).

Tabela 1. Estádios e principais características morfológicas dos embriões de galinha.

Estádios	**Tempo de incubação**	**Morfologia e número de somitos**
HH4	17 horas	Linha primitiva definitiva
HH5	18-19 horas	Formação do processo cefálico
HH6	19-21 horas	Dobra de cabeça
HH7	21-22 horas	Um par de somitos
HH8	22-24 horas	Quatro pares de somitos
HH9	29 horas	Sete pares de somitos; vesícula óptica
HH10	33 horas	10 pares de somitos; vesículas cefálicas
HH12	48 horas	16 pares de somitos; telencéfalo
HH13	50 horas	19 pares de somitos; canal atrioventricular
HH14	52 horas	22 pares de somitos; flexura do tronco
HH15	53 horas	22 a 24 pares de somitos
HH16	55 horas	Entre asas e patas 17 a 20 pares de somitos; broto dos membros
HH17	60 horas	29 a 32 pares de somitos; epífises
HH18	65 horas	30 a 36 pares de somitos
HH19	68 horas	37 a 40 pares de somitos estendidos até a cauda
HH20	3.0-3.5 dias	40-43 pares de somitos; pigmentação nos olhos
HH21	3.5 dias	43-44 pares de somitos
HH22	3.5-4.0 dias	Presença de somitos até a ponta da cauda
HH23	4 dias	Dorsal contour from hindbrain to tail is a curved line
HH24	4.5 dias	Placa dos dígitos
HH25	4.5-5.0 dias	Articulação do tornozelo e ombro
HH26	5 dias	Dígitos 1 e 3
HH27	5.0-5.5 dias	Bico
HH28	5.5-6.0 dias	3 dígitos anteriores; 4 dígitos posteriores
HH29	6.0-6.5 dias	Rudimento do quinto digito do pé
HH30	6.5-7.0 dias	Folículos das penas
HH31	7.0-7.5 dias	Presença da membrana interdigital
HH35	8 dias	Falanges nos membros posteriores

Tabela 2. Estádios e principais características morfológicas dos embriões de peixe-zebra.

Estádio	**Hpf**	**Morfologia**
1 célula	0 hora	Formação do blastodisco
64 células	2 horas	3 camadas regulares de blastômeros
128 células	2,25 horas	5 camadas de blastômeros
256 células	2,50 horas	7 camadas de blastômeros
512 células	2,75 horas	9 camadas de blastômeros; formação do vitelo
1000 células	3 horas	11 camadas de blastômeros
Camada germinativa	5,5 horas	Camada germinativa visível do polo animal; 50%-epibolia
Escudo	6 horas	Escudo embrionário visível do polo animal; 50%-epibolia
75%-epibolia	8 horas	Espessamento do lado dorsal; zona de evacuação visível
90%-epibolia	9 horas	Placa neural ; precursor dos cérebro e notocorda
Broto (Bud)	10 horas	Broto da cauda; 100%-epibolia
1-4 somitos	10,5 horas	Formação do primeiro somito
14-19 somitos	16 horas	Placóide ótico; neurômeros cerebrais
20-25 somitos	19 horas	Lentes, vesicular ótica, rombencéfalo
Prim-5	24 horas	Pigmentação inicial; batimentos cardíacos
Prim-15	30 horas	Pigmentação da retina
Prim-25	36 horas	Mobilidade inicial; Pigmentação da cauda
High-pec	42 h	Precursores das nadadeiras peitorais

4.4 Extração de RNA total de embriões de galinha e peixe-zebra

Amostras de RNA total foram obtidas a partir dos embriões de galinha (HH16), e peixe-zebra (36 hpf). Para tanto, embriões inteiros desses animais foram transferidos para tubos de 1,5mL livres de RNAse e adicionados a eles TRIZOL (Invitrogen, Carlsbad, CA) para homogeneização no vórtex até que todo o tecido fosse macerado. Em seguida, as amostras homogeneizadas foram incubadas por 5 min. em temperatura ambiente. Para cada 300µL do homogenado, adicionou-se 200µL de clorofórmio seguido de homogeneização em vórtex durante 30 segundos. Após 5 min. em temperatura ambiente o homogenado foi submetido à centrifugação por 15 min. a 12000 x g a 4°C. A fase aquosa foi transferida para um novo tubo de 1,5mL e a ela foi acrescentada 500µL de álcool isopropílico, e após homogeneização suave, as amostras foram mantidas por 10 min. à temperatura ambiente. Após esse período, as amostras foram centrifugadas a 12000 x g por 10 min. a 4°C e após completa remoção do sobrenadante, adicionou-se 1mL de etanol 70% gelado para nova centrifugação por 10 min. a 7500 x g a 4°C. O sobrenadante foi descartado e ao *pellet* acrescentado 1mL de etanol absoluto gelado. Em seguida, as amostras foram centrifugadas a 7500 x g a 4°C por 10 min. Após, o sobrenadante foi removido e o *pellet* foi solubilizado em 40µL de H_2O tratada com DEPC e estocado a - 80°C.

4.5 Síntese de DNA complementar (cDNA)

A partir do RNA obtido em 4.4, realizou-se a síntese do cDNA para posterior Reação em Cadeia da Polimerase (PCR) utilizando o Kit *SuperScript II* (Invitrogen, Carlsbad, CA). Para tanto, ao RNA total foi acrescentado RNAse H_2O tratada com DEPC a fim de se obter volume final igual 10µL. Em seguida, esses reagentes foram incubados a 65°C por 5 min. para que a denaturação

do RNA fosse realizada e após, incubados em gelo. Posteriormente acrecentou-se Tampão 10X (Tris-HCl 200mM pH 8,4 e KCl 25 mM), $MgCl_2$ (3mM), dNTPs (0,5mM de cada nucleotídeo), RNA *Inhibitor* e a enzima Transciptase Reversa (Invitrogen, Carlsbad, CA). A reação foi incubada por duas horas a 42°C e por fim incubada a 95°C por 5 min. para que ocorresse a inativação da enzima Transciptase Reversa. Os cDNAs obtidos nesta etapa foram utilizados em reações de PCR posteriormente.

4.6 Reação em cadeia da polimerase (PCR)

Para os ensaios de RT-PCR foram utilizados *primers* apropriados para cada amostra de cDNA de interesse. Cada reação de PCR foi feita em volume final igual a 25µL que incluíam 1µL de cDNA, 10pmol de *primer* direto e reverso, 0,5mL de dNTP (0,2mM de cada nucleotídeo), 1,5 mM de $MgCl_2$, 4,5µl de tampão de PCR 10X, 2,5% de DMSO e 1U de Taq DNA polimerase (LGC Biotecnologia, Brasil). As condições de todas as reações de PCR foram: Denaturação a 95°C por 30s; Anelamento dos *primers* a 60°C por 30s; Extensão a 72°C por dois minutos. Foram feitos 35 ciclos e a extensão final a 72°C por 10 min.

4.7 Síntese de ribossonda

Duas metodologias diferentes para síntese de ribossondas foram empregadas neste trabalho: (1) sondas obtidas a partir de plasmídeos e (2) sondas sintetizadas com *primers* específicos contento a região promotora da enzima RNA polimerase T7.

(1) Plasmídeos contendo os cDNAs de interesse foram submetidos à PCR utilizando os *primers* M13 direto e M13 reverso a fim de amplificar a seqüência-molde para a síntese da ribossonda.

(2) Essa categoria de ribossonda foi preparada a partir dos cDNAs de interesse, o qual foi submetido à reação em cadeia da polimerase (PCR) utilizando *primers* específicos que possuíam a sequência da região promotora da enzima RNA polimerase T7 acoplada a extremidade 5´. Essa técnica permite a obtenção de sequências-moldes para a síntese da ribossonda, uma vez que o fragmento amplificado apresenta o sítio promotor para a RNA polimerase.

Os produtos de PCR obtidos em (1) e (2) foram submetidos à extração com fenol:clorofórmio (1:1) e clorofórmio 100%, com o intuito de eliminar eventual atividade de RNAses. Os produtos de PCR foram precipitados e ressuspendidos em água tratada com Dietilpirocarbonato (H_2O DEPC). Depois de efetuada a ressuspensão, o DNA purificado foi utilizado para a transcrição e marcação da ribossonda. Para tanto, adicionamos, a 1µg de DNA purificado, 2µL de tampão de transcrição 10X (10X *transcription buffer*-Ambion), 2µL de 0,1M de DTT, 2µL de uma mistura contendo ribonucleotídeos e UTP conjugado a Digoxigenina (DIG), 0,5µL de inibidor de RNAse, 1µL da T3 RNA polimerase e água livre de ribonucleases para completar o volume final de 20µL e incubamos a 37°C por duas horas. Após a incubação, adicionou-se ao tubo 2µL de DNAse I (2U) (Fermentas) para remover o produto de PCR utilizado como molde. Esta mistura foi incubada durante 15 min. a 37°C e depois colocada em gelo. O RNA transcrito foi purificado em coluna (Sigma S5059) e ressuspendido em 30µL em água livre de ribonucleases e armazenados a -20°C.

Para verificar a qualidade da ribossonda sintetizada, eletroforese de 1µL da solução final ressuspendida foi realizada utilizando gel de agarose 1%. A qualidade da ribossonda sintetizada foi avaliada através da intensidade e definição da banda obtida após a eletroforese.

4.8 Processamento dos embriões para hibridação *in situ*

Tanto os embriões de galinha quanto os de peixe-zebra foram coletados e fixados em paraformaldeído 4% (PFA 4%) a 4°C durante 16 horas, lavados em PBT (PBS + 0,1% Tween-20) e desidratados em uma sequência de soluções de metanol a 25%, 50% e 75% em PBST, sendo finalmente armazenados em metanol 100% a -20°C para serem utilizados nos ensaios de hibridação *in situ*.

4.9 Ensaios de hibridação *in situ (Whole mount)* de embriões de galinha.

Os embriões foram reidratados através de banhos seriados decrescentes de metanol em PBT (75%, 50% e 25%) por 5 min. em cada solução e duas lavagens em PBT por 5 min. à temperatura ambiente. Em seguida, foram incubados em solução de peróxido de hidrogênio (H_2O_2) a 6% em PBT por uma hora à temperatura ambiente. Após serem lavados em PBT, os embriões foram tratados com Detergente mix (Igepal 1%, SDS 1%, Deoxicolato de sódio 0,5%, Tris-HCl 50mM ph 8.0, EDTA 1mM pH8,0 e NaCl 150mM). Este tratamento consiste em três banhos com a solução de Detergente Mix por 20 min. cada, à temperatura ambiente. Essas lavagens são fundamentais, pois permitem o acesso ao RNAm pela ribossonda no interior de cada célula no momento da hibridação, sem que o embrião tenha sua integridade comprometida. A ação do detergente mix é interrompida lavando-se os embriões duas vezes em PBT durante 5 min. à temperatura ambiente. Após esse período os embriões são refixados

em solução de PFA 4% contendo glutaraldeído a 0,25% em PBS por 20 min. e lavados em seguida três vezes por cinco minutos em PBT à temperatura ambiente. Os embriões fixados foram incubados em tampão de Pré-Hibridação (formamida 50%; SSC 5X pH 4,5; 50 µg/mL de RNA de levedura; SDS 1% e 50 µg/mL de heparina) durante duas horas a 65°C. A hibridação foi feita em Tampão de Hibridação (tampão de Pré-Hibridação contendo 1µg/mL da ribossonda), durante pelo menos 12 horas a 65°C. Em seguida, os embriões foram lavados a 65°C em Solução X (formamida 50%, SSC 2X pH 4,5 e SDS 1%) pré-aquecida quatro vezes durante 30 minutos. Após o tratamento com Solução X, os embriões foram lavados por 10 min. a 65°C em Solução X 50% pré-aquecida e $MAB_{Lev,Tw}$ 50%. Após esse período os embriões foram lavados rapidamente por três vezes em solução tampão $MAB_{Lev,Tw}$ (Ácido Maléico 100mM, NaCl 150mM, Levamisole 2mM e Tween-20 0,1%, em pH 7,5) à temperatura ambiente. Em seguida, os embriões foram lavados duas vezes por 30 min. em solução tampão $MAB_{Lev,Tw}$ à temperatura ambiente. Após essa etapa, os embriões foram pré-bloqueados em reagente de bloqueio Boehringer Mannhein (BMB) a 2% em tampão MAB em temperatura ambiente. Posteriormente, os embriões continuaram a ser pré-bloqueados em uma solução de alta concentração protéica (BMB 2%, soro de ovelha inativado 10% em tampão $MAB_{Lev,Tw}$). A etapa de pré-bloqueio é importante para bloquear sítios aos quais o anticorpo poderia eventualmente se ligar inespecificamente. Após o pré-bloqueio os embriões foram incubados em solução contendo regente de bloqueio a 2% em tampão $MAB_{Lev,Tw}$, 1% de soro de ovelha inativado e anticorpos anti-DIG conjugados à fosfatase alcalina na titulação de 1:2000 durante pelo menos 12 horas a 4°C. Em seguida, os embriões foram lavados em tampão $MAB_{Lev,Tw}$ à temperatura ambiente (oito banhos de uma hora), e pelo menos por mais 12 horas a 4°C. Antes de começar a revelação do sinal, os embriões foram

lavados quatro vezes por 10 min. em solução tampão NTMT (NaCl 100mM, Tris 100mM pH 9,5, $MgCl_2$ 50mM Tween-20 0,1%, Levamisole 2mM) à temperatura ambiente. Após essas lavagens, os embriões foram tratados com Tampão NTMT juntamente ao substrato para fosfatase alcalina, BCIP/NBT (117 µg/mL de BCIP, 225 µg/mL de NBT em NTMT), protegidos da luz, a fim de detectar a ação da fosfatase alcalina até a reação atingir intensidade desejada. Para interromper a reação, os embriões foram lavados em PBT 1X, fixados em PFA 4% a 4°C por pelo menos 12 horas. Após a fixação os embriões foram lavados em PBS 1X e armazenados em glicerol 80% em PBT (banhos seriados crescentes de glicerol em PBT 25%, 50% e 80% por 5 min. em cada solução à temperatura ambiente).

4.10 Ensaios de hibridação *in situ* em lâmina de membros de galinha

Os membros posteriores de galinha foram dissecados após a coleta, fixados *overnight* em PFA 4%, desidratados e incluídos em parafina. Após, cortes com 8µm de espessura foram obtidos em micrótomo rotativo (Leica, RM2145) e posteriormente coletados em lâminas adesivas (Starfrost, B4 0303). As lâminas foram desparafinizadas em três banhos de xilol seguidos de uma série etanólica decrescente (100-50%) e lavadas em PBS. Em seguida deixou-se as lâminas em solução contendo 0,5µL ProteinaseK/mL PBS) durante 45 minutos. Após esse período, as lâminas foram incubadas por 10min. a 37°C em solução de glicina 0,2%. Em seguida, as lâminas foram refixadas em PFA 4% por 5 min. e lavadas em PBS. Logo após, foram adicionados 300µL de solução de pré-hibridação (formamida 50%; SSC 5X pH 4,5; 50 µg/mL de RNA de levedura; SDS 1% e 50 µg/mL de heparina) por lâmina, as quais foram cobertas com filme plástico (Parafilm, 01852-AB) e colocadas em câmara úmida 65°C por quatro horas.

Posteriormente, adicionou-se a solução de hibridação (tampão de Pré-Hibridação contendo 1µg/mL da ribossonda) e as lâminas foram deixadas pelo menos 12 horas em câmara úmida a 65°C. Após, foram realizadas quatro lavagens com tampão SSC pH4,5; duas com solução X (formamida 50%, SSC 2X pH 4,5 e SDS 1%); três com PBT (PBS + 0,1% Tween-20) e quatro com MABT (Ácido Maléico 100mM, NaCl 150mM, e Tween-20 0,1%, em 7,5). Após as sucessivas lavagens as lâminas foram bloqueadas utilizando a solução de BMB/MABT 5% por uma hora. Após o bloqueio, as lâminas foram incubadas em câmara úmida por pelo menos 12 horas com anticorpo anti-DIG conjugado com fosfatase alcalina na titulação de 1:2000. Em seguinda, as lâminas foram lavadas quatro vezes em MABT, duas vezes em NTMT (NaCl 100mM, Tris 100mM pH 9,5, $MgCl_2$ 50mM Tween-20 0,1%) e posteriormente incubadas no escuro com solução de revelação (2,5µl NBT/BCIP por mLde NTMT – Roche, 11681451001). Após o término da coloração, as lâminas foram lavadas com NTMT e montadas com lamínulas em glicerol 80% e analisadas.

4.11 Ensaios de hibridação *in situ (Whole mount)* de embriões de peixe-zebra

Os embriões de peixe-zebra foram reidratados através de banhos seriados decrescentes de metanol em PBT (50% e 25%) por 5 min. em cada solução seguidas por quatro lavagens em PBT por 5 min. à temperatura ambiente. Após a reidratação, os embriões foram incubados por 40 min. em solução contendo Proteinase K (1mg/mL de PBT). Em seguida, os embriões foram refixados com PFA 4% por 20 min. em temperatura ambiente. Transcorrido esse período, os embriões foram lavados com PBT por quatro vezes de cinco min. cada. A solução de PBT foi substituída pela solução de pré-hibridação (Formamida 50%, SSC 5X, Tween-20 0,1%, 50 µg/mL

Heparina e 1mg/mL de tRNA em pH 6,0) e deixada por no mínimo 2 horas em contato com os embriões a 68°C. A solução de pré-hibridação foi retirada e aos embriões foi adicionada a solução de hibridação (solução de Pré-hibridação contendo 1µg/mL da ribossonda) e deixada por pelo menos 12 horas a 68°C. Em seguida os embriões foram lavados quatro vezes com solução de pré-hibridação a 68°C por 30 min. Após três lavagens de 15 min. com SSC 0,2X foram realizadas a 68°C e três lavagens de 15 min. em PBT à temperatura ambiente. Em seguida, os embriões foram incubados por duas horas à temperatura ambiente em solução de bloqueio (Boehringer Mannhein (BMB) a 2% em tampão MAB (Ácido Maléico 100mM, NaCl 150mM, Levamisole 2mM e Tween-20 0,1%, em pH 7,5). Após, aos embriões foi adicionada a solução de MABT contendo anticorpo anti-DIG conjugados à fosfatase alcalina na titulação de 1:6000 e deixada por pelo menos 12 horas a 4°C. Em seguida, os embriões foram lavados seis vezes por 15 min. com PBT e três vezes por 5 min. com tampão NTMT (NaCl 100mM, Tris 100mM pH 9,5, $MgCl_2$ 50mM Tween-20 0,1%). Após essas lavagens, iniciou-se a etapa de revelação do sinal, para tanto, os embriões foram tratados com solução NTMT juntamente ao substrato para fosfatase alcalina, BCIP/NBT (117 µg/mL de BCIP, 225 µg/mL de NBT em NTMT), protegidos da luz. Após o término da reação os embriões foram lavados com PBS 1X e fixados em PFA 4% a 4°C por pelo menos 12 horas. Finalizada a etapa de fixação, os embriões foram lavados em PBS 1X e armazenados em glicerol 80% após lavagens seriadas crescentes de glicerol em PBS 25%, 50% e 80%.

4.12 Análise dos embriões inteiros (*Whole mount*)

Após as hibridações *in situ*, os embriões de galinha e peixe-zebra foram analisados ao microscópio estereoscópico (Olympus, SzX7 e Leica MZ16 F, respectivamente) a fim de identificar o padrão de expressão obtido. Os resultados obtidos foram registrados em fotomicrografias organizadas em pranchas. Os embriões foram fotografados pela câmera *Cool SNAP-Pro-color – Media Cybernetics* e as fotos capturadas pelo programa *Image-Pro Plus* versão 4.1.0.0 para Windows 95/NT/98 – Media Cybernetics.

4.13 Cortes dos membros dos embriões de galinha em vibrátomo

Para maior detalhamento do padrão de expressão, peças foram incluídas em gelatina 20%, fixadas em PFA 4% *overnight* e cortadas em vibratome (OTS-3000; Electron Microscopy Sciences) com aproximadamente 50µm de espessura.

4.14 Imunolocalização de β-catenina ativada.

A localização tecidual da molécula β-catenina ativa foi realizada através do método o método da imunoperoxidase indireto. Após desparafinização e hidratação dos cortes (8mm de espessura), as lâminas foram incubadas a elevada temperatura com o tampão Citrato de Sódio 0,01M (pH6,0), a fim de recuperar a capacidade antigênica do tecido. Após, lavagens com 0,05M de solução tampão salina-trisma (TBS, pH7,4) foi realizado o bloqueio da peroxidase endógena com 3% de H_2O_2 em Metanol. Em seguida, os sítios de ligação inespecífas foram bloqueados, para tanto, as lâminas foram incubadas por uma hora com TTBS (0,1% Tween 20 e 5% de leite desnatado seco em TBS). Após, foi realizado a incubação do anticorpo primário na diluição 1:50 (anti-ABC, Milipore) durante 12 horas mantidos a 4°C. Os cortes foram então lavados com TBS e

incubados à temperatura ambiente por 40 min. com o anticorpo secundário biotinilado (diluição 1:100; Jackson Immuno Research), e depois com solução HRP-estreptavidina (diluição 1:200; Invitrogen) durante 30 min. à temperatura ambiente. Em seguida, os cortes foram tratados com 10% de 3,3′-Diaminobenzidina (DAB, em tampão Tris-HCl 0,1M, pH7,4) (Sigma) e 0,2% de H_2O_2 em TBS. Finalmente, os cortes foram contracorados com hematoxilina de Ehrlich e montados para observação em microscopia óptica.

Capítulo 1

Padrão de expressão dos genes Dpr durante o desenvolvimento dos membros de galinha (Gallus gallus)

Introdução – Capítulo 1

Os membros de vertebrados são apêndices torácicos envolvidos em funções cruciais para a vida desses animais, dentre elas — locomoção, alimentação, copulação e comunicação (Barrow, 2011; Capdevila & Belmonte, 2001). Ademais, os membros reúnem a habilidade de executar movimentos dos mais diversos, desde os mais grossos até os mais finos e delicados, atenuando ou aumentando a intensidade e robustez da força aplicada (Watson *et al*., 2009). Para tanto, os membros são dotados de diversos músculos, elementos esqueléticos, tendões, vasos sanguíneos e nervos que estão interconectados, desempenhando suas funções de maneira coordenada e precisa (Johnson & Tabin 1997; Tickle, 2003). Diversos estudos buscam desvendar como os detalhes anatômicos e funcionais dos membros de cada espécie são formados e regulados (Tickle, 1995; Tabin, 1991). Diante disso, o desenvolvimento dos membros tem sido considerado um poderoso modelo de estudo para o entendimento de variados processos — estabelecimento da posição espacial, coordenação do sistema tridimensional, determinação do padrão estrutural, diferenciação e especificação celular (Tickle, 2003; Johnson & Tabin 1997; Tickle, 1995; Tabin, 1991).

Desenvolvimento dos membros de vertebrados

Os membros dos vertebrados são originados a partir do mesoderme lateral parietal e somítico (Johnson & Tabin 1997). Através da proliferação celular de regiões específicas do flanco, ao nível do coração e rins, são formadas estruturas conhecidas como broto (botão) do membro anterior (MA) e posterior (MP), respectivamente (Figura 7A) (Tickle, 1995; Tabin, 1991). Pouco depois dessa formação, células provenientes das bordas laterais próximas aos somitos migram para dentro do broto do membro (Tickle, 2003). Todos os músculos, nervos e componentes vasculares, que

compõem o membro adulto, são derivados dessas células migratórias (Johnson & Tabin 1997). Enquanto os outros tecidos dos membros, incluindo cartilagem, tendões e ossos, são derivados das células provenientes do mesoderme lateral parietal (Figura 7B) (Johnson & Tabin 1997).

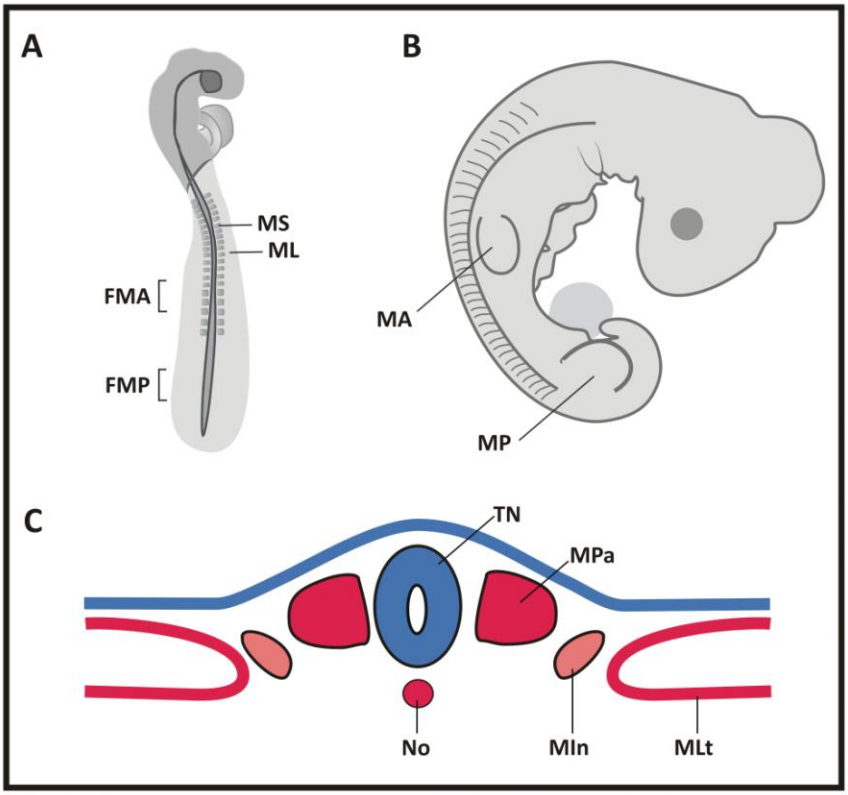

Figura 7. Locais e tecidos envolvidos no desenvolvimento anatômico dos membros de galinha. (A) Representação de um embrião de galinha com aproximadamente 70 horas de incubação. As futuras regiões formadoras do membro anterior (FMA) e posterior (FMP) estão localizadas na mesoderme paraxial adjacente aos somitos e na mesoderme paraxial não segmentada, respectivamente. (B) Esquema de um embrião de quatro dias, no qual o padrão de localização da asa (MA) e perna (MP) já estão estabelecidos e surgem na forma de brotos salientes da região do flanco. (C) Diagrama de um corte transversal de embrião de galinha com aproximadamente 50 horas de incubação. TN (tubo neural); MIn (mesoderme intermediária); MPa (mesoderme paraxial); MLt (mesoderme lateral); No (notocorda); MS (mesoderme somítica); ML (mesoderme lateral). Adaptado de Johnson & Tabin, 1997.

A anatomia do botão do membro é descrita em relação aos três eixos ortogonais — ântero-posterior (AP), dorso-ventral (DV) e próximo-distal (PD) — sendo que a denominação AP refere-se à região anterior e posterior (no membro humano adulto, da ponta do polegar até a ponta do dedo mínimo); DV denomina a região dorsal e ventral (no membro humano adulto, do dorso da mão até a palma da mão); PD determina a região proximal e distal do membro estendido em relação ao plano corpóreo (em humano adulto, do ombro até a ponta dos dedos) (Tickle, 2006; Johnson & Tabin 1997).

O botão do membro é revestido por uma camada espessa de células epiteliais ectodérmicas que são responsáveis pela formação da estrutura denominada crista apical, ou Crista Ectodérmica Apical (AER), que expressa genes da família FGF e que é responsável pelo crescimento do membro ao longo do eixo PD (Tickle, 2006). Logo abaixo da AER encontra-se uma região chamada de Zona de Progresso (PZ), que é composta por células mesenquimais indiferenciadas e de rápida proliferação (Tickle, 2006; Johnson & Tabin 1997). Acredita-se que a PZ seja o local no qual as células adquirem informação posicional que determinará em qual estrutura essas células se desenvolverão, pois somente quando as células deixam essa zona é que elas começam a se diferenciar (Johnson & Tabin, 1997). Na extremidade posterior do broto há um pequeno grupo de células, também mesenquimais indiferenciadas, denominado Zona de Atividade Polarizadora (ZPA) que está envolvida na padronização do eixo AP do membro em formação e expressa altos níveis de *Sonic hedgehog* (Shh) (Figura 8) (Tickle, 2006; Johnson & Tabin 1997).

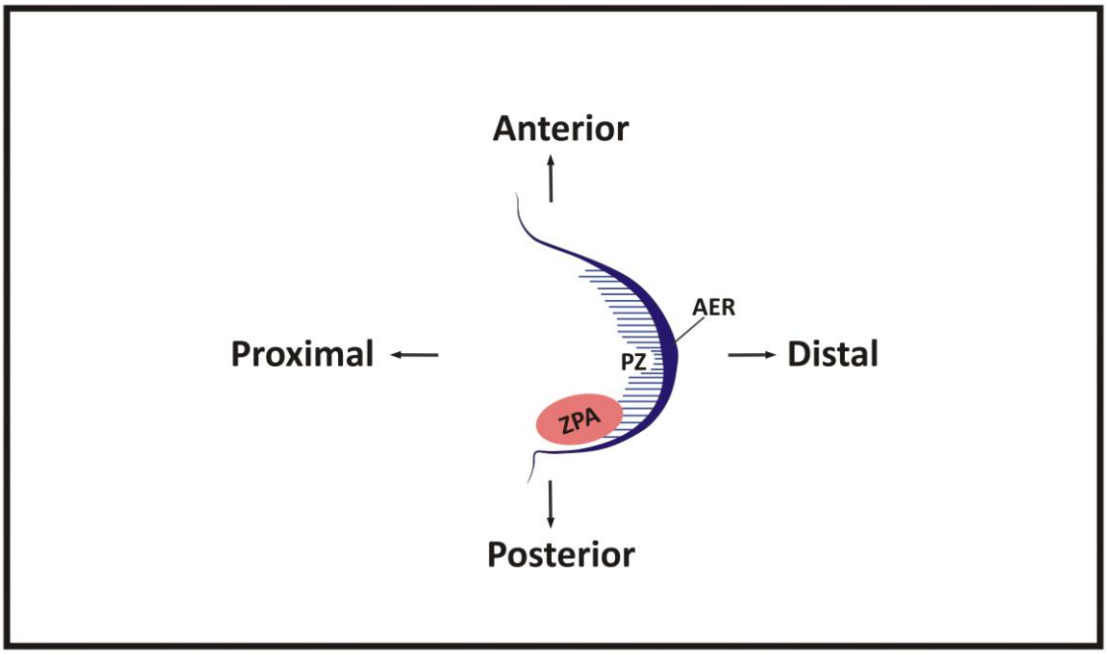

Figura 8. Diagrama da estrutura básica do broto do membro em vertebrados. O broto do membro de vertebrados é composto por células mesenquimais indiferenciadas envolvidas por uma camada de células ectodérmicas e possuí regiões específicas responsáveis pela padronização dos eixos ântero-posterior, dorso-ventral e próximo-distal. AER (Crista Ectodérmica Apical); PZ (Zona de Progresso); ZPA (Atividade Polarizadora). Adaptado de Johnson & Tabin, 1997.

Existem dois modelos que descrevem o desenvolvimento dos membros em vertebrados, especificação progressiva e especificação inicial, que serão brevemente descritos abaixo (Barrow, 2011; Towers & Tickle, 2009; Tabin & Wolpert, 2007).

O modelo de especificação progressiva foi estabelecido por Summerbell e colaboradores no ano de 1973 e por ter sido utilizado durante décadas ficou conhecido como o modelo clássico para exemplificar a padronização dos membros de vertebrados (Barrow, 2001; Towers & Tickle, 2009). Esse modelo consiste na ideia de que o crescimento dos membros se dá no sentido próximo-distal e é influenciado pela região AER (Towers & Tickle, 2009; Tabin & Wolpert, 2007). Assim, as células da PZ que permanecem por mais tempo perto da AER serão as últimas a se diferenciarem e

os elementos que compõem a região proximal — úmero/fêmur (segmento estilopódio) — serão os primeiros a serem formados (Figura 9A) (Towers & Tickle, 2009; Tabin & Wolpert, 2007; Tickle, 2003). Posteriormente, células mesenquimais se agregam para formar os elementos intermediários, rádio/fíbula e ulna/tíbia (segmento zeugópode) e em seguida, há a formação dos elementos punho/tornozelo e por fim os dígitos (segmento autópode) (Figura 10) (Tickle, 2006; Tickle, 2003; Johnson & Tabin 1997). Esse modelo pode ser explicado através de diversos experimentos clássicos que consistiam na excisão da região AER do broto de membros de galinha (Towers & Tickle, 2009; Tabin & Wolpert, 2007). Esses ensaios demonstraram que quando a região AER era totalmente retirada, os animais manipulados apresentavam asas truncadas (Towers & Tickle, 2009; Tabin & Wolpert, 2007). Além disso, a região do membro onde o truncamento ocorria estava relacionada com a fase do desenvolvimento em que a AER havia sido removida, ou seja, quando removida precocemente, apenas elementos proximais eram formados; quando removida tardiamente, tanto estruturas proximais quanto as mais distais estavam presentes (Towers & Tickle, 2009; Tabin & Wolpert, 2007). Em concordância com esses resultados, em 1979, Wolpert e colaboradores, utilizando altas doses de irradiação do tipo X, destruíram células da AER nas fases iniciais do desenvolvimento (revisado por Barrow, 2011; Towers & Tickle, 2009; Tabin & Wolpert, 2007). Os membros obtidos não apresentavam estruturas distais, contudo as estruturas proximais eram formadas normalmente (Barrow, 2011; Towers & Tickle, 2009; Tabin & Wolpert, 2007). Dessa forma, podemos dizer que o modelo clássico (especificação progressiva) padroniza o desenvolvimento do membro no sentido próximo-distal e depende do crescimento celular e do tempo em que as células indiferenciadas (ZP) ficam em exposição aos sinais da AER (Towers & Tickle, 2009). Esse modelo tem sido fortemente criticado, pois a remoção da zona AER resulta em morte celular maciça e

atualmente, acredita-se que esse fato possa ter influenciado os resultados obtidos por Summerbell e colaboradores na década de setenta (Figura 9A) (Duboc & Longon, 2009; Mariani *et al*., 2008; Dudley *et al*., 2002; Capdevila & Belmonte, 2001; Johnson & Tabin, 1997).

Em 2002, Dudley e colaboradores propuseram outro modelo de padronização próximol-distal dos membros de vertebrados (Dudley *et al*., 2002). O novo modelo, especificação inicial, propõe que a padronização é especificada prematuramente no desenvolvimento do botão do membro que, então, irá expandir e formar os elementos proximais, mediais e distais à medida que é influenciado pelos sinais provenientes da AER (Figura 9B) (Dudley *et al*., 2002). Dudley e colaboradores acreditavam que os resultados obtidos por Summerbell em 1973 são na realidade um aterfato de técnica, uma vez que a maciça morte celular ocasionada pela remoção da AER é responsável pela perda de células que já estavam comprometidas com o desenvolvimento das estruturas distais e assim, apenas elementos proximais permaneciam intactos e por isso eram os únicos presentes nos membros truncados (Dudley *et al*., 2002). No entanto, o modelo proposto por Dudley não é amplamente aceito pela comunidade científica, uma vez que os experimentos de mapeamento do destino celular realizados por ele não são reproduzíveis (Barrow, 2011; Pearse *et al*., 2007; Sato *et al*., 2007). Além disso, outra limitação apresentada pelo modelo de Dudley é a falta de explicação de como o padrão inicial é configurado nos botões dos membros (Duboc & Longon, 2009; Towers & Tickle, 2009; Mariani *et al*., 2008; Tabin & Wolpert, 2007).

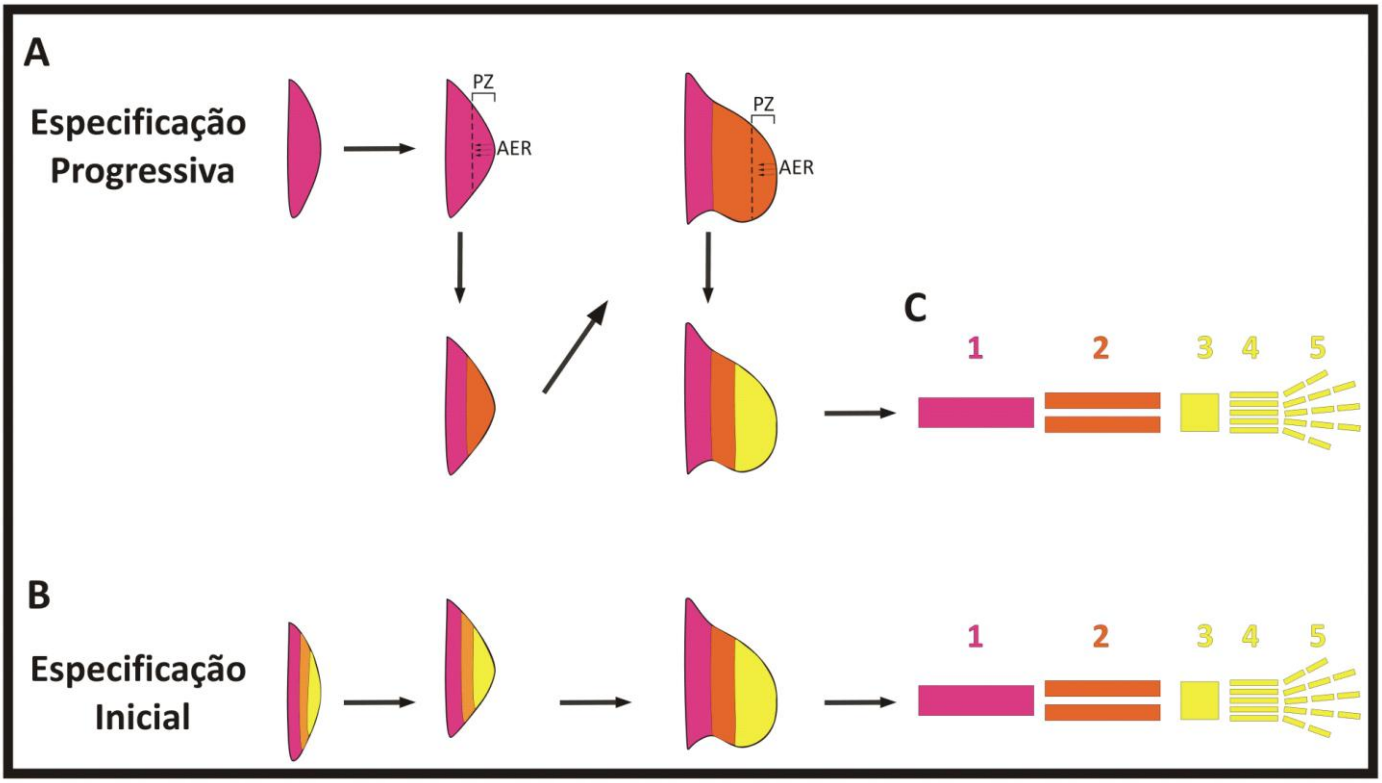

Figura 9. Modelos propostos para o desenvolvimento dos membros de vertebrados. (A) O modelo de especificação progressiva propõe que inicialmente todo o broto do membro possui identidade de formação de elementos proximais (rosa). A mesoderme da extremidade distal dos brotos dos membros constitui a PZ (zona de progresso) e ela recebe continuamente sinais da AER (Crista Ectodérmica Apical) para se diferenciar em elementos distais (amarelo). Contudo, à medida que o botão do membro cresce algumas células deixam a PZ e se comprometem coma diferenciação de elementos intermediários do membro. (B) O modelo de especificação inicial sugere que em uma fase precoce do membro, as células já estão pré-determinadas a formar cada uma das três partes do membro. (C) Diagrama representando o tamanho e o número de elementos no membro posterior de humano: 1 (fêmur), 2 (fíbula e tíbia), 3 (tarso), 4 (metatarso) e 5 (falanges). Adaptado de Tabin & Wolpert, 2007.

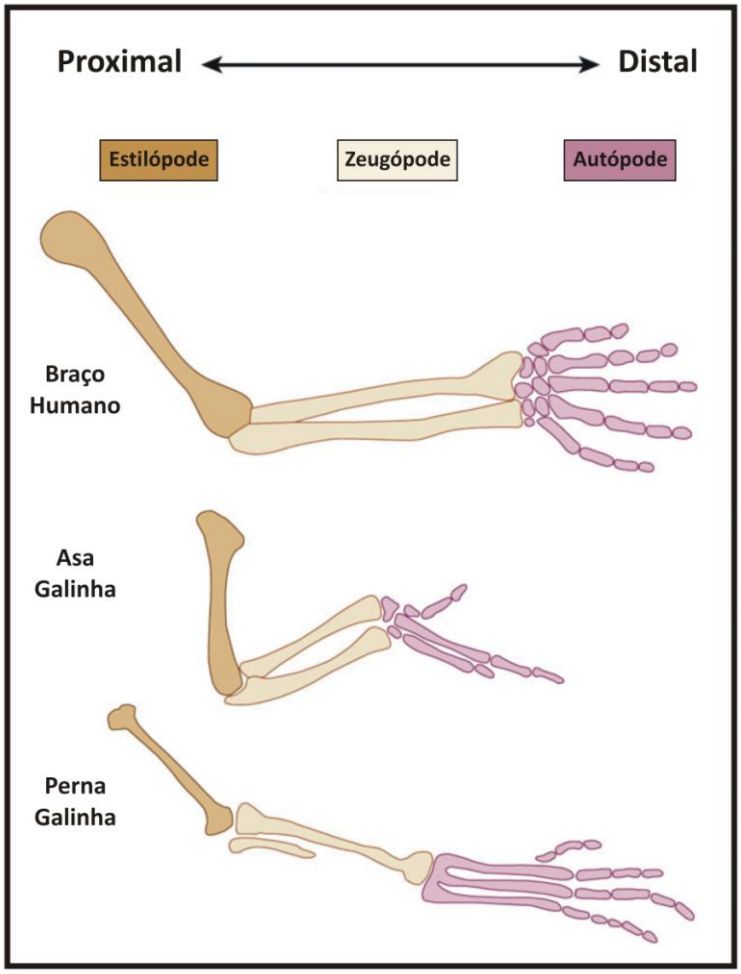

Figura 10. Comparação dos elementos esqueléticos de membros humanos e de galinha. Elementos que compõem a região proximal — úmero/fêmur (segmento estilopóde); elementos intermediários — rádio/fíbula e ulna/tíbia (segmento zeugópode); elementos distais — punho/tornozelo e por fim as falanges (segmento autópode). Adaptado de Mariani & Martin, 2003.

Por fim, nenhum dos modelos propostos até o momento para o desenvolvimento dos membros de vertebrados é totalmente aceito pela comunidade científica e todo o conhecimento disponível nesse campo de pesquisa é, de certa forma, bastante fragmentado (Barrow, 2011; Duboc & Longon, 2009; Towers & Tickle, 2009). Estudos recentes têm reavaliado os resultados obtidos pelos experimentos clássicos e unido essas informações aos dados moleculares obtidos nas últimas

décadas (Barrow, 2011; Duboc & Longon, 2009; Towers & Tickle, 2009). Dessa forma, será possível entender de que maneira essas estruturas são padronizadas e como esses princípios são compartilhados entre as diferentes espécies de vertebrados ao longo da evolução (Duboc & Longon, 2009; Towers & Tickle, 2009).

Principais vias de sinalizações envolvidas no desenvolvimento de membros de vertebrados

Os exatos mecanismos da indução da formação dos membros são ainda controversos, embora existam fortes evidências de que sinais FGF, TGF-β, Shh e Wnt coordenem os eventos necessários para o desenvolvimento dessas estruturas — integração das informações provenientes das três regiões do broto do membro (AER, PZ e ZPA); regulação dos processos de proliferação e diferenciação celular; e modulação de todos os sinais de indução ao longo do tempo e espaço (Duboc & Longon, 2009; Church & Francis-West, 2002; Capdevila & Belmonte, 2001; Johnson & Tabin, 1997).

Fator de Crescimento Fibroblástico (FGF): padronização próximo-distal do botão dos membros de vertebrados

Diversos estudos afirmam que a padronização PD durante o desenvolvimento dos membros de vertebrados é controlada pela estrutura AER presente nos brotos dessas estruturas (Capdevila & Belmonte, 2001; Johnson & Tabin, 1997). Sabe-se que a região AER apresenta forte expressão dos genes da família *FGF* que assumem, nesse contexto, importante papel na modulação das atividades exercidas por esse centro de sinalização (Bénazet & Zeller, 2009; Duboc & Longon, 2009; Capdevila & Belmonte, 2001; Niswander *et al*., 1993). Um estudo clássico — que demonstra a importância dos genes *FGF* para o correto desenvolvimento dos membros — foi realizado por

Niswander e colaboradores em 1993 (Bénazet & Zeller, 2009; Niswander *et al*., 1993). Eles demonstraram que em galinhas que tiveram a região AER removida, os sinais FGFs quando restaurados, por meio de implantação de *beads*, reestabeleciam o crescimento distal dessas estruturas (Bénazet & Zeller, 2009; Niswander *et al*., 1993). A partir desses resultados, a família FGF passou a ser amplamente estudada no que concerne a padronização do eixo PD dos membros (Bénazet & Zeller, 2009; Duboc & Longon, 2009; Capdevila & Belmonte, 2001). *FGF4*, *FGF8*, *FGF9* e *FGF17* são expressos na AER e diversas análises genéticas demonstraram que esses genes atuam de forma redundante e em sobreposição para a padronização PD dos membros em camundongo (Bénazet & Zeller, 2009; Duboc & Longon, 2009; Capdevila & Belmonte, 2001). A perda da expressão de *FGF8*, único gene presente em toda a extensão da AER, interrompe a formação dos elementos esqueléticos do estilopódio, gerando membros truncados (Bénazet & Zeller, 2009). Quando inativados simultaneamente durante as fases iniciais do desenvolvimento, *FGF4* e *FGF8* impedem a completa formação dos brotos dos membros (Bénazet & Zeller, 2009). Outros estudos revelam que a expressão transitória de *FGF4* e *FGF8* durante o início da formação dos membros é suficiente para a total especificação do eixo PD, no entanto, a especificação dos diferentes segmentos (estilopódio, zeugópode e autópode) é interrompida (Bénazet & Zeller, 2009). Recentemente, Mariani e colaboradores demonstraram que camundongos mutantes para *FGF4*, *FGF8*, *FGF9* e *FGF17* apresentavam diferentes fenótipos de malformações dos membros (Bénazet & Zeller, 2009; Mariani *et al*., 2008). Porém a perda dos elementos intermediários (zeugópode) e a manutenção dos elementos proximais (estilopódio) e distais (autópode) eram características consistentes desses mutantes (Mariani *et al*., 2008). Esses resultados estão em total desacordo com os dois modelos de padronização dos membros de vertebrados aceitos hoje em dia (Bénazet & Zeller, 2009; Duboc &

Longon, 2009; Mariani *et al*., 2008). Dessa forma, os dados obtidos por Mariani e colaboradores surgem com uma terceira hipótese, especificação intermediária, para o desenvolvimento e formação dos membros (Bénazet & Zeller, 2009; Duboc & Longon, 2009; Mariani *et al*., 2008).

Sonic Hedgehog (Shh): padronização do eixo ântero-posterior e dígitos

Os membros da família *Shh* são expressos e secretados por células que compõem a ZPA e são necessários para ativação de mais de 50 genes da família *Hox* durante o crescimento e padronização dos membros e dígitos dos vertebrados (Duboc & Longon, 2009; Tarchini & Duboule, 2006; Tickle, 2006; Tickle, 2003; Sanz-Ezquerro & Cheryll, 2000; Johnson & Tabin 1997). Dois modelos foram propostos para explicar a atividade dos genes *Shh* durante o desenvolvimento dos membros — (1) o modelo clássico, baseado em gradiente de concentração; e (2) o modelo que considera tanto a difusão do morfógeno pela estrutura, quanto o tempo em que as células ficarão expostas a eles (Duboc & Longon, 2009; Tickle, 2003; Sanz-Ezquerro & Cheryll, 2000).

O modelo clássico propõe que moléculas de Shh estabelecem um gradiente de concentração ao longo do eixo AP (Duboc & Longon, 2009; Sanz-Ezquerro & Cheryll, 2000; Tickle, 2003) As células expostas a concentrações elevadas de Shh irão formar os dígitos da região posterior do membro, ao passo que células mais distantes da ZPA, expostas a concentrações progressivamente mais baixas de Shh, contribuirão para o desenvolvimento dos dígitos mais anteriores (Duboc & Longon, 2009; Towers & Tickle, 2009; Tarchini & Duboule, 2006; Tickle, 2003; Sanz-Ezquerro & Cheryll, 2000).

O segundo modelo sugere que a padronização e especificação dos diferentes tipos de dígitos dependem não somente do gradiente de concentração das moléculas de Shh, mas também

da duração do tempo que as células progenitoras ficarão expostas a esses sinais (Tickle, 2003; Sanz-Ezquerro & Cheryll, 2000). Esse modelo sugere que o fator temporal é importante para o comprometimento das células a um tipo de dígito específico (Duboc & Longon, 2009). Dessa forma, dígitos posteriores serão definidos pela quantidade de tempo que estão expostos aos sinais Shh, ao passo que o gradiente de concentração dessas moléculas irá especificar os dígitos anteriores (Duboc & Longon, 2009).

Independente de qual modelo esteja correto, todos os ensaios de função, envolvendo as moléculas Shh, demonstram que essa família gênica está fortemente relacionada com a expansão e especificação do eixo AP e com a determinação da quantidade e identidade dos dígitos (Duboc & Longon, 2009; Towers & Tickle, 2009; Tarchini & Duboule, 2006; Tickle, 2003; Sanz-Ezquerro & Cheryll, 2000).

Sinais Wnt: padronização dos eixos ântero-posterior e dorso-ventral

As moléculas envolvidas na via de sinalização Wnt controlam diferentes processos ao longo do desenvolvimento dos membros — ativação e padronização do crescimento e regulação da diferenciação das células em diferentes tecidos (ten Berge *et al*., 2008; Church & Francis-West, 2002). Os genes *Wnt* podem ser detectados tanto na AER quanto nas células mesenquimais que compõem o broto do membro (Church & Francis-West, 2002; Enomoto-Iwamoto *et al*., 2002; Tickle & Münsterberg, 2001). Wnt8c e Wnt2b (também conhecido como Wnt13) são brevemente expressos no mesoderme lateral e induzem o crescimento das patas e asas, respectivamente (ten Berge *et al*., 2008; Enomoto-Iwamoto *et al*., 2002). Experimentos de expressão ectópica dos genes Wnts, na região entre os flancos de embriões de galinha HH13/14, induzem a expressão de FGF10 e

consequentemente a formação de um membro adicional (Barrow, 2011; Church & Francis-West, 2002; Tickle & Münsterberg, 2001). Por sua vez, o gene FGF10 promove a expressão do gene Wnt3a na região da AER, que em resposta ativa a expressão de FGF8 que, portanto, será responsável pela manutenção do estado proliferativo das células da PZ (ten Berge *et al*., 2008; Church & Francis-West, 2002; Enomoto-Iwamoto *et al*., 2002; Tickle & Münsterberg, 2001). Wnt3a é expresso na AER durante todo o desenvolvimento dos membros, ativando FGF8 e garantindo o funcionamento dessa estrutura (Barrow, 2011; Church & Francis-West, 2002). Acredita-se que as moléculas Wnts juntamente com as FGFs regulam a expressão de genes envolvidos na manutenção das junções comunicantes que desempenham importante papel para o estabelecimento da morfologia da AER (Barrow, 2011; Church & Francis-West, 2002).

Outro membro da família Wnt também relacionado com o crescimento dos membros é o Wnt5a (Barrow, 2011; tem Berge *et al*., 2008). Camundongos mutantes para esse gene apresentam encurtamento dos membros e um retardo global no desenvolvimento (Barrow, 2011; Church & Francis-West, 2002). Todas as estruturas esqueléticas são afetadas, mas a gravidade das malformações é maior nas regiões mais afastadas do corpo, ou seja, encurtamento dos elementos proximais e ausência das falanges distais (Church & Francis-West, 2002). Outras áreas do corpo também se apresentam truncadas — o eixo rostrocaudal, mandíbula e genitália — sugerindo, assim, um mecanismo comum, mediado por Wnt5a, no controle do desenvolvimento de todas essas estruturas (Barrow, 2011; Church & Francis-West, 2002).

Os genes da família Wnt também atuam na padronização do eixo DV durante o desenvolvimento dos membros (Church & Francis-West, 2002). Na ausência de Wnt7a, os ossos

sesamóides e o coxim da pata são duplicados estando presentes tanto do lado ventral como dorsal, enquanto os tendões dorsais, por sua vez, assumem um padrão ventral (ten Berge *et al*., 2008; Church & Francis-West, 2002). O gene *Wnt7a* também foi descrito como regulador da padronização do eixo AP nos membros de camundongo, uma vez que ele é responsável pela ativação da expressão das moléculas de Shh na região ZPA (Church & Francis-West, 2002; Enomoto-Iwamoto *et al*., 2002; Tickle & Münsterberg, 2001). Animais mutantes para Wnt7a não possuem os dígitos posteriores, consistente com o fenótipo apresentado por camundongos deficientes em Shh (ten Berge *et al*., 2008).

Além disso, alguns pesquisadores acreditam que as moléculas Wnt estejam envolvidas na indução da miogênese dos membros de vertebrados (ten Berge *et al*., 2008; Church & Francis-West, 2002). Sabe-se que as células precursoras de músculo ao migrarem para o interior do botão do membro ainda não estão comprometidas com a diferenciação miogênica, contudo, uma vez que elas se encontram no botão do membro elas ativam a expressão dos genes *MyoD* (fator de diferenciação miogênica) e *Myf5* (fator miogênico 5) e passam a se diferenciar em mioblastos (ten Berge *et al*., 2008; Church & Francis-West, 2002; Tickle & Münsterberg, 2001). Dentro do broto do membro e mesmo durante a migração, essas células entram em contato com diferentes proteínas Wnts, tais como Wnt5a e Wnt11 (no mesênquima) e Wnt3 e Wnt4 (na ectoderme) (Church & Francis-West, 2002). O papel desempenhado pelos genes *Wnt* no controle da ativação miogênica ainda não é claro (Church & Francis-West, 2002). Contudo, foi demonstrada a habilidade das proteínas Wnt em induzir o processo de miogênese em células provenientes de somito, fato que corrobora a hipótese do envolvimento dessas proteínas na diferenciação da musculatura nos membros (Church & Francis-

West, 2002; Petropoulos & Skerjanc, 2002; Cossu *et al*., 2000). Por fim, sinais Wnts podem estar envolvidos em outros aspectos do desenvolvimento da musculatura — migração celular e morfologia. Tufan & Tuan demonstraram que o gene *Wnt7a* ativa a expressão de N-caderinas essenciais para a migração de células envolvidas na miogênese e condrogênese, reforçando a ideia de que as moléculas Wnt possuam múltiplos papeis ao longo do desenvolvimento dos membros (ten Berge *et al*., 2008; Church & Francis-West, 2002; Tufan & Tuan, 2001).

Sinais TGF-β e BMP: controle no posicionamento dos dígitos e morte celular nas áreas interdigitais

Diversos membros da superfamília TGF-β e BMP são expressos em diferentes estádios do membro em desenvolvimento, sendo que os territórios de maior expressão dessas moléculas são as regiões digitais e interdigitais no autopódio (Lorda-Diez *et al*., 2011; Newman & Bhat, 2007; Granan *et al*., 1996). Diversos estudos indicam que diferentes tipos de moléculas da superfamília TGF-β — fatores de secreção juntamente com seus receptores, moduladores extracelulares e transdutores de sinais intracelulares — controlam a escolha celular entre o destino digital ou interdigital (Lorda-Diez *et al*., 2011; Newman & Bhat, 2007; Capdevila & Belmonte, 2001; Granan *et al*., 1996). As moléculas de BMPs possuem um duplo papel durante a formação do autopódio, ora são indutoras da programação de morte celular (PMC), ora promotoras da condrogênese (Newman & Bhat, 2007; Capdevila & Belmonte, 2001). Os genes *BMP2*, *BMP4*, *BMP5* e *BMP7* são fortemente expressos nas regiões interdigitais dos botões de membros, local de ativação da PMC (Capdevila & Belmonte, 2001). Quando *beads* embebidas de proteínas BMPs são implantadas em regiões interdigitais de brotos de membros jovens, a PMC é induzida precocemente (Lorda-Diez *et al*., 2011; Newman & Bhat, 2007; Capdevila & Belmonte, 2001; Granan *et al*., 1996). Interessantemente, quando as

mesmas *beads* são implantadas próximas a regiões digitais, há maior proliferação de cartilagem nesses locais, indicando que as BMPs também atuam na proliferação e diferenciação de cartilagem (Lorda-Diez *et al*., 2011; Newman & Bhat, 2007; Capdevila & Belmonte, 2001; Granan *et al*., 1996). Experimentos envolvendo ativação constitutiva e bloqueio dos receptores de BMP concordam como a ideia de que moléculas BMPs desempenham duas funções distintas durante o desenvolvimento dos membros (Capdevila & Belmonte, 2001). Estudos dos receptores dos sinais BMPs (BMPR1A e BMPR1B) demonstraram que eles possuem funções distintas: BMPR1A, expresso no mesênquima distal, está envolvido com a PMC e BMPR1B, presente em condensações pré-condrogênicas, induz o crescimento de cartilagem (Lorda-Diez *et al*., 2011; Capdevila & Belmonte, 2001). Ademais, camundongos deficientes para ambos receptores exibiam condroplasias severas e generalizadas (Lorda-Diez *et al*., 2011).

Outra molécula da superfamília das TGF-βs, TGF-β2, atua como indutora endógena para o desenvolvimento dos dígitos no autopódio, sendo expressa em condensações pré-condrogênicas nas regiões formadoras dessas estruturas (Capdevila & Belmonte, 2001). *Beads* embebidas da proteína TGF-β2 são capazes de induzir a formação de dígitos extras quando implantadas em regiões interdigitais (Capdevila & Belmonte, 2001). Estudos indicam que a molécula TGF-β2 atua sobre as células que deixam a PZ, tornando-as capazes de se diferenciar em cartilagem quando influenciadas pelos sinais BMPs (Capdevila & Belmonte, 2001). Nas regiões interdigitais, onde TGF-β2 é ausente, BMPs podem ativar a morte celular e, dessa forma, não há formação de dígitos (Capdevila & Belmonte, 2001). Importante destacar que a indução para formação de elementos esqueléticos ao longo do eixo PD parece ser controlada por diferentes sinais, uma vez que TGF-β2 não é expresso

nos precursores esqueléticos das regiões mais proximais, estilopódio e zeugopódio (Capdevila & Belmonte, 2001).

Genes *Dpr*: possível envolvimento na formação dos membros de vertebrados

As proteínas da família Dpr são conhecidos moduladores da via de sinalização Wnt e TGF-β (Cheyette *et al*., 2002; Gloy *et al.,* 2002; Hisaka & Sokol, 2004; Zang *et al*., 2004; Brot & Sokol, 2005a). Considerando que estes sinais são essenciais para a formação dos membros durante o desenvolvimento dos vertebrados, buscamos descrever o padrão de expressão dos genes da família *Dpr* (*Dpr1* e *Dpr2*) durante o desenvolvimento dessas estruturas em embriões de galinha. A fim de estabelecer uma relação entre os domínios de expressão dos genes *Dpr* com marcadores tecido-específicos e/ou vias de sinalizações específicas, analisamos o padrão de expressão para marcadores de musculatura esquelética, tendões, articulações, bem como para precursores das vias de sinalização Wnt e TGF-β.

Nossos resultados demonstraram que os genes *Dpr* possuem um padrão dinâmico durante a ontogênese dos membros de galinha. Em membros HH24, transcritos *Dpr1* foram encontrados no mesênquima indiferenciado dos dígitos, bem como nas regiões progenitoras de cartilagem. Em HH25, *Dpr1* apresentou-se fortemente expresso nas células que contornam a região de condensação de cartilagem. Um pouco mais adiante no desenvolvimento (membros HH28-34), *Dpr1* estava expresso no pericôndrio, tendões e articulações (HH32-34). Por sua vez, *Dpr2* foi detectado nas células precursoras condrogênicas dos botões dos membros (HH24-25), no mesênquima que coincide com o local de desenvolvimento dos dígitos vestigiais I e V, nas extremidades dos dígitos em crescimento (HH28-30) e nas articulações e tendões (HH32-34).

A seguir, os resultados obtidos nessa etapa do doutorado serão expostos pelo artigo científico, "*Dact genes expression profiles suggest a role of this gene family in integrating Wnt and TGF-β signaling during chicken limb development",* aceito para publicação pela revista *Developmental Dynamics*.

Resultados – Artigo Científico

Developmental Dynamics

Dact genes expression profiles suggest a role of this gene family in integrating Wnt and TGF-β signaling pathways during chicken limb development

Lucimara Aparecida Sensiate‡, **Débora R. Sobreira**‡, Fernanda Cristina da Veiga, Denner Jefferson Peterlini, Angelica Vasconcelos Pedrosa, Thaís Rirsch, Paulo Pinto Joazeiro, Frank R. Schubert, Carla Beatriz Collares-Buzato, José Xavier-Neto, Susanne Dietrich and Lúcia Elvira Alvares

‡ Contribuição equivalente

ABSTRACT

Background: *Dact* gene family encodes multifunctional proteins that are important modulators of Wnt and TGF-β signaling pathways. Given that these pathways coordinate multiple steps of limb development, we investigated the expression pattern of the two chicken *Dact* genes (*Dact1* and *Dact2*) from early limb bud up to stages when several tissues are differentiating.

Results: During early limb development (HH24-HH30) *Dact1* and *Dact2* were mainly expressed in the cartilaginous rudiments of the appendicular skeleton and perichondrium, presenting expression profiles related, but distinct. At later stages of development (HH31-HH35), the main sites of *Dact1* and *Dact2* expression were the developing synovial joints. In this context, *Dact1* expression was shown to co-localize with regions enriched in the nuclear β-catenin protein, such as developing joint capsule and interzone. In contrast, *Dact2* expression was restricted to the interzone surrounding the domains of *bmpR-1b* expression, a TGF-β receptor with crucial roles during digit morphogenesis. Additional sites of *Dact* expression were the developing tendons and digit blastemas.

Conclusions: Our data indicate that *Dact* genes are good candidates to modulate and, possibly, integrate Wnt and TGF-β signaling during limb development, bringing new and interesting perspectives about the roles of Dact molecules in limb birth defects and human diseases.

Running-title: *Dact1* and *Dact2* expression during chicken limb development.

Key words: *Dact*, *Dapper*, Frodo, chicken embryo, Wnt, TGF-β, limb, chondrogenesis, appendicular skeleton, *Sox9*, cartilage, perichondrium, joint, digit blastema, tendon, digit morphogenesis, limb evolution.

INTRODUCTION

The *Dact* (*Dapper*/*Frodo*) gene family encodes an important group of adaptor proteins, which coordinate several developmental processes by modulating Wnt and TGF-β signaling in different cellular contexts (Brott and Sokol, 2005a). This family is represented by three members in mouse (*Dact1,2,3*), two in chicken and zebrafish (*Dact1,2*) and two highly related copies of a single *Dact* in *Xenopus* (*Dact1)* (Fisher et al., 2006; Alvares et al., 2009; Gillhouse et al., 2004; *Cheyette et al., 2002; Gloy et al., 2002*). Its members have been related to a plethora of roles during development ranging from morphogenetic movements and mesoderm specification (Waxman et al., 2004; Zhang et al., 2004) to organogenesis of brain, eye, teeth, kidney and heart (Cheyette et al., 2002; Hikasa and Sokol, 2004; Kettunen et al., 2010; Lee et al., 2010; Brott and Sokol, 2005b). Growing evidences suggest that *Dact* gene function is also crucial for biological processes occurring postnatally. For instance, *Dact1* works as a key regulator of adult adipogenesis (Lagathu et al., 2009) and different types of cancer have been associated to altered levels of *Dact* gene expression (Yau et al., 2005; Jiang et al., 2008; Xi et al., 2010; Jia et al., 2012).

In accordance to their role as adaptors, the Dact proteins physically interact with different molecules to regulate development and postnatal homeostasis. *Dact1* is certainly the most studied representative of the Dact family. This protein is able to modulate Wnt signaling by interacting with Dishevelled (Dsh), a cytoplasmatic protein that plays key roles on canonical and non-canonical Wnt pathways (Suriben et al., 2009). However, conflicting results have been reported in different studies, in which both positive and negative effects of *Dact1* on Wnt/β-catenin signaling were described (Cheyette et al., 2002; Gloy et al., 2002; Waxman et al., 2004; Zhang et al., 2006; Gao et al., 2008).

This controversy may in part be explained by the fact that *Dact1* is sensitive to phosphorylation, acting as an enhancer of Wnt signaling when phosphorylated, but inhibiting Wnt signaling when unphosphorylated (Teran et al., 2009). Dact1 also controls Wnt signaling at the level of target gene expression, since this protein physically associates with the transcriptional factor Tcf3, converting it from transcriptional repressor to activator in the presence of stabilized β-catenin, and with XDbf4, a protein involved in chromatin remodeling that inhibits β-catenin signaling (Hikasa and Sokol, 2004; Brott and Sokol, 2005b). Interestingly, the phenotype of *Dact1* mutant mice is not related to Wnt/β-catenin signaling but rather it is primarily caused by defective behavior of the transmembrane protein Vangl2, another Dact1 interacting protein, leading to a variety of posterior malformations (Suriben et al., 2009).

Dact2, the second member of the *Dact* family, is specialized in attenuating signals of the TGF-β pathway (Zhang et al., 2004). This protein directs the Alk4 and Alk5 TGF-β/Nodal receptors to degradation through a process dependent of lysosomes. In zebrafish, *Dact2* overexpression partially inhibits Nodal dependent mesoderm formation (Zhang et al., 2004). Accordingly, in *Dact2* mutant mice it was observed an acceleration of the cutaneous wound healing mediated by increased TGF-β signaling (Meng et al., 2008). However, *Dact2* seems to have additional roles since this molecule is required for convergent extension movements working as an enhancer of the Wnt/PCP pathway (Waxman et al., 2004). *Dact3* was the last member of the *Dact* gene family to be identified and, so far, no mutants were developed for this gene. Similarly to *Dact1*, *Dact3* seems to play an important role in the modulation of canonical Wnt pathway. This molecule was shown to work as a potent

inhibitor of Wnt/β-catenin signaling, which is transcriptionally repressed in colorectal cancer (Jiang et al., 2008).

The ontogenesis of limbs requires the coordinated action of Wnt and TGF-β signals. Initially, Wnt/β-catenin signaling is recruited to promote limb bud initiation through Wnt2b/Wnt8c activity in the lateral plate mesoderm of limb-forming regions, leading to stable *FGF10* expression. Shortly after, early limb patterning demands Wnt3a activity to induce the expression of other specific fibroblast growth factors, FGF4 and 8, in the ectodermal ridge at the tip of the limb bud (apical ectodermal ridge - AER), which in turn establish a positive feedback loop with FGF10 in the underlying mesenchyme that drives growth and proximo-distal patterning (Kawakami et al., 2001). The FGF system interacts with the zone of polarizing activity (ZPA) located at the posterior limb mesenchyme that secrets the signaling molecule Shh and sets up the anteroposterior pattern (Yang and Niswander, 1995). Dorso-ventral patterning is generated by polarized expression of *Wnt7a* in the dorsal and of the transcription factor *Engrailed-1* in the ventral limb ectoderm (Riddle et al., 1995). The coordinate action of AER, ZPA and non-AER ectoderm culminates with the formation of a standardized arrangement of skeletal elements, comprising a single long bone in the proximal limb segment (stylopod), two long bones in the intermediate segment (zeugopod) and several small bones and, usually, five digits in the most distal segment (autopod) (Newman and Bhat, 2007). During late limb morphogenesis, Wnt and TGF-β systems are tightly integrated to promote endochondral bone formation and joint development [reviewed in (DeLise et al., 2000)]. While Wnts usually have a negative effect on chondrogenesis, members of the TGF-β family display remarkable chondrogenic properties. For instance, bone morphogenetic proteins (BMPs), TGF-β proteins and

activins are all able to induce cartilage formation when ectopically expressed in the interdigital membrane of developing limbs (Millan et al., 1991; Ganan et al., 1996; Merino et al., 1999a; Merino et al., 1999b). Besides, BMPs act at multiple steps of chondrogenesis, being necessary for recruitment of mesenchymal cells to the chondrogenic fate, as well as to the condensation and maturation of chondrocytes in a process that leads to activation of *Sox9,* a transcription factor necessary and sufficient to promote chondrogenesis (Duprez et al., 1996a; Duprez et al., 1996b; Zou and Niswander, 1996). Wnt3a was shown to have an antagonistic effect on BMP-2 mediated chondrogenesis at the stage of mesenchymal condensation (Fischer et al., 2002). This Wnt inhibitory effect on chondrogenesis results in transcriptional repression of *Sox9* (ten Berge et al., 2008). Interestingly, a reverse regulatory loop seems to exist between *Sox9* and Wnts, since *Sox9* inhibits the anti-chondrogenic effects of the canonical Wnt signaling by inhibiting the transcriptional activation of β-catenin and increasing the rate of β-catenin degradation (Topol et al., 2009). In spite of the strong evidences indicating an inhibitory effect of canonical Wnt signaling on chondrogenesis, it is possible that different Wnts and/or Wnt pathways have different roles on chondrogenesis. This view is supported by the fact that several Wnts are expressed at chondrogenic areas of the developing limb such as perichondrium, prehypertrophic chondrocytes and joints (Hartmann and Tabin, 2000; Witte et al., 2009). Besides, non-canonical Wnt signaling has been related to limb elongation, chondrocyte proliferation and differentiation (Yamaguchi et al., 1999; Yang et al., 2003). At later phases of development, *Wnt4* and *Wnt9a* act to direct chondro-synovioprogenitors to the synovial fate maintaining joints integrity during development, in a process that occur in concert with the activity of *Gdf5,* a TGF-β molecule that works as a master regulator of joints development (Francis-West et al., 1999; Storm and Kingsley, 1999; Spater et al., 2006). Thus, Wnt and TGF-β

signaling play crucial roles and interact at multiple points during limb development, although the mechanisms by which this coordinated action is promoted are not well understood.

In order to address possible roles of the *Dact* gene family in regulating Wnt and/or TGF-β dependent processes during chicken limb development it is paramount to determine their spatial-temporal expression profiles. To do that we investigated *Dact* gene expression during chicken limb outgrowth, patterning and tissue differentiation, and compared their expression with known markers for muscle, tendon, muscle connective tissue, cartilage, bone and synovial joint development. Our results showed that *Dact* genes are dynamically expressed in the developing cartilaginous rudiments of bones, perichondrium and joints, suggesting that this gene family collaborate to build the chicken appendicular skeleton. Moreover, *Dact* genes are expressed in developing tendons, as well as in the digit blastemas. Taken together, our data suggest that *Dact1 and Dact2* act in concert to promote the development of multiple chicken appendage structures, possibly by modulating and/or integrating Wnt and TGF-β signaling pathways.

RESULTS

Time-course of Dact1 and Dact2 expression during limb outgrowth, patterning and early development of the appendicular skeleton

To investigate the expression of the chicken *Dact* genes during early limb development, we determined their expression patterns from stage HH24/E4 to HH30/E6 (Hamburger and Hamilton, 1992). This encompasses stages from outgrowth and patterning of the limb bud to the assembling of several tissues, including the cartilaginous rudiments of the appendicular skeleton. For each

developmental stage analyzed we also determined the expression of *Sox9*, an early marker for chondrogenesis whose dynamic expression gradually reveals the cartilaginous elements formed in the developing limbs, prefigurating the appendicular skeleton (Chimal-Monroy et al., 2003). The time-course of *Dact* genes and *Sox9* expression was established by whole-mount *in situ* hybridization (ISH) of fore and hindlimbs. Details were obtained by vibratome sections, or by ISH in paraffin sections.

By HH24, *Dact1* expression was observed in a wide domain in the proximal central core of developing fore and hindlimb buds (Fig.1A,E). Cross-sections revealed that *Dact1* transcripts were associated to the pluripotent mesenchymal cells, while no expression was observed in the overlying ectoderm (Fig.1Ai,Ei). *Dact2* also displayed a mesenchymal expression, however its transcripts were enriched in a subpopulation of cells with prechondrogenic characteristics. In the forelimb, these *Dact2* expressing cells were concentrated at the border between the stylopod and trunk, where the cartilaginous template for the humerus bone forms (Fig.1I arrowhead, Ii). In the hindlimb, *Dact2* expression was associated to prechondrogenic condensations of femur (Fig.1M, arrowhead), tibia and fibula, as well as to the digital arch (Fig.1M,Mi), which contains cartilaginous precursors for autopodial bones. As previously described by others (Chimal-Monroy et al., 2003), *Sox9* expression was detected in prechondrogenic cells of fore and hindlimb buds (Fig.1Q,Qi,U,Ui), in a pattern similar but not identical to the one observed for *Dact2*.

At stage HH25, *Dact1* expression extended distally in the fore and hindlimbs reaching the developing autopod, although its expression was weaker in that compartment than in the zeupopod and stylopod segments (Fig.1B,F). Cross-sections showed that *Dact1* transcripts were concentrated

in the central domain of developing limb buds (Fig.1Bi,Fi), in a region known to contain cells that are initiating the process of cartilage condensation and differentiation (Kulyk et al., 1989). Similarly, *Dact2* expression remained associated to prechondrogenic mesenchymal cells, which were already aggregating to build cartilaginous templates for wing and leg bones (Fig.1J,Ji,N,Ni). In the forelimb, *Dact2* expression was prominent in the radio precursor as well as in the digital arch, but it was faint in the ulna template (Fig.1J,Ji). Likewise, in the hindlimb stronger *Dact2* expression was observed antero-distally in the developing anlagens for femur (Fig.1N, arrowhead), tibia and digital arch, including the precursors for metatarsal bones, while a weaker expression was associated to the posterior fibula cartilaginous template (Fig.1N,Ni). Further details of the *Dact1* and *Dact2* expression profiles were obtained by the analyses of planar sections of HH25 hindlimbs (Fig.1α,γ). These results showed that while *Dact1* transcripts are located mainly in the periphery of the developing skeleton rudiments, circumventing the central chondrogenic core, *Dact2* transcripts encompassed the whole cartilaginous templates. *Sox9* mRNAs were found in the cartilage rudiments of humerus/femur, radio/tibia, ulna/fibula and digital arch (Fig.1R,Ri,V,Vi), in accordance to its role as a key regulator of early chondrogenesis (Akiyama et al., 2002).

At HH28, *Dact1* expression was associated to the mesenchyme involving the cartilaginous templates, as well as to the developing joints (Fig.1C,Ci,G,Gi). Similarly, *Dact2* expression was found to avoid the condensed cartilage of digit rays, but a weak expression was observed in the anterior margin the radio (forelimb) and tibia (hindlimb) templates, as well as in the posterior margin of the ulna (forelimb) template (Fig.1K,O arrowheads). Interestingly, in the autopod the distribution of *Dact2* transcripts was also found to be polarized, with a higher concentration of mRNAs located on

its most anterior and posterior ends (Fig.1K,Ki,O,Oi). These prominent sites of *Dact2* expression encompassed the anlagens for digits I and V in the forelimb and presumptive digit I in the hindlimb, which fail to reach the condensation stage during development of the wing and leg of chicken embryos, respectively (Welten et al., 2005). Thus, it may be speculated that, in birds, *Dact2* has a role in the morphogenesis process that leads to the typical pattern of three (wing) and four (leg) digits in the autopod. Finally, a new domain of *Dact2* expression was identified at the tip of the digit blastemas in the hindlimb (Fig.1O, asterisks). This region is known to coordinate the formation of digit mesenchymal aggregates and its differentiation in chondrogenic cells, in a process mediated by high levels of TGF-β signaling (Montero et al., 2008). For this reason, this distal condensing mesenchyme is also known as phalanx-forming region or digital crescent (Witte et al. 2010). *Dact1* and *Dact2* expression profiles were also evaluated by ISH in planar sections (Fg.1β,δ). The results obtained confirmed that *Dact* genes were coexpressed in the undifferentiated limb mesenchyme and perichondrium, while *Dact2* was also expressed in the digit blastemas. During this period, most sites of *Sox9* expression were complementary to those observed for the *Dact* genes, because while its transcripts were concentrated in the differentiating chondrogenic cells (Fig.1S,Si,W,Wi), *Dact* genes seem to surround sites where cartilage differentiation is taking place.

At HH30, *Dact1* expression was still maintained in the mesenchymal cells around the developing appendicular skeleton (Fig.1D,H). Besides, a prominent expression became conspicuous in the elbow/knee (Fig.1Di,H), wrist/ankle and metacarpal/metatarsal phalangeal joints (Fig.1D,H). New domains of *Dact1* expression were identified in the digit blastemas (Fig.1H, asterisks) and around tendon anlagens (Fig.1Hi). Likewise, *Dact2* transcripts were also found in the joints of fore

and hindlimbs and in the digit blastemas (Fig.1L,Li,P,Pi). The expression domain encompassing the putative anlagens for digits I and V was still conspicuous in the developing wing, while a weaker expression was observed in the region corresponding to the anlagen for digit V in the hindlimb, thus reinforcing the hypothesis that *Dact2* is involved in digit patterning at the chicken autopod (Fig.1L,Li, arrowheads). *Sox9* mRNAs were associated to the developing joints as well as to digit blastemas (Fig.1T,Ti,X,Xi; asterisks), where its expression seems to overlap with *Dact1* and *Dact2* expression.

In order to clarify the spatial correlation between *Dact1*/*Dact2* and *Sox9* expression profiles from HH25 to HH30, we compared their expression patterns in limbs obtained from single embryos. These embryos were split into two. One half was hybridized either with *Dact1,* or with *Dact2,* while the other half was hybridized with *Sox9*, assuring that the compared limbs were exactly at the same developmental stage. These analyses confirmed our initial results showing the presence of both complementary and overlapping expression domains between *Dact* genes and *Sox9* (Suppl.Fig.S1). Thus, different populations of chondroprogenitor cells are found in the limb bud at early limb development, which are characterized by the expression of different combinations of *Dact1, Dact2* and *Sox9* mRNAs.

Overall, our analysis revealed a prominent expression of the *Dact* genes in the developing limbs at stages when the major limb tissues are being laid down. Their expression patterns indicate that the chicken *Dact* genes act synergistically to promote the formation of the appendicular skeleton. However, in spite of the similarities between the expression profiles of *Dact genes* and *Sox9*, a key regulator of chondrogenesis, their expression patterns are not spatial/temporally equivalent. This suggests that these genes may have related, but distinct functions during

endochondral bone formation in chicken. For this reason, we performed a comparison of the *Dact* expression with a panel of markers for muscle, connective tissue, tendons and developing skeletal elements.

Dact1 and Dact2 expression during tissue differentiation and digit formation

To further investigate the correlation between *Dact* expression domains and development of specific tissues, we selected a set of established markers for skeletal muscle, muscle connective tissue, tendon, joint, cartilage and bone development. Moreover, as *Dact* genes are known modulators of the Wnt and TGF-β signals, we included among these markers molecules belonging to these signaling pathways, which are known to be related to the development of particular cell types/tissues in the limb environment (see details in Suppl. Table 1). This analysis was done by whole-mount ISH in fore and hindlimbs and the details obtained by vibratome sectioning. The comparisons were performed at HH35/E8 (Fig.2) and HH31/E7 (Suppl.Fig.S2), when the main tissues of the developing limb are already differentiating.

At late limb development, *Dact1* mRNAs were profusely distributed in the undifferentiated limb mesenchyme surrounding the cartilage elements and tendons, as well as in the perichondrium (Fig.2A,Ai,Aii; Suppl.Fig.S2). In turn, *Dact2* was expressed at lower levels in these tissues, particularly at HH35 (Fig.2B,Bi,Bii; Suppl.Fig.S2). Among the markers expressed in the undifferentiated limb mesenchyme were the transcription factor *Tcf4* (Fig.2E,Ei,Eii), the Wnt antagonists *Sfrp2* (Fig.2F,Fi,Fii) and *Sfrp3* (Fig.2L,Li,Lii; Suppl.Fig.S2), the tendon/ligaments marker *Scleraxis* (Scx; Fig.2G,Gi,Gii), the transcriptional repressor *Zeb2* (Fig.2H,Hi,Hii; Suppl.Fig.S2) and the signaling molecule *Wnt9A* (Fig.2I,Ii,Iii; Suppl.Fig.S2). Among these, *Sfrp3* (Suppl.Fig.S2), *Scx* (Fig.2Gii;

Suppl.Fig.S2) and *Wnt9A* (Fig.2Iii) were also expressed in the perichondrium together with a weak expression of the joint marker *Gdf5* (Fig.2Jii). Around the developing tendons, it was possible to identify a belt of *Dact1*-expressing cells surrounding the tendon anlagens, while *Dact2* expression partially overlaped with *Scx* (Fig.2Aii,Bii; Suppl.Fig.S3). Digit blastemas exhibited a prominent *Dact2* expression accompanied by a weaker expression of *Dact1,* as observed in the previous stages of limb development (Fig.2B,Bi,A,Ai). Two other molecules were also expressed in the digit blastemas: *Gdf5* (Fig.2J,Ji) and the cartilage marker *Sox9* (Fig.2K,Ki). Finally, the developing joints were identified as sites of conspicuous *Dact* gene expression. *Dact1* transcripts were associated to different subgroups of developing joints, including the wrist, ankle and interphalangeal joints (Fig.2A,Ai). This joint-related expression was particularly strong in the mesenchyme surrounding the metatarsophalangeal and interphalangeal joints of the hindlimb, where it produced ring-like domains separating adjacent skeletal elements (Fig.2Ai). Likewise, *Dact2* displayed a remarkable expression in the developing joints of wing and leg, resembling the conspicuous pattern of *Gdf5* (Fig.2B,Bi,J,Ji). *Dact* genes were not associated to skeletal muscle (Fig.2C,Ci,Cii,D,Di,Dii), muscle connective tissue (Fig.2E,Ei,Eii), prehypertrophic cartilage (Fig.2M,Mi,Mii) and bone (Fig.2N,Ni,Nii) development.

A more detailed interpretation of the spatial distribution of *Dact* transcripts in developing joints was obtained by comparing longitudinal vibratome sections of those markers whose expression was mostly associated to digits and ankle joints (Fig.3). These results confirmed that *Dact1* is expressed in the undifferentiated mesenchyme surrounding the growing digits (Fig.3A), in a pattern related to that observed for the joint-inducing factor *Wnt9a* (Fig.3D,Di,Dii) and *Sfrp3* (Fig.3G,Gi,Gii). A remarkable mesenchymal expression was also identified for the TGF-β inhibitor

Zeb2 (Fig.3C). Moreover, it was possible to identify *Dact1* and *Dact2* transcripts at the interzones of digit and ankle joints (Fig.3A,Ai,Aii,B,Bi,Bii;asterisks), in a pattern similar to observed for *Gdf5* (Fig6.E,Ei,Eii) and *Wnt9a* (Fig.3Di,Dii), while it partially overlapped with *Sox9* domains in the regions surrounding the joints (Fig.3F,Fi,Fii). However, *Sox9* and *Sfrp3* mRNAs were mainly associated to the epiphysis of developing phalanges (Fig.3F,Fi,Fii,G,Gi,Gii). In the digit blastemas, *Dact1* and *Dact2* were co-expressed with *Gdf5* and *Sox9* (Fig.3A,B,E,F;arrowheads).

In conclusion, our data revealed that the main sites of *Dact* gene expression between HH31 and HH35 correspond to undifferentiated limb mesenchyme, perichondrium, tendons, digit blastemas and joints. The expression profile of *Dact* genes suggests that these molecules might be involved in the modulation of Wnt and TGF-β pathways during skeletogenesis including digit and joints morphogenesis. To further address this issue, we examined the distribution of nuclear β-catenin by immunohistochemistry to establish a possible spatial correlation with sites of *Dact1* transcription. In parallel, the expression of type I BMP receptor gene *bmpR-1b,* a central transducer involved in formation of digital cartilages (Merino et al., 1998), was examined with the purpose of establishing a possible association with *Dact2* expression domains and regions of active TFG-β signaling. Dact2 is known to inhibit TFG-β signals by driving TFG-β receptors to degradation via a lysosome-dependent process (Zhang et al., 2004).

***Dact1 is co-expressed with nuclear β-catenin, while Dact2 display an expression profile complementary to bmpR-1b* in the digit joints**

Examination of ISH in longitudinal tissue sections of HH35 chick digits allowed a deeper evaluation of *Dact* gene expression in the developing joints (Fig.4). For instance, it was possible to

identify the joint capsule (arrow, Fig.4A,Ai) as a new site of *Dact1* expression, while its expression in the interzone of interphalangeal joints and undifferentiated mesenchyme surrounding the growing digits confirmed our previous findings (Fig.4A,Ai). *Dact1* transcripts were located in the differentiating chondrocytes of developing phalanges. A clear correlation between sites of *Dact1* expression and the location of nuclear β-catenin was observed (Fig.4B,Bi). For instance, high levels of the β-catenin protein were observed in cells of the developing joint capsule, as well as in the interzone, which are both sites of intense *Dact1* transcription (Fig.4A,Ai,B,Bi). This finding suggests that *Dact1* is modulating Wnt/β-catenin pathway at particular sites of forming joints during late limb morphogenesis. In contrast, an opposite correlation was identified between *Dact2* and *bmpR-1b* expression profiles. While *Dact2* transcripts were clearly restricted to interzones, in a pattern similar but broader that the one observed for *Gdf5* (Fig.4C,Ci,E,Ei), *bmpR-1b* mRNAs were located in the developing phalangeal cartilages (Fig.4D,Di). *bmpR-1b* has been described as a key molecule involved in digit chondrogenesis and changes in cartilage development induced by different molecules such as FGFs, TGFs and BMPs requires previous modifications in the *bmpR-1b* expression levels (Zou and Niswander, 1996; Merino et al., 1998). Thus, we found reasonable to believe that regions of the developing digits expressing *bmpR-1b* are under the influence active TGF-β signaling. Accordingly, our data showed that *bmpR-1b* expression was restricted the developing cartilaginous templates of phalanges (Fig.4D,Di) while *Dact2* mRNAs were gathered in the phalangeal interzones (Fig.4C,Ci). These expression patterns suggest that *Dact2* might be preventing TGF-β signals from reaching the developing joints (via *bmpR-1b* or other TGF-β receptors), since this could lead interzone cells to follow the chondrogenic program disrupting joint formation.

DISCUSSION

Dact proteins are multifunctional molecules implicated in a myriad of developmental processes due to their ability to interact with multiple molecules depending on the cellular context. Recent findings have shown that these molecules are able to form homo and heterodimers in addition to being able to interact with several kinases, expanding the number of potential Dact partners (Kivimae et al., 2011). This possibly suggests that new functions of the Dact proteins remain to be unveiled both in development and in the maintenance of homeostasis during postnatal life.

In this study, we described the dynamic expression of the *Dact* genes during limb development, from limb bud outgrowth and patterning, to tissue differentiation. *Dact1* was found to be expressed throughout the undifferentiated limb mesenchyme at the onset of chondrogenic progenitor condensation (HH24). However, slightly later (HH25), this gene was upregulated in cells circumventing the cartilaginous condensations in a pattern partially complementary to *Dact2*. Given that Dact1 was shown to regulate Vangl2, a key component of the planar cell polarity (PCP)/Wnt pathway (Suriben et al., 2009), it is possible that this protein has a role in controlling cartilaginous precursor condensation by modulating the activity of adhesion molecules. Alternatively, considering that Wnt/β-catenin activity has an inhibitory role during chondrogenesis, it might be speculated that *Dact1* would regulate Wnt signaling at the border between chondrogenic and prechondrogenic regions (Hartmann and Tabin, 2000).

Likewise, *Dact2* expression was clearly associated to chondroprogenitor cells of the appendicular skeleton. This expression seems to precede *Sox9* activation in the cartilaginous templates. suggesting that *Dact2* acts upstream of *Sox9* during the initial phase of chondrogenesis,

probably during the aggregation of prechondrogenic cells. Considering that *Dact2* has an established role in inhibiting TGF-β signaling by promoting the degradation of Alk4/5 type I receptors (Zhang et al., 2004), it is possible that this gene inhibits precocious activation of TGF-β signaling in the subset of mesenchymal cells committed to the cartilage fate, playing a role complementary to *Sox9*. Thus, *Dact2* might be acting in parallel to adhesion molecules such as N-cadherin and N-CAM (Widelitz et al., 1993) to coordinate the condensation of chondromesenchymal precursors, while maintaining these cells in an undifferentiated stage. This hypothesis is reinforced by the complementarity between several *Dact2* and *Sox9* expression domains between HH25 and HH30. At later stages of chondrogenesis, both *Dact1* and *Dact2* are coexpressed in the perichondrium, possibly maintaining these cells in a proliferative and undifferentiated state.

The anteroposteriorly polarized expression of *Dact2* between HH28-HH30 limbs suggests that the inhibitory role of *Dact2* in chondrogenesis has been adapted to drive the characteristic morphogenesis of the chicken appendicular skeleton, which is composed by three digits in the wing and four digits in the leg. It was observed that the anlagens for digits I/V (wing) and I (leg) start to develop, but fail to reach the condensation stage of chondrogenesis (Welten et al., 2005). Thus, it is possible that, by maintaining low levels of TGF-β signaling at specific sites during skeleton morphogenesis, *Dact2* disrupts the chondrogenic program that would allow these digits to further proceed in development. This is an interesting possibility that deserves further investigation by functional and/or evolutionary studies.

In parallel to their expression in the developing cartilaginous rudiments, *Dact* genes are conspicuously expressed in the forming joints. Joint development occurs in parallel to

chondrogenesis and requires the suppression of the cartilage fate in a specific region of the chondrogenic condensation to form the interzone. In this region, molecules such as Wnt9a (previously Wnt14) and BMP inhibitors are expressed to block the activation of the chondrogenic program (Hartmann and Tabin, 2001). The expression pattern of the *Dact* genes identified in this study strongly suggests the *Dact1* is cooperating with *Wnt9a* to generate a non-chondrogenic domain in the interzone, since these genes are co-expressed at that domain. The high levels of nuclear β-catenin in the *Dact1* positive domains of developing joints confirms that this gene is expressed in sites of active canonical Wnt signaling. In this context, *Dact2* seems to act synergistically with *Dact1* by inhibiting TGF-β signaling in the interzone, probably by degrading specific TGF-β receptors, which is crucial to suppress chondrogenesis and promote joint formation. Besides, our data suggest a possible cooperation between *Dact2* and *Gdf5* in the process of joint development, although the mechanisms through which it occurs remain to be established.

Developing tendons were also associated to sites of *Dact* activity at late stages of limb development. Given that *Dact1* transcripts are distributed as a belt surrounding *Scx* positive cells, it may be speculated that this molecule is contributing to the recruitment of precursor cells to tendon anlagens by modulating Wnt signaling around the forming tendons. A balance between Wnt and FGF signals is required to coordinate the separation of skeletal versus soft connective tissue during limb morphogenesis (ten Berge et al., 2008). Interestingly, a second wave of tendon formation is TGF-β dependent (Schweitzer et al., 2010). Given the molecular properties of *Dact2* protein, it is possible that this gene regulates the second wave of tendon formation.

Another possible role of the *Dact* genes is suggested by their expression domain in the digit blastemas. These genes might be responsible for the maintenance of a pool of cells in an undifferentiated and proliferative state, promoting digit outgrowth. Interestingly, it has been shown that the tip of developing digits are regions of high level of TGF-β signaling that drive the incorporation and differentiation of precursor cells in the digit rays (Merino et al., 1999a; Montero et al., 2008). It will be important to establish if the *Dact2* and TGF-β molecules are expressed in different subgroups of cells at the digit blastemas. Considering the role of *Dact2* as inhibitor of TGF-β signaling, it would be possible that this molecule is being expressed in a subgroup of cells at the tip of the digits to protect these cells from a premature contact with TGF-β signals, maintain its population in a precursor state.

Taken together, our findings suggest that the *Dact* genes work synergistically to promote the development of several tissues/structures in the avian appendage, including the cartilaginous skeleton, tendons and joints. Moreover, the expression of *Dact* genes in sites such as undifferentiated mesenchyme, perichondrium, tendon anlagens and digit blastema suggest that *Dact* genes might be involved in the maintenance of a multipotent state in different sub-groups of mesenchymal precursors.

EXPERIMENTAL PROCEDURES

Embryos

Fertilized eggs were acquired from Yamaguishi Community Organic Farm (Yamaguishi, Brazil) and incubated at 38.5°C in a humidified atmosphere. Chicken embryos were harvested and had the

extra-embryonic membranes removed in phosphate-buffered saline (PBS) before being fixed in 4% paraformaldehyde/PBS overnight at 4°C. Staging was performed according to (Hamburger and Hamilton, 1992).

Clones and probes synthesis

The plasmids used to synthesize the probes for chicken *Dact1* and *Dact2* were previously described (Alvares et al., 2009). Chicken clones employed to generate probes for several tissue specific markers or Wnt/TGF-β signaling related molecules were either cloned by others or purchased from Source BioScience UK Ldt, Nottingham. Antisense and control RNA probes were digoxygenin-labeled using specific RNA polymerases. After being synthesized, each probe was run on a 1.5% agarose gel to check its integrity. The information about the probes used in this work was summarized in Table 1.

***In situ* hybridization of whole-mount and tissue sections of limbs**

Whole-mount ISH and vibratome sectioning of limbs were performed as previously described (Mootoosamy and Dietrich, 2002). The protocol for ISH on tissue sections was adapted from Moorman et al. (Moorman et al., 2001) with some modifications. Briefly, paraffin sections were 8µm-thick and proteinase K treatment was performed with 10µg/mL enzyme during 4 min. Hybridization and post-hybridization temperature was 55°C. The specificity of staining was monitored using sense RNA probes. Whole-mount limb images were captured on a Leica MZ16 F stereo microscope with transmitted light. Vibratome and paraffin sections were photographed on a Nikon Eclipse E800 microscope.

Immunolocation of active beta-catenin

The tissue location of active beta-catenin was performed by using a standard indirect immunoperoxidase method. After paraffin removal, embryo sections (8 µm) were rehydrated and treated at high temperature with 0.01M sodium citrate buffer (pH 6.0) to retrieve the tissue antigenicity. After washing with 0.05M Trisma-buffered saline (TBS, pH 7.4) and blockage of the endogenous peroxidase activity with 3% H_2O_2 in methanol, the sections were incubated for 1 h with TTBS (0.1% Tween 20 and 5% of dry skimmed milk in TBS) followed by incubation with the primary antibody (dilution 1:50; anti-ABC, Millipore) overnight at 4^{o}C. After washing with TBS, the sections were incubated at room temperature (RT) for 40 min with a specific biotinylated secondary antibody (dilution 1:100; Jackson ImmunoResearch) and then with HRP–Streptavidin solution (dilution 1:200; Invitrogen) for 30 min at RT. Then, sections were treated with 10% 3,3'diaminobenzidine (DAB, in Tris HCl buffer 0.1 M, pH 7.4) (Sigma) and 0.2% H_2O_2 in TBS. Finally, the sections were quickly stained with Ehrlich's Hematoxylin and mounted for optical microscopy observation.

ACKNOWLEDGEMENTS

We thank Natália Roberta dos Santos, Célia Aparecida Almeida Chaves Garcia and Luana Nunes Santos for technical help during the development of this work. This work was supported by grants from FAPESP (2006/05892-3) to Lúcia Elvira Alvares and from AFM (The Association Française Contre les Myopathies) to Susanne Dietrich.

REFERENCES

Akiyama H, Chaboissier MC, Martin JF, Schedl A, de Crombrugghe B. 2002. The transcription factor Sox9 has essential roles in successive steps of the chondrocyte differentiation pathway and is required for expression of Sox5 and Sox6. Genes Dev 16:2813-2828.

Alvares LE, Winterbottom FL, Jorge EC, Rodrigues Sobreira D, Xavier-Neto J, Schubert FR, Dietrich S. 2009. Chicken dapper genes are versatile markers for mesodermal tissues, embryonic muscle stem cells, neural crest cells, and neurogenic placodes. Dev Dyn 238:1166-1178.

Bober E, Brand-Saberi B, Ebensperger C, Wilting J, Balling R, Paterson BM, Arnold HH, Christ B. 1994. Initial steps of myogenesis in somites are independent of influence from axial structures. Development. 120, 3073-82.

Brott BK, Sokol SY. 2005a. Frodo proteins: modulators of Wnt signaling in vertebrate development. Differentiation 73:323-329.

Brott BK, Sokol SY. 2005b. A vertebrate homolog of the cell cycle regulator Dbf4 is an inhibitor of Wnt signaling required for heart development. Dev Cell 8:703-715.

Cheyette BN, Waxman JS, Miller JR, Takemaru K, Sheldahl LC, Khlebtsova N, Fox EP, Earnest T, Moon RT. 2002. Dapper, a Dishevelled-associated antagonist of beta-catenin and JNK signaling, is required for notochord formation. Dev Cell 2:449-461.

Chimal-Monroy J, Rodriguez-Leon J, Montero JA, Ganan Y, Macias D, Merino R, Hurle JM. 2003. Analysis of the molecular cascade responsible for mesodermal limb chondrogenesis: Sox genes and BMP signaling. Dev Biol 257:292-301.

DeLise AM, Fischer L, Tuan RS. 2000. Cellular interactions and signaling in cartilage development. Osteoarthritis Cartilage 8:309-334.

Duprez D, Bell EJ, Richardson MK, Archer CW, Wolpert L, Brickell PM, Francis-West PH. 1996a. Overexpression of BMP-2 and BMP-4 alters the size and shape of developing skeletal elements in the chick limb. Mech Dev 57:145-157.

Duprez DM, Kostakopoulou K, Francis-West PH, Tickle C, Brickell PM. 1996b. Activation of Fgf-4 and HoxD gene expression by BMP-2 expressing cells in the developing chick limb. Development 122:1821-1828.

Francis-West, P. H., et al., 1999. Mechanisms of GDF-5 action during skeletal development. Development. 126**,** 1305-15.

Fischer L, Boland G, Tuan RS. 2002. Wnt signaling during BMP-2 stimulation of mesenchymal chondrogenesis. J Cell Biochem 84:816-831.

Fisher DA, Kivimae S, Hoshino J, Suriben R, Martin PM, Baxter N, Cheyette BN. 2006. Three Dact gene family members are expressed during embryonic development and in the adult brains of mice. Dev Dyn 235:2620-2630.

Francis-West PH, Abdelfattah A, Chen P, Allen C, Parish J, Ladher R, Allen S, MacPherson S, Luyten FP, Archer CW. 1999. Mechanisms of GDF-5 action during skeletal development. Development 126:1305-1315.

Ganan Y, Macias D, Duterque-Coquillaud M, Ros MA, Hurle JM. 1996. Role of TGF beta s and BMPs as signals controlling the position of the digits and the areas of interdigital cell death in the developing chick limb autopod. Development 122:2349-2357.

Gao X, Wen J, Zhang L, Li X, Ning Y, Meng A, Chen YG. 2008. Dapper1 is a nucleocytoplasmic shuttling protein that negatively modulates Wnt signaling in the nucleus. J Biol Chem 283:35679-35688.

Goulding M, Lumsden A, Paquette AJ. 1994. Regulation of Pax-3 expression in the dermomyotome and its role in muscle development. Development. 120, 957-71.

Gillhouse M, Wagner Nyholm M, Hikasa H, Sokol SY, Grinblat Y. 2004. Two Frodo/Dapper homologs are expressed in the developing brain and mesoderm of zebrafish. Dev Dyn 230:403-409.

Gloy J, Hikasa H, Sokol SY. 2002. Frodo interacts with Dishevelled to transduce Wnt signals. Nat Cell Biol 4:351-357.

Hamburger V, Hamilton HL. 1992. A series of normal stages in the development of the chick embryo. 1951. Dev Dyn 195:231-272.

Hartmann C, Tabin CJ. 2000. Dual roles of Wnt signaling during chondrogenesis in the chicken limb. Development 127:3141-3159.

Hartmann C, Tabin CJ. 2001. Wnt-14 plays a pivotal role in inducing synovial joint formation in the developing appendicular skeleton. Cell 104:341-351.

Healy C, Uwanogho D, Sharpe PT**.** 1996. Expression of the chicken Sox9 gene marks the onset of cartilage differentiation. Ann N Y Acad Sci. 785**,** 261-2.

Hikasa H, Sokol SY. 2004. The involvement of Frodo in TCF-dependent signaling and neural tissue development. Development 131:4725-4734.

Jia Y, Yang Y, Brock MV, Zhan Q, Herman JG, Guo M. 2012. Epigenetic Regulation of DACT2, A Key Component of the Wnt Signaling Pathway in Human Lung Cancer. J Pathol.

Jiang X, Tan J, Li J, Kivimae S, Yang X, Zhuang L, Lee PL, Chan MT, Stanton LW, Liu ET, Cheyette BN, Yu Q. 2008. DACT3 is an epigenetic regulator of Wnt/beta-catenin signaling in colorectal cancer and is a therapeutic target of histone modifications. Cancer Cell 13:529-541.

Kardon G, Harfe BD, Tabin CJ. 2003. A Tcf4-positive mesodermal population provides a prepattern for vertebrate limb muscle patterning. Dev Cell. 5**,** 937-44.

Kawakami Y, Capdevila J, Buscher D, Itoh T, Rodriguez Esteban C, Izpisua Belmonte JC. 2001. WNT signals control FGF-dependent limb initiation and AER induction in the chick embryo. Cell 104:891-900.

Kettunen P, Kivimae S, Keshari P, Klein OD, Cheyette BN, Luukko K. 2010. Dact1-3 mRNAs exhibit distinct expression domains during tooth development. Gene Expr Patterns 10:140-143.

Kivimae S, Yang XY, Cheyette BN. 2011. All Dact (Dapper/Frodo) scaffold proteins dimerize and exhibit conserved interactions with Vangl, Dvl, and serine/threonine kinases. BMC Biochem 12:33.

Kulyk WM, Upholt WB, Kosher RA. 1989. Fibronectin gene expression during limb cartilage differentiation. Development 106:449-455.

Lagathu C, Christodoulides C, Virtue S, Cawthorn WP, Franzin C, Kimber WA, Nora ED, Campbell M, Medina-Gomez G, Cheyette BN, Vidal-Puig AJ, Sethi JK. 2009. Dact1, a nutritionally regulated preadipocyte gene, controls adipogenesis by coordinating the Wnt/beta-catenin signaling network. Diabetes 58:609-619.

Ladher RK, Church VL, Allen S, Robson L, Abdelfattah A, Brown NA, Hattersley G, Rosen V, Luyten FP, Dale L, Francis-West PH. 2000. Cloning and expression of the Wnt antagonists Sfrp-2 and Frzb during chick development. Dev Biol. 218**,** 183-98.

Lee WC, Hough MT, Liu W, Ekiert R, Lindstrom NO, Hohenstein P, Davies JA. 2010. Dact2 is expressed in the developing ureteric bud/collecting duct system of the kidney and controls morphogenetic behavior of collecting duct cells. Am J Physiol Renal Physiol 299:F740-751.

Meng F, Cheng X, Yang L, Hou N, Yang X, Meng A. 2008. Accelerated re-epithelialization in Dpr2-deficient mice is associated with enhanced response to TGFbeta signaling. J Cell Sci 121:2904-2912.

Merino R, Ganan Y, Macias D, Economides AN, Sampath KT, Hurle JM. 1998. Morphogenesis of digits in the avian limb is controlled by FGFs, TGFbetas, and noggin through BMP signaling. Dev Biol 200:35-45.

Merino R, Macias D, Ganan Y, Rodriguez-Leon J, Economides AN, Rodriguez-Esteban C, Izpisua-Belmonte JC, Hurle JM. 1999a. Control of digit formation by activin signalling. Development 126:2161-2170.

Merino R, Rodriguez-Leon J, Macias D, Ganan Y, Economides AN, Hurle JM. 1999b. The BMP antagonist Gremlin regulates outgrowth, chondrogenesis and programmed cell death in the developing limb. Development 126:5515-5522.

Millan FA, Denhez F, Kondaiah P, Akhurst RJ. 1991. Embryonic gene expression patterns of TGF beta 1, beta 2 and beta 3 suggest different developmental functions in vivo. Development 111:131-143.

Montero JA, Lorda-Diez CI, Ganan Y, Macias D, Hurle JM. 2008. Activin/TGFbeta and BMP crosstalk determines digit chondrogenesis. Dev Biol 321:343-356.

Moore MA, Gotoh Y, Rafidi K, Gerstenfeld LC.1991. Characterization of a cDNA for chicken osteopontin: expression during bone development, osteoblast differentiation, and tissue distribution. Biochemistry. 30, 2501-8.

Moorman AF, Houweling AC, de Boer PA, Christoffels VM. 2001. Sensitive nonradioactive detection of mRNA in tissue sections: novel application of the whole-mount in situ hybridization protocol. J Histochem Cytochem 49:1-8.

Mootoosamy RC, Dietrich S. 2002. Distinct regulatory cascades for head and trunk myogenesis. Development 129:573-583.

Newman SA, Bhat R. 2007. Activator-inhibitor dynamics of vertebrate limb pattern formation. Birth Defects Res C Embryo Today 81:305-319.

Riddle RD, Ensini M, Nelson C, Tsuchida T, Jessell TM, Tabin C. 1995. Induction of the LIM homeobox gene Lmx1 by WNT7a establishes dorsoventral pattern in the vertebrate limb. Cell 83:631-640.

Schweitzer R, Chyung JH, Murtaugh LC, Brent AE, Rosen V, Olson EN, Lassar A, Tabin CJ. 2001. Analysis of the tendon cell fate using Scleraxis, a specific marker for tendons and ligaments. Development 128:3855-3866.

Schweitzer R, Zelzer E, Volk T. 2010. Connecting muscles to tendons: tendons and musculoskeletal development in flies and vertebrates. Development 137:2807-2817.

Smith A, Graham A. 2001. Restricting Bmp-4 mediated apoptosis in hindbrain neural crest. Dev Dyn 220:276-283.

Spater D, Hill TP, O'Sullivan R J, Gruber M, Conner DA, Hartmann C. 2006. Wnt9a signaling is required for joint integrity and regulation of Ihh during chondrogenesis. Development 133:3039-3049.

Storm EE, Kingsley DM. 1999. GDF5 coordinates bone and joint formation during digit development. Dev Biol 209:11-27.

Suriben R, Kivimae S, Fisher DA, Moon RT, Cheyette BN. 2009. Posterior malformations in Dact1 mutant mice arise through misregulated Vangl2 at the primitive streak. Nat Genet 41:977-985.

ten Berge D, Brugmann SA, Helms JA, Nusse R. 2008. Wnt and FGF signals interact to coordinate growth with cell fate specification during limb development. Development 135:3247-3257.

Teran E, Branscomb AD, Seeling JM. 2009. Dpr Acts as a molecular switch, inhibiting Wnt signaling when unphosphorylated, but promoting Wnt signaling when phosphorylated by casein kinase Idelta/epsilon. PLoS One 4:e5522.

Topol L, Chen W, Song H, Day TF, Yang Y. 2009. Sox9 inhibits Wnt signaling by promoting beta-catenin phosphorylation in the nucleus. J Biol Chem 284:3323-3333.

Tylzanowski P, De Valck D, Maes V, Peeters J, Luyten FP. 2003. Zfhx1a and Zfhx1b mRNAs have non-overlapping expression domains during chick and mouse midgestation limb development. Gene Expr Patterns. 3**,** 39-42.

Vortkamp A, Lee K, Lanske B, Segre GV, Kronenberg HM, Tabin CJ. 1996. Regulation of rate of cartilage differentiation by Indian hedgehog and PTH-related protein. Science. 273**,** 613-22.

Waxman JS, Hocking AM, Stoick CL, Moon RT. 2004. Zebrafish Dapper1 and Dapper2 play distinct roles in Wnt-mediated developmental processes. Development 131:5909-5921.

Welten MC, Verbeek FJ, Meijer AH, Richardson MK. 2005. Gene expression and digit homology in the chicken embryo wing. Evol Dev 7:18-28.

Widelitz RB, Jiang TX, Murray BA, Chuong CM. 1993. Adhesion molecules in skeletogenesis: II. Neural cell adhesion molecules mediate precartilaginous mesenchymal condensations and enhance chondrogenesis. J Cell Physiol 156:399-411.

Witte F, Chan D, Economides AN, Mundlos S, Stricker S. 2010. Receptor tyrosine kinase-like orphan receptor 2 (ROR2) and Indian hedgehog regulate digit outgrowth mediated by the phalanx-forming region. Proc Natl Acad Sci U S A 107:14211-14216.

Witte F, Dokas J, Neuendorf F, Mundlos S, Stricker S. 2009. Comprehensive expression analysis of all Wnt genes and their major secreted antagonists during mouse limb development and cartilage differentiation. Gene Expr Patterns 9:215-223.

Xi S, Yang M, Tao Y, Xu H, Shan J, Inchauste S, Zhang M, Mercedes L, Hong JA, Rao M, Schrump DS. 2010. Cigarette smoke induces C/EBP-beta-mediated activation of miR-31 in normal human respiratory epithelia and lung cancer cells. PLoS One 5:e13764.

Yamaguchi TP, Bradley A, McMahon AP, Jones S. 1999. A Wnt5a pathway underlies outgrowth of multiple structures in the vertebrate embryo. Development 126:1211-1223.

Yang Y, Niswander L. 1995. Interaction between the signaling molecules WNT7a and SHH during vertebrate limb development: dorsal signals regulate anteroposterior patterning. Cell 80:939-947.

Yang Y TL, Lee H, Wu J. 2003 Wnt5a and Wnt5b exhibit distinct activities in coordinating chondrocyte proliferation and differentiation. Development 130:1003-1015.

Yau TO, Chan CY, Chan KL, Lee MF, Wong CM, Fan ST, Ng IO. 2005. HDPR1, a novel inhibitor of the WNT/beta-catenin signaling, is frequently downregulated in hepatocellular carcinoma: involvement of methylation-mediated gene silencing. Oncogene 24:1607-1614.

Zhang L, Gao X, Wen J, Ning Y, Chen YG. 2006. Dapper 1 antagonizes Wnt signaling by promoting dishevelled degradation. J Biol Chem 281:8607-8612.

Zhang L, Zhou H, Su Y, Sun Z, Zhang H, Zhang Y, Ning Y, Chen YG, Meng A. 2004. Zebrafish Dpr2 inhibits mesoderm induction by promoting degradation of nodal receptors. Science 306:114-117.

Zou H, Niswander L. 1996. Requirement for BMP signaling in interdigital apoptosis and scale formation. Science 272:738-741.

Zou H, Wieser R, Massagué J, Niswander L. 1997. Distinct roles of type I bone morphogenetic protein receptors in the formation and differentiation of cartilage. Genes Development 11(17):2191-203.

LEGENDS

Figure 1 – Time-course of *Dact1* and *Dact2* expression during chicken limb development. *Sox9* expression was determined to follow changes in the appendicular skeleton. *Dact1* (A-H;α,β), *Dact2* (I-P;χ,δ) and *Sox9* (Q-X) *in situ* hybridizations of whole-mount fore (FL) and hindlimbs (HL) between HH24 to HH30. Dorsal views of FL and HL are oriented anterior to the top, distal to the right. White arrowheads in I, and M,N,V indicate humerus and femur rudiments, respectively. Black arrowheads in K and O indicate lateral expression of *Dact2* in the radius, ulna and tibia. Black arrowheads in L and Li indicate putative anlagens for digits I/V which fail to further develop in the chick wing. Asterisks in L, O, P and X indicate the digit blastemas. Abbreviations: Aj (ankle joint); c (cartilaginous condensations); Da (digital arch), DI-V (digits I to V); Ej (elbow joint); Et (extensor tendon); Fb (fibula); Ft (flexor tendon); Hu (humerus); Kj (knee joint); McI-V (metacarpus I to V); MtI-V (metatarsus I to V); p (perichondrium); R (radius); Sj (shoulder joint); T (tibia); Ul (ulna); Wj (wrist joint).

Figure 2 – Comparison of *Dact1* and *Dact2* expression with markers for specific tissues at HH35 (E8) chicken limbs. Dorsal views of whole-mount ISH of fore (FL) and hindlimbs (HL) are shown, anterior to the top, distal to the right. Hindlimbs were cross-sectioned in order to detail the expression patterns. Markers: Skeletal muscle (*Pax7, MyoD*); muscle connective tissue (*Tcf4, Sfrp2*); tendon (*Scx*); interdigital mesenchyme (*Zeb2*); joints (*Wnt9a, Gdf5*); cartilage (*Sox9*); epyphysis

(*Sfrp3*); hypertrophied cartilage (*Ihh*) and osteoblasts (*Spp1*). Abbreviations: Aj (ankle joint); Edc (extensor digitorium communis muscle); Ej (elbow joint); Fdp (flexor digitorium profundus tendon); Ft (flexor tendon); Hc (hypertrophic cartilage); Ij (interphalangeal joint); It (interosseous muscle); Lb (lumbrical muscle); m (mesenchyme); Mcj (metacarpophalangeal joint); Mtj (metatarsophalangeal joint); o (osteoblast); p (perichondrium); Wj (wrist joint).

Figure 3 – Details of *Dact1* and *Dact2* expression in the phalangeal and ankle joints at HH35 chicken embryos. Longitudinal vibratome sections of hindlimb digits (A-G), magnified view of phalangeal (Ai-Gi) and ankle (Aii-Gii) joints. Distal to the top. Markers: Synovial joints formation (*Wnt9a, Gdf5*); cartilage (*Sox9*), Wnt (Sfrp3) and TGF-β inhibitor (Zeb2) were also analyzed. Asterisks indicate interzones, arrowheads the digit blastemas.

Figure 4 – *Dact1* and *Dact2* expression during interphalangeal joints development. Longitudinal serial sections from HH35 digits were processed for tissue ISH (A,C-E), immunohistochemistry (B) or histology (F). Distal to the top. Asterisks indicate interzones and arrows the developing joint capsule.

Supplemental Figure S1 – Comparison of *Dact1/Sox9* and *Dact2/Sox9* expression profiles from HH25 to HH30 in limbs obtained from single embryos. *Dact1* (A-D), *Sox9* (Ai-Di); *Dact2* (E-J), *Sox9* (Ei-Ji). Dorsal views of fore (FL) and hindlimbs (HL) are oriented anterior to the top, distal to the right. Black and red arrowheads indicate overlapping and complementary sites of expression, respectively.

Supplemental Figure S2 – Comparison of *Dact1* and *Dact2* expression with markers for specific tissues at HH31 (E7) chicken limbs. Dorsal views of whole-mount *in situ* hybridizations of fore (FL) and hindlimbs (HL) are shown, anterior to the top, distal to the right. Markers: Skeletal muscle

(*Pax7, MyoD*); muscle connective tissue (*Tcf4, Sfrp2*); tendon (*Scx*); interdigital mesenchyme (*Zeb2*); joints (*Wnt9a, Gdf5*); cartilage (*Sox9*); epyphisis (*Sfrp3*); hypertrophied cartilage (*Ihh*) and osteoblasts (*Spp1).*

Supplemental Figure S3 – Details of *Dact1*, *Dact2*, and *Scleraxis* (Scx) in HH35 chicken hindlimbs. Whole-mount ISH of *Dact1* (A), *Dact2* (B) and *Scx* (C). Ventral views of hindlimbs are oriented distal to the top, anterior to the left. Vibratome sections at the level of digits (Ai-Ci) and metatarsals bones (Aii-Cii). Arrowheads indicate tendons.

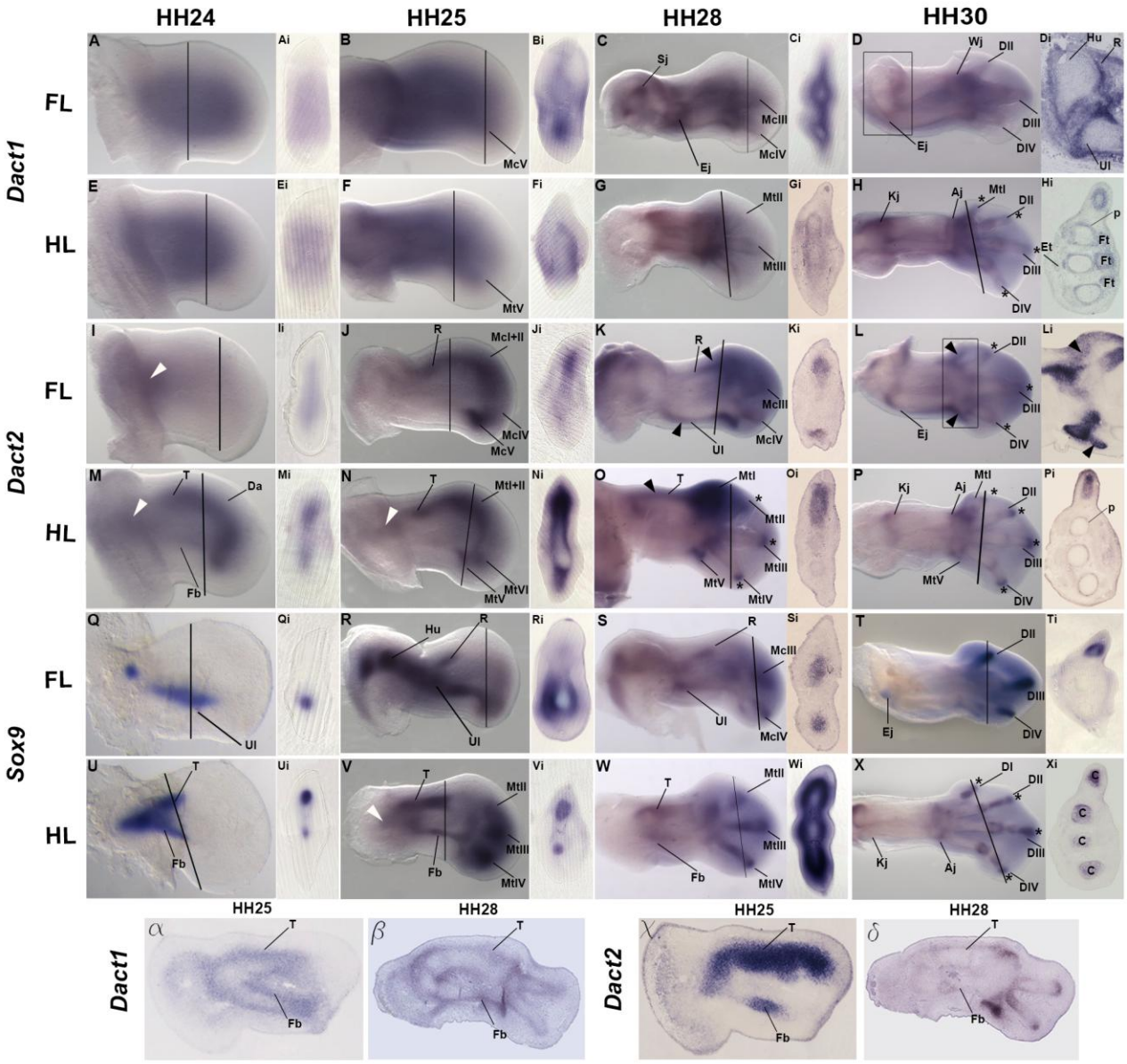
HH24
HH25
HH28
HH30
Dact1
FL
HL
Dact2
FL
HL
Sox9
FL
HL
HH25
HH28
HH25
HH28
Dact1
Dact2

Figure 1

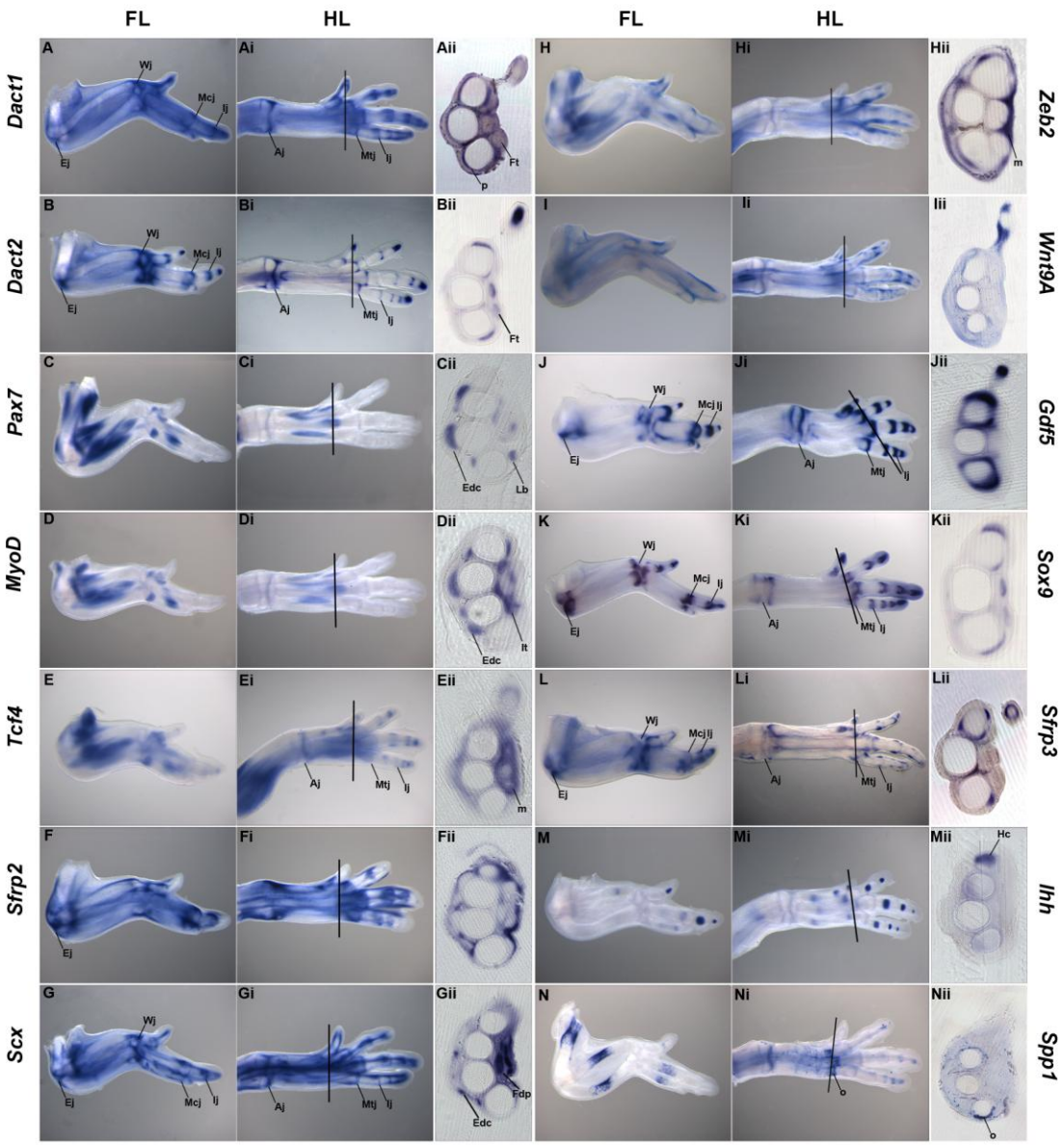
FL
HL
FL
HL
Dact1
Dact2
Pax7
MyoD
Tcf4
Sfrp2
Scx
Zeb2
Wnt9A
Gdf5
Sox9
Sfrp3
Ihh
Spp1
A
Ai
Aii
B
Bi
Bii
C
Ci
Cii
D
Di
Dii
E
Ei
Eii
F
Fi
Fii
G
Gi
Gii
H
Hi
Hii
I
Ii
Iii
J
Ji
Jii
K
Ki
Kii
L
Li
Lii
M
Mi
Mii
N
Ni
Nii
Wj
Mcj
Ij
Ej
Aj
Mtj
Ft
p
Edc
Lb
It
m
Hc
Fdp
o

Figure 2

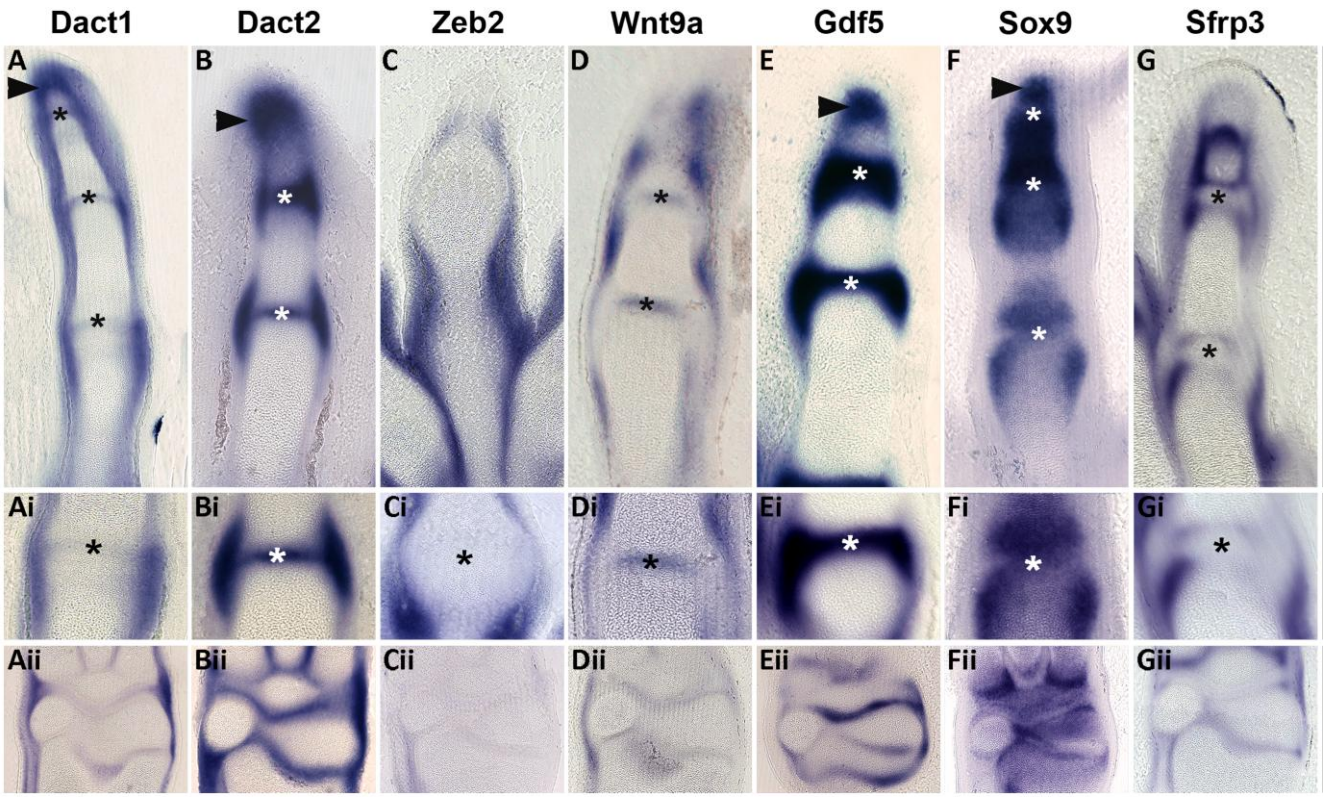
Dact1
Dact2
Zeb2
Wnt9a
Gdf5
Sox9
Sfrp3
A
B
C
D
E
F
G
Ai
Bi
Ci
Di
Ei
Fi
Gi
Aii
Bii
Cii
Dii
Eii
Fii
Gii

Figure 3

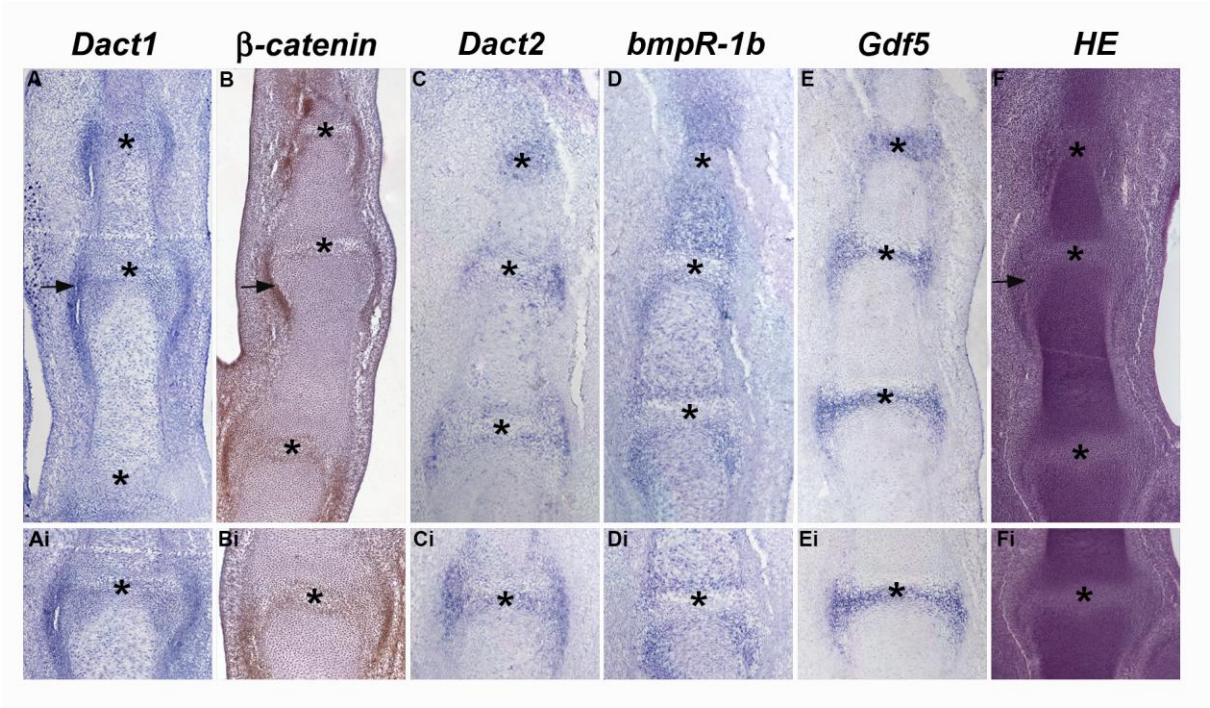

Figure 4

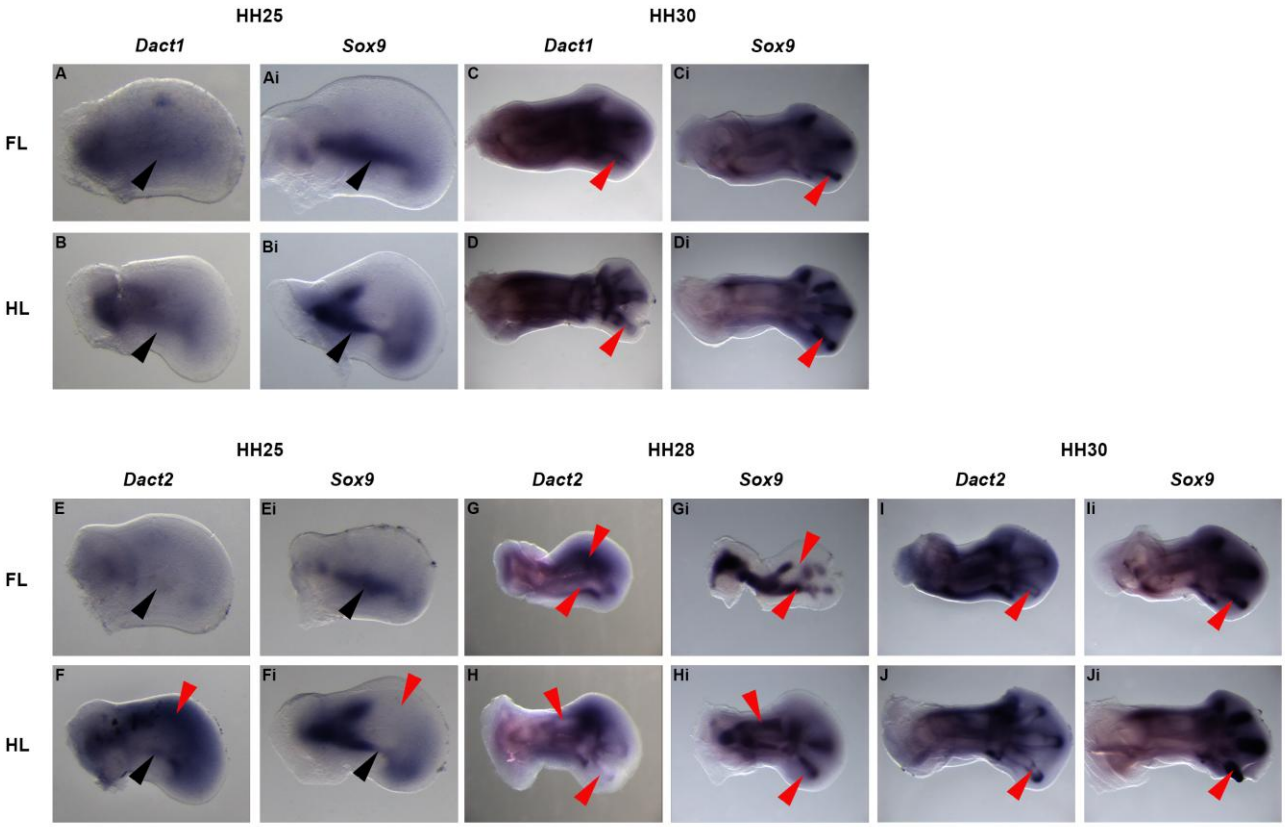

Supplemental Figure S1

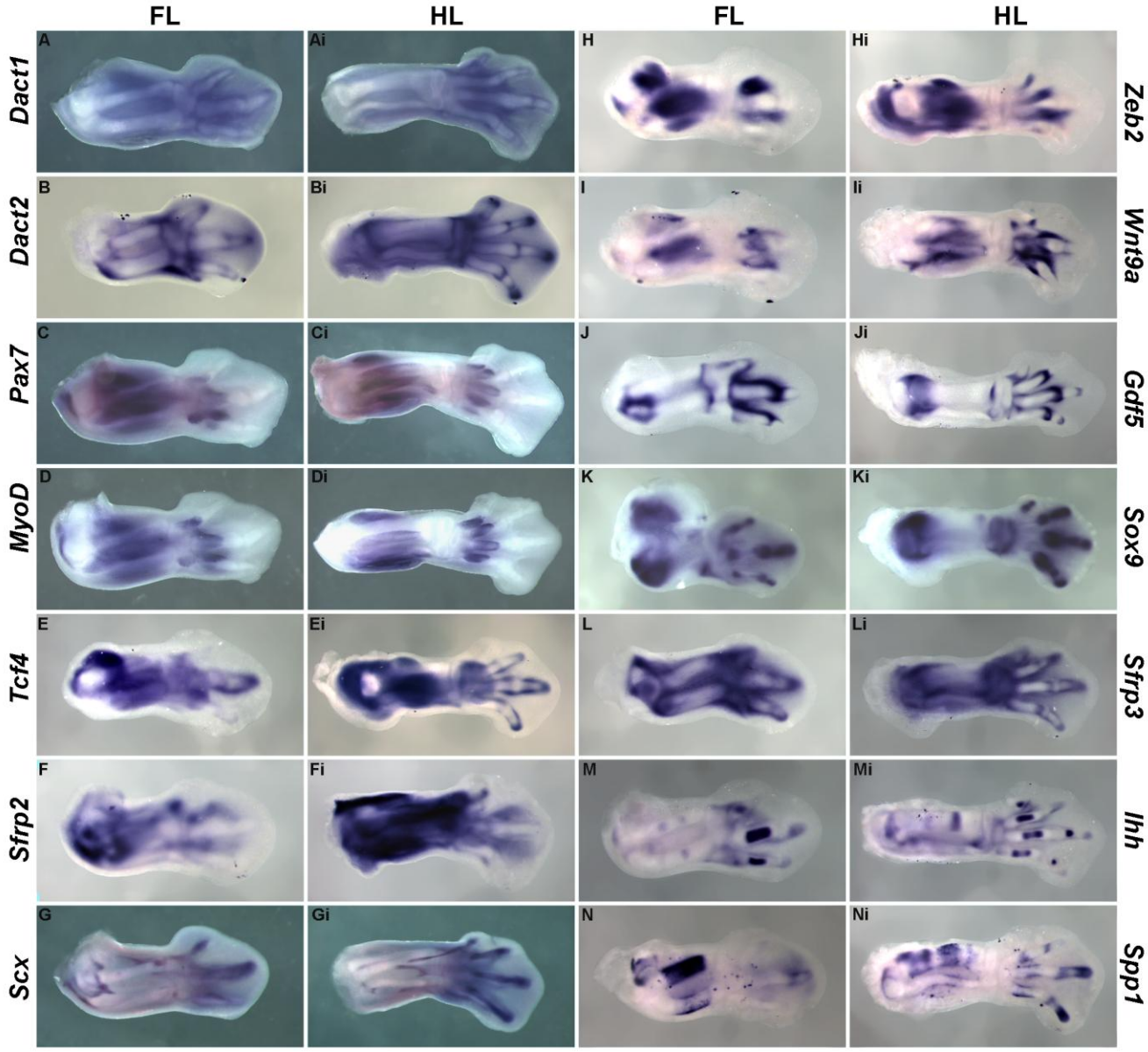

Supplemental Figure S2

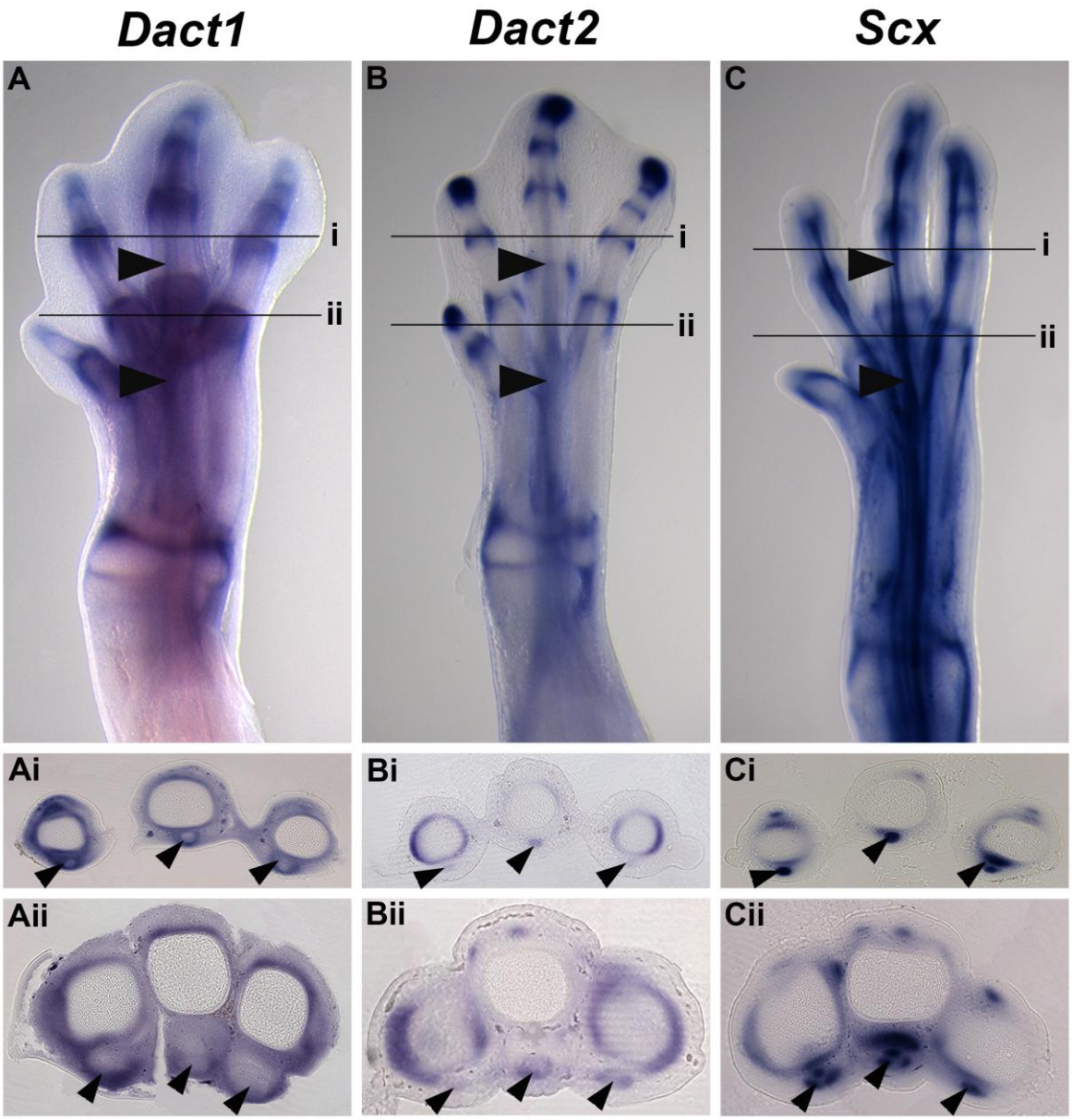

Supplemental Figure S3

Supplemental Table 1. Probes, expected and observed expression patterns

Gene	*In situ* probe	Expected expression according to literature	Found at E7	Found at E8
BmpR-1b	(Smith & Graham, 2001)	Distal phalanx of the digit, subridge mesoderm and undifferentiated mesenchyme (Merino et al., 2008)	-	Digit blastema and cartilage
Dact1	(Alvares et al., 2009)	-	Undifferentiated mesenchyme between cartilage elements and perichondrium, joints	Undifferentiated mesenchyme between cartilage elements and around tendons, pre-chondrogenic mesenchyme, perichondrium and joints
Dact2	(Alvares et al., 2009)	-	Perichondrium, pre-chondrogenic mesenchyme and joints	Perichondrium, pre-chondrogenic mesenchyme, joints and tendons
Gdf5	ChEST347d16*	Joints and perichondrium (Francis-West et al., 1999)	Joints and perichondrium	Joints and perichondrium (weak)
Ihh	PCR fragment corresponding to nucleotides 167-530 of the cDNA	Hypertrophied cartilage (Vortkamp et al., 1996)	Hypertrophied cartilage	Hypertrophied cartilage
MyoD	(Bober et al., 1994)	Differentiating muscle (Bober et al., 1994)	Muscle	Muscle
Pax7	(Goulding et al., 1994)	Muscle precursors (Goulding et al., 1994)	Muscle precursors	Muscle precursors
Scleraxis (Scx)	ChEST871m16*	Tendons, ligaments (Schweitzer et al., 2001)	Tendons and ligaments	Tendons, ligaments and perichondrium (weak)
Sfrp2 (Sdf5)	(Ladher et al., 2000)	Mesenchyme around muscles (Ladher et al., 2000)	Mesenchyme around muscle and bones, interdigital mesenchyme and tendons	Mesenchyme around muscle and bones, interdigital mesenchyme and tendons
Sfrp3 (Frzb)	(Ladher et al., 2000)	Prechondrogenic mesenchyme, perichondrium, pre-hypertrophied cartilage (Ladher et	Prechondrogenic mesenchyme and perichondrium	Epiphysis

		al., 2000)		
Sox9	(Healy et al., 1996)	Cartilage condensations/ pre-chondrogenic mesenchyme, pre-hypertrophied cartilage (Akiyama et al., 2002; Chimal-Monroy et al., 2003; Healy et al., 1996)	Cartilage condensations/ pre-chondrogenic mesenchyme	Cartilage condensations/ pre-chondrogenic mesenchyme
Spp1 (Osteopontin)	ChEST176k23*	Osteoblasts (Moore et al., 1991)	Osteoblasts and prechondrogenic mesenchyme (weak)	Osteoblasts,
Tcf4 (Tcf7l2)	pctcf4.1	Muscle connective tissue (Kardon et al., 2003)	**Muscle connective tissue, undifferentiated mesenchyme between cartilage elements and around tendons	**Muscle connective tissue, undifferentiated mesenchyme between cartilage elements and around tendons
Wnt9a (Wnt14)	ChEST867g3*	Interdigital mesenchyme, joints, perichondrium (Spater et al., 2006); (Hartmann and Tabin, 2001)	Interdigital mesenchyme, joints (weak) and perichondrium	Interdigital mesenchyme, joints (weak) and perichondrium
Zeb2 (Sip1)	Chest4489*	Interdigital mesenchyme, perichondrium, muscle (or muscle connective tissue*) (Tylzanowski et al., 2003)	Interdigital mesenchyme, muscle or muscle connective tissue	Interdigital mesenchyme, perichondrium, muscle or muscle connective tissue

* Clone ID (Source Bioscience UK Ltd)

** Muscle-associated expression was not investigated in detail in this study.

Capítulo 2

Origem e evolução dos genes da família Dpr

Introdução – Capítulo 2

A Biologia Evolutiva do Desenvolvimento (EvoDevo) tem suas origens nos estudos de Embriologia Comparativa realizados no século XIX por Karl Ernst von Baer e Ernst Haeckel, ainda sabendo que as ideias propostas por Haeckel estavam incorretas em muitos detalhes (Müller, 2005; Taylor *et al*., 2003; Arthur, 2002). Após quase um século em repouso, em 1980, a EvoDevo voltou a ser explorada devido à descoberta dos genes homeóticos em drosófilas e ao fato deles serem filogeneticamente conservados (Arthur, 2002). Vale destacar que a EvoDevo não é simplesmente a fusão do campo da Biologia do Desenvolvimento com o da Biologia Evolutiva, nem a incorporação dos conceitos de desenvolvimento nos estudos evolutivos, ou vice-versa (Müller, 2005; Taylor *et al*., 2003; Holland *et al.*, 1994). A EvoDevo moderna procura unificar as áreas de Genômica; Desenvolvimento; Biologia Populacional; Ecologia; e critérios de Seleção Natural às mudanças evolutivas, utilizando abordagens e métodos empregados na Embriologia, Paleontologia, Biologia Molecular e Sistemática (Müller, 2005; Taylor *et al*., 2003; Arthur, 2002; Holland *et al.*, 1994). Os estudos de EvoDevo buscam elucidar duas questões fundamentais: quais são as bases genéticas da variação fenotípica; e de que maneira essa variação produz a biodiversidade existente (Holland *et al.*, 1994).

Diversos estudos apontam os genes *Dpr* como moduladores das vias de sinalização Wnt e TGF-β, através das quais regulam diversos processos ao longo do desenvolvimento embrionário e durante a vida adulta dos organimos (Brot & Sokol, 2005a; Zang *et al*., 2004; Hisaka & Sokol, 2004; Cheyette *et al*., 2002; Gloy *et al*., 2002). Contudo, enquanto as vias de sinalização Wnt e TGF-β estão presente em todo o reino animal, os *Dprs* são uma das poucas famílias que são restritas aos

vertebrados e sua origem ainda permanece desconhecida (Brot & Sokol, 2005a; Hisaka & Sokol, 2004; Waxman *et al*., 2004; Zang *et al*., 2004; Cheyette *et al*., 2002; Gloy *et al*., 2002). Ademais, aparentemente, diferentes vertebrados recrutaram um conjunto particular de genes da família *Dpr* capaz de regular e interagir diferencialmente com as vias Wnt e TGF- β (Brot & Sokol, 2005a; Hisaka & Sokol, 2004; Waxman *et al*., 2004). Diante disso, esta tese de doutorado empregou também uma abordagem evolutiva para buscar entender as funções originais e as adquiridas ao longo da evolução e também o surgimento dos genes *Dpr* durante a evolução dos metazoários.

Para tanto, utilizando ferramentas de *Bioinformática*, analisamos as sequências disponíveis de todos os ortólogos dos genes *Dpr* em todo o reino animal e dessa forma, estabelecemos a filogenia dessa família gênica. Além disso, as análises filogenéticas revelaram a presença de um gene *Dpr* ancestral em *Branchiostoma floridae*, entretanto, nenhuma sequência de *Dpr* foi encontrada em protostomios nem em deuterostômios não-cordados. Foram também identificados novos genes *Dprs,* formando assim um grupo de quatro parálogos nos vertebrados (*Dpr4*). Porém, o conjunto completo de quatro genes *Dpr* foi encontrado apenas em teleósteos, lagartos e cobras, mas não em anfíbios, mamíferos e aves. Análises de sintenia dos *loci* gênicos dos quatro parálogos dos *Dprs* corroboram os dados filogenéticos e reforçam a hipótese de que os quatro *genes Dpr* surgiram a partir de um ancestral comum após sucessivas duplicações completas do genoma nos vertebrados.

Ainda neste trabalho, uma análise dos motivos protéicos das proteínas Dprs e ensaios de hibridação *in situ* utilizando embriões de peixe-zebra foram realizados a fim de fornecer uma visão mais abrangente sobre as propriedades dessa família gênica durante o desenvolvimento embrionário ao longo da evolução.

Os resultados obtidos nessa etapa do doutorado serão apresentados em forma de manuscrito, *Origin and Evolution of Dact genes, key regulators at the intersection of Wnt and Tgf beta pathways,* submetido à publicação.

Resultados - Manuscrito

Dact genes are chordate specifc regulators at the intersection of Wnt and Tgf beta pathways

Débora Rodrigues Sobreira, Ricardo Janousek, Frank Richard Schubert, Lúcia Elvira Alvares and Susanne Dietrich

ABSTRACT

Vertebrate Dact proteins have been implicated in Wnt and Tgfβ signaling, and thus, may serve as a nodal point in the regulation of cell proliferation, differentiation, migration, stem cell behavior, tissue homeostasis, tissue regeneration, embryonic development and cancer. However, the number of vertebrate *Dact* paralogs, their origin, evolution and the evolution of Dact function is not known.

We screened for *Dact* genes in the animal kingdom and established their phylogeny and conserved sequence motifs. While unable to detect any *dact* genes in protostomes and non-chordate deuterostomes, we readily detected *Dact* genes in chordates such as the lancelet and jawless vertebrates such as the lamprey. We also identified novel *Dact* genes in jawed vertebrates and show that they belong to four paralogous groups, with *Dact1* and *Dact3* arising from one, *Dact2* and *Dact4* from the other ancestral gene that was generated during the first round of vertebrate genome duplication.

Protein motifs shared by vertebrate and chordate Dacts suggest an evolutionarily basic role in the control of Wnt signaling. In contrast, specific motif combinations in Dact2 and 4 suggest that the ability to inhibit Tgfβ signaling may have evolved with the gnathostome Dact2,4 precursor. The novel Dact4 is the most derived Dact, and its combination of motifs raises the possibility that it may antagonize the function of the other Dacts. Importantly, *Dact* genes have overlapping expression patterns, suggesting that in a given tissue, the combination of Dact proteins will determine the outcome of Wnt and Tgfβ signal transduction events.

Keywords: Dact, Dapper, Frodo, Wnt signaling, Tgfβ signaling, evolution, phylogeny, protein motifs, expression, protostomes, deuterostomes, chordates, actinopterygian vertebrates, sarcopterygian vertebrates.

INTRODUCTION

Wingless and Transforming growth factor beta (Tgfβ) signaling are two cell-cell signaling systems that are well conserved in the animal kingdom and that control a plethora of processes ranging from embryonic development, cell proliferation, differentiation and migration, tissue homeostasis, stem cell behavior, tissue regeneration and cancer (Croce and McClay, 2008; Huminiecki et al. 2009). Tgfβ signaling is initiated when Tgfβ ligands bind to the membrane-based type 2 receptor dimer which forms a heterotetrameric complex with type 1 receptors, in most cases Alk5 [reviewed in (Wu and Hill, 2009)]. Alk5 in turn phosphorylates the intracellular regulatory factors Smad2 or 3 which bind the co-factor Smad4. Smad2/3-Smad4 complexes translocate to the nucleus, recruit chromatin remodeling factors and positively or negatively regulate gene transcription. Wnt signaling operates a β-Catenin-dependent ("canonical") and a number of β-Catenin-independent pathways, with ligands having a preference but not a strict association with a particular pathway, and some ligands being able to activate several pathways dependent on the receptors they interact with [reviewed in (Kestler and Kuhl, 2008)]. The β-Catenin-dependent pathway is initiated when Wnt ligands such as Wnt1 or Wnt3a bind to their Frizzled transmembrane receptors and the lipoprotein receptor-related protein 5 or 6 co-receptor (Lrp5/6), leading to receptor clustering and the recruitment and polymerization of the cytosolic protein Dishevelled (Dvl). This provides a platform for the recruitment of a multiprotein complex including Casein kinase 1 (CK1), Axin, Glycogen Synthase Kinase 3 (GSK3) and adenomatous polyposis coli (APC) to the cell membrane. This protein complex normally phosphorylates free β-Catenin (i.e. not associated with α-Catenin and Cadherins) and admits it to proteasomal degradation. In the presence of Wnt, however, the clustered receptors

initiate a number of phosphorylation events including the phosphorylation of Dvl by CK1 that results in the dissociation of the β-Catenin destruction complex, thus stabilizing β- Catenin. β-Catenin translocates to the nucleus, and together with T cell factor/lymphoid enhancer binding factor (Tcf/Lef) transcription factors and additional co-factors, it activates transcription of Wnt target genes. The planar cell polarity (PCP) pathway is activated when Wnt ligands such as Wnt11 trigger the recruitment of Dvl and the relocation of a Frizzled-Dvl-Diversin complex to the distal side and the transmembrane protein Vangl together with Prickle to the proximal side, leading to cell polarization. Together with heterodimeric G-proteins Dvl activates Rho and Rac GTPases, Rho Kinase (ROCK) and c-Jun N-terminal kinase (JNK). The results of this pathway are changes in cytoarchitecture and cell polarity, and thus changes in cell adhesion and motility. The Ca^{2+} pathway is initiated when ligands such as Wnt5a bind to the Frizzled receptor and Ror1/2 co-receptor. This recruits a complex consisting of Dvl, Axin and GSK3 that phosphorylates Ror1/2, which activates the membrane-based phospholipase C (PLC), leading to the generation of the second messengers 1,2 diacylglycerol (DAG) and Inositol 1,4,5 triphosphate (IP3). IP3 interacts with Calcium channels located on the endoplasmatic reticulum to release Calcium which activates Calcium-Calmodulin-dependent protein kinase type II (CaMKII) and Calcineurin; Calcium and DAG activate protein kinase C (PKC). The kinases activate a number of transcription factors including NFκB, nuclear factor of activated T cells (NFAT) and cAMP response element binding protein (CREB); Wnt 1 and Wnt7a may also target the adenylate cyclase pathway directly, activating protein kinase A (PKA), which in turn allows CREB to activate its targets (Chen et al. 2005). Notably, the Ca^{2+} pathway, similar to the β-Catenin dependent pathway, results in changes of gene transcription. However, Wnt5a via CamKII activates a mitogen activated protein kinase (MAPK) cascade consisting of TAK1 and the Nemo-like kinase NLK that phosphorylates

Tcf and prevents the Tcf-β Catenin complex from binding DNA (Ishitani et al. 2003). Moreover Wnt5a is able to target phosphorylated as well as unphosphorylated β-Catenin for proteasomal degradation via an alternative E3 ubiquitin ligase complex that contains APC, Ebi, and Siah1 or 2 (Topol et al. 2003). Thus, this pathway antagonizes the "canonical" cascade.

Superficially, there seems to be no overlap between the various Wnt and Tgfβ signaling cascades. However, evidence is accumulating that both pathways are linked, most prominently by Dact/Dapper/Frodo proteins. Dact proteins are intracellular multi-adapter proteins with the ability to bind Dvl, CKIδ/ε, Vangl, PKA, PKC as well as Alk5 (Kivimae et al. 2011). In line with these properties, gain and loss of function studies have shown that Dact proteins positively and negatively regulate the Wnt/β-Catenin pathway and positively regulate the Wnt/PCP pathway (involvement in the Wnt/Ca^{2+} has not been investigated). In addition, specifically Dact2 has been implicated in the suppression of Tgfβ dependent wound healing and Nodal dependent mesoderm induction due to its ability to facilitate lysosomal degradation of Alk5 (Zhang et al. 2004; Su et al. 2007; Meng et al. 2008). Furthermore, Dact proteins have been shown to stabilize p120 Catenin (a mediator of Cadherin function and Rho GTPases) which in turn sequesters the transcriptional repressor Kaiso, thus leading to the activation of Kaiso targets (Park et al. 2006). Since the p120-Dact interaction is stimulated by Wnt and is mediated by Dvl, and because many Kaiso targets are also Tcf/Lef targets, the p120 Catenin/Kaiso pathway is seen as a parallel pathway to the Wnt/β-Catenin pathway. Dact proteins have been shown to also modulate Wnt signaling mediators in a ligand independent fashion: Dact proteins shuttle between the nucleus and cytoplasm, and can block nuclear β-Catenin function by disrupting β-Catenin/Lef1 complexes and enhancing Lef1-HDAC interaction (Gao et al. 2008).

However, they can also promote Tcf/Lef function when the Dact N-terminal domain interacts with these transcription factors (Hikasa and Sokol, 2004). In addition, Dact proteins can interact with Dbf4 which, independent from is role in cell cycle regulation, inhibits β-Catenin targets (Brott and Sokol, 2005). Finally, Dact function has been shown to depend on its phosphorylation state which is controlled in two ways (Teran et al. 2009; Chen et al. 2011): firstly, in the absence of Wnt, Dact is unphosphorylated, binds to Dvl and blocks its ability to protect β-Catenin from phosphorylation, thus promoting β-Catenin degradation. In the presence of Wnt, CKIδ/ε not only phosphorylates Dvl but also Dact; this decreases their affinity and promotes the resolution of β-Catenin destruction complex, thereby stabilizing β-Catenin. It also allows Dact to promote the function of Tcf/Lef molecules, thus further enhancing the Wnt response (Teran et al. 2009). Secondly, cyclic AMP activated PKA phosphorylates Dact; this allows the binding of 14-3-3 beta which also blocks the ability of Dact to promote Dvl degradation, thus enhancing Wnt signal transduction (Chen et al. 2011). Taken together, Dact proteins have emerged as nodal points in the simultaneous control of the various Wnt and Tgfβ signaling pathways.

Given that Dact proteins interact with a number of proteins, it is not surprising that they are modular proteins, and domains devoted to the interaction with specific partners are now being recognized. A leucine zipper located in the N-terminal half of the protein is required for homo-and hetero-dimerization, a C-terminal PDZ binding domain together with a domain located in the center of the protein is crucial for Dvl binding, a serine-rich domain upstream of the PDZ binding domain is required for the interaction with Vangl2, the sequences encoded by the first three and the start of the fourth exon are sufficient to inhibit Alk5, a region encoded by the end of the 3rd and start of the

4th exon has been implicated in Tcf3 binding and a not well characterized central portion of the protein interacts with p120 Catenin (Cheyette et al. 2002; Gloy et al. 2002; Wong et al. 2003; Hikasa and Sokol 2004; Park et al. 2006; Zhang et al. 2006; Su et al. 2007; Suriben et al. 2009; Kivimae et al. 2011). Furthermore, nuclear export and import signals have been identified (Gao et al. 2008). However, in vitro binding studies showed that binding affinity and specificity of Dact proteins with their various partners is variable, with mouse Dact2 being the only Dact showing significant affinity to Tcf/Lef and Alk5 and, in comparison to Dact1 and Dact3, weak binding to Vangl2 (Kivimae et al. 2011). Knock out studies in the mouse implicated Dact1 in Wnt/PCP and Dact2 in Tgfβ signaling, yet morpholino knockdown experiments in zebrafish implicated dact1 in Wnt/β-Catenin and dact2 in Wnt/PCP signaling (Waxman et al. 2004; Meng et al. 2008; Suriben et al. 2009; Wen et al. 2010). This indicates that the structure-function relationship of Dact proteins is still unclear.

A key factor in our limited understanding of Dact function is the fact that the number of *Dact* genes that animals may have to regulate Wnt and Tgfβ signaling is not known, and therefore, *Dact* functions may have been overlooked or misinterpreted due to gene redundancy. Moreover, *Dact* genes have so far only been found in jawed vertebrates. However, in this animal group the genome has been duplicated twice (teleost fish: three times), followed by subsequent gene loss or gene diversification (Holland et al. 1994; Taylor et al. 2001; Postlethwait, 2007). Thus, the origin of *Dact* genes and their evolutionarily basic function is not known. To begin to understand the original and derived roles of *Dact* genes and proteins, we took an evolutionary approach. We searched for so far elusive *Dact* family members in the animal kingdom, and, using bioinformatic tools, we determined their phylogeny. Moreover, we searched for conserved amino acid stretches that may serve as

functional domains. Finally, we determined the expression of *dact* genes in the zebrafish, the organism with the highest number of *dact* genes, in comparison with that of the chicken that has only two.

Our study shows that *Dact* genes are unique to chordate animals since in non-chordate deuterostomes and in protostomes, no genes with *dact* homology were found. In jawed vertebrates, four distinct *Dact* paralogs were identified, with *Dact1* and D*a*ct3 originating from one, *Dact2* and *Dact4* from the second *Dact* gene that was present after the first round of genome duplication. Remarkably, all four genes are still present in *Latimeria* (a lobe-finned animal related to tetrapods), turtles (anapsid reptiles) as well as lizards and snakes (diapsid reptiles), but mammals, birds and amphibians have independently lost particular *Dact* genes. In most teleosts, a *dact1*, *dact2*, two *dact3* and one *dact4* gene have been kept; zebrafish and the spotted gar, a holost fish, have an additional, intron-less and hence possibly retrotranscribed *dact4r*. Motif comparison suggests that the ability to dimerize, shuttle between cytoplasm and nucleus, bind Tcf/Lef and Vangl molecules and to interact with various kinases may have been present already in the ancestral Dact protein. The ability to interact with Alk5 may have evolved with Dact2 and 4. Yet motif combinations in extant Dact4 proteins suggest that these molecules may sequester Dact binding partners, thereby inhibiting their function. Significantly, the various *Dact* genes show similar expression patterns, suggesting that in a given tissue, the regulation of Wnt and Tgfβ signaling will depend on the combinatorial action of Dact proteins.

RESULTS

1. Identification of novel *Dact* genes

1.1. Identification of gnathostome Dact genes

Currently, three *Dact* family members are known in mouse and humans, two *Dact* genes have been identified in the chicken, one in *Xenopus* (with a *Dact1a* and *Dact1b/ Frodo* gene in the pseudo-tetraploid *Xenopus laevis*) and two in the zebrafish; no *dact* genes have been found in invertebrates, and *Dact* genes are thought to be vertebrate specific (Cheyette et al. 2002; Gloy et al. 2002; Gillhouse et al. 2004; Fisher et al. 2006; Hunter et al. 2006; Suriben et al. 2006; Alvares et al. 2009). To understand when and how *Dact* genes, and with them the integration of Wnt and Tgfβ signaling systems evolved, we first aimed at obtaining a comprehensive overview of *Dact* genes in jawed vertebrates (gnathostomes). We therefore searched the genomes of selected lobe-finned/lobe-limbed (=sarcopterygian) bony vertebrates including humans, mouse, cattle, dog, African elephant (placental mammals); opossum (marsupial mammals); platypus (monotreme mammals) all representing the lineage of synapsid amniotes; chicken, turkey, zebrafinch, duck, budgerigar (birds, representing archosauromorph diapsid amniotes); Anole lizard, python (lepidosauromorph diapsid amniotes); Western painted and Chinese soft shield turtles (anapsid amniotes); *Xenopus tropicalis* and *Xenopus laevis* (amphibians) and *Latimeria chalumnae* (coelacanths) for traces of *Dact* sequences. We also searched the genomes of ray-finned (actinopterygian) bony vertebrates including the spotted gar (holosts) and the following teleosts: zebrafish (ostariophysian teleosts); atlantic cod (paracanthopterygian teleosts); Fugu, the green spotted pufferfish *Tetraodon*, three-spined stickleback, Medaka and the Nile *Tilapia* (acanthopterygian teleosts). Finally, we searched the

genomic databases for the elephant shark, a cartilaginous (=chondrichthyan) vertebrate. To perform these searches, we interrogated the Ensemble and NCBI data bases using the human and mouse Dact1,2,3; chicken Dact1,2; *Xenopus laevis* Dact1a,1b and zebrafish Dact1,2 protein sequences as baits. Moreover, we performed searches with protein sequences encoded by individual exons. Since some of the selected genomes are not fully sequenced, assembled or annotated, we also used the query sequences to interrogate the NCBI EST database. Using this approach, we searched for *Dact* ESTs in the aforementioned species, in additional sarcopterygian and actinopterygian bony vertebrates as well as in the spiny dogfish shark, Pacific electric ray and little skate (chondrichthyan vertebrates). All species analyzed are summarized in Supplementary Table1.

Sequences identified by our searches were aligned using ClustalW and T-Coffee. Further manual refinement was used to accommodate for varying sequence length and to ensure that functionally confirmed motifs were aligned. Moreover, PSort and NetNes 1.1 motif prediction programs were used to identify further putative motifs. Using this approach, we identified novel Dact sequences in sarcopterygians and actinopertygians, and we found matching sequences in chondrichthyans (Fig.1/Table1). Moreover, while we found sequence motifs typical for all Dact proteins, we also identified motifs and sequence variations that distinguish Dact family members. Based on the presence and linear order of these motifs (summarized in Fig.2 and Supplementary Table 2; for longer conserved sequences stretches, refer to the full alignments shown as Supplementary Figs. 1-5 or the gnathostome Dact consensus sequences show as Supplementary Fig. 6), a pattern of four distinct types of Dact proteins emerged.

Dact1-type sequences

A first set of sequences encompassed in total 800-850 amino acids (aa) which were encoded by four exons. The first exon encoded some 98-122aa, beginning with MK or MN, after a short variable stretch continuing with a sequence akin to ER-Q/V-RTRER-L/Q-EATLAGL-A/G/T-EL-E/D/G-Y/F-LR-Q/H/R-RQE, followed by a conserved LLV group (Suppl. Fig. 1, Fig.2 and Suppl. Table 2, motif 1; core underlined); PSort predicted this motif as nuclear export signal. Exon1 encoded sequences ended with a conserved EEK group followed by **L**EENILL**L**RKQL (Suppl. Fig. 1, Fig.2 and Suppl. Table 2, motif 2a); the bold 2 L contributed to a leucine zipper. Exon2 encoded 43-45aa that continued the highly conserved region, encompassing three distinguishable elements. The sequence began with NC**L**RRRDAG**L**, followed by the sequence E**L**D-K/R-QISD**L**RLDV that has been suggested as nuclear export signal (Gao et al. 2008), and ended with ETDSRPSS (Suppl. Fig. 1, Fig.2 and Suppl. Table 2, motifs 2b,c,d). The bold L and two further leucines contributed to the in total 6x leucine-zipper that has been implicated in homo-and heterodimerization (Kivimae et al. 2011). Exon3 encoded 52-53aa that further extended the conserved domain. The exon2/3 splice created the coding sequence for an invariant glycine, followed by the sequence FY-E/D-LSDG-A/T-SG linked to SLSNSSNSVFSECLSSC (Suppl. Fig. 1, Fig.2 and Suppl. Table 2, motifs 2e,f). Overall, the exon3 derived sequences were enriched in serines.

Exon3 sequences ended with D/E-G-R/C/Q-P/L/A-KSA (Suppl. Fig. 1, Fig.2 and Suppl. Table 2, motif 3a), linked to a conserved DLI sequence encoded by the start of exon4 (Fig.2 and Suppl. Table 2, motif 3c). This last exon contributed the remaining 560-634aa to the protein. About 25aa from the exon3/4 splice site, a 20aa stretch enriched in serines and prolines was located (Suppl. Fig. 1, Fig.2

and Suppl. Table 2, motif 4a; VCRS-L/F/P-S-T/A-P-H/Q-S/F-N in most tetrapods, VRRSFSAPYS in gar and teleosts), followed by DV-H/N/Q and PKYQCDLVSKNGND-V/I-YRYPSPLHAVAVQSPMF (Suppl. Fig. 1, Fig.2 and Suppl. Table 2, motif 4b). Some 120-150aa from the splice site, a further conserved sequence stretch starting with KK and followed by M/I/L-D-G/S-YILSL-V/L/I-Q-K/R-K/R was found (Suppl. Fig. 1, Fig.2 and Suppl. Table 2, motif 5a), followed by V and RTNKPRTS-L/V/I (motif 5b) and, linked by K-G/S-I/L-L, continued with R-H/Q/N-GS-M/V/L/I-CVR (motif 5c). The region encompassing motifs 3c-5b has been implicated in Tcf3 binding; the region encompassing motifs 5b,c was shown to participate in Dvl binding (Hikasa and Sokol, 2004; Suriben et al. 2009). 100aa downstream of this region and approximately 250aa from the start of exon4 encoded sequences, we found the conserved stretch EERP-A/P/I-L-D/E-F/L-KS-E/L-GSSSQSL-D/E-E/D-G (Suppl. Fig. 1, Fig.2 and Suppl. Table 2, motif 7a), linked to LVN followed by A-Q/H-Y/F-IPAQQQ (Suppl. Fig. 1, Fig.2 and Suppl. Table 2, motif 7b) and K/R-NV followed by KI-L/V-KVKSS-T/A/S-LKHR (Suppl. Fig. 1, Fig.2 and Suppl. Table 2, motif 7c). Thereafter, a sequence enriched in basic aa including REK-(x)-K/R (Suppl. Fig. 1, Fig.2 and Suppl. Table 2, motif 8a), KKCRFP-D/E-D/E (Suppl. Fig. 1, Fig.2 and Suppl. Table 2, motif 8b), and KK-(xx)-KK (Suppl. Fig. 1, Fig.2 and Suppl. Table 2, motif 8c; x represent variable aa) was located, of which the sequences constituting motif 8b have been identified as bipartite nuclear localization signal (Gao et al. 2008). Subsequently, a serine-rich region (SESSL in cartilaginous fish; reminiscent of motif 9 in other Dact proteins) linked to the sequence GRE-V/A/Q/P-V-V/L-A which was denoted motif 10.

The last 200aa stood out most, starting with the sequence blocks KPKHKR-A/T/G/N-DY (Suppl. Fig. 1, Fig.2 and Suppl. Table 2, motif 11a), RRWKSSAEISYEEA; (motif 11b) and RRARR-R/N-Q/A/N-RRE (motif 11c). This was followed by a block of 32 highly conserved aa with stereotype acidic aa,

repetitive neutral aa (mainly serines) and glycines, starting with SDSEYSAEC and ending with TTNC (motif 11d), and a second, similar block of 28aa, starting with FGDSESS and ending with ESGG (motif 11e); the sequence concluded with L-I/N/V-W-S/P-QF (motif 11f). Of these conserved stretches, motif11a is being predicted by NetNes 1.1 as further nuclear localization signal; motifs 11d-f are located in the region that has been implicated in the binding of Vangl proteins (Suriben et al. 2009). The proteins invariably ended with the sequence K-A/T-FV followed by KIKASHNLKKKILRFRSGSLKLMTTV that encompasses the PDZ binding motif K-L/V-MTTV (Fig.2 and Suppl. Table 2, motif 11g; (Suriben et al. 2009). Notably, the combination of features described here is typical for all the known (human, mouse, chicken, *Xenopus*, zebrafish) Dact1 proteins. Sequences of this type were found in all gnathostomes with the exception of pufferfish. In all species, only a single *Dact1* gene was present.

Dact2-type sequences

A second set of sequences was 750-850aa long and also encoded by 4 exons. The 1st exon accounted for 67-97aa, starting with ML or MW, further downstream encoding a variant of the Dact1 motif1 (DR-G/S/C/R-RVGERLQAALAGLQEL-(xx)-LR-E/D-K/R-Q) and ending with E-Q/H and a variant of motif2a (R**L**EATL-T/A/S-A**L**K- E/Q-QL; Fig.2 and Suppl. Table 2), with the bold leucines contributing to a leucine zipper. The 2nd exon encoded a stereotype set of 44-45aa, starting with a sequence akin to SR**L**RRQD VG**L** (Fig.2 and Suppl. Table 2, motif 2b), followed by K-S/T-HL-D/Q-Q linking to Q**L**D-Q/R-Q/R-ISE**L**KLDV (motif 2c) and almost invariably ending with L-E/D-SDSRPSS (motif 2d). Conserved leucines contributed further 4L to a 6x L zipper. Notably, motif2c located in the center of exon2 encoded sequences and following the L-zipper was similar but not identical to the Dact1 nuclear

export signal. The 3rd exon encoded 82-101aa, beginning with GFY-E/D-LSDGGSC and followed by SLSNSCTSVYSE-S/C-L/I/M-SSS (Fig.2 and Suppl. Table 2, motifs 2e,f). Towards the end of exon3 encoded sequences, a bipartite motif was found. The first part consisted of DY (sarcopterygians, elephant shark), followed by R-P/R-R/K-SA and a conserved DE pair, the second set read RPRPVST. Both parts are similar to the sequences encoded by the end of Dact1 exon3 (Fig.2 and Suppl. Table 2 motif 3a), suggesting that they represent an internal duplication. Therefore, the sequences have been named motifs 3a,b.

Exon 4 contributed the remaining 557-620aa. The sequence began with G-DL (Fig.2 and Suppl. Table 2, motif3c), followed by conserved E/D-R. This was followed by a conserved D and PK-Y/F-Q-S/N/R/C-D/N-LVS-K/R-N/S/G-G-(x)-D/E-VY-P/H/L/R-YPSPLHAVALQSPLFS, reminiscent of the YPSPLHAVAV containing sequence in Dact1 (Fig.2 and Suppl. Table 2, motif 4b). Some 120aa from the splice site, sequences akin to GYI-N/D-K/R-LL-Q/R-R were found (Fig.2 and Suppl. Table 2, motif 5a), followed by a serine rich but variable stretch of aa (GGVKINSSSSQLEK in birds and reptiles) that aligned with Dact1 motif 5c. This was followed by a conserved stretch reading EFVH followed by A-Q/K-FVPA-E/G-S-H/Q-Q/R that resembled Dact1 motif 7b and KT followed by KAVK-L/I/V-KRR-N/S-SEK that resembled Dact1 motif 7c (Fig.2 and Suppl. Table 2, motifs 7b,c). Moreover, rudimentary versions of motifs 8a (E-K/R-(x)-R) and 8c (RRP) were also found while motif 8b that had been associated with nuclear localization was absent. Downstream at the position where Dact1 sequences carried a serine enriched but loosely conserved stretch, the current group of proteins carried a defined RSCSESSL sequence (Fig.2 and Suppl. Table 2, motif9).

The start of the conserved C-terminus was marked by a variation of motif 11a (KKKQ), followed by RKWQSTVEIS (Fig.2 and Suppl. Table 2, motif 11b) and, in sarcopterygians and the gar, followed by PR-Q/P-P/A-A/G-RRAG (Fig.2 and Suppl. Table 2, motif 11c). Similar to Dact1 proteins, the sequence continued with a highly conserved stretch of 30aa, starting with R/K-SESD-(x)-SEYSAEC and ending with T-T/A-NR (motif 11d) and a second, related stretch, starting with FGDSESS and ending with a block of acidic aa (motif 11e); this was followed by a recognizable but more varied L-V/I-W sequence (motif 11f). The protein terminated in P-(x)-LPP-V/E-P-(xx)-C and RIKASKALKKKIRRFQPASLKVMT-M/L-V (Fig.2 and Suppl. Table 2, motif11g), thus showing a related but different sequence compared to Dact1. The combination of features is typical for the known (human, mouse, chicken, zebrafish) Dact2 proteins. Dact2 type sequences were found in all gnathostomes with the exception of amphibians. As for *Dact1*, only a single *Dact2* gene was found in a given species.

Dact3-type sequences

A third set of sequences encompassed proteins with significant length variations, ranging from 420aa (*Xenopus*), 540-660 (teleosts), 610-630 (mammals) to 820 (*Latimeria*). However, these proteins shared a number of features that distinguished them from the other Dact-type proteins. Notably, in teleosts two distinct representatives of this group of proteins were found, in line with the idea that teleosts underwent 3 rounds of genome duplication (Taylor et al. 2001). Proteins belonging to this 3rd group of Dact proteins typically started with MIRAFSFP (most tertrapods) or MHRAFSFP (1st set of teleost sequences), followed by ER-S/G-R-L/N/T and a version of Dact1 motif1 that read K/R-G/S-WLEGSLAGLCEL-H/P/Q-W/L-LRERQE in amniotes or K/R-ERLEASLAGLCELEL-L/R-K/R-Q/E-RQE in

non-amniotes (Fig.2 and Suppl. Table 2, motif1). The subsequent sequence stretch encoded by exon1 varied in length, therefore the sequences encoded by this exon encompassed 46-83aa in total. In placental mammals, this stretch contained the repetitive sequence EAEDEEDADEDEDAAAARRAAAA which was not shared by other animals. In most cases, exon1 encoded sequences ended with L/P-EEQL (amniotes) or L-R/K-R/K-QL (*Latimeria*, gar, "a"-type of teleost sequences and zebrafish dact3b), with bold L contributing to a L-zipper (Fig.2 and Suppl. Table 2, motif2a). The exon 2 encoded sequences (33-45aa) lacked a conserved start, and the nuclear export signal found in Dact1 and 2 sequences was changed to L-E/G/Q-QQ-V/L-GEL-R/S/K-L/V/I-D/E (Fig.2 and Suppl. Table 2, motif2c). However, exon2 contributed further leucines to continue the L-zipper. Yet in *Latimeria*, the gar and the "a"-type teleost sequences, a loss of 3aa shifted the array of leucines, thus interrupting this L-zipper (Suppl. Fig.7). Since these animals represent both the sarcopterygian and the actinopertygian lineage, we concluded that the interruption of the L-zipper occurred before the sarcopterygian-actinopterygian split. In the sarcopterygian lineage, tetrapods lost an additional 4aa, such that 2-4 correctly placed leucines completed a 3x-5x L-zipper. In teleost 3a-type proteins, even though further leucines were present, they were not all in the position required for a L-zipper, leaving a 3+2x (*Latimeria*, gar, Tetraodon and *Tilapia* "a" sequences), 3x (Dr "a") or 2+2x (Medaka "a") zipper arrangement. In "b" type teleost sequences, the L-zipper was further reduced: in many species, two exon 2 encoded leucines were in the position to form a rudimentary L-zipper; however, the Tetraodon "b" sequence lacked a L-zipper altogether.

Most exon2 derived sequences terminated in 2-3 serines. However, only sequences from placental mammals (EQESGRSS), reptiles (ETDSWPSS), the gar, and most teleosts "a" type proteins

(DSRPSS) showed the full sequence motif found in Dact1 and Dact2 (Fig.2 and Suppl. Table 2, motif 2d). In line with the ill-conserved end of exon2-coding sequences, teleost "b" type proteins (exception zebrafish dact3b), lacked any sequences normally encoded by the 3rd exon and immediately proceeded to sequences typical for exon4. For both zebrafish proteins and for sarcopterygian and "a"-type teleost sequences, however, 32-52aa encoded by a 3rd exon and showing the hallmarks of Dact exon3 encoded sequences were found. These sequence began with GFYE (motif 2e; exception: *Xenopus*), followed by P/S-SS in amniotes and SSEG-Q/P/L-SP for teleost dact3a which may functionally replace the serine rich motif 2f found in Dact1 and Dact2. Moreover, these exon3 encoded sequenced terminated in ERPKS-V/L/A (Fig.2 and Suppl. Table 2, motif 3a), thus resembling the arrangement of exon3 encoded sequences of specifically Dact1.

Exon4 encoded sequences ranged from 310aa (*Xenopus*) to 637aa (*Latimeria*). They typically began with the sequence G-D-A/P/V, a rudimentary version of Dact1/2 motif3c, some 20aa downstream followed by a fairly conserved stretch reading V/L-PRSFSAPYP (Fig.2 and Suppl. Table 2, motif 4a; YP not conserved in teleost dact 3b) and a varied stretch enriched acidic aa and glycines. In sarcopterygians, further conserved prolines and the FLYPSPLHAVA-L/M motif (Fig.2 and Suppl. Table 2, motif 4b) followed. In a number of teleost "b" type proteins, the sequence HATLA (Tetraodon), HAAVA (Fugu) or HAIVT (*Tilapia*) may represent the remainder of this motif; however, in all other teleost sequences, the motif was replaced by a sequence enriched in tryptophans. Interestingly, the subsequent R/H-R/K-V/L/A-E-G/T/S/N-YI-L/S/F-G/S/A/R-L-I/L-Q/R-RR and RP-S/C/G-K/Q-PRT-S/T-L motifs (Fig.2 and Suppl. Table 2, motifs 5a,b) were well recognizable, and the serine-rich stretch thereafter that was variable in other Dacts, was well conserved here (RRQ-S/N-SL-C/R/H); Fig.2 and

Suppl. Table 2, motif 5c). Likewise, the sequence L/M-V-S/K/N followed by AQYIP-G/A-Q/A (most) or LV-S/N-A-Q/K/E/S-YIP-G/A-Q (teleosts) aligned well with LVNA-Q/H-Y/F-IPAQQQ of Dact1 (Fig.2 and Suppl. Table 2, motif 7b). Approximately 100aa further downstream, the sequence RE-K/R-P-R/K reminiscent of Dact1 motif 8a was found in sarcopterygians except *Xenopus*; followed in non-mammalian sarcopterygians and teleost dact3b by K/R-K/R-C/G/N-R/H-(xx)-E-D/R/E that resembles the Dact1 nuclear localization signal (Fig.2 and Suppl. Table 2, motif 8b) and, subsequently, a rudiment of motif 8c (R/K-R/K). This was followed by RSQSENSL which resembles Dact2 motif 9 (Fig.2 and Suppl. Table 2, motif 9) and V/A/L-PE-(xxx)-R/P-K/R-Y-(x)-T-(x)-ER-D/E that bears some resemblance to Dact1 motif 10 but may equally represent a unique Dact3 motif.

The C-terminus of the third group of proteins strongly resembled that of Dact1, in sarcopterygians (except *Xenopus*) and the gar starting with R-P/Q-RR, for teleost dact3b starting with R/K-(x)-R/K-R/K (Fig.2 and Suppl. Table 2, motif 11a). In all, this was followed by RRW-R/C-S-T/N-L/A-E-L/I-SQDE-G/A-E (motif 11b) and RR-(xx)-RR-(x)-R (motif 11c). Further downstream, a 26aa S-rich stretch that started with E/D-SESS, ended with ESGG and aligned well with the 2nd S-rich stretch in Dact1 (Fig.2 and Suppl. Table 2, motif 11e) was found, followed by an invariant LVWPQQLPP (motif 11f). The proteins terminated in K-A/V-F-VKIKASHALKKKI-L/M-RFR-S/T-GSLKVMTTV, which is near-identical to the C-terminus of Dact1 (Fig.2 and Suppl. Table 2, motif 11g). The features described here are typical for the known human and mouse Dact3 proteins, and so we concluded that we have identified novel Dact3 proteins in further placental mammals, and in addition, marsupial and monotreme mammals, reptiles, amphibians, coelacanths, teleosts and cartilaginous fish. Yet we were unable to detect the third type of Dact sequences in birds. Thus, while amphibians retained a *dact3*

gene and lost *dact2*, birds kept the *Dact2* gene and lost *Dact3*. In contrast, teleosts have a *dact1* (lost in pufferfish), *dact2*, *dact3a* and *dact3b* gene.

Dact4-type sequences

Given that the vertebrate Dact family is thought to consist of three members only (Fisher et al. 2006; Hunter et al. 2006; Suriben et al. 2006; Alvares et al. 2009; Cheyette et al. 2002; Gloy et al. 2002; Gillhouse et al. 2004), we were surprised to find a fourth set of sequences in cartilaginous fish, ray-finned fish, and the following sarcopterygians: the coelacanth *Latimeria*, lizards and snakes (representing lepidosauromorph diapsid amniotes) and in turtles (representing anapsid amniotes). The sequences displayed Dact-specific but also unique features. They encompassed some 700 (Anole lizard), 830 (*Latimeria*), 990 (zebrafish) to 1070-1120aa (acanthopterygian teleosts). Like Dact1,2,3/3a sequences, Dact4 sequences were encoded by four exons, with exon1 contributing 52-99aa, exon2 52-81aa, exon3 68-106aa and exon4 ranging between 430 (Anole lizard) and 780-840 (teleosts) aa. The exception is a second gar and zebrafish dact4 protein which stems from an intron-free gene that possibly was retrotranscribed (hence the gene was named *dact4r*).

Type 4 Dact proteins typically shared a very similar N-terminus (MA-A/-/G-RR, exception Anole lizard and fish 4r sequences), and, following the stretch SLWSG-T/S, they displayed a variation of the exon1 core motif reading E/D-RVRIGERL-K/Q-A-T/S-LAG-V/I/L-LELE-L/V-LR-(x)-K/R-H/Q-L-E/D-MV-D/E (Dact4) or GRKRIRDRFCATVAGLLELEVLRVKHKVMVE (dact4r, Fig.2 and Suppl. Table 2, motif 1). In stickleback, Medaka and *Tilapia*, an extended stretch of glutamic acids reminiscent of the acidic stretch in mammalian Dact3 was found; yet this was not shared by other species. Importantly, exon1 encoded sequences (except dact4r) typically terminated in R/G/Q/P-QQV, a modification of Dact1-3

motif2a, but did not contribute leucines to a L-zipper. Likewise, exon2 was neither enriched in leucines nor did it contain leucines positioned to contribute to a L-zipper. Thus, Dact4 proteins lack this particular protein-protein interaction domain.

While overall exon2-encoded sequences were somewhat divergent, all ended with the complete DSRPSS motif (dact4r: K/Q-SR-A/S-SS) typical for Dact1 and Dact2 (Fig.2 and Suppl. Table 2, motif 2d). Exon3 derived sequences began with a variation of the GFY-led motif (sarcopterygians: GFY-E/D-T/V-S-E/D-M/S-G, actinopterygian dact4: GFYSVSGS, dact4r: GFC-E/D), followed by SLS-D/N-S-C/S-(x)-S-V/M-S/H/C-S-E/D-(xx)-PGG , thus showing the typical Dact motif 2e,f arrangement (Fig.2 and Suppl. Table 2). In sarcopterygians (RP-R/H-ST-DE) and in the gar and cyprinid teleost dact4 (RP-R/H-S-L/A-DH), a variation of motif 3a was found, followed by the terminal motif RRP-V/F-ST (Fig.2 and Suppl. Table 2, motif3b). This arrangement specifically resembles that of Dact2. Also akin to Dact2, many Dact4 exon4 sequences began with GD-L/V/P-E (Fig.2 and Suppl. Table 2, motif3c), and, 20-30aa further downstream, all continued with LD followed by P-R/K-Y-C/K/R-T/S/C-DLVSR-R/N/K/S-T-K/S-EVY-H/S/P/R-YPSPLHAVALQSPLF (Fig.2 and Suppl. Table 2, motif4b). Further 100aa downstream, with the exception of dact4r, the sequence L-D/E- Q/R-YI-S/A-R/K-L-(xx) R/Q was found (Fig.2 and Suppl. Table 2, motif5a), followed by K/R-SH-(x)-S-(x)-Q/S-S-L/V-S/C reminiscent of motif5c. In teleosts, a 40aa stretch of highly repetitive NLNL followed; thereafter, all Dact4s continued with a conserved motif of basic aa (R/K-I/S/T-R-R/P-RISTC; Fig.2 and Suppl. Table 2, motif 6) not found in any other Dact protein. This was in teleosts followed by a second repetitive stretch of 100aa enriched serines, histidines and prolines. In all proteins, approximately 280aa before the C-terminus we identified a conserved stretch reading LY-R/K-GKHAS-H/R-E/K -LV-R/K not present in other Dacts

(Fig.2 and Suppl. Table 2, motif10; no sequences available for dact4r). This was followed by a block of alkaline aa that may represent a rudimentary version of motif 11a; in sarcopterygians and the elephant shark (no sequence available for the gar) also motif 11b (KW-T/A/V/M-SVLEIS) was found. Sequences concluded with a S-rich domain that was ill conserved between sarcopterygians and actinopterygians but may represent a rudiment of motif 11e, and L-H/R/Y-R-S/T-RSFKELKK-R/M/V-V (sarcopterygians; followed by 11-16aa enriched in serines) or L-Q/T-RSRSLRDLGRKVFGSMRSLSLKRKPSKK (most teleosts; no C-terminal sequences are available for the gar, cartilaginous fish and Dact4r), which shared a number of alkaline and neutral aa with Dact1-3 motif 11g (Fig.2 and Suppl. Table 2). Notably, the novel Dact proteins lacked the PDZ binding domain, suggesting that they may not be able to interact with Dvl.

Our findings suggest that we have identified a fourth Dact family member. Remarkably, while this fourth Dact type was present in anapsid and diapsid reptiles and in *Latimeria* (all sarcopterygians), in actinopterygians and in chondrychthians; it could not be identified in mammals, birds and amphibians. This suggests that after the two rounds of vertebrate genome duplications, *Dact4* genes persisted well beyond the actinopterygian-sarcopterygian split, the coelacanth-tetrapod split, the amphibian-amniote split and the segregation of the amniote lineages, and was lost independently in the avian, mammalian and amphibian lineage. Since both the gar and the zebrafish have a possibly retrotranscribed dact4r, this suggests that the gene occurred before the teleost-specific third genome duplication, but in most teleosts, it was eliminated together with the duplicate of the genuine Dact4 gene.

1.2. Identification of agnathan Dact genes

Gnathostome vertebrates are thought to have split from the agnathan lineage some 536 million years ago (Kumar and Hedges, 1998). It is currently controversial whether the first of the two rounds of vertebrate genome duplication happened before or after this split (Kuraku et al. 2009). Yet, given the close relationship of jawed and jaw-less vertebrates, we reasoned that agnathans would have at least one Dact gene. We therefore searched the Ensembl and NCBI databases, using gnathostome full-length Dact1-4 protein sequences, sequences derived from individual exons and the conserved sequence motif as baits. We were able to identify several contigs encoding Dact-like sequences in the 2008 Ensemble release 50 preview of the sea lamprey genome. When the current version of the lamprey genome was released, unfortunately all but the sequences previously located on contig 364339, now GL476511, had been removed. However, since several of these contigs encoded a number of the Dact motifs in the correct order, some of these sequences may be trustworthy.

Contig 2707 encoded a sequence that included the stretch ERGRGRRRSEATLSGKGDPEQMFGAVA which resembled motif1 of gnathostome exon1 encoded Dact sequences (Fig.2, Suppl. Table 2, Suppl.Fig.5; aa matching the gnathostome core motif are underlined) and IFTSALLVRQPI which may mark the end of sequences encodes by this exon. Contig 36439 (now GL476511) encoded protein sequences that encompassed motifs 2e (G-FYELSDAGTG), 2f (SLSTSCNSVFSDLVPSP) and 3b (ERRPLST) in gnathostomes encoded by the third Dact exon. Contig 54804 encoded exon4-typcial sequences including rudimentary motifs 3c (GPSP) and motif 4a (PPLPPGPAPPH), and a clearly recognizable motif 4b (RRFARDVPSLDGSGLYRYPSALHAVAIQSPAL), 5a

(YIARLLER) and 5b (CRLSRPRRTP; Fig.2, Suppl. Table 2, Suppl.Fig.5). Thus, with the exception of exon 2 encoded sequences, we were able to detect clear evidence for a *Petromyzon* dact gene.

Interestingly, we found a second set of sequences that also encoded exon3-4 derived sequences. Since the second set of sequences was similar but not identical to the first, it suggests that the sequences belonged to a second lamprey dact gene. The majority of these sequences were located on supercontig 37220, and they have been predicted to contribute to cDNA sequences typical for Dact exon3 (GENSCAN00000056301) and the 5' end of exon4 encoded sequences (GENSCAN00000136320), including motifs 2e (G-YYDLSDG), 2f (SLSNSCNSIFNDCLSDS), 3b (VPPSSST), 3c (GDLL), possibly 4a (TPGPPPPAGCP), 4b (GRYVSDLTSRDGSDVYRYPSPLHAVAIQSPLF), 5a (YICSLLDR), 5b (NGRLKPKHEE) and 7c (ARPPKVEEQRARRRDEDR; Fig.2, Suppl. Table 2, Suppl.Fig.5). Contig 20195 encoded 79aa that included a HAVA motif identical to that encoded by sc37220, suggesting that both contigs are overlapping clones from the same gene. Following an uncharacterized stretch, c20195 encoded a well recognizable Dact C-terminus with a serine/acidic aa rich stretch and a PVV motif similar to gnathostome motifs 11e,f. Sequences terminated with motif 11g (C-RIKASRSLKKKMMHFRSGSLKVITTV, which contains a close match to the established PDZ binding domain K-L/V-MTTV.

In addition to these contigs, we found a further contig (c46758) encoding a HAVAI sequence. Moreover, a probable Dact C-terminus was encoded by contig 2487 (KAFVTAVIHILKKKILTTFRP-Stop-HKRSSSGVMVTTV. However, these contigs were riddled with Stop codons in all reading frames, and hence, cannot currently be interpreted. Nevertheless, our data suggests the existence of two

independent lamprey *dact* genes, which we named dact A (c36439/54804) and dact B (sc37220/c20195).

1.3. Identification of invertebrate dact genes

In order to understand the origin and distribution of *dact* genes in eukaryotes, we next searched the Ensembl and NCBI genome and EST collections for *Oikopleura dioica*, *Ciona intestinalis*, *Ciona savignyi* (non-vertebrate chordates, subphylum tunicates), of *Branchiostoma floridae* (non-vertebrate chordates, subphylum cephalochordates), of *Saccoglossus kowalevskii* (hemichordates) and *Strongylocentrotus purpuratus* (echinoderms). These are all deuterostome animals. In addition, we searched the sequences available for *Aplysia californica*, a mollusc representing lophotrochozoan protostomes, and the sequences available for *Drosophila melanogaster*, *Tribolium castaneum*, *Bombyx mori* (insects, ecdysozoan protostomes) and of *C. elegans*, *C. briggsae* and *Loa loa* (nematodes, ecdysozoan protostomes). Finally we interrogated the remaining NCBI protist and fughi genomes. The searches were performed as before, using full length or exon-specific Dact protein sequences or protein motifs as baits. However, the only invertebrate harboring dact sequences was the cephalochordate *Branchiostoma floridae*, the Florida lancelet. In *Branchiostoma*, the blast hits matched with exons 8-10 of a predicted 10-exon cDNA on a single scaffold (s65). Exons 1-7 were confirmed by ESTs, encoding however the lancelet homologue of the *RPA2* gene. Exons 8-10 were confirmed by two further sets of ESTs. The first set encompassed exon 8, 9 and start to mid-exon 10. The second set carried middle and end of exon10. There are no ESTs to suggest that exons 1-10 are linked in a transcript. Moreover, as will be shown below, exons 8-10 carry the complete sequence for a *dact* gene. We therefore renamed the exons that belong to *Branchiostoma dact* exons1,2,3.

Exon1 encoded 73aa with loose homology to exon1 derived sequences in vertebrate Dacts, including the sequence DRSLQ and ARLMASEAAMEELRLLRQRQE that resembles motif1 and CINSIDK**L**RNAV that partially matches motif2a and contributes one leucine (bold) to a L zipper (Fig.2, Suppl. Table 2, Suppl.Fig.5; motifs 1,2a). Exon2 accounted for 58aa that aligned well with exon2-derived sequences of gnathostome Dact1-3, began with CINSIDK**L**RNAV (motif 2b), delivered further four leucines in the correct position to form an in total 5x L zipper and provided the nuclear export sequence **L**NTQILQ**L**KLA (Fig.2, Suppl. Table 2, motif 2c). Different to vertebrates, however, the *Branchiostoma* exon2-3 boundary encoded an extended serine-rich stretch, and the in vertebrates exon2-encoded motif 2d (DSRRSS) was provided by sequences on the other side of the splice.

Exon3 encoded in total 872aa that encompassed sequences which in vertebrates are encoded by the 3' end of exon2, and by exons3 and 4. Indeed, the lancelet DSRRSS motif was followed by G-FFDASSP (vertebrate motif 2e; Fig.2, Suppl. Table 2), SPPLTPDIASPEKLHHY (similar to motif 2f), GESD (similar to motif 3c), FKLALRPRSKTGLSVCYPYPSPMHAIAIQSDM (motif 4b) and SAGLLRPV (similar to motif 5a). Motifs 5b (KAPRKPKPTP) and 5c (RQSLLK) were also recognizable; however, compared to vertebrates, they were separated from motif 5a by and extended stretch of 130aa.

Towards the end of exon3 encoded sequences, the sequence RRCNEN, reminiscent of gnathostome motif 8b that serves as nuclear localization signal, was found (Fig.2, Suppl. Table 2, motif 8b). This was followed by acidic aa and serines that aligned well with the SE rich sequence at the C terminus of vertebrate Dact proteins (Fig.2, Suppl. Table 2, motif 11e). The sequence terminated in LVL (possibly motif 11f) and ATRRRLSSQDSLSRMFPSCHLVTEL that partially matched the gnathostome Dact1-3 C-terminus but, importantly, lacked the K-L/V-MTTV sequence (Fig.2, Suppl.

Table 2, motif 11g). Thus, the lancelet *dact* gene structure differs from that of gnathostome *Dact* genes, and the protein lacks a number of motifs found in vertebrates, most notably the PDZ binding motif. Nevertheless, our data suggest that *dact* genes were already present in deuterostome animals before the split between the cephalochordate lineage and the lineage leading to vertebrates.

2. Organization and relationship of gnathostome *Dact* gene loci

Our study revealed novel vertebrate Dact sequences that were allocated to four paralog groups, based on the combination of aa sequence features. To further corroborate this allocation, we analyzed the organization of vertebrate *Dact* loci, reasoning that *Dact* orthologs would have similar genomic loci. We focused on humans, mouse (placental mammals); opossum (marsupial mammals), platypus (monotreme mammals); chicken, zebrafinch (archosauromorph diapsid amniotes); Anolis lizard (lepidosauromorph diapsid amniotes); Western painted turtle (anapsid amniotes); *Xenopus tropicalis* (amphibians), *Latimeria* (coelacanths) all representing sarcopterygians, the spotted gar (holosts), zebrafish (ostariophysian teleost); atlantic cod (paracanthopterygian teleost); Fugu, Tetraodon, three-spined stickleback, Medaka and Nile *Tilapia* (acanthopterygian teleosts) representing actinopterygians, as their genomes are reasonably well characterized. We first determined the location of a given *Dact* gene, performing a Blast search on the Ensembl data base. We then established the order of neighboring genes in a 1-2 Mb radius (Fig.3), exploiting the Ensembl gene annotations or performing Blast-searched for these genes. During this process, we noticed that, following inversions and other forms of recombination events, genes associated with a particular *Dact* gene in sarcopterygians often had been placed in the wider environment of the orthologous

Dact gene in teleosts, and vice versa. We therefore also established the wider environment of *Dact* genes (Suppl. Figs. 8-11).

Dact1 *loci*

Genes for the proteins that we had allocated to the Dact1 group were located on human chromosome (chr) 14, mouse chr12, opossum chr1, platypus supercontig 214, chicken and finch chr5, lizard contig GL343459 (Ensemble release 50: scaffold (s) 5), turtle scaffold JH584658, *Xenopus* contig GL172704 (s68), *Latimeria* contig JH126564, gar linkage group LG7, zebrafish chr17, cod s909, stickleback group (gr) XV, Medaka chr22 and *Tilapia* GL831368 (Fig.3A). In sarcopterygians, the *Dact1* gene was invariably placed between *ActR10*, *Psma3*, *Arid4* and *Timm9* on one side and *Daam1* and *Rtn1* on the other. In tetrapods, the *Talpid3* gene was inserted between *Timm9* and *Dact1*; in *Latimeria*, *Irf2bp* like was found instead. In the gar, *dact1* was on one side associated with *psma3*, *timm9, arid4a* and both *irf2bpl2* and *talpid3*, on the other, *daam1* was found. Moreover, *gpr135* that in most tetrapods was placed between *Daam1* and *Rtn1*, was also linked to the gar *dact1-daam1* group, suggesting that both loci are related. In most of the teleosts, *dact1* was on one side associated with *psma3*, *arid4a* and *timm9* (cod: genes on two short scaffolds). On the other side of *dact1*, *fbxo34* and /or *tbpl2* were located, which in sarcopterygians were found in a gene group linked to *actR10*. In zebrafish, stickleback and Medaka, *irf2bpl* was found between *timm9* and *dact1* as in *Latimeria* and the gar. In zebrafish, *talpid3* was placed between *dact1* and *fbxo34*. In *Tilapia*, *irf2bpl* and *talpid3* were linked and situated on one side of the *dact1* gene. Thus, although there is some variation in gene order, the same genes are associated with *dact1* in sarcopterygians and actinopterygians. Of the genes tightly associated with *dact1* genes, *actR10*, *psma3*, *timm9* and *talpid3* are single genes

without any paralogs. Hence, they serve as unique identifiers of the *dact1* locus. Within the 1Mb radius around the actinopterygian *dact1* genes, genes were located that were found in the nearer environment of bird *Dact1* and in the wider environment of mammalian *Dact1* genes (example *Rcor1*), or that were in the nearer environment of *Xenopus Dact1* and the wider environment of *Dact1* in amniotes (example *Ehd4*); furthermore, numerous genes and gene groups were in the wider environment of both sarcopterygian and actinopterygian *Dact1* genes (Suppl. Fig.8). Taken together, our analysis suggests that genes we had allocated to the *Dact1* group are true *Dact1* genes. Remarkably, the genomic *Dact1* environment was well preserved in puffer fish, suggesting that these animals lost the *dact1* gene only recently.

Dact2 *loci*

Proteins we had allocated to the second Dact group encompassed amniote and coelacanth (no amphibian Dact2) as well as actinopterygian Dact2 proteins. Genes encoding these proteins were located on human chr6, mouse chr17, opossum chr2, platypus c22096, chicken and finch chr3, Anole lizard chr1, turtle JH584758, *Latimeria* JH129292, gar LG16, zebrafish chr13, cod s609, Fugu s53, Tetraodon chr17, stickleback grVI, Medaka chr15 and *Tilapia* GL831145 (Fig.3B). The platypus and *Latimeria* scaffolds were small and did not carry accompanying genes; however partial or near-complete genomic information was available for the other species. In amniotes, *Dact2* was associated with *Unc93a*, *Mllt4*, *Kif25* and *Frmd1* on one side and with *Smoc2*, *Thbs2*, *Wdr27*, *Phf10*, *Dll1*, *Tbp* on the other (*Kif25* and *Frmd1* not found in mouse; *Phf10* and *Dll1* not found in the lizard, *Dll* not present on the *Dact1* carrying scaffold of the turtle). In mammals and birds, the strongly conserved region also included *Agpat4* and *Map3k4* which were linked to *Unc93a*; in the lizard, the *Agpat4*-

Map3k4 group was placed on the opposite side of *Dact2*. Similarly, in the lizard and in birds, *Tbp* was flanked by *Galnt2*, *Sipa1l2*, *Kcnk1*, *Irf2bp2*, *Tomm20*, *Arid4b* and *Gng4*; this gene group was on the opposite, *Unc93a*-carrying side in *Monodelphis*, and on separate chromosomes in humans and mouse. Of the genes associated with amniote *Dact2*, *Mllt4*, *Wdr27* and *Phf10* are unique and serve as locus identifiers. *Kif25* has further homologues, but they are not associated with any *Dact* gene. Thus, the gene may have translocated to the *Dact2* locus secondarily, but now also serves as locus identifier. In the gar, *agpat4*, *map4k3*, *frmd1* were found on one and *smoc2* on the other side of *dact2*, and additional genes located in the sarcopterygian *Dact2* environment were also in the gar *dact2* environment, indicating that the close relationship of the sarcopterygian and holost *Dact2* loci. In teleosts, *dact2* was associated with a variable array of *herc4*, *cox5b*, *fam160b*, *ablim1a*, *cdh23*, *lrrfip*, *mlh1* and *ate*, and hence at first sight, the locus looks distinct. However, also in teleosts, *dact2* is tightly associated with *smoc2*. Moreover, the *agpat4-map3k4* group, the *sipa1l2- irf2bp2-tomm20-arid4b-gng4* group, the *wdr27-thbs2* group as well as *frmd1* and *kcnk1* are all in the nearer environment of teleost *dact2*. Numerous additional genes are shared by teleosts and specifically birds – the *Dact2* locus is more dispersed in mammals (Suppl. Fig.9). Taken together, our data suggested that we identified *Dact2* orthologs and gene loci correctly. However, in teleosts, a number of genes have invaded the locus after this lineage split from the holost lineage and most likely before the 3rd genome duplication occurred. Remarkably, traces of *Dact2* locus can still be found in *Xenopus* since a number of *Dact2* associated genes are well preserved on contig GL172638.

Dact3 *loci*

Proteins in the third group encompassed mammalian, reptile, amphibian, coelocanth and gar Dact3 (no Dact3 in birds) and teleost dact3a and 3b. The sarcopterygian *Dact3* genes were located on human chr19, mouse chr7, *Monodelphis* chr4, platypus c69853, Anole lizard GL343568 (Ensemble release 50 s1268), turtle JH58447, *Xenopus* GL172667and *Latimeria* JH128225. Gar *dact3* was found on LG2. The teleost *dact3a* genes were located on zebrafish chr18, cod s3150, Fugu s165, Tetraodon s14072, stickleback grI, Medaka chr13, *Tilapia* GL831147; the *dact3b* genes were on zebrafish chr10, cod s4338, Fugu s455, Tetraodon chr7, stickleback grVII, Medaka chr14 and *Tilapia* GL831515 (Fig.3C). For platypus and *Latimeria*, genes were on individual contigs that did not allow to determine gene order.

In placental mammals, *Dact3* was flanked by *Mark4-Fosb2-Rtn2-Vasp-Opa3-Eml2-Snrpd2-Fbxo46-Six5-Dmpk-Foxa3-Irf2bp1-Nova2-Pglyrp1-Hif3a-Ppp5c-Calm3-Ptgir-Gng8* on one side and *Prkd2-Strn4-Fkrp-Arhgap35-Npas1-Sae1-C5ar1-Meis3-Napa-Ehd2* on the other. This arrangement was near-identical in marsupials. In the lizard, turtle and *Xenopus*, *Dact3* was linked to *Ptgir-Gng8* on one side and to *Fkrp* on the other, with orthologs of genes found in the mammalian *Dact3* environment close by. Specifically, *Dmpk*, *Vasp*, *Pglyrp1, Snrpd2* and *Arhgap35*, albeit in a somewhat varying order, were always present. In birds, almost all of the *Dact3* associated genes were absent, suggesting that the entire locus has been lost. In the gar, *dact3* was flanked by *akt2, fosb, ttc9b, sipa1l3* on one and by *c5ar, dmpk, fbxo46, numbl2* on the other side, with *arhgap35*, *snrpd2*, *pglyrp1*, *vasp* and the genes associated with mammalian *Dact3* located in the wider environment. The teleosts *dact3a* gene was invariably linked with *c5ar* and, in a less stringent arrangement, with *vasp*, *snrpd2*

and *pglyrp* on one side and with *gramd1b*, *clmp* and/or *kirre3* on the other. In acanthopterygians as well as cod, *polr2i* was placed between *c5ar* and *pglyrp1*/*snrpd2*; this gene was linked to *pglyrp2* in the zebrafish and located in the wider *Dact3* environment in mammals (Suppl. Fig.9). Moreover, numerous genes including *C5ar* were found in the wider environment of mammalian *Dact3* and teleost *dact3a* genes, indicating that these loci are closely related. The teleost *dact3b* genes were tightly linked with *dmpk*, and in a more variable fashion with *akt2*, *nova2*, *dll3*, *rtn2* and *arhgap35* genes. Moreover, the genes were linked with *rexo2*, *hlcs* and a second set of *gramdb1*, *clmp1* genes. Thus, although the locus is less preserved than the *dact3a* locus, it is clearly identifiable as a second *dact3* locus that originated from the teleost-specific 3rd genome duplication (Taylor et al. 2001). Of the genes linked to tetrapod *Dact3* as well as teleost *dact3a* and *dact3b* genes, *Polr2i*, *Opa3*, *Snrpd2*, *Fkrp* and *Sae1* are unique, and *Ppp5c* and *C5ar1* have no paralogs linked to other *Dact* genes. Hence, these serve as locus identifiers for *Dact3*-type genes.

Dact4 *loci*

Dact4-type proteins were only found in lizards, snakes, turtles, *Latimeria*, the gar and in teleosts. The corresponding genes were located on Anole lizard GL343928 (Ensembl release 50 s1205), turtle JH584543, *Latimeria* JH126593, gar LG28, zebrafish chr14, cod s3610, Fugu s187, Tetraodon chr1, stickleback grIV, Medaka chr10 and *Tilapia* GL831165; the intron-less *Dact4r* genes were found on gar LG14 and zebrafish chr24 (Fig.3D, Supplementary Material 7). In the lizard and turtle, *Dact4* was flanked by *Bscl2*, *Gng3*, *Hnrnpul2*, *Ttc9c* on one side and *Zbtb3* on the other. In *Latimeria*, *Bscl2* was found in the wider environment; *Dact4* itself was flanked by *Mark2, Rcor2, Dpf2, Rom1, Taf6l, Ttc9c* and *Map1lc3c, Zbtb3, Polr2g, Stx5*. Also in the gar, *bscl2* was in the wider *dact4*

environment, and *dact4* was surrounded by *stx5, ganab, rom, lrrn4cl, cdc42bpg, hnrnpul2, ttc9c* and *ehd1, cfl1, fosl1*. Most of these genes were in the wider environment of *Dact4* in *Latimeria*, suggesting that the loci are related. In acanthopterygian teleosts and the cod, the *dact4* gene was typically linked to *pola2, dpf2, ttc9c* and *map1lc3c, ehd1, ubxn1, prpf39, ganab, ints5, scyl1, rom1, ccdc88b, flrt1, fermt3*, with *bscl2, hnrnpul2* and in most cases also *polr2g, zbtb3* and *stx5* residing in the near environment; a similar arrangement was found in the zebrafish. Most of these genes were also found in the *Latimeria* and gar *Dact4* environment, suggesting that all these loci are related. Interestingly, the gar and zebrafish *dact4r* loci resembled each other, but did not share any genes with other *dact* loci. This reinforces the notion that a *dact4* mRNA was retrotranscribed and secondarily inserted into this genomic position in the ancestor of holost and teleost fish, but shed from most teleost genomes thereafter. Of the genes associated with the original *Dact4* loci, *Bscl2*, *Ints5*, *Polr2g* and *Stx5* are unique and hence, identify this site. Searching for *Dact4* associated genes in vertebrates that have lost *Dact4*, we noticed that the locus was very well conserved in mammals and in amphibians, suggesting that their *Dact4* gene disappeared recently. In contrast, in birds, a few dispersed genes formerly associated with *Dact4* were present, suggesting that the entire locus has been lost.

3. Phylogenetic analysis of Dact protein sequences

Our genomic analysis supported the idea that until recently, sarcopterygian and actinopterygian vertebrates had four distinct *Dact* genes, in line with the view that two rounds of genome duplications occurred during the evolution of jawed vertebrates (Holland et al. 1994). In order to further corroborate this finding and in addition, determine which of the *Dact* genes are more

related and hence, originated from a common ancestor, we carried out a phylogenetic analysis of Dact proteins, using the using a maximum likelihood method (PhyML). To ensure that the major chordate taxa are represented, we focused on sequences from humans, opossum, chicken, Anole lizard, the Western painted turtle, *Xenopus* tropicalis, *Latimeria*, the spotted gar, zebrafish, Fugu, *Tilapia* and *Branchiostoma* that were full length or near full length, in addition including the partial sequences from the elephant shark, and from *Petromyzon* dact A and dact B. We used and unbiased approach, i.e. an unrooted tree (Fig.4A), as well as rooting the tree from the *Branchiostoma* sequences (Fig.4B).

In all phylogenetic trees, the sequences previously allocated to the Dact1 group (Fig.4A,B; red branches) were grouped. Likewise, Dact2 sequences (Fig.4A,B; turquoise branches) were grouped, as were Dact3 (Fig.4A,B; pink branches) and Dact4 (Fig.4A,B; green branches) sequences, respectively. Within the Dact3 group, the Dact3, 3a and 3b sequences formed the expected subgroups. Likewise, the gar and zebrafish dact4r sequences formed a subgroup within the Dact4 group. Thus the phylogenetic tree analysis supports our previous Dact1-4 group allocations. Within the individual Dact groups, sarcopterygian and actinopterygian Dact sequences formed subgroups; and together, the sequences from bony vertebrates were separated from the elephant shark sequences. The exception is the shark dact3 sequence that, possibly because it is incomplete, grouped with tetrapod Dact3 sequences.

Interestingly, in both the unrooted and the rooted tree, the gnathostome Dact1 and Dact3 sequences formed a meta-group, supported by bootstrap value of 96. The gnathostome Dact2 and Dact4 sequences formed a second metagroup, supported by a bootstrap value of 51. This suggests

that of the two *Dact* genes created during the first vertebrate genome duplication, one gave rise to *Dact1* and *3*, the other to *Dact2* and *4* genes.

In our phylogenetic trees, the *Petromyzon* sequences were grouped, separated from the others Dacts by a bootstrap value of 91. However, the lamprey sequences seemed to be more closely related to gnathostome Dact2,4 than to Dact1,3 sequences, suggesting that they are a duplicate of the Dact2,4 precursor gene. However, the bootstrap value that separated the agnathan dacts from the gnathostome Dact2,4 sequences was 51, the bootstrap value that separated the lamprey dacts from the *Branchiostoma* sequence was 47. Thus the allocation of lamprey sequences to the Dact2,4 group is not well supported, and consequently the evolution of the agnathan sequences cannot be determined with certainty.

4. Phylogenetic analysis of *Dact* associated genes

When analyzing the genomic organization of *Dact* loci, we identified unique genes associated with a particular type of *Dact* gene. On the other side, we found a number of *Dact*-associated genes whose paralogs were linked with a paralogous *Dact* gene. This suggests that the ancestors of these *Dact* associated genes were part of the original *Dact* locus before the genome became duplicated. It also infers that the phylogenetic relationship of these *Dact*-associated genes may shed further light onto the relationship of the four *Dact* genes. We thus scanned the environment of *Dact* genes for genes that have four paralogs in all vertebrates, each associated with a particular *Dact* locus, making allowanced for teleost genes that, after the third round of genome duplication were kept at the locus that shed the duplicated *Dact* gene. These criteria applied to *Ehd1-4; Eml1-4; Fos, Fosb, Fosl1, Fosl2; Mark1-4; Rtn1-4 and Sipa1, Sipa1l1, 1l2, 1l3* (genomic location: see Suppl. Figs. 8-11). We next

extracted the protein sequences encoded by these genes, and wherever possible, the corresponding lamprey, *Branchiostoma*, tunicate or *Drosophila* sequences. Using the *Drosophila* sequences at outgroups, we then constructed phylogentic trees, using the same procedure as before (Suppl. Fig. 12). In all cases, orthologous sequences were grouped. Notably, in the phylogenetic tree for Ehd proteins, Ehd4 (*Dact1* locus) and Ehd2 (*Dact3* locus) formed a well-supported metagroup, as did Ehd3 (*Dact2* locus) and Ehd1 (*Dact4* locus) sequences (bootstrap values 72 and 87, respectively; Suppl. Fig.12A). In the Eml tree, Eml4 (*Dact2* locus) and Eml3 (*Dact4* locus) sequences formed a metagroup supported by the bootstrap value of 100 (Suppl. Fig.12B). In the tree for Mark protein sequences, Mark3 (*Dact1* locus) and Mark4 (*Dact3* locus) were grouped, as were Mark 1 (*Dact2* locus) and Mark2 (*Dact4* locus) sequences (bootstrap values 92 and 80, respectively; Suppl. Fig.12C). In the Fos tree, Fosl2 (*Dact2* locus) and Fosl1 (*Dact4* locus) were grouped (bootstrap value 55; Suppl. Fig.12D), in the Rtn tree Rtn1 (*Dact1* locus) and Rtn2 (*Dact3* locus) were grouped (bootstrap value 53; Suppl. Fig.12E), and in the Sipa tree, Sipa1l1 (*Dact1* locus) and Sipa1l3 (*Dact3* locus) were grouped (bootstrap value 82; Suppl. Fig.12F). Thus, Dact sequences as well as sequences from Dact-associated genes followed a Dact1,3 and Dact2,4 pattern; the other possible permutations (Dact1,2; Dact1,4; Dact3,2; Dact3,4) were never observed (summarized in Fig.5A). It thus seems likely that during the 2nd round of vertebrate gene duplication *Dact1-Dact3* arose from one, *Dact2-Dact4* from the other *Dact* precursor (Fig.5B).

5. Comparative expression analysis

Our analysis showed that initially, jawed vertebrates were equipped with four *Dact* genes, of which mammals lost one (*Dact4*), puffer fish lost one (*dact1*), amphibians lost two (*dact2, dact4*) and

birds lost two (*Dact3, Dact4*). On the other hand, after their teleost-specific third genome duplication, these animals kept two *dact3* genes and hence, gained a *dact* gene. Zebrafish and gar, by retaining the retrotranscribed *dact4r* gene, gained a further *dact* gene. In order to understand whether there still is a common denominator of *Dact* gene expression, at least a conserved expression pattern for orthologous *Dacts*, or whether expression domains have been redistributed, and to determine tissues in which several *Dact* genes may contribute to the regulation of cell-cell signaling, we comparatively analyzed *Dact* gene expression, focusing on the extreme cases: chicken (2 *Dact* genes) versus zebrafish (6 *dact* genes). We investigated pharyngula-early somite stage embryos since at this stage, vertebrate embryos are the most similar (phylotypic stage; (Irie and Sehara-Fujisawa, 2007) and references therein). At this stage, chicken *Dact1* was expressed in the somites, the craniofacial mesenchyme, the splanchnopleural lateral mesoderm, the limb mesenchyme, the epibranchial placodes and weekly, the dorsal root ganglia (Fig.6A and (Alvares et al. 2009). Chicken *Dact2* was expressed in the somites, the neural crest derived pharyngeal arch and periocular mesenchyme, the mesenchyme surrounding cranial and dorsal root ganglia, the limb buds, the lung bud, the eye (Fig.6B and (Alvares et al. 2009). Thus, expression overlaps in the somites, the craniofacial mesenchyme and the limb buds. Zebrafish *dact1* was expressed in the craniofacial mesenchyme, the somites, the neural tube, the otic vesicle, the pectoral fin bud and the surface ectoderm (Fig.6C). A very similar expression pattern was found for *dact2* (Fig.6D), which also showed strong expression in the pharyngeal arches. *dact3a* specifically labeled the hindbrain whereas *dact3b* had a more widespread expression in the fore-, mid- and hindbrain, the pharyngeal arches and notochord (Fig.6E,G). *dact4* and *dact4r* displayed similar expression patterns, encompassing the brain, the otic vesicle and the pectoral fin bud (Fig.6F,H). Taken together, for both vertebrates at least one member of the Dact1,3

gene group as well as of the Dact2,4 gene group was expressed in the somites, the fin/limb buds and the mesenchyme of the pharyngeal arches, suggesting that these are sites of original *dact* function.

DISCUSSION

Aim of this study was to shed light on the evolution of *Dact* genes, important regulators at the intersection of Wnt and Tgfβ signaling (Cheyette et al. 2002; Zhang et al. 2004; Kivimae et al. 2011). Here we show that *Dact* genes evolved late in the deuterostome lineage. We also identified novel gnathostome *Dact* genes and show that, with the exception of a retrotranscribed gene in actinopterygians, they arose during the two (teleosts, three; (Holland et al. 1994; Taylor et al. 2001; Postlethwait, 2007). rounds of whole genome duplications, with *Dact1,3* originating from one, *Dact2,4* from the second gene generated in the first duplication round. Subsequently, *Dacts* diversified mainly at protein level, such that combinatorial expression of *Dacts* in a given tissue will determine the outcome of Wnt and Tgfβ signaling events.

Gnathostomes were originally equipped with 4 *Dact* genes - and many still are

Previous studies identified a *Dact1,2,3* gene in placental mammals, a *Dact1* and *2* gene in chicken, a *Dact1* gene in frogs (duplicated in the pseudotetraploid *Xenopus laevis*), and a *Dact1* and *2* gene in zebrafish (Cheyette et al. 2002; Gloy et al. 2002; Gillhouse et al. 2004; Fisher et al. 2006; Hunter et al. 2006; Suriben et al. 2006; Alvares et al. 2009). Searching all available databases for avian sequences, we can confirm here that birds (archosauromorph diapsids) have only *Dact1,2* genes. However, we identified novel homologs of the mammalian *Dact1-3* genes in various actinopterygian and sarcopterygian lineages and in cartilaginous fish (chondrichthyans), with amphibians having shed

their *Dact2* gene. Importantly, we identified a 4th *Dact* homologue in the following sarcopterygians: lizards and snakes (lepidosauromorph diapsids), turtles (anapsids) and *Latimeria* (coelacanth). Moreover, a 4th *Dact* gene was found in actinopterygians including the gar (holosts) and all teleosts examined. Furthermore, a 4th *Dact* was present in chondrichthyans. The Dact4 proteins shared unique sequence motifs not found in other Dacts, they grouped in a phylogenetic tree, and the organization of their genomic loci was very similar. This suggests that the *Dact4* genes we identified are orthologs, and they are paralogs to *Dact1-3*. Since *Dact4* genes were found in both the actinopterygian and sarcopterygian lineages of osteichthyans as well as in chondrichthyans, we conclude that they were present in early gnathostomes. The presence of *Dact4* in lepidosauromorph diapsids and in anapsids, and the conservation of the gene locus in mammals and frogs suggests that in tetrapods, the gene persisted well after the split of the amphibian and the various amniote lineages, and was independently shed in frogs, birds and mammals.

***Dact1,3* arose from one and *2,4* from another precursor during 2R**

The analysis of *Dact* genomic loci revealed that each of the four gnathostome *Dacts* is associated with unique genes that identify the respective locus. However, we also found genes which have four paralogs, each associated with a particular *Dact*. In phylogenic trees, both the Dact proteins and the proteins encoded by *Dact*-associated genes formed well supported groups. Moreover, a given *Dact* gene was always linked with a particular paralog of the associated genes. This indicates that precursors of these genes were already associated with the ancestral *Dact* precursor. It furthermore suggests that *Dact* genes and *Dact* loci were generated during the two rounds of vertebrate genome duplication (2R) rather than individual gene duplication events.

Comparing the organization of protein motifs, we found a number of motifs and motif variations that distinguish Dact1,3 from Dact2,4 proteins. In tree analyses, Dact1 and Dact3 proteins formed a metagroup, and Dact2,4 formed another metagroup. Similarly, proteins from *Dact1,3* associated genes and/or from *Dact2,4* associated genes formed metagroups. Metagroups linking *Dact1*,*2*; *Dact1*,*4*; *Dact3*,*2* or *Dact3*,*4* associated genes were never observed. This infers that *Dact1*,*3* arose from one ancestor and *Dact2*,*4* from another ancestor, both of which had been generated during the 1st round of vertebrate genome duplication (1R).

Tracing the teleost *dacts*

In teleost fish, the genome was duplicated a third time (3R, (Taylor et al. 2001; Postlethwait, 2007)). However, we were only able to identify single *dact1* and *2* genes, located in a conserved, *dact1*- and *dact2*-specific genomic environment, respectively. This suggests that immediately after the 3rd genome duplication and before the radiation of teleosts, one of the *dact1* and *dact2* genes was shed. In pufferfish, while the *dact1* locus environment was clearly recognizable, the *dact1* gene itself was absent, suggesting a more recent gene loss.

In contrast to *dact1* and *dact2*, consistently two genes and gene loci were found for teleost *dact3*. In phylogenetic trees, the dact3a and 3b protein sequences formed well supported subgroups. Moreover, *dact3a* and *dact3b* loci were related but clearly distinguishable loci. This suggests that teleosts kept both *dact3* genes and gene loci that were generated during 3R.

Interestingly, two *dact4* genes were found in the gar and the zebrafish. The 1st gene closely resembled the *Dact4* of other vertebrates and consisted of the typical 4 exons. The second gene was intronless. It resided in a similar genomic environment in the gar and the zebrafish, but this

environment was unrelated to that of the 1st *dact4* gene. Significantly, the gar is a holost fish that had not undertaken the teleost-specific 3rd genome duplication (Taylor et al. 2001; Postlethwait, 2007). Together, this suggests that the 2nd *dact4* is a retrotranscribed gene (hence called *dact4r*) that appeared in actinopterygians before the holost-teleost split, and, together with the genuine 3R-derived *Dact4b* was eliminated in all teleosts analyzed here except cyprinids.

Dact genes evolved late in the deuterostome lineage

Gnathostome Dact proteins are important regulators of Wnt and Tgfβ signal transduction, two pathways that evolved prior to the split of deuterostome and protostome lineages (Croce and McClay, 2008; Huminiecki et al. 2009). This seems at odds with the view that *Dact* genes are gnathostome-specific (Cheyette et al. 2002; Gloy et al. 2002; Gillhouse et al. 2004; Fisher et al. 2006; Hunter et al. 2006; Suriben et al. 2006; Alvares et al. 2009). Our study for the first time identified dact sequences in agnathan vertebrates and in non-vertebrate chordates. However, despite intensive searches, no dact sequences were found outside chordates, suggesting that *dact* genes appeared late in the deuterostome lineage.

In the agnathan *Petromyzon marinus*, our searches identified several small genomic fragments encoding aa sequences with homology to gnathostome *dacts*. As most of these fragments were unlinked, it was not possible to determine the number of *dact* genes present in this animal. However, we also identified two sets of overlapping fragments that encoded partial sequences of two distinct *dacts*. Currently, it is controversial whether agnathans and gnathostomes shared the 1st round of genome duplication, whether an independent genome duplication occurred in the lamprey, or

whether individual genes were duplicated (Kuraku et al. 2009). Unfortunately, the currently available sequence is insufficient to clarify the relationship of agnathan and gnathostome Dacts.

For non-vertebrate chordates, we were able to identify a *dact* gene in the Florida lancelet, but not in any of the tunicates searched. This is astonishing, given that tunicates are thought to be more closely related to vertebrates than cephalochordates (Delsuc et al. 2006). However, tunicates have reduced their body plan during evolution, and it is possible that they secondarily lost their *dact* gene. It is tempting to speculate that the loss of regulators of signaling cascades may have facilitated the reduction of tunicate body structures.

The original chordate dact may have served in Wnt signaling

Dact proteins are multi-domain multiadaptor proteins {(Cheyette et al. 2002 ; Gloy et al. 2002; Wong et al. 2003; Hikasa and Sokol, 2004; Park et al. 2006; Zhang et al. 2006; Su et al. 2007; Gao et al. 2008; Suriben et al. 2009;Kivimae et al. 2011). We found that a number of protein motifs, but not all, were shared by Dacts from gnathostomes and the lancelet, including motifs 1, 2a-f, 3c, 4b, 5a-c, 8b, 11e,f, and the basic aa of the C-terminal motif 11g. Thus, these motifs may represent the original repertoire of the ancestral dact. Motifs 1-5 occupy the N-terminal half of Dact proteins and encompass the L-zipper essential for homo- and heterodimerization, a functionally characterized and a further predicted nuclear export signal, a domain that assists binding to Dvl and a domain that in gnathostome Dact1 has been implicated in Tcf3 binding ((Hikasa and Sokol, 2004; Gao et al. 2008; Kivimae et al. 2011), and this study). The motifs located in the C-terminal half provide a functionally characterized (motif8) nuclear localization signal and contribute to the Vangl binding domain (motifs 11e,f; (Gao et al. 2008; Suriben et al. 2009; Kivimae et al. 2011), and this study). All proteins are

enriched with serines, particularly in the area containing motifs 2f, 11e. Thus, the ancestral dact protein may have served as a multi-adaptor protein, capable of interacting with molecules in the β Catenin dependent and PCP Wnt signaling pathway, possibly able to shuttle between the nucleus and cytoplasm, and subject to extensive regulation by phosphorylation.

In gnathostomes Dacts 1,2,3, motif 11g contains the K-L/V-MTTV sequence, a PDZ binding domain and key for the interaction of Dact with Dvl (Cheyette et al. 2002; Gloy et al. 2002; Wong et al. 2003; Kivimae et al. 2011). In lamprey dact B (no C-terminal sequences available for dact A), the related sequence KVITTV was found, suggesting that this molecule has similar properties to gnathostome Dact1-3. In the lancelet, motif 11g does not contain a recognizable PDZ binding motif. Thus, either *Branchiostoma* dact has secondarily lost this sequence, or alternatively, this sequence appeared in the vertebrate lineage. Consequently, it cannot be decided when the main Dvl-interacting ability of Dacts emerged during evolution. However, this function was firmly established in the vertebrate lineage.

In addition to the PDZ binding domain, further motifs (3b, 4a, 7c) are found in gnathostome and agnathan Dacts, suggesting that they arose in the vertebrate lineage. Gnathostome proteins exhibit a number of additional motifs (3a, 7b, 8a, 8c, 9,11a-d), and the region encompassing motifs 2-f and 11a-g is strongly conserved. This suggests that the stabilized protein domains carry out essential molecular roles. Unfortunately, not all of the gnathostome specific sequence motifs have been functionally characterized. Yet motif 4a resides in the Tcf3 binding domain, and motif 11d maps to the region implicated in Vangl binding (Zhang et al. 2006; Suriben et al. 2009; Kivimae et al. 2011). Thus, it is possible that these motifs improved the ability to control Wnt signaling events.

The ability to inhibit Alk5 may have evolved with *Dact2,4* genes

Functional studies on mammalian and zebrafish *Dact2* showed that this molecule can regulate both Wnt and Tgfβ signaling (Waxman et al. 2004; Zhang et al. 2004; Su et al. 2007). The corresponding test has not been carried out for Dact1,3; however, in binding assays using mouse Dact proteins, only Dact2 showed significant Alk5 affinity (Kivimae et al. 2011). Interestingly, the region that had been implicated in Dact2-Alk5 interaction is very similar in all Dact2 and 4 proteins. Moreover, this region contains the motif 3b, possibly a duplicated version of motif 3a, that has been shed in Dact1,3 proteins. Furthermore, gnathostome Dact2, 4 have secondarily lost the S-P rich motif 4a in the Tcf3 binding domain and motif 5b in the internal Dvl binding domain. Molecular studies are required to test whether these differences account for the ability of Dact proteins to interact with Alk5. However, it is quite possible that the ability to regulate Tgfβ signaling evolved with or was stabilized in the ancestor of Dact2,4, at the expense some functions in the Wnt signaling system.

Could the gnathostome Dact4 be an "anti-Dact"?

After the two (teleosts: three) rounds of vertebrate genome duplications, while re-diploidization occurred for many genes, duplicated genes involved in signaling have been preferentially retained, and this has been interpreted as an evolutionary platform to increase complexity (Huminiecki and Heldin, 2010). However, immediately after these duplication events, biological systems are potentially deregulated and instable. Specifically, the ancestral vertebrate now had four *Dact* genes, all possibly interfering with Wnt signaling. Moreover, with the duplication of *Dact2,4*, possibly also the capacity to inhibit Tgfβ signaling was enhanced. Furthermore, in the

actinopterygian lineage, the *Dact4r* gene appeared, potentially further destabilizing the system. How did vertebrates cope with this?

In a number of vertebrate lineages, *Dact* genes were shed: mammals lost *Dact4*, birds lost *Dact3* and *4*, frogs lost *Dact2* and *4* (remarkably, *Xenopus Dact3* is rather divergent and may have taken over some *Dact2* function), teleosts rid themselves of the duplicated *dact1* (pufferfish lost both *dact1* copies), *dact2*, *dact4*, and most also lost *dact4r*. In animals that kept a complement of *Dact1, 2, 3*, the Dact3 L-zipper was reduced or incapacitated, thus inhibiting the ability to dime rise. In teleost dact3 proteins, the motif4b in the Tcf3 binding domain was reduced (dact3b) or removed (dact3a), possibly reducing Tcf3-binding capacity. Furthermore, in most (except zebrafish) *dact3b* genes the 3rd exon was lost. Thus, specifically in teleosts, *dact3* may have evolved into a less potent version of *dact1*.

Amongst gnathostome *Dacts*, however, *Dact4* is the most derived. The protein lost (motifs 2b,c, 7b,c, 8a-c, 9, 11c,d,f), modified (motifs 2a, 3a, 11a,b,e,g) and gained (motifs 6, 10) a number of motifs. Significantly, the lost motifs encompass the L-zipper; thus, the proteins are unable to dime rise. The modified motifs encompass the internal and the C-terminal (loss of MTTV sequence) Dvl binding domain, and hence, Dact4 proteins may be unable to regulate this key molecule essential for all Wnt pathways. Since some motifs have been maintained and new motifs have been stabilized, we can assume, however, that the protein is able to carry out some protein-protein interactions. This may lead to a sequestering of Dact-interacting proteins, and hence the antagonization of Dact1,2,3 function.

The combinatorial expression of *Dact* genes may determine the outcome of Wnt and Tgfβ signaling events in gnathostomes

In addition of gene loss, and sub- and neo-functionalization of proteins, duplicated genes may diversify at the level of their cis-regulatory sequences leading to expression divergence (Huminiecki and Heldin, 2010). However, our expression analysis of chicken (*Dact1,2* genes only) and zebrafish *dacts* (*dact1,2,3a,3b,4,4r*) suggests that at the pharyngula- early somite stage of development, i.e. the vertebrate phylotypic stage (Irie and Sehara-Fujisawa, 2007), *Dact* genes are co-expressed in many tissues. Notably, *Dact1* and *2* genes were expressed in somites, the fin/limb buds and the mesenchyme of the pharyngeal arches. These domains have also been shown to express *Dact1*, *Dact2* and *Dact3* in the mouse (Cheyette et al. 2002; Gloy et al. 2002; Gillhouse et al. 2004; Fisher et al. 2006; Hunter et al. 2006; Suriben et al. 2006; Alvares et al. 2009), suggesting that these domains are the sites of original *Dact* function before the split of the Dact1,3 and the Dact2,4 groups. Given that *Dact* genes are coexpressed in a number of tissues, we have to postulate that the outcome of Wnt and Tgfβ signaling events depends on the combinatorial activity of these *Dacts*.

In the zebrafish, *dact3* and *dact4* genes are mainly expressed in the brain, nevertheless still labeling the pharyngeal arches (*dact3b*) and the pectoral fin buds (*dact4, 4r*). The latter is remarkable since the expression of a retrotranscribed gene depends on the regulatory elements present at the integration site. It is tempting to speculate that this potential anti-dact has been kept since, together with the original *dact4*, it may counterbalance the function of the numerous dact1-3 gene products. However, the net outcome of *Dact* function in the chicken (few *Dacts*, no potential anti-*Dact*) and in the fish (many *dacts*, but potentially counterbalanced by *dact4* and *4r*) may be similar.

CONCLUSIONS

This study traced the evolution of vertebrate *Dact* genes and with it, the evolution of a molecular system that allows the simultaneous control of Wnt and Tgfβ signaling. Our study suggest that *Dact1,3* arose from one, *Dact2,4* from another precursor during the second round of vertebrate genome duplications. The protein motifs present in cephalochordate and gnathostome Dacts suggests that while the control of Wnt signaling may have been the ancestral role of these proteins, the ability to inhibit Tgfβ signaling may have evolved with the gnathostome *Dact2,4* precursor. Moreover, our study raises the possibility that in those vertebrates that kept Dact4, this protein may inhibit the function of the other Dacts. Our study provides the basis for structural and molecular biologists to systematically test the function of the shared and divergent Dact protein motifs, and for cell and developmental biologists to explore the combinatorial aspects of Dact function.

MATERIALS AND METHODS

Database searches

Genomes of Humans, mouse, cattle, dog, African elephant, opossum, platypus, chicken, turkey, zebrafinch, duck, budgerigar, Anole lizard, Western painted turtle, Chinese soft shield turtle, *Xenopus* tropicalis, *Latimeria* chalumnae, spotted gar, zebrafish, Atlantic cod, Fugu, Tetraodon, stickleback, Medaka, Nile *Tilapia*, Southern platyfish, sea lamprey, Ciona intestinalius, Ciona savignyi, *Drosophila* melanogaster;, C.elegans, saccharomyces cerevisiae were searched using the Ensemble browser (http://www.ensembl.org/index.html; genome editions 2012 and 2008). Genomes of the Burmese python, Oikopleura dioica, *Branchiostoma* floridae, Saccoglossus kowalevskii,

Strongylocentrotus purpuratus, Aplysia californica, Tribolium castaneum, Bombyx mori, C.briggsae, Loa loa and of the groups Kinetoplastida including Trypanosoma and Funghi were searched using the NCBI browser (http://www.ncbi.nlm.nih.gov/; 2011 genome editions). The genome of the elephant shark was searched at the portal of the elephant shark genome project (http://esharkgenome.imcb.a-star.edu.sg/). EST databases for the above species and for *Xenopus* laevis and for the taxonomical groups lungfish, chondrosts, holosts, teleosts, chondrichthyans, agnathans, ascidians, protostomes and for protists were performed, using the NCBI browser. The first round of data base searches were performed using the human and mouse Dact1,2,3; chicken Dact1,2; *Xenopus* laevis Dact1a,1b and zebrafish Dact1,2 protein sequences as baits. Subsequently, we also used the newly identified zebrafish, lizard and turtle Dact3 and Dact4 sequences, the lamprey and the *Branchiostoma* sequences as baits. Moreover, we performed searches with protein sequences encoded by individual exons.

Molecular phylogenetic analyses

For molecular phylogenetic analyses, protein sequences were pre-aligned (with invertebrate outgroup sequences included) using ClustalW (Thompson et al. 1994) and T-Coffee (Notredame et al. 2000). The alignments were then finalized manually using BioEdit (Hall, 1999) and trimmed to remove non-significant residues. Phylogenetic tree reconstruction was carried out using maximum likelihood method. Finished alignments were fed into PhyML 3.0 (Guindon et al. 2010) on the phylogeny.fr server (Dereeper et al. 2008). The resulting tree was visualized using iTOL (Letunic and Bork, 2007).

Motif prediction

To identify potential functional domains in the Dact proteins, protein sequences were searched using PSort (Nakai and Horton, 1999) and NetNes 1.1 (la Cour et al. 2004).

Embryos and *in situ* hybridization

Fertilized chicken eggs (Winter Farm, Royston) were incubated in a humidified atmosphere at 38.5°C. Embryos were staged staged according to (Hamburger and Hamilton, 1951). Zebrafish embryos (Biological Services Unit, King's College London) were raised at 28°C in egg water (0.3 gl/l Instant Ocean Salt, 1 mg l/l Methylene Blue; after 24hpf supplemented with 0.2 mM 1-phenyl-2-thiourea (PTU, Sigma) to prevent pigmentation) and staged according to (Kimmel et al. 1995). All embryos were harvested in 4% PFA and subjected to in situ hybridization as described in (Alvares et al. 2009) (chicken embryos) and (Thisse and Thisse, 2008) (zebrafish embryos). Probes for chicken *Dact1* and *Dact2* are detailed in (Alvares et al. 2009), Probes for zebrafish *Dact1* and *Dact2* were amplified from cDNA obtained from 36hpf embryos, using the primers zfDact1F 5'-GTTGCTTAGGAAACAGTTGAA-3', zfDact1R 5'- GATGATGTCTGGGAGCCTAC-3', zfDact2F 5'-TGGTGGTTCAGGCTCATTGT-3' and zfDact2R 5'- GTTGAGGTCCATTCAGCGAT-3'. Probes for zebrafish *Dact3a, 3b, 4, 4r* were obtained from the plasmids IMAGp998P2412045Q (*Dact3a*), IMAGp998G1214848Q (*Dact3b*); IMAGp998F2414609Q (*Dact4*); IMAGp998I1217623Q (*Dact4r*) obtained from Source Bioscience.

ACKNOWLEDGEMENTS

We are grateful to Karl Wotton and Simon Kolstoe for helpful discussions and advice. The work was supported by grants from the Association Française contre les Myopathies (AFM N°14153) and the Anatomical Society to S.D, the European Regional Development Fund grant Trans Channel Neuroscience Network (TC2N) to F.R.S. and FAPESP (2006/05892-3) to L.E.A.

REFERENCES

Alvares L.E., Winterbottom F.L., Jorge E.C., Rodrigues Sobreira D., Xavier-Neto J., Schubert F.R., Dietrich S. **Chicken dapper genes are versatile markers for mesodermal tissues, embryonic muscle stem cells, neural crest cells, and neurogenic placodes.** *Dev Dyn.* May;238(5):1166-78. 2009.

Brott B.K, Sokol S.Y. **A vertebrate homolog of the cell cycle regulator Dbf4 is an inhibitor of Wnt signaling required for heart development**. *DevCell*. 8(5):703-715. 2005.

Chen AE, Ginty DD, Fan CM. **Protein kinase A signalling via CREB controls myogenesis induced by Wnt proteins**. Nature. Jan 20;433(7023):317-22. Epub 2004 Nov 28. 2005.

Chen H., Liu L., Ma B., Ma T.M., Hou J.J., Xie G.M., Wu W., Yang F.Q., Chen Y.G. **Protein kinase A-mediated 14-3-3 association impedes human Dapper1 to promote dishevelled degradation**. *J Biol Chem*. 2011.

Cheyette, B.N.R., Waxman, J.S., miller, J.R., Takemaru, K., Sheldahl, L.C., Khlebtsova, N., Fox, E.P., Earnest, T., Moon, R.T. **Dapper, a Dishevelled-associated antagonist of betacatenin and JNK signaling, is required for notochord formation.** *Dev Cell*. 2: 449-461. 2002.

Croce JC and McClay DR**. Evolution of the Wnt Pathways.** Methods Mol Biol. 2008; 469: 3–18.

Delsuc F, Brinkmann H, Chourrout D, Philippe H. Tunicates and not cephalochordates are the closest living relatives of vertebrates. Nature. Feb 23;439(7079):965-8. 2006

Dereeper A, Guignon V, Blanc G, Audic S, Buffet S, Chevenet F, Dufayard JF, Guindon S, Lefort V, Lescot M, Claverie JM, Gascuel O. **Phylogeny.fr: robust phylogenetic analysis for the non-specialist.** Nucleic Acids Res. Jul 1;36(Web Server issue):W465-9.

Fisher DA, Kivimae S, Hoshino J, Suriben R, Martin PM, Baxter N,Cheyette BNR: **Three Dact Gene Family Members are Expressed During Embryonic Development and in the Adult Brains of Mice**. *DevDyn*. 235:2620-2630. 2006.

Gao X., Wen J., Zhang L., Li X., Ning Y., Meng A., Chen Y.G. **Dapper1 is a nucleocytoplasmic shuttling protein that negatively modulates wnt signaling in the nucleus**. *J Biol Chem.* 283(51):35679-35688. 2008.

Gillhouse M., Nyholm M.W., Hikasa H., Sokol S.Y., Grinblat Y. **Two Frodo/Dpr homologs are expresssed in the developing brain and mesoderm of zebrafish.** *Developmental Dynamics*, 230: 403-9. 2004.

Gloy, J., Hikasa, H. & Sokol, S.Y. **Frodo interacts with Dishevelled to transduce Wnt signals.** *Nat Cell. Biol*. 4: 351-357. 2002.

Guindon S, Dufayard JF, Lefort V, Anisimova M, Hordijk W, Gascuel O. New algorithms and methods to estimate maximum-likelihood phylogenies: assessing the performance of PhyML 3.0. Syst Biol. May;59(3):307-21. 2010.

Hall TA. BioEdit**: a user-friendly biological sequence alignment editor and analysis program for Windows 95/98/NT.** Nucleic acids symposium series. **1999**

Hikasa H., Sokol S.Y. **The involvement of Frodo in TCF-dependent signaling and neural tissue development**. Development. 131(19):4725-4734. 2004.

Holland P.W.H., Garcia-Fernindez J., Williams N.A., Sidow A. **Gene duplications and the origins of vertebrate development**. *Development*, 125-133. 1994.

Horton P, Park KJ, Obayashi T, Fujita N, Harada H, Adams-Collier CJ, Nakai K. WoLF PSORT: protein localization predictor. Nucleic Acids Res. Jul;35(Web Server issue):W585-7. Epub 2007 May 21. 2007.

Huminiecki L, Goldovsky L, Freilich S, Moustakas A, Ouzounis C, Heldin CH. **Emergence, development and diversification of the TGF-beta signalling pathway within the animal kingdom**. BMC Evol Biol. Feb 3;9:28. 2009.

Hunter N.L., Hikasa H., Dymecki S.M., Sokol S.Y. **Vertebrate homologues of Frodo are dynamically expressed during embryonic development in tissues undergoing extensive morphogenetic movements.** *Dev Dyn.* Jan;235(1):279-84. 2006.

Irie N, Sehara-Fujisawa A. **The vertebrate phylotypic stage and an early bilaterian-related stage in mouse embryogenesis defined by genomic information**. BMC Biol. Jan 12;5:1. 2007

Ishitani T, Ninomiya-Tsuji J, Matsumoto K. Regulation of lymphoid enhancer factor 1/T-cell factor by mitogen-activated protein kinase-related Nemo-like kinase-dependent phosphorylation in Wnt/beta-catenin signaling. Mol Cell Biol. Feb;23(4):1379-89. 2003

Kestler HA, Wawra C, Kracher B, Kühl M. **Network modeling of signal transduction: establishing the global view**. Bioessays. Nov;30(11-12):1110-25.2008.

Kivimäe S., Yang X.Y., Cheyette B.N. **All Dact (Dapper/Frodo) scaffold proteins dimerize and exhibit conserved interactions with Vangl, Dvl, and serine/threonine kinases.** *BMC Biochem*. Jun 30;12:33. doi: 10.1186/1471-2091-12-33. 2011.

Kumar S, Hedges SB. **A molecular timescale for vertebrate evolution**. Nature. Apr 30;392(6679):917-20. 1998

Kuraku S, Meyer A, Kuratani S. Timing of genome duplications relative to the origin of the vertebrates: did cyclostomes diverge before or after? Mol Biol Evol. Jan;26(1):47-59. 2009.

la Cour T, Kiemer L, Mølgaard A, Gupta R, Skriver K, Brunak S. Analysis and prediction of leucine-rich nuclear export signals. Protein Eng Des Sel. Jun;17(6):527-36. Epub 2004 Aug 16. 2004

Letunic I, Bork P. Interactive Tree Of Life (iTOL): an online tool for phylogenetic tree display and annotation. Bioinformatics. Jan 1;23(1):127-8. Epub 2006 Oct 18. 2007.

Meng F., Cheng X., Yang L., Hou N., Yang X., Meng A. **Accelerated reepithelialization in Dpr2-deficient mice is associated with enhanced response to TGFbeta signaling.** *J Cell Sci.* 121(Pt 17):2904-2912. 2008.

Notredame C, Higgins DG, Heringa J. T-Coffee: A novel method for fast and accurate multiple sequence alignment. J Mol BiolSep. 8;302(1):205-17. **2000.**

Park M., Moon R.T.**The planar cell-polarity gene stbm regulates cell behaviour and cell fate in vertebrate embryos.** *Nat Cell Biol.* Jan;4(1):20-5. 2002.

Su Y., Zhang L., Gao X., Meng F., Wen J., Zhou H., Meng A., Chen Y.G.**The evolutionally conserved activity of Dapper2 in antagonizing TGF-beta signaling.** *FASEB J*. 21(3):682-690. 2007.

Suriben R., Kivimae S., Fisher D.A., Moon R.T., Cheyette B.N. **Posterior malformations in Dact1 mutant mice arise through misregulated Vangl2 at the primitive streak**. *Nat Genet*. 41(9):977-985. 2009.

Taylor J.S., Braasch I., Frickey T., Meyer A**,** Van de Peer Y**. Genome duplication, a trait shared by 22000 species of ray-finned fish**. Genome Res. Mar;13(3):382-90.2003.

Teran E., Branscomb A.D., Seeling J.M. **Dpr Acts as a molecular switch, inhibiting Wnt signaling when unphosphorylated, but promoting Wnt signaling when phosphorylated by casein kinase Idelta/epsilon**. *PLoS One*. 4(5):e5522. 2009.

Thompson JD, Higgins DG, Gibson TJ.**CLUSTAL W: improving the sensitivity of progressive multiple sequence alignment through sequence weighting, position-specific gap penalties and weight matrix choice**. Nucleic Acids Res. Nov 11;22(22):4673-80. 1994.

Topol L, Jiang X, Choi H, Garrett-Beal L, Carolan PJ, Yang Y. **Wnt-5a inhibits the canonical Wnt pathway by promoting GSK-3-independent beta-catenin degradation**. J Cell Biol. Sep 1;162(5):899-908. 2003.

Waxman J.S, Hocking A.M., Stoick C.L., Moon R.T. **Zebrafish Dapper1 and Dapper2 play distinct roles in Wnt-mediated developmental processes**. *Development*. 131(23):5909-5921. 2004.

Wen J., Chiang Y.J., Gao C., Xue H., Xu J., Ning Y., Hodes R.J., Gao X., Chen Y.G. **Loss of Dact1 disrupts planar cell polarity signaling by altering dishevelled activity and leads to posterior malformation in mice.** *J Biol Chem.* 285(14):11023-11030. 2010.

Wu M.Y., Hill C.S. **Tgf-beta superfamily signaling in embryonic development and homeostasis**. *Dev Cell.* Mar;16(3):329-43. 2009.

Zhang L, Gao X, Wen J, Ning Y, Chen Y.G. **Dapper 1 antagonizes Wnt signaling by promoting dishevelled degradation.** *JBiolChem*. 281:8607-8612. 2006.

Zhang, L., Zhou, H., Su, Y., Sun, Z., Zhang, H., Zhang, L., Zhang, Y., Ning, Y., Chen, Y.G. & Meng, A. **Zebrafish Dpr2 inhibits mesoderm induction by promoting degradation of nodal receptors.** *Science.* 306: 114-117. 2004.

LEGENDS

Fig.1 and Table 1. Occurrence of *Dact* genes in bilateria

Searching bilaterian DNA databases with known Dact protein or protein motif sequences as baits, novel Dact genes were identified. However, Dact genes were only found in gnathostome and agnathan vertebrates and in cephalochordates, suggesting that these genes arose late during deuterostome evolution. Judged by linear amino acid sequence similarity, presence of specific sequence motifs, phylogenetic analyses and the organization of the corresponding genomic loci, gnathostome Dact sequences fell into four paralog groups, in line with the two rounds (2R) of genome duplication. In teleosts, a third round of genome duplication (3R) occurred. However, of the teleost-specific duplicates only *dact3a* and *3b* genes were maintained. In actinopterygians, *dact4* was retrotranscribed before the holost-teleost split, but this gene was only maintained in the gar and in zebrafish.

Fig.2. Features of Dact proteins

Graphical representation of conserved sequences stretches and motifs in Dact proteins. Exon1 and exon3 encoded sequences are represented by dark blue and exon2 and 4 encoded sequences by black lines; gaps introduced to align similar sequences are shown by thin grey lines (large gaps only). In the lamprey, the genomic fragment carrying dact exon1 sequences was not linked to the fragments carrying exons 3-4 of dact A and B, hence the exon1 carrying fragment may belong to either dact A or B (dotted grey lines). Exon boundaries are indicated below a set of sequences; note that the exon2-3 boundary in vertebrate and *Branchiostoma* Dacts is different; for ease of comparison, the vertebrate nomenclature was applied throughout.

Protein motifs are depicted as purple boxes; where Dact1 and 3 proteins share a specific variation of a motif, this is shown in red, Dact2,4 shared motif variations are shown in green, the motif11g variation shared by gnathostome Dact2 and lamprey dact B is depicted in turquoise, motifs typical for a particular Dact paralog are shown in yellow. The leucine zipper is marked by mid-blue, higher boxes; the light blue and lilac shading indicates the most conserved areas of Dact proteins. Motifs are numbered according to their position in the Dact gapped alignment; linked motifs are marked by

letters, rudimentary versions of a motif are in brackets. Known roles of motifs or sequence stretches are indicated at the top, predicted roles are marked in grey and with dotted lines.

Note that gnathostome Dacts carry specific combinations of sequence motifs and can be assigned to four paralogous groups. Motifs 1, 2e, 2f, 4b, 5a, 5b, 11e, 11f and the alkaline aa of motif 11g are found in vertebrate and *Branchiostoma* Dacts and may account for their evolutionarily basic roles. The leucine zipper and motifs 2a-d, 3c, 5c and 8b are found in gnathostome Dacts and in the dact protein of *Branchiostoma*, suggesting that also these belong to the original repertoire of Dact proteins (all marked by arrowheads). Motifs 3b, 4a, 7c and the PDZ binding domain of motif 11g are found in gnathostome and the lamprey Dacts, suggesting that they arose in the vertebrate lineage (arrows). Motifs 3a, 7b, 8a, 8c, 9,11a-d are shared by the majority of gnathostome Dacts but not he lamprey dacts, suggesting that these domains arose after the agnathan-gnathostome split but prior to the two rounds of gnathostome genome duplication (crosses).

Gnathostome Dact1 and Dact3 proteins share a similar variant of motifs 1, 4a, 5b, 7b, 11e, 11 g and lack motif 3b, while Dact 2 and 4 have similar motif variants for motifs 1, 2f, 3a-c and lack motif 4a, 5b and 8b. This suggests that *Dact1,3* may have arisen from one, *Dact2,4* from the second *Dact* gene generated during the 1st round of gnathostome genome duplication. However, subsequently Dact3, and more prominently Dact4, lost a number of motifs and gained new motifs, suggesting that they evolved novel functions.

Individual Dact1,3 (red) or Dact 2,4 (green) motif variants could be traced back to the lamprey and lancelet, suggesting that they represent the original form of that motif.

Fig.3. Organization of gnathostome *Dact* genomic loci

Shape code: circle - *Dact* gene; square - gene with paralogs also associated with *Dact* genes; triangle, tip down - unique gene without any paralogs; triangle, tip up - gene with paralogs not associated with *Dact* loci.

Shape infill: yellow infill- *Dact* genes; colored infill - genes associated with tetrapod and teleost *Dact* loci. A rainbow color scheme was applied to the human locus in the case of *Dact1,3* and *4*; in the case of *Dact2*, the mammalian loci are fragmented, hence the rainbow color scheme was applied to the

better preserved chicken locus. Orthologous genes are displayed in the same color. Gray infill - genes associated with teleost *Dact* genes only; striped pattern - genes associated with *Dact* loci in teleosts, non-mammalian tetrapods and the opossum, but dispersed in placental mammals. The color of the stripes corresponds to that of the neighboring filled-in shape in teleosts. A diagonal bar in the boxes representing *Six* genes indicates the presence of several *Six* paralogs at this site.

Underlying shading: yellow shading - *Dact* genes; colored shading - core genes associated with a particular *Dact* gene; grey shading - genes within 1Mb distance from Dact genes.

Double slash - genes or gene groups separated by more than 3Mb.

Species names (abbreviations: see Suppl. Table 1) and genomic localization of genes are indicated on the left side of the figures if the loci are continuous. If genes are distributed over several scaffolds or chromosomes, the names of these sites are shown next to the corresponding genomic fragment.

Note that the same genes, albeit not always in the same order, are associated with a particular *Dact* ortholog, also note that the teleost *Dact3a* and *3b* loci are similar. This supports our assignment of gnathostome Dact sequences to the four paralog groups. A number of genes are only found in conjunction with teleost *Dact* genes, suggesting that they have invaded the locus after the two round of genome duplication shared by sarcopterygians and actinopterygians, but before the third, teleost-specific genome duplication.

Fig.4. Phylogenetic tree of Dact proteins

(A) Unrooted phylogenetic tree of full length and near full length Dact protein sequences from humans (Hs), opossum (Md), chicken (Gg), Anole lizard (Ac), the Western painted turtle (Cpb), *Xenopus tropicalis* (Xt), Latimeria (Lc), the spotted gar (Lo), zebrafish (Dr), Fugu (Tr), Tilapia (On) and *Branchiostoma floridae* (Bfl), and of partial sequences from the elephant shark (Cm), and the lamprey (Pm). (B) Phylogenetic tree for the same sequences rooted from the *Branchiostoma* sequences. Both trees are based on the same alignment. Sequences are annotated using the abbreviation for the species, followed by the Dact ortholog number and in (B), the genomic localization. Note that in both trees, the gnathostome Dact1 (red branches) and Dact3 sequences (pink branches) formed a well-supported metagroup. Dact2 (turquoise branches) and Dact4 sequences (green branches) formed a

second metagroup. This corroborates that *Dact1* and *Dact3* arose from one, *Dact2* and *Dact4* from the other *Dact* gene generated during the first round of vertebrate genome duplication.

Fig.5. Summary of the phylogentic analysis of gnathostome *Dact* and *Dact* associated genes

(A) Grouping of gnathostome *Dact* and *Dact* associated genes as suggested by the phylogenetic analysis of the cognate protein sequences. Genes genomically colocalizing with a particular *Dact* gene are depicted in the same color as the associated *Dact* gene. Black boxes link genes that form a well-supported group in the corresponding phylogenetic protein tree (Suppl. Fig.12). Note that in all cases, *Dact1*,*3* and/ or *Dact2,4* associated sequences were grouped.

(B) Model for the evolution of gnathostome *Dacts*. The pairwise grouping of *Dact1,3* and *Dact2,4* and their associated genes suggests that during the first round of gnathostome genome duplication (R1), a *Dact1,3* and a *Dact2,4* precursor was generated which during the second round of genome duplication (R2) gave rise to the individual *Dact1*, *Dact3*, *Dact2* and *Dact4* genes. Subsequently, in Dact3 the L-zipper required for Dact dimerization and specifically in teleost dact3, motif4b located in the center of the Tcf3 interacting region were reduced (dact3b) or eliminated (dact3a). In Dact4, the L-zipper and PDZ binding domain of motif 11g was lost, motifs 11d-f (Vangl binding domain) were reduced, and motifs 6 and 10 were gained. This suggests that Dact3 and, more prominently, Dact4 proteins have altered molecular properties compared to Dact1, Dact2, and the original dact.

Fig.6. Comparison of *Dact* gene expression in the zebrafish and chicken

(A,B) Lateral views of E3 (HH20-21) chicken embryos, anterior to the top, and (C-H) lateral views of 36 hours post fertilization (36hpf) zebrafish embryos, anterior to the left, assayed for mRNA expression of *Dact* genes as indicated in the panel. Note that for members of both the *Dact1,3* paralog group, as well as for the *Dact2,4* paralog group, prominent expression is found in the somites, pharyngeal arches and developing paired limbs/ fins, suggesting that these are original sites of *Dact* function. It furthermore suggests that Wnt and Tgf beta signal transduction is controlled by combinatorial Dact activity rather than individual Dact genes.

Abbreviations: drg; dorsal root ganglion; ect, surface ectoderm; fl, fore limb; hb, hindbrain; hl, hind limb; ht, hart; ov, otic vesicle; pf, pectoral fin; pa, pharyngeal arches; s, somites; V, trigeminal ganglion; VII facial ganglion.

Suppl. Table 1

Bilaterians searched for *Dact* genes, abbreviations of species names are indicated on the left. *Dact* EST sequences are represented by a tick; for genomic sequences, the genomic localization is indicated, following the nomenclature of ensemble (http://www.ensembl.org/index.html), NCBI (http://www.ncbi.nlm.nih.gov/), and the elephant shark genome project (http://esharkgenome.imcb.a-star.edu.sg/).

Suppl. Table 2

Overview over the position and sequence of well conserved protein motifs in Dact proteins; consensus sequences are shown. Underlined aa – core of motifs; blue highlighter - leucines contributing to a leucine (L) zipper; leucines are also bold. Yellow highlighter - unique motif for a specific Dact paralog; red highlighter - shared by Dact1/3 proteins; green highlighter - shared by Dact2/4 proteins. Light blue and lilac shading – extended conserved sequence stretches.

Note that a number of protein motifs are shared by vertebrate and *Branchiostoma* Dacts, suggesting that they account for the evolutionarily basic Dact function. Additional motifs are shared by the majority of gnathostome Dacts, suggesting that they were present in the ancestral Dact prior to the two rounds of genome duplication. Lamprey dact B and gnathostome Dact1-3 proteins have a PDZ binding domain that is not conserved in gnathostome Dact4, suggesting that Dact4 proteins may have lost the ability to interact with Dvl. Moreover, Dact3 and Dact4 proteins have lost parts or all of their leucine zipper, suggesting a compromised ability to dime rise. Nevertheless, many sequence motifs encoded by the first three exons, and hence possible protein-protein interactions associated with these sequences are conserved in all four paralogs. A number of motifs or motif variations are shared by Dact1,3 and Dact2,4 proteins, respectively, suggesting that these pairs of proteins may share some molecular roles.

Abbreviations: actinopt., actinopterygians; aa, amino acids; Bfl, *Branchiostoma floridae*; Cm, *Callorhinchus milii*; Dr*, Danio rerio*, Pm, *Petromyzon marinus*; sarcopt., sarcopterygians.

Suppl. Figs. 1-5

Gapped alignment of Dact protein sequences, protein motifs are annotated. Additional gaps have been introduced to facilitate the identification of exon boundaries.

Suppl. Fig. 6

Consensus sequences of gnathostome Dact1-4 proteins, based on the gapped alignments. Protein motifs are indicated by solid lines, flanking amino acids conserved in a particular Dact paralog are indicated by stippled lines. Partially conserved motifs are indicated in brackets.

Suppl. Fig. 7

Arrangement of the leucine zipper in Dact1,2,3 proteins; legend included with Fig.6.

Suppl. Figs. 8-11

Wider environment of gnathostome *Dact* loci, using the same shape and color codes as in Fig.3. Note the extended similarity of genomic loci for the individual *Dact* paralogs.

Suppl. Fig. 12

Phylogenetic protein trees for genes associated with all four *Dact* loci, color code and abbreviations as in Fig.4. Note that wherever statistically well supported metagroups appeared in these trees, they encompassed *Dact1,3*and/or *Dact2,4* associated genes; all other permutations (linking *Dact1,2*; *Dact1,4*; *Dact3,2* or *Dact3,4* associated genes) did not occur. This supports the idea that *Dact1* and *Dact3* loci arose from one, *Dact2* and *Dact4* loci from the second locus generated during the 1st round of vertebrate genome duplication.

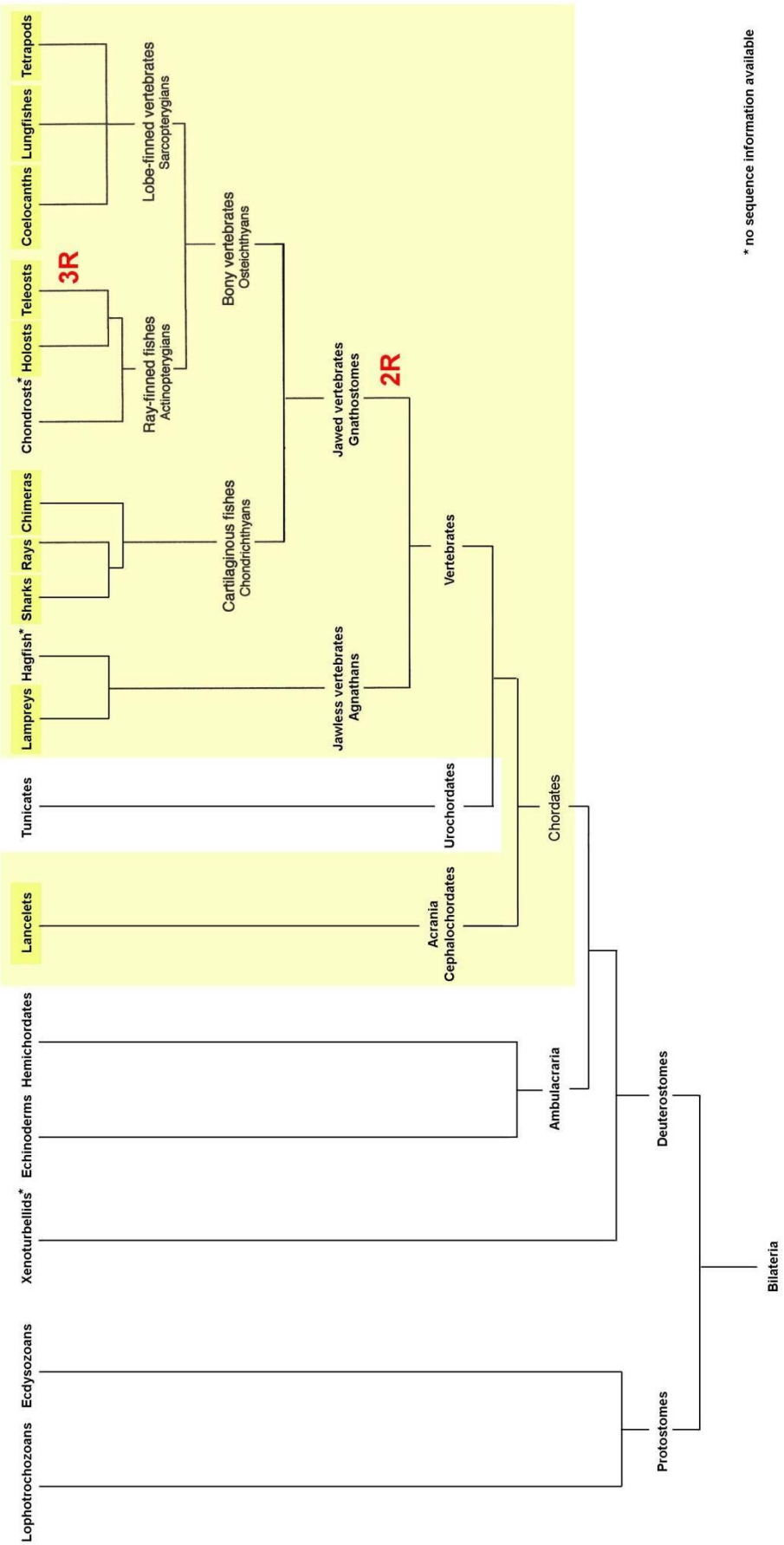
Lophotrochozoans
Ecdysozoans
Xenoturbellids*
Echinoderms
Hemichordates
Lancelets
Tunicates
Lampreys
Hagfish*
Sharks
Rays
Chimeras
Chondrosts*
Holosts
Teleosts
Coelocanths
Lungfishes
Tetrapods
Protostomes
Deuterostomes
Bilateria
Ambulacraria
Acrania
Cephalochordates
Urochordates
Chordates
Jawless vertebrates
Agnathans
Cartilaginous fishes
Chondrichthyans
Ray-finned fishes
Actinopterygians
Lobe-finned vertebrates
Sarcopterygians
Bony vertebrates
Osteichthyans
Jawed vertebrates
Gnathostomes
Vertebrates
2R
3R
* no sequence information available

Figure 1

Table 1

					Dact	Dact1	Dact2	Dact3		Dact4
Deuterostomes										
Jawed vertebrates										
	Bony vertebrates									
		Lobe-finned/limbed vertebrates incl. tetrapods*1								
			Mammals			✓	✓	✓		-
			Birds			✓	✓	-		-
			Lizards, snakes			✓	✓	✓		✓
			Turtles			✓	✓	✓		✓
			Amphibians			✓	-	✓		-
			Lungfishes			*1	✓*1	*1		*1
			Coelocanths			✓	✓	✓		✓
		Ray-finned fish								
			Holosts	Spotted gar		✓	✓	✓		✓*2
			Teleosts					3a	3b	
				Zebrafish		✓	✓	✓	✓	✓*2
				Atlantic cod		✓	✓	✓	✓	✓
				Pufferfishes		-	✓	✓	✓	✓
				Stickleback		✓	✓	✓	-	✓
				Medaka		✓	✓	✓	✓	✓
				Nile Tilapia		✓	✓	✓	✓	✓
	Cartilaginous vertebrates			Elephant shark		✓	✓	✓		✓
Jaw-less vertebrates				lamprey	✓*3					
Non-vertebrate chordates	***Cephalochordates***			Lancelet	✓					
	Tunicates (=Urochordates)				-					
Hemichordates					-					
Echinoderms					-					
Protostomes					-					

*1 Insufficient sequence information for lungfishes; however a Dact2 gene was found for Protopterus aethiopicus

*2 gar and zebrafish have a 2nd, intron-less Dact4 gene that possibly was retrotranscribed

*3 2 distinct sets of Dact sequences and additional short sequence stretches

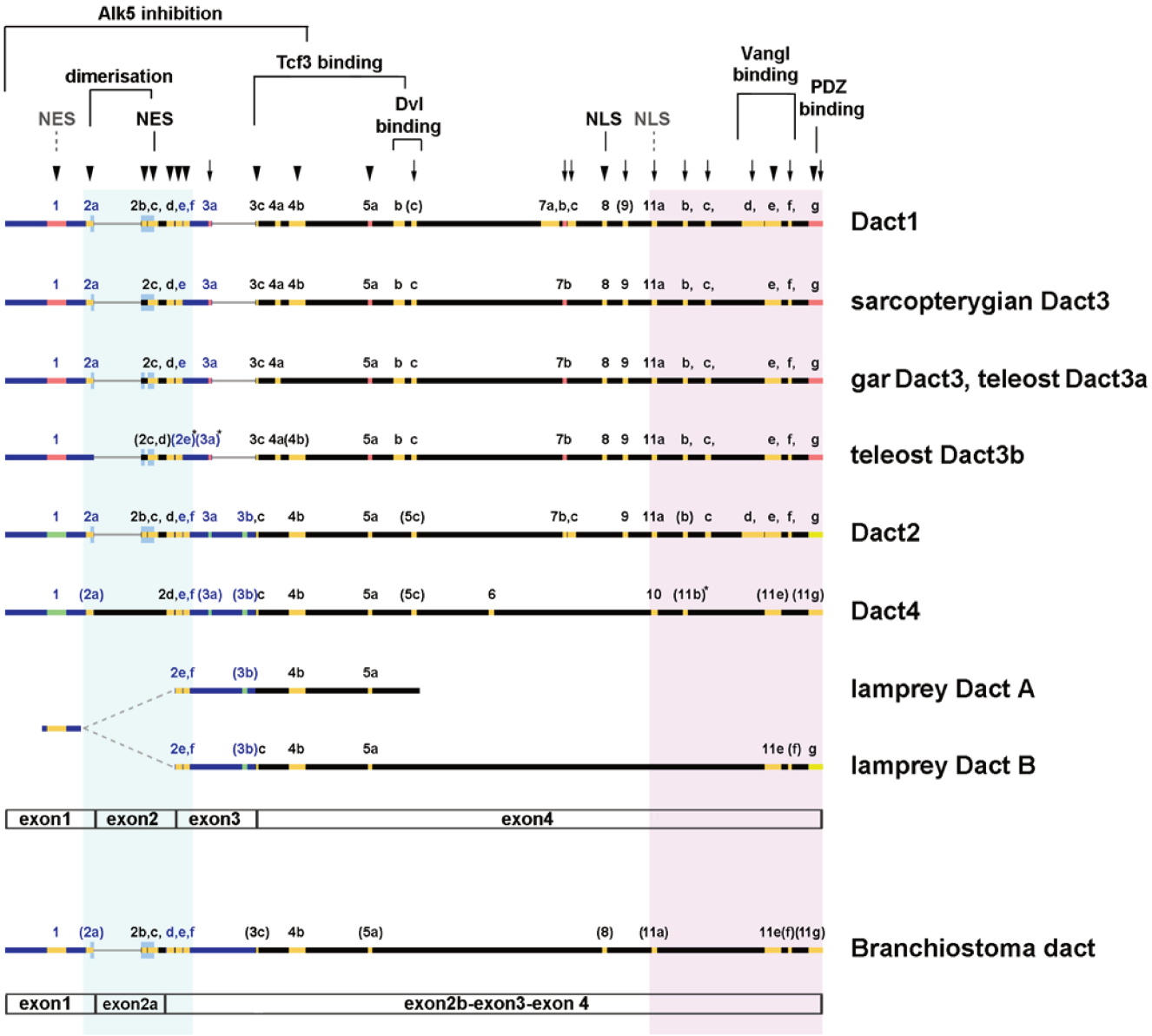
Alk5 inhibition
dimerisation
Tcf3 binding
Vangl binding
PDZ binding
NES
NES
Dvl binding
NLS
NLS
Dact1
sarcopterygian Dact3
gar Dact3, teleost Dact3a
teleost Dact3b
Dact2
Dact4
lamprey Dact A
lamprey Dact B
exon1
exon2
exon3
exon4
Branchiostoma dact
exon1
exon2a
exon2b-exon3-exon 4

Figure 2

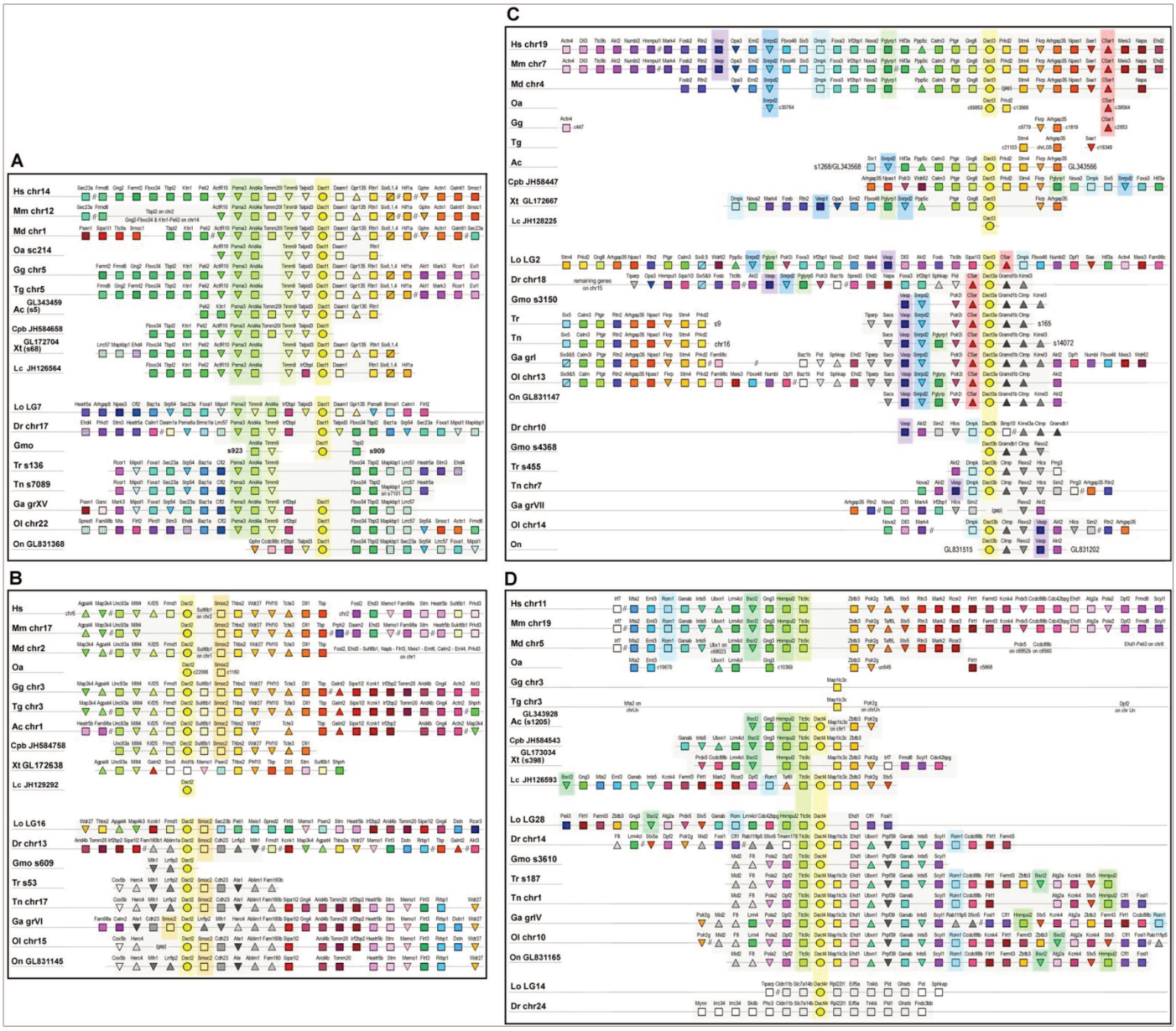
A
Hs chr14
Mm chr12
Md chr1
Oa sc214
Gg chr5
Tg chr5
GL343459
Ac (s5)
Cpb JH584658
GL172704
Xt (s68)
Lc JH126564
Lo LG7
Dr chr17
Gmo
s923
s909
Tr s136
Tn s7089
Ga grXV
Ol chr22
On GL831368
B
Hs
Mm chr17
Md chr2
Oa
Gg chr3
Tg chr3
Ac chr1
Cpb JH584758
Xt GL172638
Lc JH129292
Lo LG16
Dr chr13
Gmo s609
Tr s53
Tn chr17
Ga grVI
Ol chr15
On GL831145
C
Hs chr19
Mm chr7
Md chr4
Oa
Gg
Tg
Ac
s1268/GL343568
GL343566
Cpb JH58447
Xt GL172667
Lc JH128225
Lo LG2
Dr chr18
Gmo s3150
Tr
s9
Tn
chr16
s165
Ga grI
s14072
Ol chr13
On GL831147
Dr chr10
Gmo s4368
Tr s455
Tn chr7
Ga grVII
Ol chr14
On
GL831515
GL831202
D
Hs chr11
Mm chr19
Md chr5
Oa
Gg chr3
Tg chr3
GL343928
Ac (s1205)
Cpb JH584543
GL173034
Xt (s398)
Lc JH126593
Lo LG28
Dr chr14
Gmo s3610
Tr s187
Tn chr1
Ga grIV
Ol chr10
On GL831165
Lo LG14
Dr chr24

Figure 3

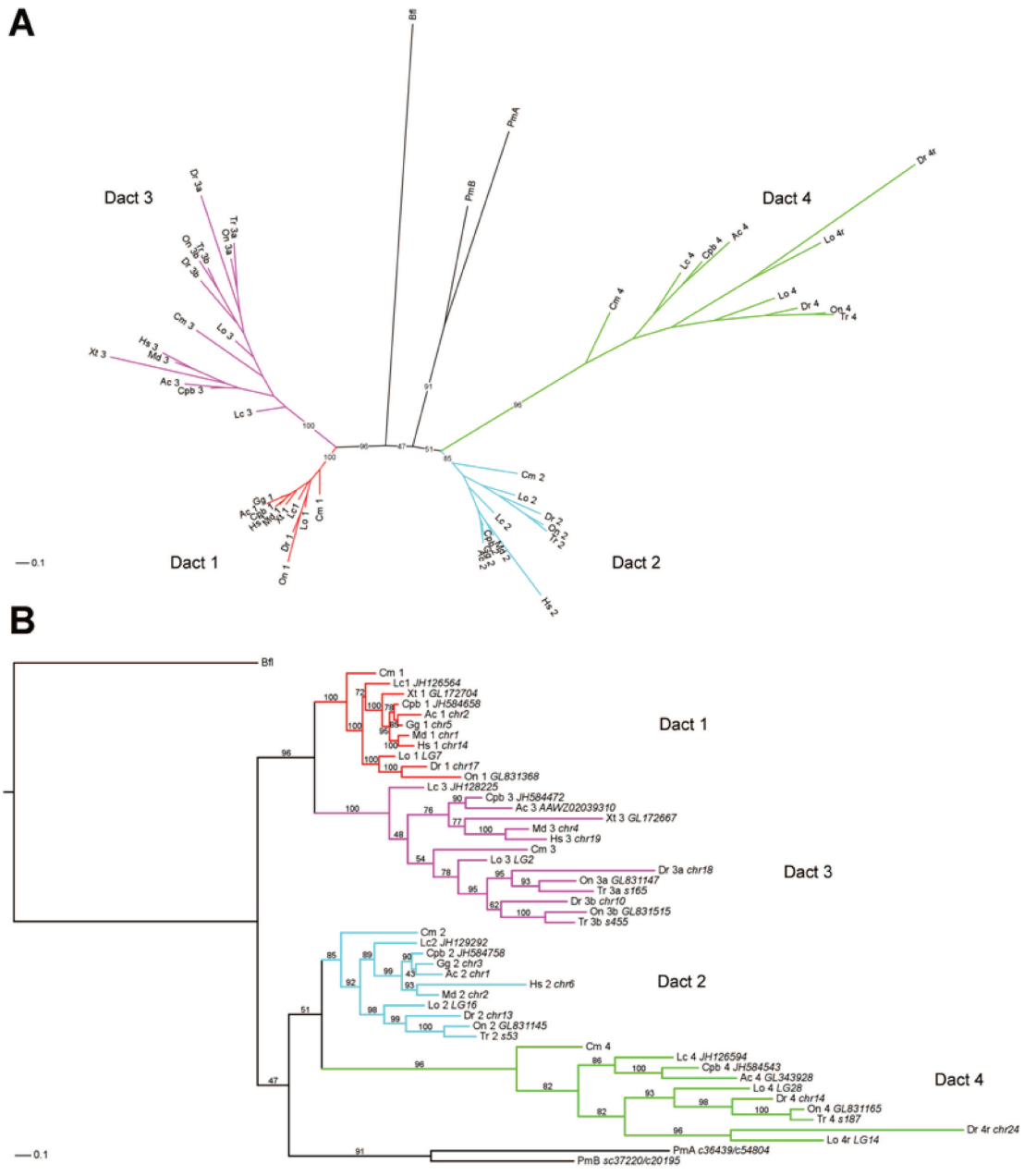
A
Bfl
PmA
PmB
Dact 3
Dact 4
Dact 1
Dact 2
0.1
B
Bfl
Cm 1
Lc1 JH126564
Xt 1 GL172704
Cpb 1 JH584658
Ac 1 chr2
Gg 1 chr5
Md 1 chr1
Hs 1 chr14
Lo 1 LG7
Dr 1 chr17
On 1 GL831368
Lc 3 JH128225
Cpb 3 JH584472
Ac 3 AAWZ02039310
Xt 3 GL172667
Md 3 chr4
Hs 3 chr19
Cm 3
Lo 3 LG2
Dr 3a chr18
On 3a GL831147
Tr 3a s165
Dr 3b chr10
On 3b GL831515
Tr 3b s455
Dact 1
Dact 3
Cm 2
Lc2 JH129292
Cpb 2 JH584758
Gg 2 chr3
Ac 2 chr1
Hs 2 chr6
Md 2 chr2
Lo 2 LG16
Dr 2 chr13
On 2 GL831145
Tr 2 s53
Dact 2
Cm 4
Lc 4 JH126594
Cpb 4 JH584543
Ac 4 GL343928
Lo 4 LG28
Dr 4 chr14
On 4 GL831165
Tr 4 s187
Dr 4r chr24
Lo 4r LG14
Dact 4
PmA c36439/c54804
PmB sc37220/c20195
0.1

Figure 4

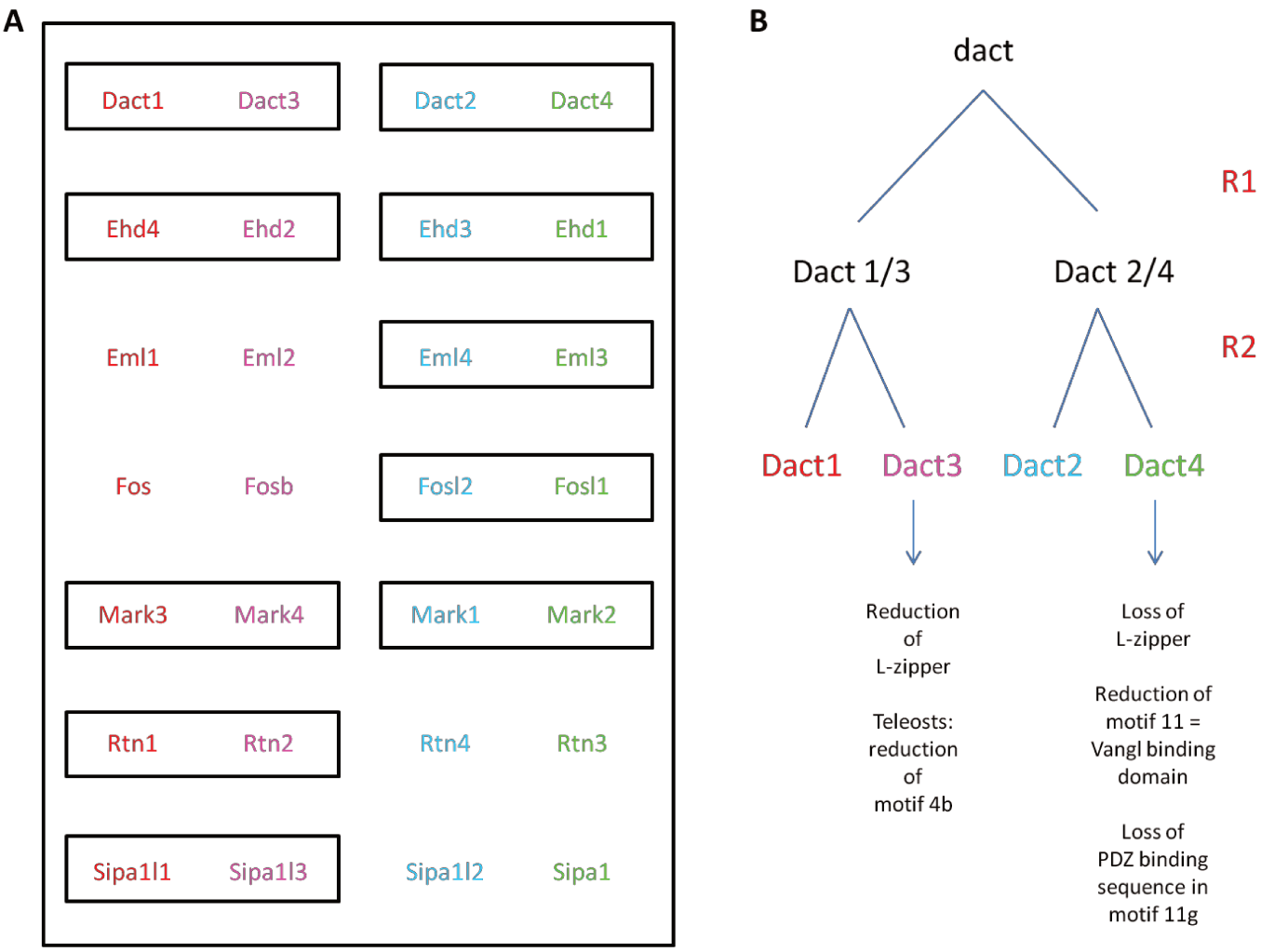
A
Dact1
Dact3
Dact2
Dact4
Ehd4
Ehd2
Ehd3
Ehd1
Eml1
Eml2
Eml4
Eml3
Fos
Fosb
Fosl2
Fosl1
Mark3
Mark4
Mark1
Mark2
Rtn1
Rtn2
Rtn4
Rtn3
Sipa1l1
Sipa1l3
Sipa1l2
Sipa1
B
dact
R1
Dact 1/3
Dact 2/4
R2
Dact1
Dact3
Dact2
Dact4
Reduction of L-zipper
Teleosts: reduction of motif 4b
Loss of L-zipper
Reduction of motif 11 = Vangl binding domain
Loss of PDZ binding sequence in motif 11g

Figure 5

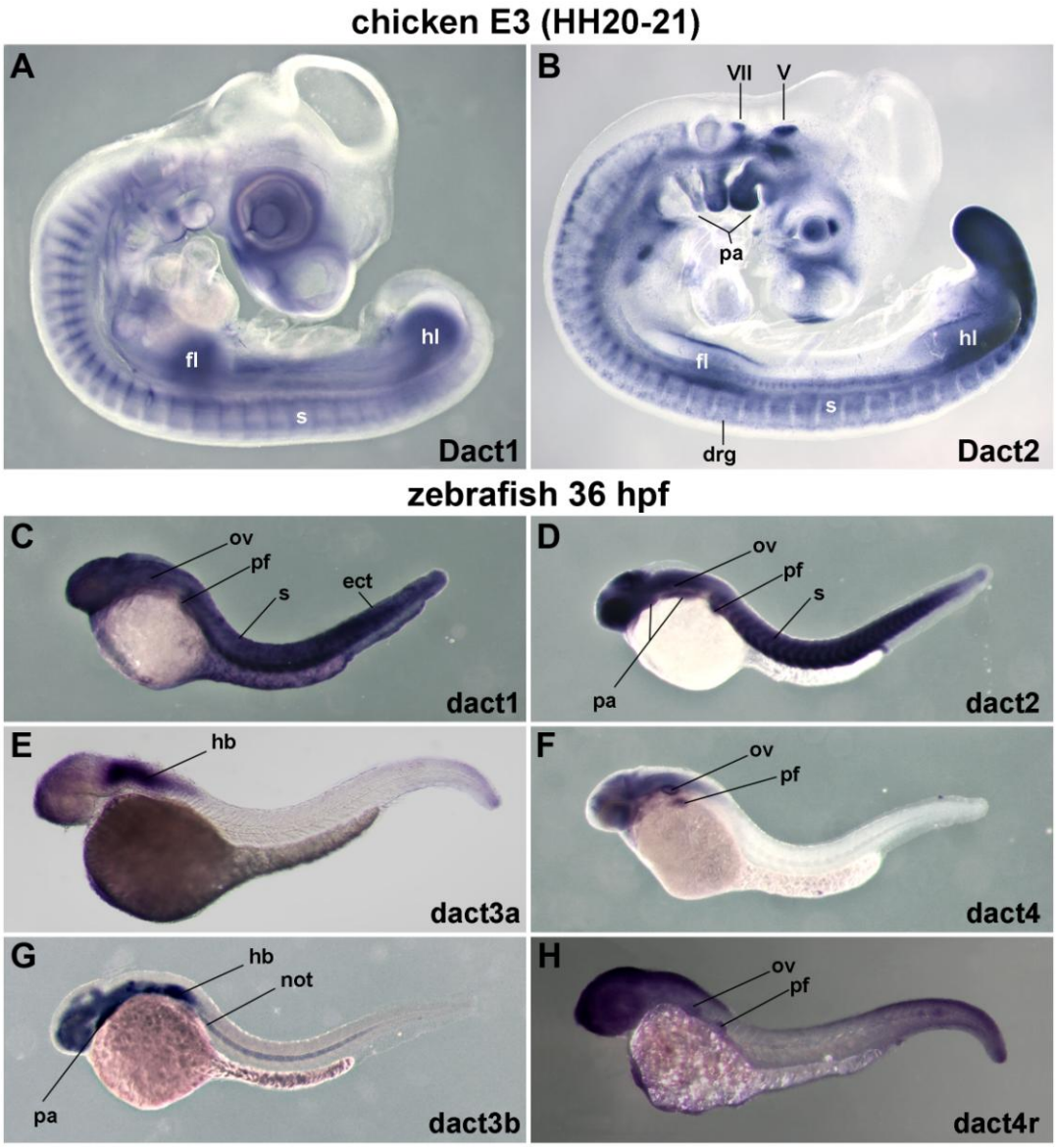
chicken E3 (HH20-21)
A
fl
hl
s
Dact1
B
VII
V
pa
hl
fl
s
drg
Dact2
zebrafish 36 hpf
C
ov
pf
s
ect
dact1
D
ov
pf
s
pa
dact2
E
hb
dact3a
F
ov
pf
dact4
G
hb
not
pa
dact3b
H
ov
pf
dact4r

Figure 6

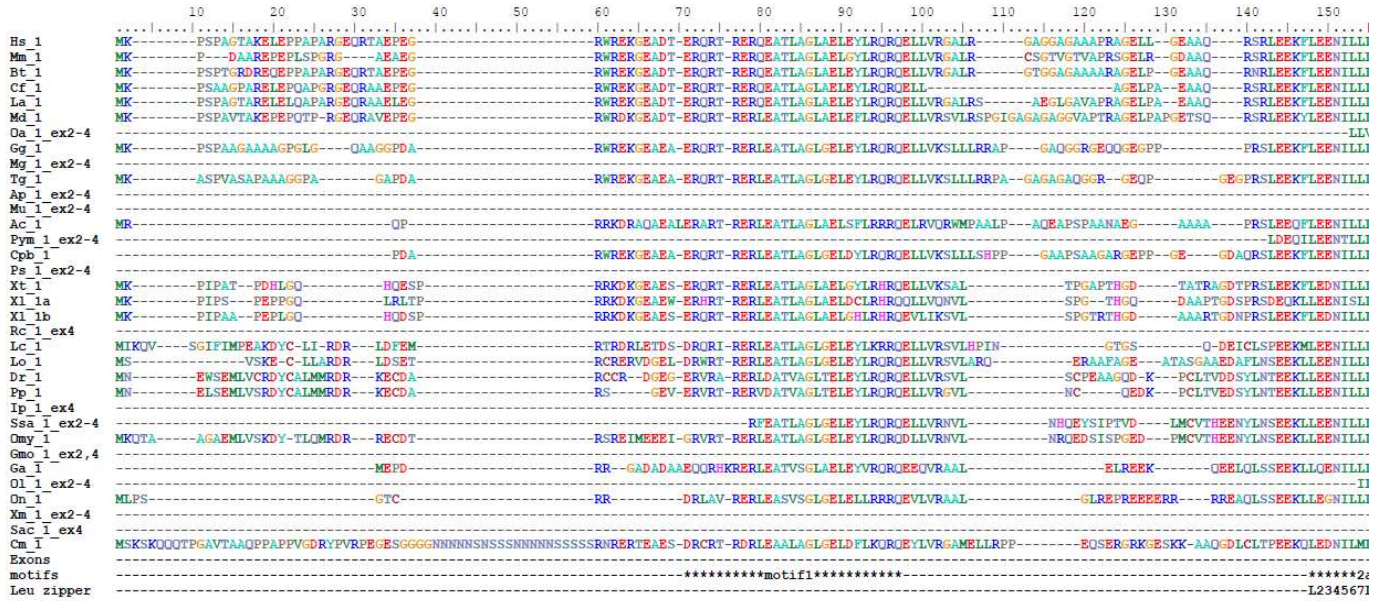

Supplemental Figure 1

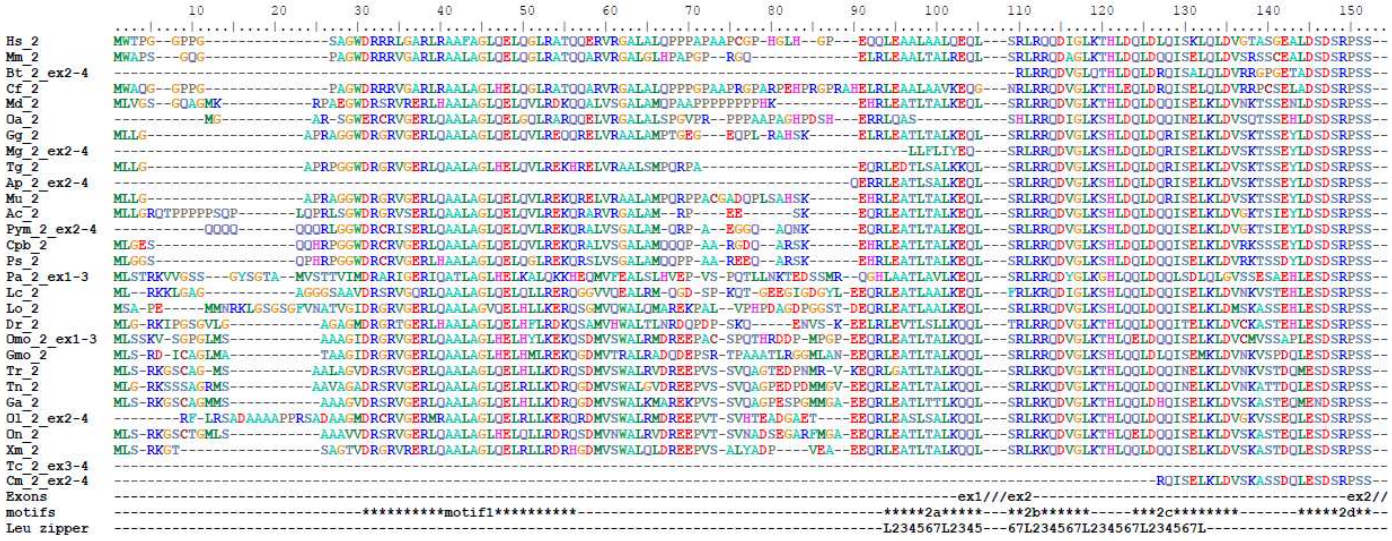

Supplemental Figure 2

Supplemental Figure 3

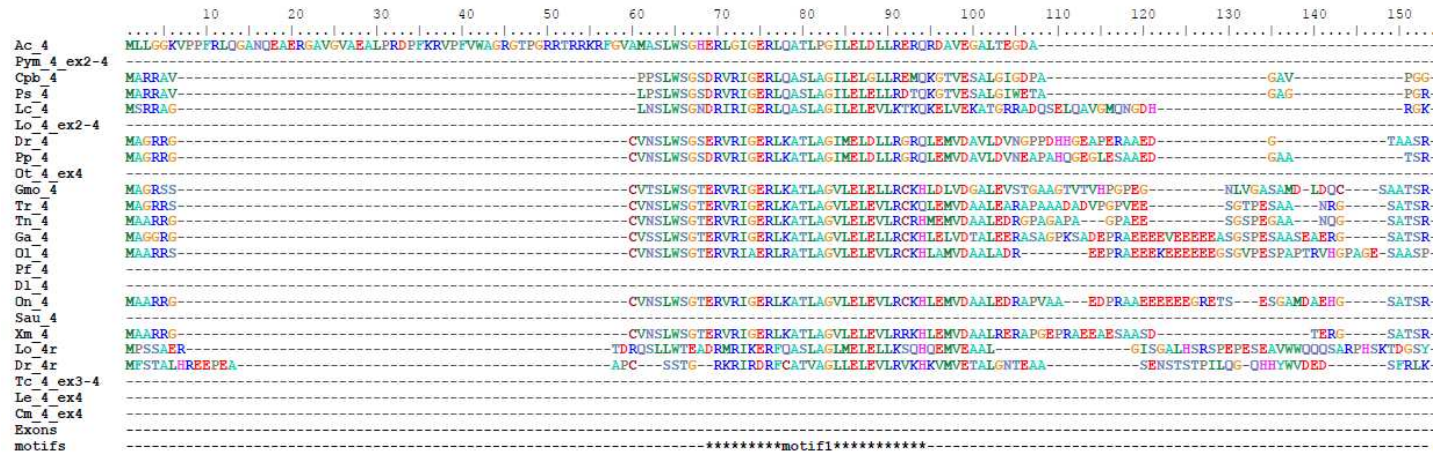

Supplemental Figure 4

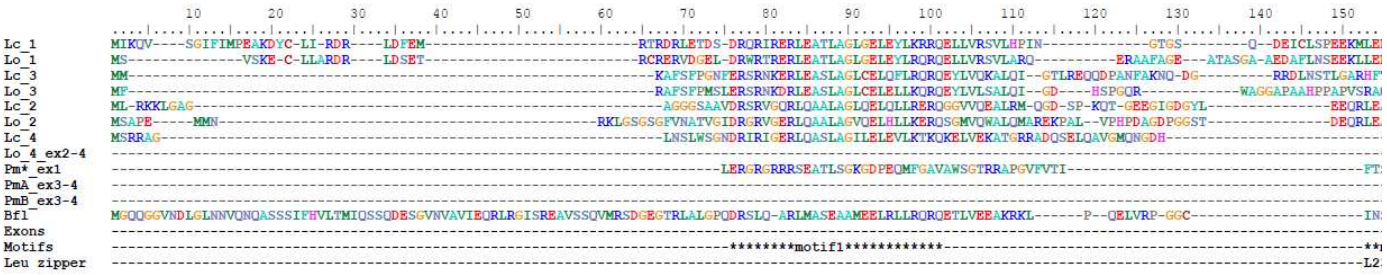

Supplemental Figure 5

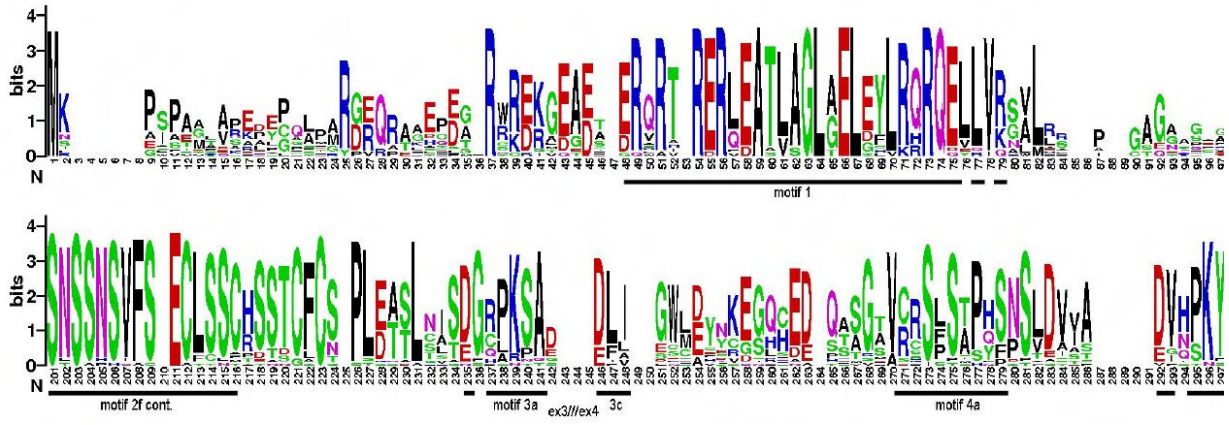

Supplemental Figure 6

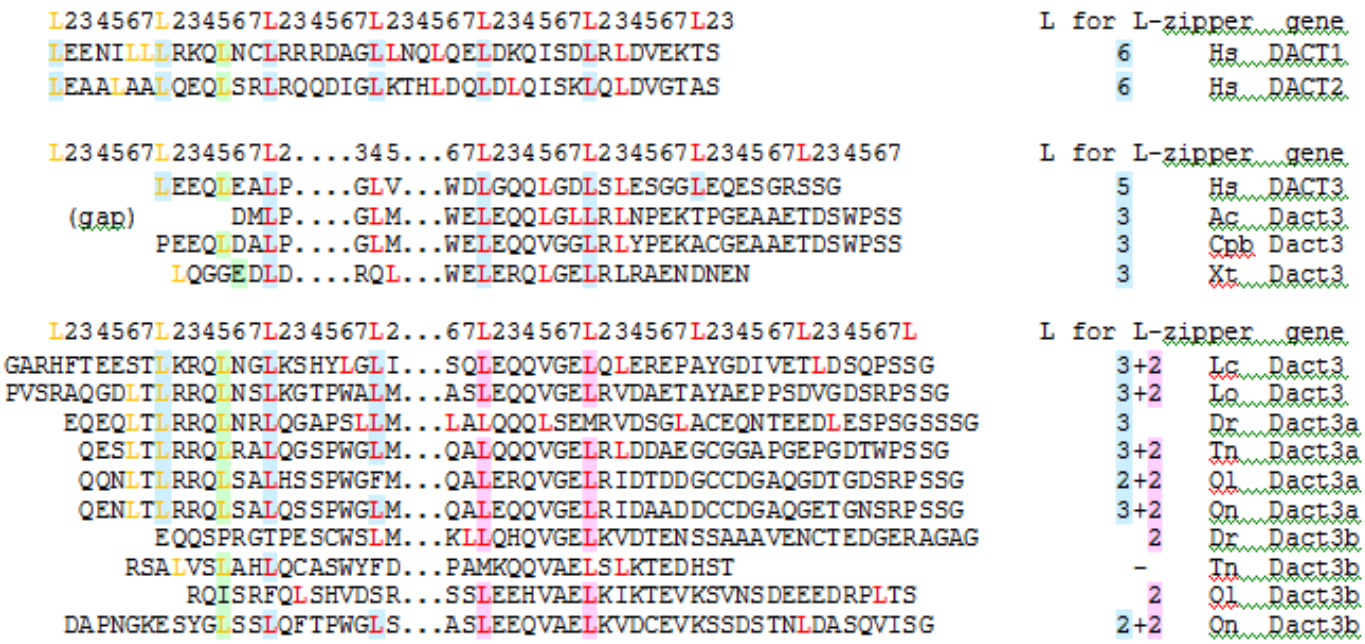

Supplemental Figure 7

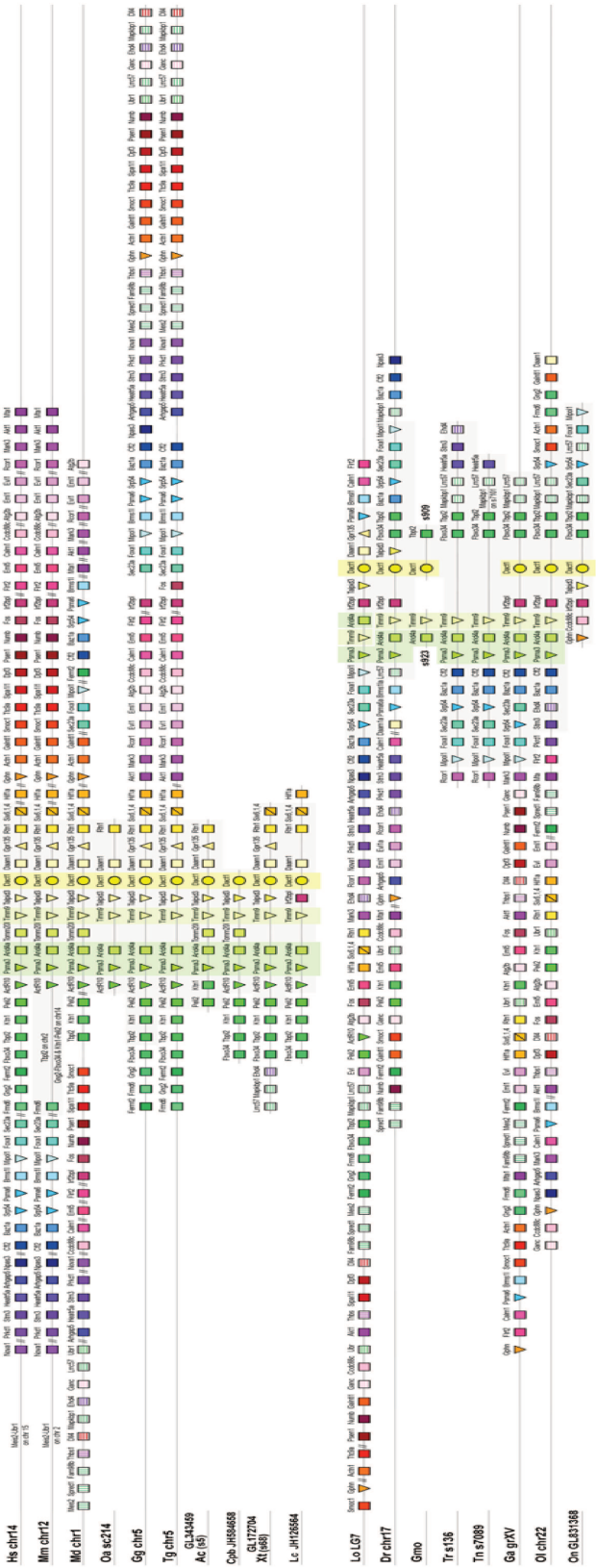

Supplemental Figure 8

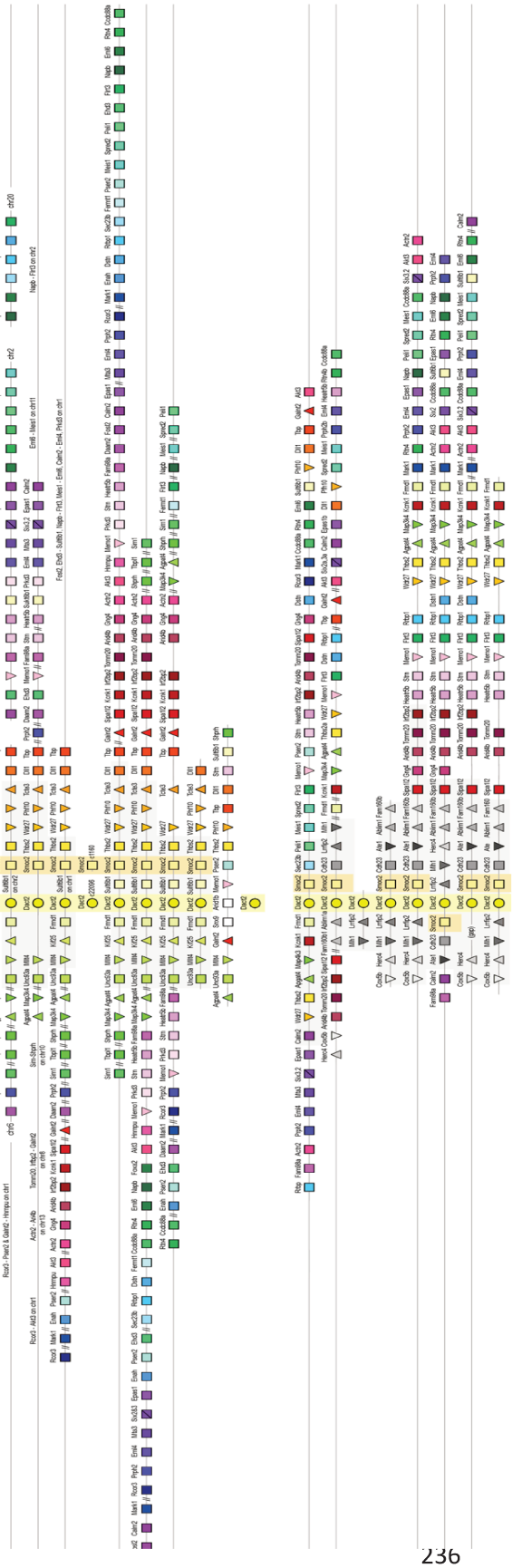

Supplemental Figure 9

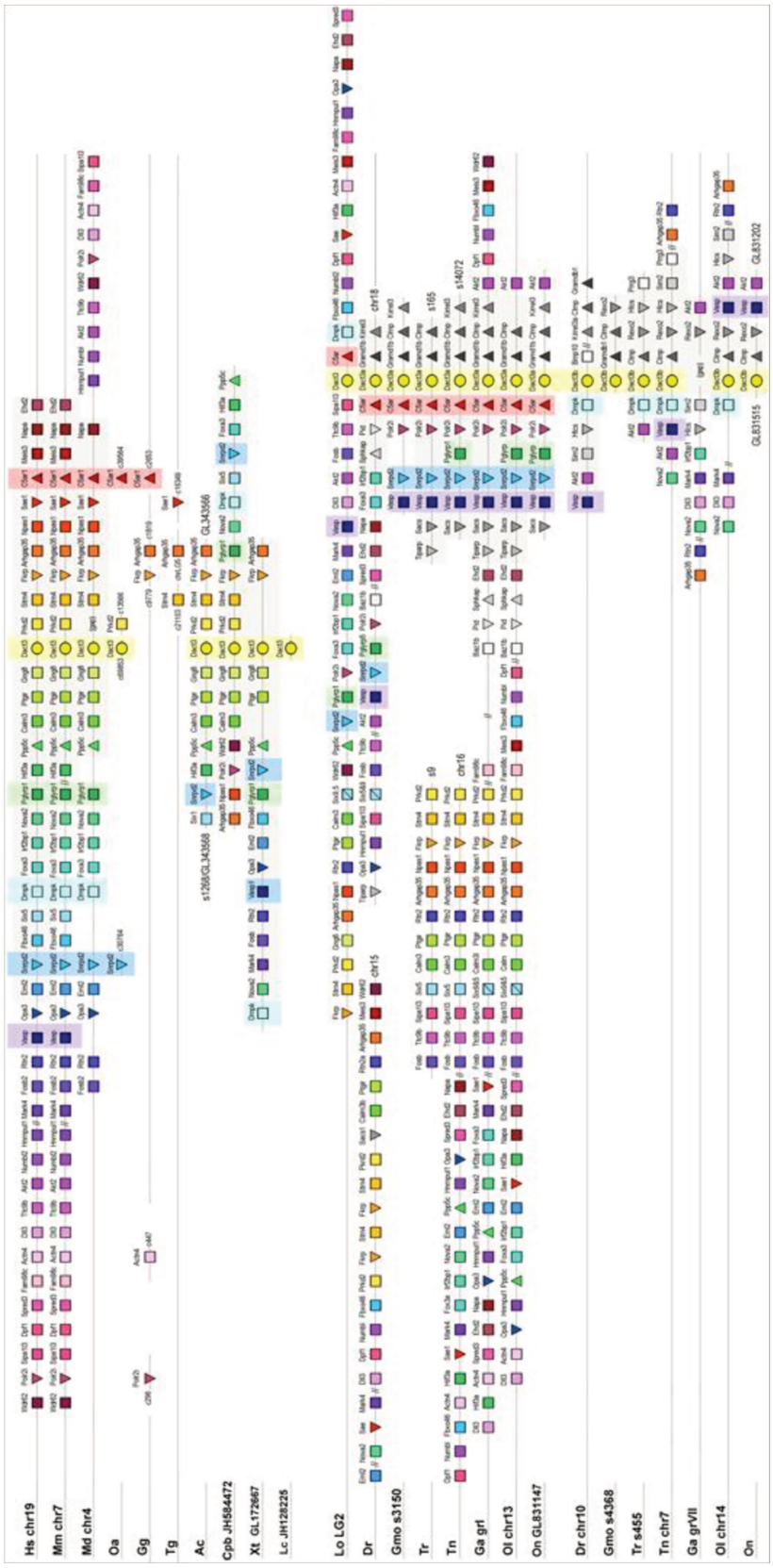

Supplemental Figure 10

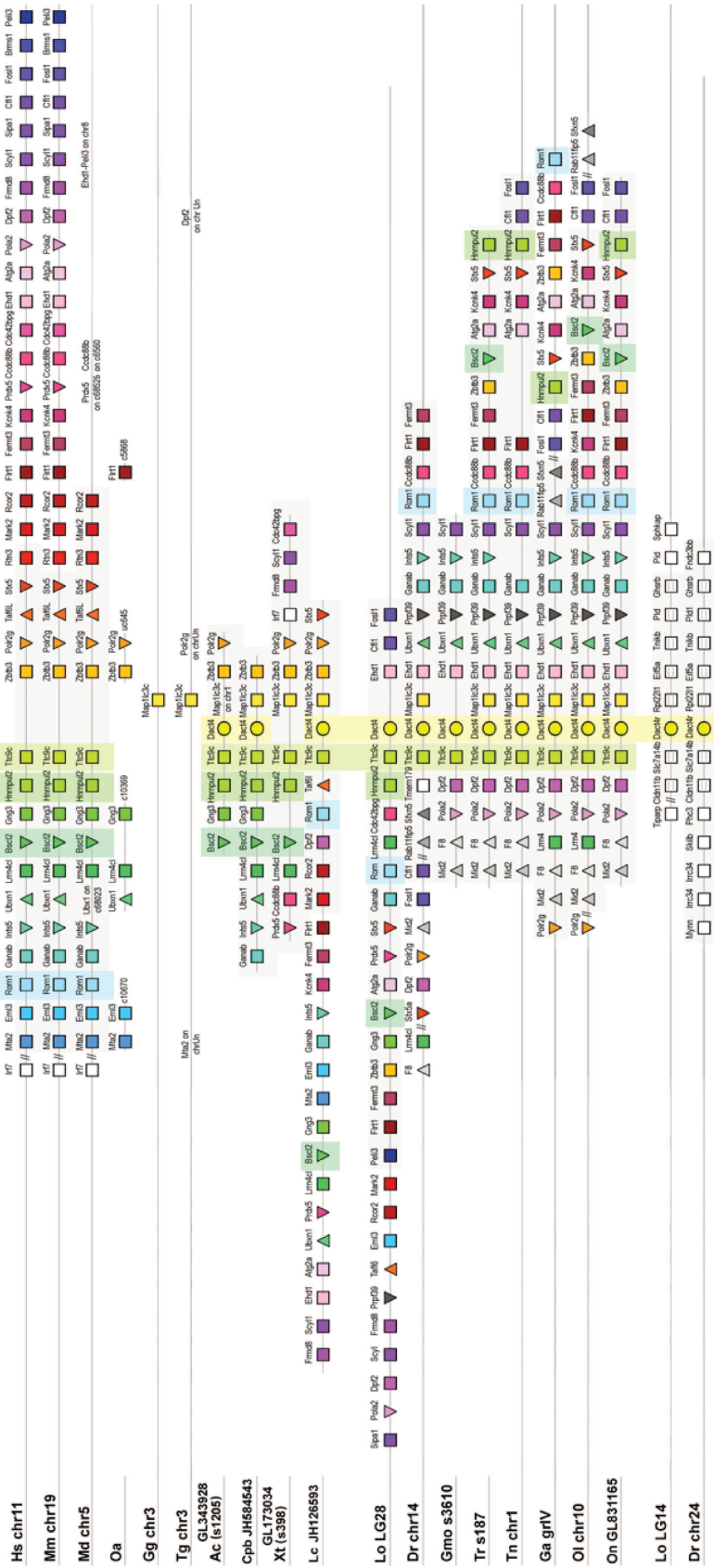

Supplemental Figure 11

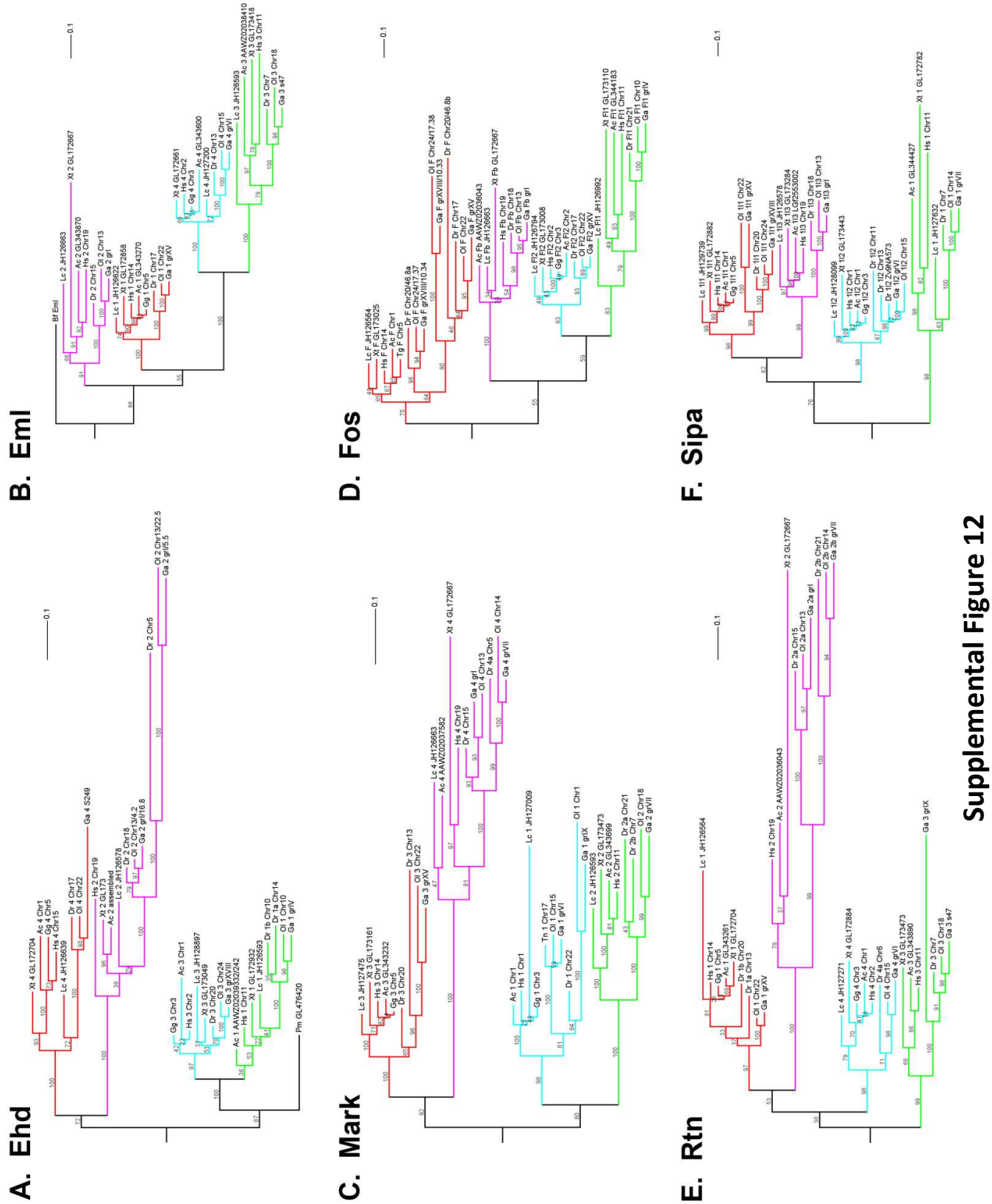

Supplemental Figure 12

Supplemental Table 1

Bilaterians searched for Dact genes, abbreviations of species names are indicated on the left. Dact EST sequences are represented by a tick, for genomic sequences, the genomic localisation is indicated, following the nomenclature of the 2012 edition of the ensemble (http://www.ensembl.org/index.html), NCBI (http://www.ncbi.nlm.nih.gov/), and the elephant shark genome project databases (http://esharkgenome.imcb.a-star.edu.sg/). For the Anole lizard, Xenopus tropicalis, Latimeria, and the lamprey, in addition the nomenclature used in the 2008 edition of ensemble is shown.

abbreviation	species	common name	classification	Dact1	Dact2	Dact3 or 3a	Dact3b	Dact4	comments
			Deuterostomes						
			Phylum: chordata; **Subphylum vertebrata**;						
			Infraphylum: Gnathostomata						
			Superclass: Osteichthyes						
			Class: Sarcopterygii,						
			Subclass: Tetrapodomorpha						
Hs	Homo sapiens	human	Amniota; Synapsids - Infraclass: Mammalia; Placentalia	chr14✓	chr6✓	chr19✓		(locus chr11)	Dact4 locus is identifiable but lacks a Dact gene
Mm	Mus musculus	Mouse	"	chr12✓	chr17✓	chr7✓		(locus chr19)	"
Bt	Bos Taurus	Cattle	"	chr10	chr9	chr18		(locus chr29)	"
Cf	Canis familiaris	Dog	"	chr8	chr1	chr1		(locus chr18)	"
La	Loxodonta africana	African elephant	"	s2755		s4446			
Md	Monodelphis domestica	Opossum	Infraclass: Mammals; Marsupials	chr1	chr2	chr4		(locus chr5)	"
Oa	Ornithorhynchus anatinus	Platypus	Infraclass: Mammals; Monotremes	c214, 26117; c164635 (ex4)	c20694, c22096	c69853 (ex1), c289003 (ex4)			
Gg	Gallus gallus	Chicken	Amniota; Diapsids; Archosauromorpha; Infraclass: Aves	chr5✓	chr3✓				Dact3 and 4 loci not preserved
Mg	Meleagris gallopavo	Turkey	"	chr5	chr2				Dact3 and 4 loci not preserved
Tg	Taeniopygia guttata	Zebrafinch	"	chr5	chr3				Dact3 and 4 loci not preserved
Ap	Anas platyrhynchos	Duck	"	s626	s530				Dact3 and 4 loci not preserved
Mu	Melopsittacus undulatus	Budgerigar		JH556483	JH556595				
Ac	Anolis carolinensis	Anole lizard	Amniota; Diapsids; Infraclass: Lepidosauromorpha, o: squamata-subo:lacertilia	GL343459 (formerly s5, s29) and chr2	chr1 (formerly s549)	GL343568 (formerly s1268)		GL343928 (formerly s71, s1206)	
Pym	Python molurus	Burmese python	o: squamata-subo:serpentes	c26513843 c26939	c24659227 c2656349	c26582260		c26563039 c26110406 c25444438	

				700	7 c26659464 c26922077			c24942884	
Cpb	Chrysemys picta bellii	Western painted turtle	Amniota; Anapsids; Infraclass: Testudines (turtles and tortoises)	JH584658	JH584758	JH584472		JH584543	
Ps	Pelodiscus sinensis	Chinese soft shield turtle	"	JH212506	JH208515	JH209944		JH206113	
Xt	Xenopus tropicalis	Western clawed frog	Infraclass: Amphibia	GL172704 (formerly s68) ✓		GL172667 (formerly s31 (ex4) ✓		(locus GL173034, formerly s398)	Dact4 locus is identifiable but lacks a Dact gene
Xl	Xenopus laevis	African clawed frog	Infraclass: Amphibia	1a, b✓					
Rc	Rana catesbeiana		Infraclass: Amphibia	✓					
Pa	Protopterus aethiopicus	African or marbled lungfish	Subclass: Dipnoi (lungfishes); f: Protopteridae		✓				
Lc	Latimeria chalumnae		Subclass: Coelocanthimorpha	JH126564 (formerly c002619-17)	JH129292 (formerly c230613-11)	JH128225 (formerly c190000,13,18,22)		JH126593 (formerly c015702)	
			Class: Actinopterygii						
			Subclass: Chondrostei (birchirs, sturgeons)						
			o:Squaliformes						
			Subclass: Neopterygii Infraclass: Holostei (bowfins, gars)						
Lo	Lepisosteus oculatus	Spotted gar	o: Lepisosteiformes	LG7	LG16	LG2		LG28	2nd Dact4 on LG14 but may be a retrotranscribed gene: no introns
			Infraclass: Teleostei						
			so: Osteoglossomorpha						
			so: Elopomorpha						
			so: Clupeomorpha						
			so: Ostariophysi						
Dr	Danio rerio	Zebrafish	o: Cypriniformes, f: Cyprinidae	chr17✓	chr13✓	chr18✓	chr10✓	chr14✓	2nd Dact4 on chr24 ✓- but may be a retrotranscribed gene: no introns
Pp	Pimephales promelas	Fathead minnow	o: Cypriniformes, f: Cyprinidae	✓		✓		✓	
Ip	Ictalurus punctatus	Channel catfish	o: Siluriformes, f: Ictaluridae	✓					
			so: Protacanthopterygii						
Ssa	Salmo salar	Altlantic salmon	o: Salmoniformes, f: Salmonidae	✓					
Ot	Oncorhynchus tshawytscha	Chinook salmon	o: Salmoniformes, f: Salmonidae					✓	
Omy	Oncorhynchus mykiss	Rainbow trout	o: Salmoniformes, f: Salmonidae	✓			✓		
Omo	Osmerus mordax	Rainbow smelt	o: Osmeriformes, f: Osmeridae		✓				
			so: Stenopterygii (may						

			belong in Protacanthopterygii)						
			so: Cyclosquamata						
			so: Scopelomorpha						
			so: Lampridiomorpha						
			so: Polymyxiomorpha						
			so: Paracanthopterygii						
Gmo	Gadus morhua	Atlantic cod	**o:Gadiformes=Anacanthini**	s909/c572298, c143687,	s609/c360826	s3150	s4368	s3610; partial sequences on c76676	
			so: Acanthopterygii						
Tr	Takifugu rubripes	Fugu	o: Tetraodontiformes, f: Tetraodontidae	(locus on s136)	s53	s165	s455	c187	Dact1 locus present, but no Dact1 gene
Tn	Tetraodon nigroviridis	Green spotted pufferfish	o: Tetraodontiformes, f: Tetraodontidae	(locus on s7089)	chr17	chrUn/s14702	chr7	chr1	Dact1 locus present, but no Dact1 gene
Ga	Gasterosteus aculeatus	three-spined stickleback	o: Gasterosteiformes, f: Gasterosteidae	grXV✓	grVI	grI✓	(locus on grVII)	grIV✓	Sequence gap at the position of the Dact3b gene
Ol	Oryzias latipes	Medaka	o: Beloniformes, f: Adrianichthyidae	chr22✓	chr15✓	chr13	chr14✓	chr10✓	
Pf	Perca flavescens	Yellow perch	o: Perciformes, f: Percidae					✓	
Dl	Dicentrarchus labrax	European seabass	o: Perciformes, f: Moronidae					✓	
On	Oreochromis niloticus	Nile Tilapia	o: Perciformes, f: Chichlidae	GL831368	GL831145	GL831147	GL831515 ✓	GL831165	
Hb	Haplochromis burtani	African cichlid	o: Perciformes, f: Chichlidae				✓		
Sau	Sparus aurata	Gilthead seabream	o: Perciformes, f: Sparidae					✓	
Xm	Xiphophorus maculatus	Southern platyfish	o: Cyprinodontiformes f: Poeciliidae	JH557083	JH556663	JH556880		AGAJ01047724 & JH556834	
			Super/Class: Chondrichthyes						
			Subclass: Elasmobranchii;						
			Subdivision Selachii; so: Galeomorphi						
Sac	Squalus acanthias	Spiny dogfish shark	Subdivision Selachii; so: Squalomorphi, f: squalidae	✓					
Tc	Torpedo californica	Pacific electric ray	Subdivision / so: Batoidea, f: Torpedinidae		✓			✓	
Le	Leucoraja erinacea	Little skate http://www.marinegenomics.org/node/27111	Subdivision / so: Batoidea, f: Rajidae					✓	
			Subclass: Holocephali						
Cm	*Callorhinchus milii*	Elephant shark	o: Chimaeriformes; f: Callorhynchidae	AAVX014209261.1 AAVX012216041.1 AAVX012367601.1 AAVX011797251.1 AAVX012767631.1	AAVX01057442.1 AAVX01184388.1	AAVX01159308.1		AAVX01316550.1	
			Infraphylum: Agnatha						
Pm	Petromyzon marinus	Sea lamprey	Class Hyperoartia/Petromyzontida	Exon3 + exon4 on c37200/c20195; 2nd exon 3 on c36439; 2nd exon 4 on c54804					Possibly 2 genes
			Class Myxonoidea						

Oik	Oikopleura dioica		Phylum: Chordata; **Subphylum: Tunicata/Urochordata**; Class: Appendicularia; o:Copelata						No significant hit
Cii	Ciona intestinalis	Vase tunicate	Class: Ascidiacea; o:Enterogona						No significant hit
Cis	Ciona savignyi		Class: Ascidiacea; o:Enterogona						No significant hit
Bfl	Branchiostoma floridae	Florida lancelet	Phylum: chordata; **Subphylum: Cephalochordata;** Class Leptocardii; o:Amphioxiformes			s65 ✓			
Sak	Saccoglossus kowalevskii	Acorn worm	Phylum: Hemichordata; Class: Enteropneusta						No significant hit
Spu	Strongylocentrotus purpuratus	California purple sea urchin	Phylum: Echinodermata; Class: Echinoidea						No significant hit
			Protostomes-lophotrochozoa						
Apc	Aplysia californica	California sea slug or California sea hare	Phylum: Mollusca, Class: Gastropoda						No significant hit
			Protostomes-ecdysozoa						
Drm	Drosophila melanogaster	Fruit fly	Phylum: Arthropoda; Class: Insecta						No significant hit
Trc	Tribolium castaneum	Red flour beetle	Phylum: Arthropoda; Class: Insecta						No significant hit
Bom	Bombyx mori	domesticated silkmoth	Phylum: Arthropoda; Class: Insecta						No significant hit
Cel	C.elegans		Phylum: Nematoda						No significant hit
Cbr	C.briggsae		Phylum: Nematoda						No significant hit
Loa	Loa loa	African eye worm	Phylum: Nematoda						No significant hit

Supplemental Table 2

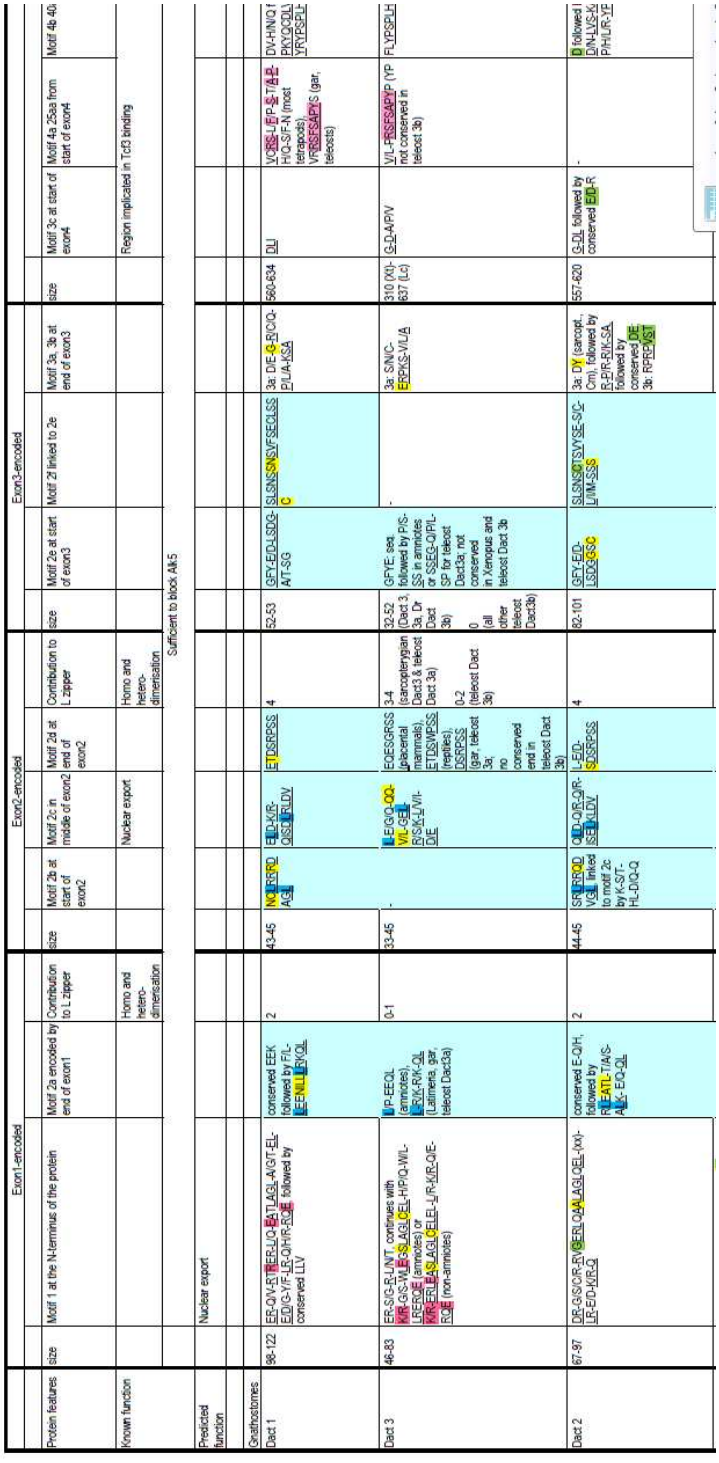

		Exon1-encoded			Exon2-encoded						Exon3-encoded					
Protein features	size	Motif 1 at the N-terminus of the protein	Motif 2a encoded by end of exon1	Contribution to L zipper	size	Motif 2b at start of exon2	Motif 2c in middle of exon2	Motif 2d at end of exon2	Contribution to L zipper	size	Motif 2e at start of exon3	Motif 2f linked to 2e	Motif 3a, 3b at end of exon3	size	Motif 3c at start of exon4	Motif 4a-25aa from start of exon4	Motif 4b 40
Known function				Homo and hetero-dimerisation			Nuclear export		Homo and hetero-dimerisation						Region implicated in Tcf3 binding		
								Sufficient to block Alk 5									
Predicted function		Nuclear export															
Geathostomes																	
Dact 1	98-122	ER-QN-ET-RERLQ-EETLASL-A/GT-EL-E/Q-I-FF-LR-Q-H-R-RQE followed by conserved LLV	conserved EEK followed by FIL-EENLLERKQL	2	43-45	NQERSRQ AGT	EED-V/R-QSSTEDLDV	ETDSRPSS	4	52-53	GFY-E/D-LSDQ-A/T-SG	SLSNSSNGVFSEQLSS C	3a: D/E-S-R/Q/Q-P/LA-K/SA	566-634	DLI	V/RSS-L/F-P-S/T-A/E H/Q-S/T-N (most tetrapods) V/RSSSAPP/S (gar, teleosts)	DN-H/NQ/ PR/YQ-QLL YR/TSPLL
Dact 3	46-83	ER-S/G-R-L/N/T, continues with KR-GS-W/E-S-AGL-QEL-H/P/Q-W/L-LRERQE (ammotes) or KRERLEASLAGLQELEL-L/R-K/R-Q/E-RQE (non-ammotes)	L/P-EEQL (ammotes), E-R/K-R/K-QL (Latimeria, gar teleost Dact3a)	0-1	33-45	-	L-E/G/Q-QQ-V/L-GEL-R/S/K-L/V/I-D/E	EQESGRSS (placental mammals), ETDSVPSS (reptiles), DSRPSS (gar, teleost 3a; no conserved end in teleost Dact 3b)	3-4 (sarcopterygian Dact3 & teleost Dact 3a) 0-2 (teleost Dact 3b)	32-52 (Dact 3, 3a, Dr Dact 3b) 0 (all other teleost Dact3b)	GFYE; sea, followed by P/S-SS in ammotes or SSEG-Q/P/L-SP for teleost Dact3a; not conserved in Xenopus and teleost Dact 3b	-	3a: S/N/C-E/D/K-S-V/L/A	310 (Xl)-637 (Lc)	G-D-A/P/V	V/L-PSSFSA/P/P (YP not conserved in teleost 3b)	FL-YPSPLH
Dact 2	67-97	DR-G/S/Q/R-R/Q/ERLQ-A/A-AGL-QEL-(x)-LR-E/D-H/R-Q	conserved E-Q/H, followed by R-LEATL-T/M/S-A/L-E/Q-QL	2	44-45	SNTERQQD V/G-L linked to motif 2c by KSIT-HL-D/Q-Q	Q/E-D/R-Q/R-SSE-L/D/V	L-E/D-S/D/SRPSS	4	82-101	GFY-E/D-LSDQ-S/G-C	SLSNSSTSVYSE-S/C-L/M-SSS	3a: D/Y (sarcopt, Cm), followed by R-L/P-R/K-S/A, followed by conserved D/E 3b: R/P-P/V/ST	557-620	G-D/L followed by conserved E/D-R	-	followed DN-LVS-K P/H/LR-Y/F

Resumo dos Resultados

Resumo dos Resultados

Capítulo 1

Os dados obtidos nessa etapa do trabalho sugerem fortemente o envolvimento dos genes da família *Dpr* durante a ontogenia dos membros de galinha.

A partir desse trabalho foi possível obter os seguintes resultados:

- A família *Dpr* surge como um novo grupo de moléculas marcadoras do desenvolvimento dos membros em galinha;
- Os genes da família *Dpr* apresentam um padrão de expressão dinâmico durante o desenvolvimento dos membros;
- Inicialmente, o gene *Dpr1* é expresso no mesênquima indiferenciado do membro em formação durante a condensação dos progenitores condrogênicos;
- *Dpr2* é expresso em células progenitoras de condrócitos, e nas fases posteriores é detectado no pericôndrio;
- Tanto *Dpr1* quanto *Dpr2* podem estar relacionados com a formação das articulações dos membros de galinha;
- Os genes da família *Dpr* e o gene *Sox9* apresentam expressão complementar e sobreposta durante diversas fases do desenvolvimento dos membros de galinha;

Capítulo 2

Durante essa etapa do trabalho, revelamos a origem evolutiva da família *Dpr*. Além disso, caracterizamos as proteínas codificadas por todos os membros dessa família gênica e demonstramos o padrão de expressão desses genes em galinha e peixe-zebra.

A partir desse trabalho foi possível obter os seguintes resultados:

- A família *Dpr* surge durante a evolução dos organismos deuterostômios;
- Identificação do ancestral dos genes *Dpr* no genoma de organismos não vertebrados, lampreia e anfioxo;
- Existência de um novo gene parálogo, *Dpr4*, no genoma dos répteis, em peixes sarcopterígios (celacantos) e nos peixes teleóteos;
- O parálogo *Dpr3* foi identificado em répteis, anfíbios, e em peixes sarcopterígios e teleósteos;
- Identificação de todos quatro membros da família *Dpr* no genoma de peixes cartilaginosos;
- Os genes *Dpr1* e *Dpr3* surgiram do mesmo ancestral comum e *Dpr2* e *Dpr4* de outro.
- Os quatro membros da família *Dpr* possuem similares *loci* genômicos entre diferentes espécies ao longo da evolução;
- As proteínas codificadas pelos genes *Dpr* apresentam sete motivos conservados entre si;
- Somitos, brotos dos membros/nadadeira e arcos faríngeos são, possivelmente, os sítios originais de expressão dos genes *Dpr;*

Conclusão

Esta tese de doutorado reflete o trabalho de investigação sobre os genes da família *Dpr* durante a ontogenia dos membros de *Gallus gallus*, e também o surgimento e a evolução dessas moléculas ao longo do processo evolutivo dos metazoários.

No decorrer do Capítulo 1 foi assinalado o envolvimento dos genes *Dpr* durante a ontogenia dos membros de galinha. Podemos concluir, de acordo com os dados apresentados, que a família gênica *Dpr* surge como um novo grupo de moléculas reguladoras do desenvolvimento dos membros em vertebrados e que, possivelmente, atue na interconexão das vias de sinalização Wnt e TGF-β. Nosso trabalho abre novas perspectivas para a compreensão da padronização e crescimento dos membros, bem como para o entendimento de doenças e malfomações congênitas dessas estruturas em humanos. O desafio nessa área de pesquisa permanece na compreensão precisa de como as vias de sinalização são reguladas separadamente e em conjunto de modo a produzir uma estrutura funcional capaz de executar movimentos precisos e coordenados — os membros.

A totalidade dos dados alcançados no Capítulo 2 nos possibilitou traçar a evolução dos *Dprs* e também a construção da filogenia desses genes, além da identificação de novos ortólogos. Demonstramos, pela primeira vez, uma visão abrangente sobre o número e as propriedades dos genes *Dpr* no que se refere à organização de seu *loci* genômico e os diferentes motivos protéicos que eles codifiam. Nosso estudo sugere que os ortólogos *Dpr1* e *Dpr3* originaram-se a partir de um mesmo ancestral, enquanto *Dpr2* e *Dpr4* surgiram de outro precursor durante a segunda duplicação completa do genoma dos vertebrados. Os motivos protéicos presentes nas proteínas Dpr dos cefalocordados e gnatostômio indicam que a

capacidade de modular sinais da via de sinalização Wnt já estava presente no ancestral comum às moléculas Dpr1 e Dpr3. No entanto, a capacidade de inibir os sinais TGF-β deve ter evoluído juntamente com o precursor de Dpr2 e Dpr4 nos animais gnatostomados. Ainda nesse capítulo, a existência de novos ortólogos *Dprs* foi confirmada através de ensaios de hibridação *in situ,* que apontaram os domínios de expressão complementares e de sobreposição dos membros dessa família gênica. Assim, concluímos que nosso trabalho fornecerá subsídios para futuros ensaios moleculares e estruturais que investiguem a função dos motivos protéicos compartilhados e divergentes das moléculas Dprs, e para estudos funcionais que analisem o papel desempenhado por essa família gênica tanto no contexto celular como durante o desenvolvimento embrionário dos organismos.

Bibliografia

- Alvares L. E., Winterbottom F. L., Jorge E. C., Rodrigues Sobreira D., Xavier-Neto J., Schubert F. R., Dietrich S. **Chicken dapper genes are versatile markers for mesodermal tissues, embryonic muscle stem cells, neural crest cells, and neurogenic placodes.** *Dev Dyn.* 238(5):1166-1178. 2009.
- Angers S., Moon R. T. **Proximal events** in **Wnt signal transduction**. *Nat Rev Mol Cell Biol*. 10(7):468-477. 2009.
- Antara De. **Wnt/Ca2+ signaling pathway: a brief overview.** *Acta Biochim Biophys Sin*. 43(10):745-756. 2011.
- Arthur W. **The emerging conceptual framework of evolutionary developmental biology**. *Nature.* 415(6873):757-764. 2002.
- Barrow J. R. **Wnt/planar cell polarity signaling**. *Organogenesis*. 7 (4):260-266. 2011.
- Bartscherer K., Boutros M. **Regulation of Wnt protein secretion and its role in gradient formation.** *EMBO Rep*. 9(10):977-982. 2008.
- Bejsovec A. **Wnt pathway activation: new relations and locations**. *Cell.* 120(1):11-14. 2005.
- Bénazet J. D., Bischofberger M., Tiecke E., Goncalves A., Martin J. F., Zuniga A., Naef F., Zeller R. **A self-regulatory system of interlinked signaling feedback loops controls mouse limb patterning**. *Science.* 323(5917):1050-1053. 2009.
- Berridge M. J. Cell Signalling Biology. **Portland Press.** 2012.
- Brott B. K., Sokol S. Y. (a). **Frodo proteins: modulators of Wnt signaling in vertebrate development**. *Differentiation*. 73(7):323-329. 2005.
- Brott B. K., Sokol S. Y. (b). **A vertebrate homolog of the cell cycle regulator Dbf4 is an inhibitor of Wnt signaling required for heart development**. *DevCell*. 8(5):703-715. 2005.
- Capdevila J., Belmonte J. C. I. **Patterning mechanisms controlling vertebrate limb development.** *Annu Rev Cell Dev. Biol*. 17:87-132. 2001.
- Cayuso J., Marti E. **Morphogens in motion: growth control of the neural tube**. *J Neurobiol*. 64(4):376-387. 2005.
- Chen H., Liu L., Ma B., Ma T. M., Hou J. J., Xie G. M., Wu W., Yang F. Q., Chen Y. G. **Protein kinase A-mediated 14-3-3 association impedes human Dapper1 to promote dishevelled degradation**. *J Biol Chem*. 286(17):14.870-14.880. 2011.
- Cheyette B. N. R., Waxman J. S., Miller J. R., Takemaru K., Sheldahl L. C., Khlebtsova N., Fox E. P., Earnest T., Moon R. T. **Dapper, a Dishevelled-associated antagonist of betacatenin and JNK signaling, is required for notochord formation.** *Dev Cell*. 2(4):449-461. 2002
- Church V. L., Francis-West P. **Wnt signalling during limb development.** *Int J Dev Biol*. 46(7):927-936. 2002.
- Clevers H. **Wnt/β-Catenin Signaling in Development and Disease**. *Cell.* 127(5):469-480. 2006.
- Cossu G., De Angelis L., Borello U. , Berarducci B., Buffa V., Sonnino C., Coletta M., Vivarelli E., Bouche M., Lattanzi L., Tosoni D., Di Donna S., Berghella L., Salvatori G., Murphy P., Cusella-Deangelis M. G. Molinaro M. **Determination, diversification and multipotency of mammalian myogenic cells**. *Int J Dev Biol*. 44(6):699-706. 2000.
- Duboc V., Logan M. P. O. **Building limb morphology through integration of signaling modules**. *Current Opinion in Genetics & Development*. 19(5):497-503. 2009.
- Dudley A. T., Ros M. A., Tabin C. J. **A re-examination of proximodistal patterning during vertebrate limb development.** *Nature.* 418(6897):539-544. 2002.

- Enomoto-Iwamoto M., Kitagaki J., Koyama E., Tamamura Y., Wu C., Kanatani N., Koike T., Okada H., Komori T., Yoneda T., Church V., Francis-West P. H., Kurisu K., Nohno T., Pacifici M., Iwamoto M. **The Wnt antagonist Frzb-1 regulates chondrocyte maturation and long bone development during limb skeletogenesis**. *Dev Biol.* 251(1):142-156. 2002.
- Fisher D. A., Kivimae S., Hoshino J., Suriben R., Martin P. M., Baxter N.,Cheyette B. N. R. **Three Dact Gene Family Members are Expressed During Embryonic Development and in the Adult Brains of Mice**. *DevDyn*. 235(9):2620-2630. 2006.
- Fortini M. E. **Notch signaling: the core pathway and its posttranslational regulation**. *Dev Cell*. 16(5):633-647. 2009.
- Freisinger C. M., Fisher R. A., Slusarski D. C. **Regulator of g protein signaling 3 modulates wnt5b calcium dynamics and somite patterning**. *PLoS Genet.* 6(7):1-11. 2010.
- **F-β signaling.** *Cell Research*. 19(1):128–139. 2009.
- Gañan Y., Macias D., Duterque-Coquillaud M., Ros M. A., Hurle J. M. **Role of TGF**bs **and BMPs as signals controlling the position of the digits and the areas of interdigital cell death in the developing chick limb autopod.** *Development.* 122(8):2349-2357. 1996.
- Gao B., Song H., Bishop K., Elliot G., Garrett L., English M. A., Andre P., Robinson J., Sood R., Minami Y., Economides A. N., Yang Y. **Wnt signaling gradients establish planar cell polarity by inducing Vangl2 phosphorylation through Ror2.** *Dev Cell.* 20(2):163-176. 2011.
- Gao S., Yang Z., Zheng Z.Y., Yao J., Zhang F., Wu L.M., Xie H.Y., Zhou l., Zheng S.S. **Reduced expression of DACT2 promotes hepatocellular carcinoma progression: involvement of methylation-mediated gene silencing.** *World J. Surg. Oncol.* 7(11):57.doi: 10.1186/1477-7819-11-57. 2013.
- Gao X., Wen J., Zhang L., Li X., Ning Y., Meng A., Chen Y. G. **Dapper1 is a nucleocytoplasmic shuttling protein that negatively modulates wnt signaling in the nucleus**. *J Biol Chem.* 283(51):35.679-35.688. 2008.
- Gilbert S. F. **Developmental Biology**. 7th Edition, Sinauer Associates Inc. 2003.
- Gillhouse M., Nyholm M. W., Hikasa H., Sokol S. Y., Grinblat Y. **Two Frodo/Dpr homologs are expresssed in the developing brain and mesoderm of zebrafish.** *Developmental Dynamics*. 230(3):403-409. 2004.
- Gloy J., Hikasa H., Sokol S. Y. **Frodo interacts with Dishevelled to transduce Wnt signals.** *Nat Cell. Biol*. 4(5):351-357. 2002.
- Gordon M. D., Nusse R. **Wnt signaling: multiple pathways, multiple receptors, and multiple transcription factors.** *J Biol Chem*. 281(32):22.429-22.433. 2006.
- Hikasa H., Sokol S. Y. **The involvement of Frodo in TCF-dependent signaling and neural tissue development**. *Development.* 131(19):4725-4734. 2004.
- Holland P. W. H., Garcia-Fernindez J., Williams N. A., Sidow A. **Gene duplications and the origins of vertebrate development**. *Development*. 125-133. 1994.
- Hunter N. L., Hikasa H., Dymecki S. M., Sokol S. Y. **Vertebrate homologues of Frodo are dynamically expressed during embryonic development in tissues undergoing extensive morphogenetic movements.** *Dev Dyn.* 235(1):279-284. 2006.
- Huo Y. Y., Zhang K. T., Li B. Y., Duan R. F., Fan B. X., Xiang X. Q., Hu Y. C., Xie L., Wu D. C. **Regulation of SMAD7 gene by TGF-β 1 in process of malignat transformation.** *Ai Zheng*. 21(2):117-121. 2002

- Imai Y., Kurokawa M., Izutsu K., Hangaishi A., Maki K., Ogawa S., Chiba S., Mitani K., Hirai H. **Mutations of the SMAD4 gene in acute myelogeneous leukemia and their functional implications in leukemogenesis**. *Oncogene*. 20(1):88-96. 2001.
- Jia Y., Yang Y., Brock M. V., Zhan Q., Herman J. G., Guo M. **Epigenetic Regulation of DACT2, A Key Component of the Wnt Signaling Pathway in Human Lung Cancer.** *J Pathol*. Doi: 10.1002-path. 4073. 2012.
- Jiang X., Tan J., Li J., Kivimae S., Yang X., Zhuang L., Lee P. L., Chan M. T., Stanton L. W., Liu E. T., Cheyette B. N., Yu Q. **DACT3 is an epigenetic regulator of Wnt/beta-catenin signaling in colorectal cancer and is a therapeutic target of histone modifications**. *Cancer Cell.* 13(6):529-541. 2008
- Johnson R. L., Tabin C. J. **Molecular models for vertebrate limb development.** *Cell*. 90(6):979-990. 1997.
- Katoh M., Katoh M. **Identification and characterization of human Dapper1 and Dapper2 genes in silico.** *Int J Oncol.* 22(4):907-913. 2003.
- Kettunen P., Kivimäe S., Keshari P., Klein O. D., Cheyette B. N., Luukko K. **Dact1-3 mRNAs exhibit distinct expression domains during tooth development.** *Gene Expr Patterns.* 10(2-3):140-143. 2010.
- Kivimäe S., Yang X. Y., Cheyette B. N. **All Dact (Dapper/Frodo) scaffold proteins dimerize and exhibit conserved interactions with Vangl, Dvl, and serine/threonine kinases.** *BMC Biochem*. 12(33):1471-1483. 2011.
- Kohn A. D., Moon R. T. **Wnt and calcium signaling: beta-catenin-independent pathways.** *Cell Calcium.* 38(3-4):439-446. 2005.
- Kühl M., Sheldahl L. C., Malbon C. C., Moon R. T. **Ca (2+)/calmodulin-dependent protein kinase II is stimulated by Wnt and Frizzled homologs and promotes ventral cell fates in Xenopus.** *J Biol Chem*. 275(17):12701-12711. 2000.
- Lagathu C., Christodoulides C., Virtue S., Cawthorn W. P., Franzin C., Kimber W. A., Nora E. D., Campbell M., Medina-Gomez G., Cheyette B. N., Vidal-Puig A. J., Sethi J. K. **Dact1, a nutritionally regulated preadipocyte gene, controls adipogenesis by coordinating the Wnt/beta-catenin signaling network.** *Diabetes.* 58(3):609-619. 2009.
- Lee W. C., Hough M. T., Liu W., Ekiert R., Lindstrom N. O., Hohenstein P., Davies J. A. **Dact2 is expressed in the developing ureteric bud/collecting duct system of the kidney and controls morphogenetic behavior of collecting duct cells.** *Am J Physiol Renal Physiol.* 299(4):740-751. 2010.
- Li J. M., Shen X., Hu P. P.,Wang X. F. **Transforming growth factor beta stimulates the human immunodeficiency virus 1 enhancer and requires NF-kappaB activity.** *Mol Cell Biol.* 18(1):110-121. 1998.
- Lin S., Baye L. M., Westfall T. A. Slusarski D. C. **Wnt5b-Ryk pathway provides directional signals to regulate gastrulation movement**. *J Cell Biol*. 190:263-278. 2010.
- Li X., Florez S., Wang J., Cao H., Amendt B.A. **Dact2 Represses PITX2 Transcriptional Activation and Cell Proliferation through Wnt/beta-Catenin Signaling during Odontogenesis**. *PloS One*. 8(1):e54868. doi: 10.1371/journal.pone.0054868. 2013.
- Logan C. Y., Nusse R. **The Wnt signalling pathway in development and disease**. *Annu Rev Cell Dev Biol*. 20:781-810. 2004.
- Lorda-Diez C. I., Montero J. A., Diaz-Mendoza M. J., Garcia-Porrero J. A., Hurle J. M. **Defining the Earliest Transcriptional Steps of Chondrogenic Progenitor Specification during the Formation of the Digits in the Embryonic Limb**. *PLoS One.* 6(9):e24546.doi:10.1371/jornal.pone.0024546. 2011.

- Mariani F. V., Ahn1 C. P., Martin G. R. **Genetic evidence that FGFs have an instructive role in limb proximal–distal patterning**. *Nature*. 453(7193):401-405. 2008.
- Mariani F. V., Martin G. R. **Deciphering skeletal patterning: clues from the limb.** *Nature.* 423(6937):319-325. 2003.
- Massagué J. **How cells read TGF-β signals.** *Nat. Rev. Mol. Cell Biol*.1 (3):169-178. 2000.
- Meng F., Cheng X., Yang L., Hou N., Yang X., Meng A. **Accelerated reepithelialization in Dpr2-deficient mice is associated with enhanced response to TGFbeta signaling.** *J Cell Sci.* 121(17):2904-2912. 2008.
- Mikels A. J., Nusse R. **Purified Wnt5a protein activates or inhibits beta-catenin-TCF signaling depending on receptor context**. *PLoS Biol*. 4(4):e115. 2006.
- Miller J. R., Hocking A. M., Brown J. D., Moon R. T. **Mechanism and function of signal transduction by the Wnt/beta-catenin and Wnt/Ca2+ pathways.** *Oncogene.* 18(55):7860-7872. 1999.
- Moon R. T., Kohn A. D., De Ferrari G. V., Kaykas A. **WNT and beta-catenin signalling: diseases and therapies.** *Nat Rev Genet*. 5(9):691-701. 2004.
- Moon R. T., Shah K. **Developmental biology: Signalling polarity.** *Nature*. 417:239-240. 2002.
- Moustakas A., Pardali K., Gaal A., Heldin C. H. **Mechanisms of TGF-beta signaling in regulation of cell growth and differentiation.** *Immunol Lett*. 82(1-2):85-91. 2002.
- Müller G. B. **Evolutionary Developmental Biology.** Handbook of Evolution, Vol. 2: The Evolution of Living Systems (Including Hominids). Copyright Wiley-VCH Verlag GmbH & Co. KGaA, Weinheim. 2005.
- Newman S. A., Bhat R. **Activator-Inhibitor Dynamics of Vertebrate Limb Pattern Formation**. *Birth Defects Research*. Part C (81):305-319. 2007.
- Niehrs C. **The complex world of WNT receptor signaling.** *Nat Rev Mol Cell Biol*. 13(12):767-779. 2012.
- Niswander L., Tickle C., Vogel A., Booth I., Martin G.R. **FGF-4 replaces the apical ectodermal ridge and directs outgrowth and patterning of the limb**. *Cell.* 75(3):579-587. 1993.
- Nusse R., van Ooyen A., Cox D., Fung Y. K., Varmus H. **Mode of proviral activation of a putative mammary oncogene (int-1) on mouse chromosome 15.** *Nature*. 307(5947):131-136. 1984.
- Nusse, R. **Wnt signaling and stem cell control**. *Cell Research*. 18:523-527. 2008.
- Okerlund N. D., Kivimae S., Tong C. K., Peng I. F., Ullian E. M., Cheyette B. N. **Dact1 is a postsynaptic protein required for dendrite, spine, and excitatory synapse development in the mouse forebrain**. *J Neurosci*. 30(12):4362-4368. 2010.
- Park J. I., Ji H., Jun S., Gu D., Hikasa H., Li L., Sokol S. Y., McCrea P. D. **Frodo Links Dishevelled to the p120-Catenin/Kaiso Pathway: Distinct Catenin Subfamilies Promote Wnt Signals.** *DevCell.* 11(5):683-695. 2006.
- Park M., Moon R. T. **The planar cell-polarity gene stbm regulates cell behaviour and cell fate in vertebrate embryos.** *Nat Cell Biol.* 4(1):20-25. 2002.
- Patapoutian A., Reichardt L. F. **Roles of Wnt proteins in neural development and maintenance.** *Curr Opin Neurobiol*. 10(3):392-399. 2000
- Patterson G. I., Padgett R. W. **TGF-β-related pathways. Roles in Caenorhabditis elegans development.** *Trends Genet*. 16(1):27-33. 2000.

- Pearse R. V., Scherz P. J., Campbell J. K., Tabin C. J. **A cellular lineage analysis of the chick limb bud.** *Dev. Biol.* 310:388-400. 2007.
- Petropoulos H., Skerjanc I. S. **Beta -catenin is essential and sufficient for skeletal myogenesis in P19 cells**. *J Biol Chem*. 277(18):15393-15399. 2002.
- Pires-daSilva A., Sommer R. J. **The evolution of signalling pathways in animal development.** *Nat Rev Genet*. 4(1):39-49. 2003.
- Polakis P. **Wnt signaling and cancer**. *Genes Dev*. 14:1837-1851. 2000.
- Saneyoshi T., Kume S., Amasaki Y., Mikoshiba K. **The Wnt/calcium pathway activates NF-AT and promotes ventral cell fate in Xenopus embryos**. *Nature.* 417(6886):295-299. 2002.
- Sanz-Ezquerro J. J., Tickle C. **Autoregulation of Shh expression and Shh induction of cell death suggest a mechanism for modulating polarising activity during chick limb development**. *Development.* 127(22): 4811-4823. 2000.
- Sato K., Koizumi Y., Takahashi M., Kuroiwa A., Tamura K. **Specification of cell fate along the proximal–distal axis in the developing chick limb bud**. *Development*. 134(7):1397-1406. 2007.
- Schier A. F. **Nodal signaling in vertebrate development.** *Annu Rev Cell Dev Biol*. 19:589-621. 2003.
- Sharma R. P., Chopra V. L. **Effect of the wingless (wg1) mutation on wing and haltere development in Drosophila melanogaster**. *Dev Biol*. 48(2):461-465. 1976.
- Shen M. M. **Nodal signaling: developmental roles and regulation**. *Development.* 134(6):1023-1034. 2007.
- Shi Y., Massagué J. **Mechanisms of TGF-β Signaling Review from Cell Membrane to the Nucleus.** *Cell*. 113(6):685-700. 2003.
- Stern C. D. **The chick: A great model system becomes even greater**. *Dev Cell*. 8(1):9-17. 2005.
- Stroschein S. L., Wang W., Zhou S., Zhou Q., Luo K. **Negative feedback regulation of TGF-beta signaling by the SnoN oncoprotein.** *Science.* 286(5440):771-774. 1999.
- Su Y., Zhang L., Gao X., Meng F., Wen J., Zhou H., Meng A., Chen Y. G. **The evolutionally conserved activity of Dapper2 in antagonizing TGF-beta signaling.** *FASEB J*. 21(3):682-690. 2007.
- Suriben R., Kivimae S., Fisher D. A., Moon R. T., Cheyette B. N. **Posterior malformations in Dact1 mutant mice arise through misregulated Vangl2 at the primitive streak**. *Nat Genet*. 41(9):977-985. 2009.
- Tabin C. J. **Retinoids, homeoboxes, and growth factors: toward molecular models for limb development**. *Cell.* 66(2):199-217.1991.
- Tabin C. J., Wolpert L. **Rethinking the proximodistal axis of the vertebrate limb in the molecular era.** *Genes Dev.* 21(13):1433-1442.2007.
- Tada M., Kai M. **Noncanonical Wnt/PCP signaling during vertebrate gastrulation.** *Zebrafish*. 6(1):29-40. 2009.
- Tarchini B., Duboule D. **Control of Hoxd Genes' Collinearity during Early Limb Development.** *Dev Cell.* 10(1):93-103. 2006.
- Taylor J. S., Braasch I., Frickey T., **Meyer A, Van de Peer Y. Genome duplication, a trait shared by 22000 species of ray-finned fish**. *Genome Res*. 13(3):382-390. 2003.

- ten Berge D., Brugmann S. A., Helms J. A., Nusse R. **Wnt and FGF signals interact to coordinate growth with cell fate specification during limb development.** *Development*. 135(19):3247-3257. 2008.
- ten Dijke P., Goumans M. J., Itoh F., Itoh S. **Regulation of Cell Proliferation by Smad Proteins.** *J. Cell. Physiol*. 191(1):1-16. 2002.
- Teran E., Branscomb A. D., Seeling J. M. **Dpr Acts as a molecular switch, inhibiting Wnt signaling when unphosphorylated, but promoting Wnt signaling when phosphorylated by casein kinase Idelta/epsilon**. *PLoS One*. 4(5):e5522.doi:10.1371/jornal.pone.0005522. 2009.
- Tian T., Meng A. M. **Nodal signals pattern vertebrate embryos**. *Cell Mol Life Sci.* 63(6):672-685. 2006.
- Tickle C. **Making digit patterns in the vertebrate limb**. *Nat Rev Mol Cell Biol*. 7(1):45-53. 2006.
- Tickle C. **Patterning systems--from one end of the limb to the other**. *Dev Cell*. 4(4):449-58. 2003.
- Tickle C. **Vertebrate limb development.** *Genetics and Development*. 5:478-484. 1995.
- Tickle C., Münsterberg A. **Vertebrate limb development — the early stages in chick and mouse.** *Cur Opin in Gen & Dev*. 11(4):476-481. 2001.
- Towers M., Tickle C. **Growing models of vertebrate limb development**. *Development*. 136(2):179-190.2009.
- Tufan A. C., Tuan R. S. **Wnt regulation of limb mesenchymal chondrogenesis is accompanied by altered N-cadherin-related functions**. *FASEB J*. 15(8):1436-1438. 2001.
- Wang S., Kang W., Go M. Y., Tong J. H., Li L., Zhang N., Tao Q., Li X., To K. F., Sung J. J., Yu J. **Dapper Homolog 1 Is a Novel Tumor Suppressor in Gastric Cancer through Inhibiting the Nuclear Factor-κB Signaling Pathway.** *Mol Med*. 18(1):1402-11. 2012.
- Wang Y., Nathans J. **Tissue/planar cell polarity in vertebrates: new insights and new questions**. *Development*. 134(4):647-658. 2007.
- Watson S. S., Riordan T. J., Pryce B. A., Schweitzer R. **Tendons and muscles of the Mouse Forelimb During Embryonic Development.** *Dev Dyn*. 238(3):693-700. 2009.
- Waxman J. S, Hocking A. M., Stoick C. L., Moon R. T. **Zebrafish Dapper1 and Dapper2 play distinct roles in Wnt-mediated developmental processes**. *Development*. 131(23):5909-5921. 2004.
- Waxman J. S. **Regulation of the early expression patterns of the zebrafish Dishevelled-interacting proteins Dapper1 and Dapper2.** *Dev Dyn*. 233(1):194-200. 2005
- Wells R. G. **Fibrogenesis. V. TGF-beta signaling pathways.** *Am J Physiol Gastrointest Liver Physiol*. 279(5):845-850. 2000.
- Wen J., Chiang Y. J., Gao C., Xue H., Xu J., Ning Y., Hodes R. J., Gao X., Chen Y. G. **Loss of Dact1 disrupts planar cell polarity signaling by altering dishevelled activity and leads to posterior malformation in mice.** *J Biol Chem.* 285(14):11023-11030. 2010.
- Wodarz, A., Nusse R. **Mechanisms of Wnt signaling in development.** *Annu Rev Dev Biol*. 14: 59-88. 1998.
- Wu J. W., Krawitz A. R., Chai J., Li W., Zhang F., Luo K., Shi Y. **Structural mechanism of SMAD4 recognition by the nuclear oncoprotein Ski: insights on Ski-mediated repression of TGF-beta signaling**. *Cell*. 111(3):357-367. 2002.
- Wu M. Y., Hill C. S. **Tgf-beta superfamily signaling in embryonic development and homeostasis**. *Dev Cell.* 16(3):329-343. 2009.

- Xue H., Xiao Z., Zhang J., Wen J., Wang Y., Chang Z., Zhao J., Gao X., Du J., Chen Y.Z. **Disruption of the *Dapper3* gene aggravates ureteral obstruction-mediated renal fibrosis by amplifying Wnt/β-catenin signaling.** *J. Biol. Chem.* Epub ahead of print. 2013.
- Yang Z. Q., Zhao Y., Liu Y., Zhang J. Y., Zhang S., Jiang G. Y., Zhang P. X., Yang L. H., Liu D., Li Q. C., Wang E. H. **Downregulation of HDPR1 is associated with poor prognosis and affects expression levels of p120-catenin and beta-catenin in nonsmall cell lung cancer.** *Mol Carcinog.* 49(5):508-519. 2010.
- Yau T. O., Chan C. Y., Chan K. L., Lee M. F., Wong C. M., Fan S. T., Ng I. O. **HDPR1, a novel inhibitor of the WNT/β-catenin signaling, is frequently downregulated in hepatocellular carcinoma: involvement of methylation-mediated gene silencing**. *Oncogene*. 24(9):1607-1614. 2004.
- Yoshida Y., Kim S., Chiba K., Kawai S., Tachikawa H., Takahashi N. **Calcineurin inhibitors block dorsal-side signaling that affect late-stage development of the heart, kidney, liver, gut and somatic tissue during Xenopus embryogenesis.** *Dev Growth Differ*. 46(2):139-152. 2004.
- Zhang L., Gao X., Wen J., Ning Y., Chen Y. G. **Dapper 1 antagonizes Wnt signaling by promoting dishevelled degradation.** *JBiolChem*. 281(13):8607-8612. 2006.
- Zhang L., Zhou H., Su Y., Sun Z., Zhang H., Zhang L., Zhang Y., Ning Y., Chen Y. G., Meng A. **Zebrafish Dpr2 inhibits mesoderm induction by promoting degradation of nodal receptors.** *Science.* 306(5693):114-117. 2004.
- Zhang X., Yang Y., Liu X., Herman J.G., Brock M.V., Licchesi J.D., Yue W., Pei X., Guo M. **Epigenetic regulation of the Wnt signaling inhibitor DACT2 in human hepatocellular carcinoma.** *Epigenetics.* Epub ahead of print. 2013.
- Zhang Y. E. **Non-Smad pathways in TGF-β signaling.** *Cell Research*. 19(1):128-139. 2009.

Apêndice

Resultados obtidos em colaboração

Elastic fiber assembly in the adult mouse pubic symphysis during pregnancy and postpartum

Silvio Roberto Consonni, Claudio Chrysostomo Werneck, Débora Rodrigues Sobreira, Fabiana Kühne, Suzana Guimarães Moraes, Lúcia Elvira Alvares e Paulo Pinto Joazeiro

BIOLOGY OF REPRODUCTION (2012) 86(5):151, 1–10
Published online before print 11 January 2012.
DOI 10.1095/biolreprod.111.095653

Elastic Fiber Assembly in the Adult Mouse Pubic Symphysis During Pregnancy and Postpartum

Sílvio Roberto Consonni,[3] Claúdio Chrysostomo Werneck,[4] **Débora Rodrigues Sobreira**,[3] Fabiana Kühne,[5] Suzana Guimarães Moraes,[6] Lúcia Elvira Alvares,[3] and Paulo Pinto Joazeiro[2,3]

[3]Department of Histology and Embryology, State University of Campinas (Unicamp), Campinas, Brazil [4]Department of Biochemistry, State University of Campinas (Unicamp), Campinas, Brazil
[5]Department of Anatomy, Cell Biology and Physiology, State University of Campinas (Unicamp), Campinas, Brazil [6]Department of Morphology and Pathology, Pontifical Catholic University of Sa˜o Paulo (PUCSP), Sorocaba, Brazil

ABSTRACT

Impairment of pelvic organ support has been described in mice with genetic modifications of the proteins involved in elastogenesis, such as lysyl oxidase-like 1 (LOXL1) and fibulin 5. During pregnancy, elastic fiber-enriched pelvic tissues are modified to allow safe delivery. In addition, the mouse pubic symphysis is remodeled in a hormone-controlled process that entails the modification of the fibrocartilage into an interpubic ligament (IpL) and the relaxation of this ligament. After first parturition, recovery occurs to ensure pelvic tissue homeostasis. Because ligaments are the main supports of the pelvic organs, this study aimed to evaluate elastogenesis in the IpL during mouse pregnancy and postpartum. Accordingly, virgin, preg-nant, and postpartum C57BL/6 mice were studied using light, confocal, and transmission electron microscopy as well as Western blots and real-time PCR. Female mice exhibited the separation of the pubic bones and the formation, relaxation, and postpartum recovery of the IpL. By the time the IpL was formed, the elastic fibers had increased in profile length and diameter, and they consisted of small conglomerates of amorphous material distributed among the bundles of microfibrils. Our analyses also indicated that elastin/tropoelastin, fibrillin 1, LOXL1/Loxl1, and fibulin 5 were spatially and temporally regulated, suggesting that these molecules may contribute to the synthesis of new elastic fibers during IpL development. Overall, this work revealed that adult elastogenesis may be important to assure the elasticity of the pelvic girdle during preparation for parturition and postpartum recovery. This finding may contribute to our understanding of pathological processes involving elastogenesis in the reproductive tract.

elastogenesis, extracellular matrix, female reproductive tract, pregnancy, pubic symphysis, rodents (guinea pigs, mice, rats, voles)

INTRODUCTION

In the past decade, many studies focused on the reduced expression of proteins related to weakness of the birth canal and improper elastic fiber formation [1–3]. Despite the differences in anatomy, physiology, and biochemistry in the birth canal and pelvic floor between mice and humans [4], impaired birth canal recovery at postpartum is observed in mice with genetic modifications in genes encoding proteins involved in the formation of elastic fibers [5], such as lysyl oxidase-like 1 (LOXL1) [2, 6], fibulin 3 [3], and fibulin 5 [1]. These mutants provide important tools for studying the mechanisms underlying prolapse [7] because the mutant mice develop pelvic organ prolapse similar to that observed in primates, including the descent of the vagina, cervix, and bladder herniating through the pelvic floor musculature [1–3]. Because of the mechanical properties of pelvic tissue recovery during the normal postpartum period [8], pelvic organ prolapse is associated with impaired synthesis and organization of the extracellular matrix compounds, mainly elastic fibers, which can result in abnormal and irreversible biomechanical alter-ations in the birth canal [9]. These studies highlight the importance of elastic fiber protein synthesis and deposition for the recovery of the birth canal at postpartum.

Elastic fibers provide elastic recoil without damage in tissues and organs of the reproductive tract that need to be both strong and extensible to function, such as the vagina [10], uterine cervix [11], and uterus [12, 13]. The organization of the elastic fibers involves the synthesis and deposition of molecules in a highly regulated sequence to ensure the elastic characteristics in the early stages of development [14]. Briefly, the elastic fiber formation involves the deposition of tropoelastin on fibrillin-enriched microfibrils in the pericellular space while LOXL1 catalyzes cross-links in association with fibulin 5 [2, 15–20]. After deposition, elastic fiber production is substantially reduced, and there is little turnover because the production of new elastin ceases at maturity [14, 21].

Among the organs that form the birth canal, the pubic symphysis is part of the musculoskeletal tissues at the margins of the birth canal [22] and functions to support the pelvic organs [23, 24] and to ensure the proper relaxation of the birth canal and a safe birth in mice [24–26]. The pubic symphysis has evolved to dissipate the forces imposed on the pelvis during gait, which results in the rapid transfer of weight from one side of the pelvis to the other with the associated forces centered on and applied to the symphysis [27].

The stability of the pubic symphysis is altered during pregnancy in mice [28–31], in bats [32], and modestly in humans [33–35]. In mice, first, the pubic bones separate in a process induced by hormones, particularly relaxin, that promotes the formation of the interpubic ligament from the existing fibrocartilaginous tissue, and second, this ligament relaxes before parturition [34, 36]. The formation of this extensible ligament between the two pubic bones ensures the safe passage of the offspring during parturition [28]. However,

[1]This study was supported by FAPESP (Grant no 2008/56492-0) and by CNPq (Grant no 308169/2009-3).
[2]Correspondence: Paulo Pinto Joazeiro, Department of Histology and Embryology, State University of Campinas, CP 6109, 13083-970, Campinas, SP, Brazil. E-mail: pjoaz@unicamp.br

Received: 18 August 2011.
First decision: 11 September 2011.
Accepted: 3 January 2012.

eISSN: 1529-7268 http://www.biolreprod.org
ISSN: 0006-3363

when the pubes are widely separated by the interpubic ligament, the lower abdominal muscles normally attached to the pubes are partially displaced laterally, which explains, in part, hernias in mice [37]. In humans, it is not clear how much the relaxation of the symphysis actually contributes to the mechanisms of labor and birth, but interpubic gap widening and increased mobility at the symphysis do occur in humans, although to a lesser extent [33]. In addition, some studies report cases in which the recovery is impaired and becomes pathological, causing severe pregnancy-related pelvic girdle pain [38–45], but the causes of these pathologies need to be investigated further.

Elastic fiber formation in mammals occurs during the late fetal and early neonatal periods [14, 21] as well as during pregnancy, which is a short period in adult life [13, 46, 47]. The presence of elastic fibers on the pubic symphysis was previously described in bats [32] and rats [48], but the arrangement and the role of these fibers in ligament formation during pregnancy was not detailed. To our knowledge, only one other study observed the ultrastructure of the elastic fibers and microfibrils in the mouse pubic symphysis during pregnancy [49]. Therefore, in this study, we attempt to understand how pregnancy induces elastic fiber formation on the pubic symphysis in adult mice because this articulation does not have abundant elastic fibers before pregnancy. We analyzed virgin, pregnant, and postpartum female mice. Our findings provide morphological, biochemical, and molecular evidence that suggests that the newly forming elastic fibers may play an important role in the remodeling and recovery of the mouse pubic symphysis during normal pregnancy and the postpartum period, respectively.

MATERIALS AND METHODS

Animals

Virgin female C57BL/6/JUnib mice (3-mo old) were obtained from the Multidisciplinary Center for Biological Investigation on Laboratory Animal Science at Unicamp. Mating was encouraged by placing the young females in the same cage with breeding males overnight. Vaginal plug formation was considered to be an indicator of Day 1 of pregnancy (D1). Pubic symphyses or interpubic ligaments were obtained from the following groups: virgins in estrus (virgin, n ¼15) [50], D12, D15, D18, D19, 1 day postpartum (1dpp), and 3dpp. As control tissue, mouse uterine cervix was used in 1dpp and 3dpp. The animals were anesthetized using a mixture of 100–200 mg/kg ketamine and 5– 16 mg/kg xylazine chloride (Agribrands do Brasil), which was administered intraperitoneally, between 1100 and 1200 h. The distance between the pubic bones (the interpubic articulation gap) was measured using a caliper with a precision of 0.01 mm following laparotomy. The mice were euthanized by cervical dislocation, and the symphyses or ligaments were then removed and processed. As detailed below, three animals per group were used, for a total of 90 animals. The animal experiments were conducted in accordance with the Guide for the Care and Use of Laboratory Animals, issued by the National Institutes of Health (Bethesda, MD). All of the experimental protocols were approved by the Institutional Committee for Ethics in Animal Research (State University of Campinas, Protocol no. 1705-1).

Histology

The pubic symphyses and interpubic ligaments were fixed in situ with 4% paraformaldehyde in 0.1 M phosphate-buffered saline (PBS, pH 7.4) and then removed and immediately immersed in the same fixative solution for 24 h. After embedding in paraffin, transverse sections (antero-posterior direction) were cut out, deparaffinized, and then rehydrated. All the histological 5- and 7-lm thick sections were stained with Masson trichrome [51] and Weigert resorcin-fuchsin after oxidation with oxone [52], respectively. The sections were then examined and imaged using a Nikon Eclipse E800 light microscope.

Transmission Electron Microscopy

Small samples of pubic symphyses and interpubic ligaments were fixed in 2.5% glutaraldehyde (Electron Microscope Sciences) in 0.1 M cacodylate buffer containing 0.3% tannic acid for 4 h at 48C. The tissues were postfixed with 1% osmium tetroxide in 0.1 M cacodylate buffer for 1 h. Specimens were dehydrated through a graded series of acetone and embedded in Epon (EMbed-812; Electron Microscopy Sciences). Ultrathin sections were stained with uranyl acetate and lead citrate. The sections were examined using a LEO 906 electron microscope.

Morphometric Determination of the Length and Diameter Profiles of the Elastic Fibers

For the light microscopy analysis, 7-lm semiserial sections stained with Weigert resorcin-fuchsin. Only the medial region, where both fibrocartilage (virgin and D12) and the interpubic ligament (D15, D18, D19, 1dpp, and 3dpp) are located, was photographed and enlarged to 3203 magnification. Three randomly selected fields for each semiserial section were photomicrographed, and three different sections were used for each joint. To estimate the mean apparent profile length in a vertical projection of an elastic fiber [53], the point-counting methodology for structure length measurement was chosen, with reference to the morphometric principles of Buffon as a standard [54]. The photomicrograph was overlaid with a grid that had an area frame corresponding to 0.12 mm^2, where parallel lines were 28.12 lm apart (d). Thus, d was larger than the mean profile length of 30 elastic fibers (l ¼ 21.46 6 6.45 lm), directly measured over the photomicrograph. The apparent length profile was calculated by comparison to the estimated length of a so-called needle, that is, l ¼ (p/2) 3 (n/N) 3 d, according to Arherne and Dunnill [54], where n/N ¼ the mean of the number of intersections through elastic fiber profiles per throw (N ¼ 45).

For the transmission electron microscopy analysis, the smallest diameters of elastic fibers with round or slightly elliptical cross-sections were measured directly from electron micrographs at 21 5603 with a Bausch and Lomb measuring magnifier. At least 30 measurements were made for each experimental specimen.

Immunohistochemistry and Laser Confocal Microscopy Analysis

The cellular locations of elastin, fibulin 5, and LOXL1 were determined by immunohistochemistry. Staining was performed in cryosections (10 lm) of pubic symphyses, interpubic ligaments, and uterine cervix (as positive control) frozen in n-hexane with liquid nitrogen. The sections were fixed with acetone at ₃208C for 3 min, and then the slides were washed in 0.1 M PBS (pH 7.4). After blocking with 1% bovine serum albumin for 30 min, the sections were incubated with a primary antibody at 48C overnight. Elastin (1:200, 25041; Novotec), fibulin 5 (1:100, SC-23062; Santa Cruz Biotechnology), and LOXL1 (1:100, SC-48720; Santa Cruz Biotechnology) were all detected using polyclonal antibodies. The incubation with the primary antibodies was followed by an incubation with fluorophore-conjugated (AlexaFluor 488 or AlexaFluor 568) secondary antibodies (1:300; Invitrogen Life Technologies). The nuclei were stained using 4^0,6-diamidino-2-phenylindole (SC-3598; Santa Cruz Biotechnology). The sections were mounted with VECTASHIELD Mounting Medium (Vector Labs) and were visualized with an Axioplan LSM 510 Laser Scanning Microscope (Zeiss) using 633 1.3 NA oil-immersion objectives.

Protein Extraction, SDS-PAGE, and Western Blots

To confirm the specificity of the mouse anti-fibulin 5 and anti-LOXL1 antibodies, protein extraction, SDS-PAGE, and Western blot analysis were carried out according to Drewes et al. [1] and Rosa et al. [55]. Samples of pubic symphysis, interpubic ligament, and uterine cervix were frozen in liquid nitrogen and ground manually with a mortar and pestle. The ground tissues were suspended in a basic buffer containing protease inhibitors (16 mM potassium phosphate, pH 7.8, 0.12 M NaCl, 1 mM ethylenediaminetetraacetic acid, 0.1 mM phenylmethylsulfonyl fluoride, 10 lg/ml pepstatin A, and 10 lg/ ml leupeptin) and then centrifuged at 10 000 3 g. The supernatant was then removed, and the previous homogenization step was repeated after resuspend-ing the remaining tissue pellet in basic buffer. After the removal of the second supernatant, the remaining tissue pellet was suspended in urea buffer (6.0 M urea in above basic buffer), homogenized, and placed on a rotating rack for overnight extraction at 48C. Thereafter, the samples were centrifuged at 10 000 3 g for 30 min, and the supernatant was removed. The protein concentrations were determined using a commercial Bradford dye-binding assay (BioAgency). Samples of 50 lg of the protein homogenates were separated by SDS-PAGE and then transferred to polyvinylidene fluoride membranes (Amersham Pharmacia). The mouse anti-fibulin 5, anti-LOXL1, and anti-GAPDH antibodies were used at a dilution of 1:500 and incubated at 48C overnight. The blots were washed and incubated with horseradish peroxidase-rabbit anti-

TABLE 1. Mean values (mm) of the interpubic articulation gap (bone to bone) in the groups.

Group	Mean 6 SEM[a]	P value[b]
Virgin	1.5 6 0.08	–
D12	1.5 6 0.17	P . 0.05
D15	2.5 6 0.11	P , 0.05
D18	5.2 6 0.40	P , 0.001
D19	6.3 6 0.15	P , 0.05
1dpp	3.3 6 0.45	P , 0.01
3dpp	2.2 6 0.27	P , 0.05

[a] Arithmetic mean from the pubic articulation gaps of five animals. [b] Refers to statistical analysis relative to the group above.

goat immunoglobulin G conjugate (ZyMax) at a dilution of 1:2000, and the antigen-antibody complexes were detected using an enhanced chemiluminescence system (SuperSignal West Pico chemiluminescent substrate; Pierce).

Real-Time PCR

Gene expression was assessed by quantitative real-time PCR on the virgin, D12, D15, D18, D19, 1dpp, and 3dpp groups. Total RNA was extracted from frozen tissues using Trizol reagent (Invitrogen Life Technologies), and cDNA was synthesized using a RevertAid H Minus First Strand cDNA Synthesis Kit (Fermentas). Both procedures were carried out according to the manufacturer's recommendations. Real-time PCR was performed using SYBR Green (Applied Biosystems) in Applied Biosystems 7300. Each gene was normalized to the expression of the housekeeping gene 36b4 [56], officially known as ribosomal protein, large, P0 (Rplp0). The primers for tropoelastin, fibrillin 1, fibulin 5, Loxl1, and Rplp0 were purchased from Applied Biosystems (see Supplemental Table S1 for the primer sequences, available online at www.biolreprod.org). All the primers were optimized, and dissociation curves were prepared to ensure that only one product was amplified. A total of 20 ng of cDNA was used in each reaction according to the universal cycling conditions for the SYBR Green system. The results were normalized using the CT (threshold cycle) values of the housekeeping gene Rplp0 on the same plate. To quantify and cquire the fold increase of the genes, the mathematical model $2^{-\Delta\Delta Ct}$ was utilized, normalizing to the virgin group. The efficiencies of the tropoelastin, fibrillin 1, fibulin 5, and Loxl1 assays were calculated through the equation $E = 10^{(-1/slope)}$, with resulting values of 0.95, 0.95, 0.97, and 0.96, respectively. Three animals were used for each experimental time point, and all the reactions were performed in triplicate on the same plate.

Statistical Analysis

The data are presented as the mean values 6 SEM. The interpubic articulation gap and the relative gene expression were analyzed as groups using the Kruskal-Wallis test followed by the Mann-Whitney test. Statistical significance was defined as P , 0.05.

RESULTS

Tissue Remodeling in the Pregnant Mouse Pubic Symphysis: Cells and Extracellular Matrix

The histoarchitectural and biometrical aspects of the pubic symphysis in virgin mice and the interpubic ligament in pregnant and postpartum mice were compared (Fig. 1 and Table 1). In virgin mice, the symphysis showed the presence of fibrocartilage between the hyaline cartilage caps that cover the pubic bones (Fig. 1A). The fibrochondrocytes displayed a perpendicular orientation relative to the pelvic girdle, and the extracellular matrix displayed a thin collagen network, which is a typical organization pattern seen in fibrocartilaginous tissues (Fig. 1B).

During pregnancy, the initial aspects of the pubic bone separation and the formation of the interpubic ligament in the fibrocartilage were clearly observed (Fig. 1, C–E, and Table 1). At D15, the fibroblast-like cells of the interpubic ligament were

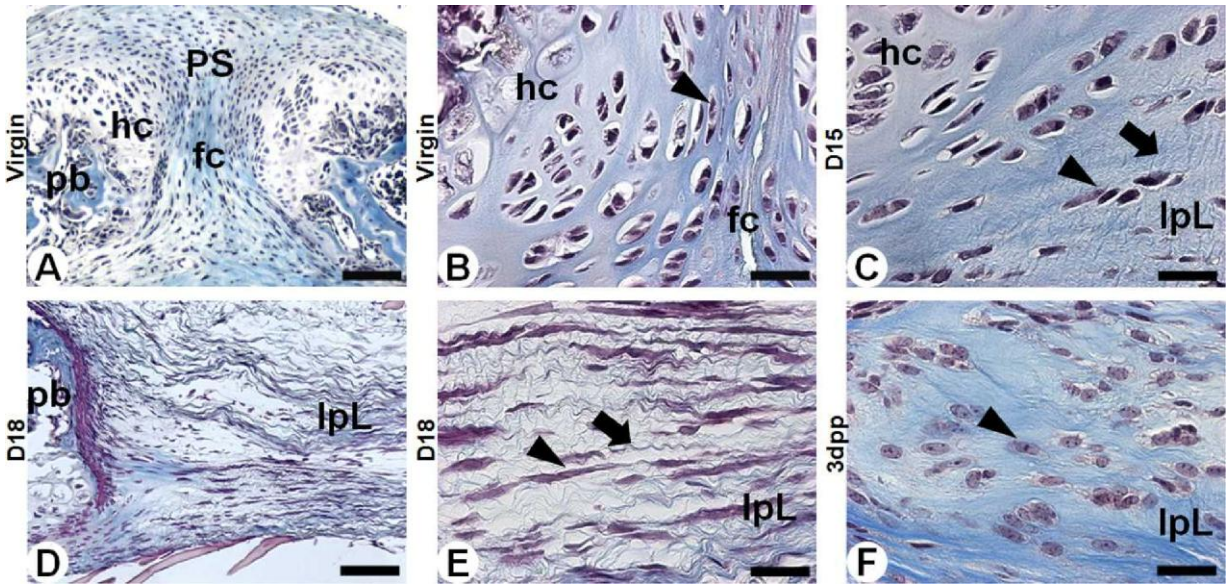

FIG. 1. Light micrographs of transverse sections of mouse pubic symphysis (A and B) and interpubic ligament (C–F) stained with Masson trichrome. A) The virgin mouse pubic symphysis (PS) is composed of fibrocartilage (fc) placed between thin layers of hyaline cartilage (hc) and pubic bones (pb) at both sides. B) The virgin mouse group showed the typical aspects of the hyaline cartilage (hc) and fibrocartilage (fc) in which the fibrochondrocytes were arranged into transverse rows (arrowhead) perpendicular to the major axis of the joint, (i.e., relative to the pubic bones). C) The D15 mouse group exhibited the initial formation of the interpubic ligament (lpL) in which the fibrochondrocytes change their orientation and became rearranged into longitudinal rows (arrowhead) parallel to the long axis of the lpL and collagen fibers (arrow). D) The lpL was formed by an oriented connective tissue placed between the pubic bones. E) The D18 group showed the crimp morphology of the fibers (arrow) and oriented fibroblast nucleus (arrowhead) relative to the opening of the pubic bones. F) The 3dpp group demonstrated the rearrangement of the extracellular matrix into a fibrocartilaginous tissue with fibrochondrocyte-like cells that showed loose chromatin and evident nucleolus (arrowhead). Bars ¼ 100 lm (A and D) and 25 lm (B, C, E, and F).

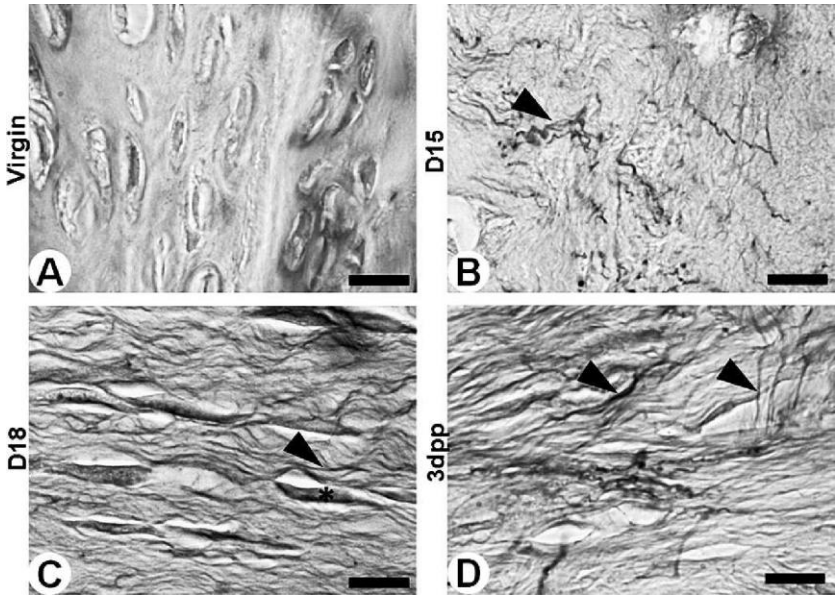

FIG. 2. Light micrographs of transverse sections from mouse pubic symphysis (A) and interpubic ligament (B–D) stained with Weigert resorcin-fuchsin with previous oxidation. A) No specific fibers were stained in the virgin group. B) Stained fibers were randomly oriented (arrowhead) in the D15 group. C) Stained fibers observed in a wavy and oriented arrangement (arrowhead) relative to the opening of the pubic bones next to the fibroblast-like cells (asterisk) in the D18 group. D) Stained fibers had a sinuous morphology (arrowheads) along the interpubic ligament at 3dpp. Bars ¼ 10 lm.

aligned parallel to the pelvic girdle, and the extracellular matrix showed wavy collagen fibers with the same orientation (Fig. 1C). At D18, the interpubic ligament showed the relaxation that occurs before parturition (Fig. 1D). There was a noticeable change from a densely packed arrangement to a loose arrangement of the collagen fibers, with flattened cells (fibroblast-like phenotype) disposed in parallel to the pubic girdle (Fig. 1E).

At 3dpp, the interpubic ligament displayed an extracellular matrix organization that was similar to that of the fibrocartilaginous tissues as well as islands of fibrocartilage containing rounded cells where flattened cells with a fibroblast-like phenotype had been previously observed (Fig. 1F). During the postpartum period, the pubic bones were closer to each other than during pregnancy, with a significant reduction of the interpubic articulation gap (Table 1).

Morphology and Morphometry of the Elastic Fibers in the Mouse Pubic Symphysis and Interpubic Ligament During Pregnancy and Postpartum

The histological preparations of virgin mouse pubic symphyses using the Weigert resorcin-fuchsin stain with previous oxidation did not detect the presence of elastic fibers in the fibrocartilaginous tissue (Fig. 2A). However, at D15, this selective stain revealed thin, wavy elastic fibers randomly distributed along the developing interpubic ligament (Fig. 2B). During the relaxation at D18, thin, wavy elastic fibers were identified parallel to the major axis of the articulation (Fig. 2C). After parturition, at 3dpp, the elastic fibers showed an irregular wavy morphology with an oblique arrangement throughout the interpubic ligament (Fig. 2D).

In the ultrastructural analysis of the fibrocartilaginous tissue of the virgin mouse pubic symphyses, identification of microfibrils was difficult because these compounds were thin and dispersed in the extracellular matrix (Fig. 3A). However, the interpubic ligament in pregnant and postpartum samples allowed the identification of the fibrillar and amorphous compounds of the elastic fibers, which are probably related to the elastogenesis process. During both the separation at D15 (Fig. 3B) and the relaxation at D18 (Fig. 3E), the ultrastructure showed parallel microfibrils intermingled with elongated patches of amorphous material, in agreement with the ultrastructural pattern of elastic fibers described elsewhere. Higher magnification of the elastic fibers showed that elastin formed a continuous, solid core for the elastic fiber, with adjacent bundles of microfibrils (Fig. 3, C, D, F, and G). After parturition, these compounds were observed along the cell surface (Fig. 3H).

The morphometric analysis indicated that the estimated profile length and diameter of the elastic fibers had progressively and significantly increased from D12 to D15 and from D15 to D18 (Table 2). At D18, D19, and 1dpp, there were no significant differences in the profile length and diameter of the elastic fibers, but at 3dpp, there was a significant decrease in profile length compared to 1dpp (Table 2).

Proteins Involved in Elastic Fiber Assembly in the Mouse Pubic Symphysis and Interpubic Ligament During Pregnancy and Postpartum

Immunohistochemical staining identified the proteins involved in elastic fiber assembly in the mouse pubic symphysis and interpubic ligament as elastin, fibulin 5, and LOXL1. The punctate staining pattern of elastin was detected in the pericellular localization of fibrochondrocytes at D12 (Fig. 4A), in the wavy, and elongated elastin-containing fibers laid

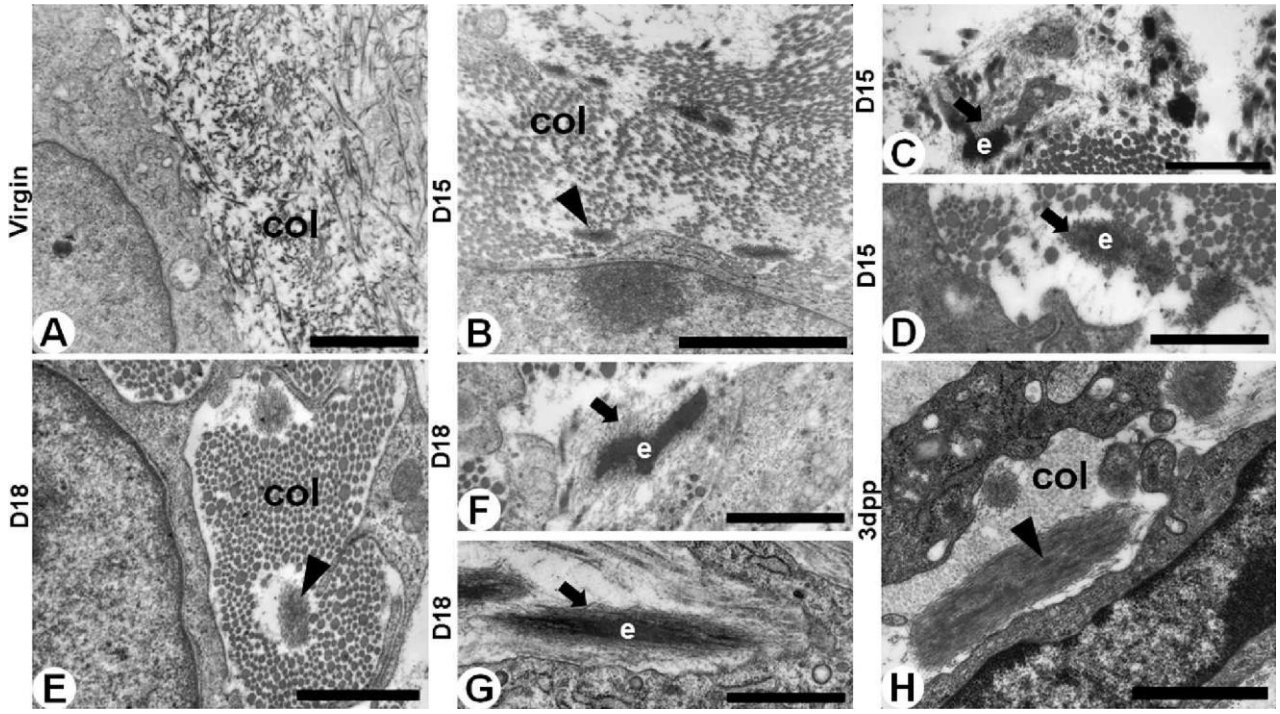

FIG. 3. Electron micrographs of transverse sections from mouse pubic symphysis (A) and interpubic ligament (B–H). A) The virgin group showed fibrochondrocytes with thin, randomly arranged collagen fibrils (col) in the pericellular space. B and E) The D15 and D18 groups, respectively, showed thin and thick collagen fibrils (col) and newly forming elastic fibers (arrowhead) next to the fibroblast-like cells. C, D, F, and G) Higher magnification showed the integration of electron-dense microfibrils (arrow) and amorphous elastin (e) in normal elastic fibers. H) The 3dpp group showed thin and thick collagen fibrils, and the elastic fibers (arrowhead) demonstrated the appearance of relatively newly forming elastic fiber in which a relatively small amount of amorphous material is surrounded by a number of microfibrils. Bars ¼ 2 lm (A, B, and H) and 1 lm (C–G).

around the surface of fibroblast-like cells at D15 (Fig. 4B), and in the branched fibers at the lamina propria of the uterine cervix (Fig. 4C).

Immunohistochemical analysis for fibulin 5 showed a punctate staining pattern consistent with a subcellular distri-bution in the fibrochondrocytes (Fig. 4D) and fibroblast-like cells (Fig. 4E). Western blot analysis detected a 66-kDa protein as expected for fibulin 5, corroborating the specificity of the primary antibody (Fig. 4F). For LOXL1, the immunohisto-chemistry identified a punctate staining pattern consistent with the subcellular distribution for this enzyme in both fibrochon-drocytes (Fig. 4G) and fibroblast-like cells (Fig. 4H). Western blot analysis confirmed the specificity of this primary antibody by detecting a 32-kDa protein, as expected (Fig. 4I). GAPDH was used as the control (Fig. 4, F and I). Negative controls with no primary antibody were performed for all the experiments, and no staining was detected (data not shown).

Comparison of Gene Expression Levels Between Mouse Pubic Symphysis and Interpubic Ligament During Pregnancy and Postpartum

The relative levels of tropoelastin, fibrillin 1, fibulin 5, and Loxl1 mRNAs were evaluated by real-time PCR in virgin mouse pubic symphysis and interpubic tissues during pregnancy and postpartum. Overall, the results showed a progres-

TABLE 2. Estimated length profile and diameter of elastic fibers in the pubic symphysis and interpubic ligament of virgin, pregnant, and postpartum mice using light and transmission electron microscopy.

	Light microscopy			Electron microscopy	
Group[a]	Mean number of intersections per throw (N ¼ 45) 6 SEM	Mean estimated profile length (l) 6 SEM	P value[b]	Mean diameter of elastic fiber (nm) 6 SEM	P value[b]
Virgin	–[c]	–	–	–[c]	–
D12	79.7 6 16.73	78.1 6 16.39	–	260 6 80	–
D15	127.1 6 27.81	124.5 6 27.22	P , 0.001	350 6 100	P , 0.001
D18	146.7 6 33.31	143.8 6 32.63	P , 0.001	460 6 180	P , 0.001
D19	141.2 6 11.40	138.4 6 11.17	P . 0.05	470 6 140	P . 0.05
1dpp	146.6 6 12.16	143.9 6 11.94	P . 0.05	430 6 100	P . 0.05
3dpp	129.7 6 18.80	127.1 6 18.52	P , 0.001	440 6 120	P . 0.05

[a] Higher magnification of representative analyzed areas is shown in Figures 2 and 3. [b] Refers to statistical analysis relative to the group above.
[c] Only fibrocartilage was analyzed.

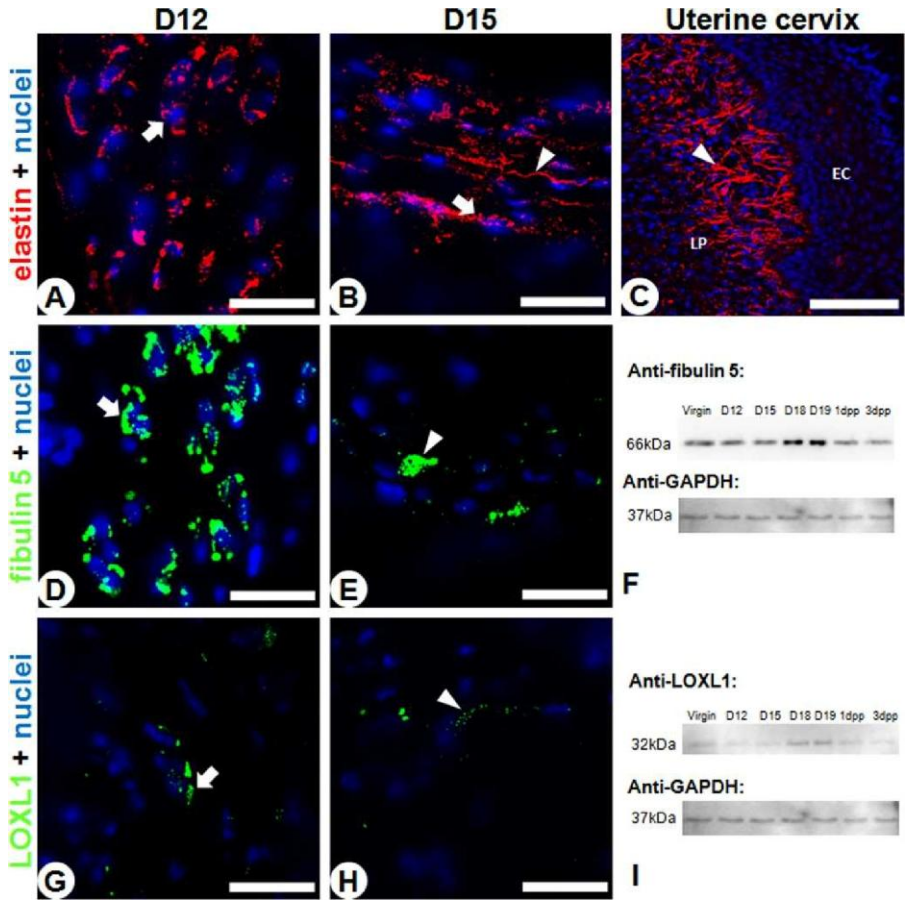

FIG. 4. Laser confocal microscopy and Western blots for proteins involved in elastogenesis: elastin (A–C), fibulin 5 (D–F), and LOXL1 (G–I). A–C) Immunohistochemistry for elastin in aggregates (white arrow) and fibers (white arrowheads) on the pubic symphysis, interpubic ligament, and uterine cervix in 1dpp (positive control), respectively. LP, lamina propria; EC, epithelium of the cervix. D and E) Immunohistochemistry for fibulin 5 (white arrow) on the pubic symphysis and interpubic ligament, respectively. F) Western blot for fibulin 5 and GAPDH. G and H) Immunohistochemistry for LOXL1 (white arrow) on the pubic symphysis and interpubic ligament, respectively. I) Western blot for LOXL1 and GAPDH. Bars ¼ 30 lm (A, B, D, E, G, and H) and 100 lm (C).

sive increase of transcript levels when the interpubic tissues during pregnancy and postpartum were compared with the pubic symphysis in virgin mice (Fig. 5). For instance, at 1dpp, the interpubic tissues presented 12-fold more tropoelastin mRNAs than virgin mouse pubic symphysis (Fig. 5A). Similarly, the fibrillin 1 relative gene expression increased significantly during the separation and relaxation of the interpubic tissues, up 10-fold in the D19 group when compared with the virgin mice (Fig. 5B). Finally, the relative gene expression of fibulin 5 and Loxl1 also increased during pregnancy and postpartum, increasing 6- and 3-fold, respectively, at D19 compared with virgin mice (Fig. 5, C and D).

DISCUSSION

This study identifies adult elastic fiber formation in a physiological process on mouse pubic symphysis during pregnancy and postpartum. First, microfibrils with small conglomerates of amorphous material are randomly assembled at the cell surface, and a clear up-regulation of tropoelastin and other proteins involved in elastogenesis is observed. Then, the newly forming elastic fibers appear to align with the major axis of the articulation as the gene expression hits its highest levels before parturition. During the postpartum period, the proper histoarchitecture of the elastic fibers, as well as highly regulated gene expression, may play an important role in the recovery of the articulation. On the basis of these observations, we propose a model in which elastic fibers are formed in adult tissue during pregnancy on the mouse pubic symphysis. These newly forming elastic fibers probably help confer the elasticity necessary in the period of preparation for parturition and the elastic recoil that may help the recovery via fibrocartilaginous tissue formation after a first pregnancy.

The fibrocartilaginous pubic symphysis of virgin female mice is subject to compressive forces and has little elasticity [31, 37], which is in agreement with the lack of fibers containing elastin in the extracellular matrix. During pregnan-cy, the rearrangement of the tissues leads to the morphogenesis of a new ligament with a distinct cellular phenotype. This process involves the deposition of collagen fibers oriented relative to the pubic bones, which ensures the maximum extensibility of this articulation during parturition. Because of the magnitude of this phenomenon, it has been previously described as a transformation or metamorphosis of the pubic symphysis into interpubic ligament [28, 34, 37].

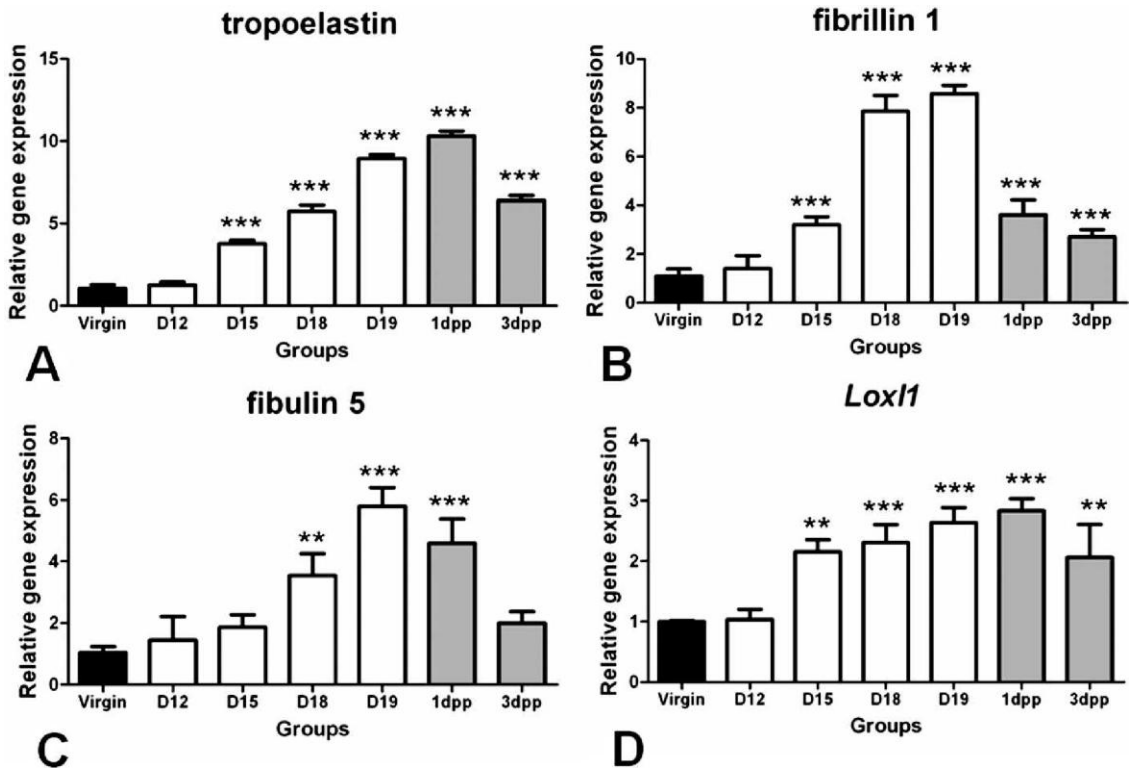

FIG. 5. Tropoelastin (A), fibrillin 1 (B), fibulin 5 (C), and Loxl1 (D) mRNA levels were measured by real-time PCR using mRNA extracted from the connective tissues of the interpubic articulation and normalized to 36b4 levels. A) Tropoelastin mRNA expression had a similar level in virgin and D12 animals and increased from D15 to 3dpp. ***P , 0.001 versus virgin. B) Fibrillin 1 mRNA expression increased from D15 to 3dpp. ***P , 0.001 versus virgin. C) Fibulin 5 mRNA expression increased from D18 to 1dpp. **P , 0.01 versus virgin; ***P , 0.001 versus virgin. D) Loxl1 mRNA expression was increased from D15 to 3dpp. **P , 0.01 versus virgin; ***P , 0.001 versus virgin. Mean 6 SEM.

During the separation of the pubic bones and interpubic ligament development at D15, Weigert resorcin-fuchsin staining and ultrastructural analysis demonstrate the initial appearance of newly forming, randomly distributed elastic fiber as well as a relatively small amount of amorphous material (elastin) surrounded by a number of microfibrils on the surfaces of fibroblast-like cells. A similar process has been observed during the dynamic imaging of elastic fiber formation by cells expressing tropoelastin tagged with a fluorescent timer construct in which the initial step in elastin assembly is the formation of small elastin aggregates on the cell surface [57].

At D18, the elastic fiber is observed to be an aggregate of microfibrils clustered in a long cylinder that lies along an infolding at the cell surface. This organization may guarantee the dynamic adaptation to the biomechanic forces necessary for parturition followed by postpartum recovery. These newly forming elastic fibers probably aid in conferring the necessary elasticity to the pelvic girdle in the period of preparation for parturition and, along with other extracellular compounds, such as hyaluronic acid and proteoglycans [58–61], may help to maintain the anatomical integrity of the interpubic ligament. This articulation begins to recover and close during the postpartum period, and the morphological aspect of the obliquely arranged elastic fibers clearly indicates a role for this extracellular compound in helping to tie the pubic bones.

Morphological evidence in this study highlight the relation-ship between the fibroblast-like cells and the thin elastic fibers deposited in the pericellular space. These cells may be associated with elastogenesis in adult tissues driven by pregnancy. This hypothesis is supported by a previous report describing elastic fiber assembly directed by connective tissue cells [15]. As in the bat pubic symphysis [32] and the human cervix [62], the elastic fibers may play a role in maintaining the mouse interpubic ligament integrity for a few hours postpartum because the collagen network, proteoglycans, and water are not well rearranged.

Morphometric data indicate a significant increase in the estimated length profile of the elastic fibers in the interpubic medial region, which may indicate rotation and elongation instead of simply elongation to increase alignment in the direction of loading at the same time that the reorientation resistance parameter of the reproductive tissue changes. Because within each section-slab the apparent profile length of a fiber is the sum of the projected fiber profile (vertical projection) and the transected profile at the surface of the section, an increase in the apparent profile length of a fiber results in a proportional increase in both the projected and the transected fiber profiles [53]. Similarly, the observation of an increase in the diameters of elastic fibers may indicate elastogenesis in the pregnant mouse pubic symphysis at a time when the entire reproductive tract is adapting to different

degrees of stress, which has been shown to occur in the uterus [13, 63].

Elastic fiber assembly requires the coordinated expression of all the molecules that constitute the elastic fiber as well as the cross-linking enzymes. This process is inefficient in adult tissues, most often resulting in the production of elastin that either does not polymerize or does not organize into a functional three-dimensional fiber [16]. However, in this work, the cellular localization and molecular analysis show an important temporal and spatial regulation of molecules involved in elastogenesis in the interpubic ligament during pregnancy and postpartum, and these results corroborate the elastogenesis model proposed by Kielty et al. [20]. The localization of elastin, fibulin 5, and LOXL1 in cells, as revealed by immunohistochemistry, supports an important spatial relationship between cells and elastic fibers that occurs in the elastogenesis process, in agreement with our ultrastruc-tural analysis. Additionally, our positive controls show the presence of elastin in fibers of the uterine cervix where it is believed that the organization of the elastic fibers is essential for the postpartum recovery of the connective tissue [1, 2].

The punctate staining pattern observed in the fibrochon-drocytes at D12 is similar to the immunostained cellular compartment of both articular cartilage and meniscal tissue in rabbits [64] and to the conversion to an elastogenic phenotype by fetal hyaline chondrocytes followed by alterations in the expression of elastin-related macromolecules [65]. Our results in the immunostained interpubic ligament show that some elastin particles seem to approach each other to form fibrillar aggregates that dynamically elongate, resulting in the elastic fibers. When two of these aggregates meet by chance, they become associated or connected and a larger aggregate is formed that is directed by long linear microfibrils in the extracellular space [57, 66]. Consistent with this process, the assembly of other extracellular molecules, such as fibulin 5 and LOXL1, on the interpubic ligament, show that cells convert to an elastogenic phenotype between D12 and D15 and that they play a direct role in shaping the fibers to respond to mechanical forces associated with the cellular cytoskeleton, cell movement, and global matrix deformation.

In this study, molecular analysis of virgin and D12 mice do not show significant alterations in the relative gene expression of tropoelastin, fibrillin 1, fibulin 5, and Loxl1. From D12 to D15, during the separation of the pubic bones and the formation of the interpubic ligament, the expression levels of these genes increase significantly. In the relaxation period, from D15 to D19, the increase of fibrillin 1 gene expression is higher and earlier than that observed for the other molecules. After parturition, all the genes are up-regulated compared to the virgin group, but their expression levels decrease gradually until 3dpp. Thus, the mouse pubic symphysis illustrates the temporal regulation of these molecules during the elastogenesis process in adult tissues. Similarly, in the rat uterus, elastin content reaches a maximum several days prior to parturition and then declines continuously until 5dpp [63].

Our molecular results indicate that there is temporal regulation of fibrillin 1 and tropoelastin mRNAs in accord with the elastic fiber assembly model [20]. The microfibril has been suggested to play a morphogenetic role in determining the shape and direction of the forming elastic fiber by serving as an extracellular scaffold that binds tropoelastin monomers in preparation for cross-linking into the functional polymer [67]. Fibulin 5 gene expression is also regulated in a similar way, suggesting that this molecule may play a role in modulating the interactions between cells and microfibrils. The binding of fibulin 5 to integrins is necessary for the tethering of newly synthesized elastic fibers to surrounding cells, which induces elastic fiber assembly and maturation by organizing tropoelas-tin and cross-linking enzymes onto the microfibrils [7, 17, 68].

Cells play an active and important role in forming elastic fiber by secreting elastin to sites where assembly can occur and where the concentration of elastin monomers is sufficient to facilitate alignment and crosslinking by lysyl oxidase [57]. In addition, LOXL1 is essential in ensuring elastic fiber homeostasis [2] as well as elastogenesis [69], all of which is consistent with Loxl1 gene expression in the interpubic ligament during pregnancy and postpartum. The levels of LOXL decreases in adults and may be a factor associated with the absence of elastogenesis in adult tissues [18]. Interestingly, the mouse interpubic ligament cells from D15 to 3dpp express higher levels of Loxl1 mRNA than the virgin group.

In the mouse pubic symphysis, a better understanding of the synthesis, deposition, and remodeling of the extracellular matrix that occurs during pregnancy and postpartum is important because these processes may affect the mechanical integrity of the birth canal [2, 5, 70, 71]. Given that this articulation drastically changes during pregnancy and after parturition, the altered attachments of the pelvic floor muscles to the widely separated interpubic ligament may be one of the factors that causes pelvic organ prolapse, particularly in animal models with null mutations for proteins involved in elasto-genesis, such as in the gross pelvic anatomy observed in Loxl1$^{-/-}$ [5] and fibulin 3$^{-/-}$ [3] models as well as in other studies. To better understand the mechanics involved, it is important to recognize the morphological differences between the pubic symphysis and interpubic ligament, for example, in the pelvic morphology of fibulin 3$^{-/-}$ null mice [3]. Nevertheless, it is important to keep in mind that this period of preparation for parturition is singular and highly regulated, where elastic fiber proteins are up-regulated during late pregnancy. Therefore, when early parturition is simulated with a balloon model in the vagina [72], the tissues that compose the birth canal are not properly prepared to receive this stimulus, and a pathological process, instead of a physiological process, may be recapitulated.

Because elastic fiber assembly in mammals occurs during late fetal and in early neonatal periods, it was necessary to show via the increase of tropoelastin, fibrillin 1, fibulin 5, and Loxl1 gene expression, ultrastructural analysis, and immuno-histochemistry that elastic fiber assembly in the interpubic ligament seems to recapitulate the elastogenesis process during pregnancy in adult tissue on the mouse pubic symphysis. The formation of an elastic network can be associated with the morphogenesis, repair, or regeneration of tissues [73]. Each new arrangement of elastic fibers represents an adaptation to the forces upon the tissues [66]. In the female reproductive tract, there is a unique adaptation to synthesize and assemble new elastic fibers [13] that allows the pubic symphysis to expand and protect the birth canal during pregnancy and guarantee a safe postpartum recovery. However, many physiological and genetic factors still remain to be investigated because some alterations of elastic fiber morphology and assembly are responsible for the development of pelvic organ prolapse [74].

Overall, the data presented in this work show a gradual differentiation of the pubic symphysis in virgin mice into a loosely organized interpubic ligament during pregnancy; determination of the morphology, morphometry, biochemistry, and relative gene expression demonstrate that, while prior to pregnancy elastic fiber is scarce, newly forming elastic fibers may play an important role in mouse pubic symphysis remodeling. The pubic symphysis appears to be capable of

recovering fibrocartilaginous tissue after the first pregnancy with the support of myofibroblasts [75], collagen crimps [59], and newly forming elastic fibers that provide tissue recoil [76]. Thus, the physiological process that prepares pelvic structures in a relatively short time for parturition involves elastic fiber synthesis and assembly as well as the coordination of other extracellular matrix molecules during pregnancy, such as an increase in the synthesis of high molecular weight hyaluronic acid and versican as well as a decrease in the expression of ADAMTS1 protease (a disintegrin-like and metalloprotease with thrombospondin type 1 motif) in the interpubic ligament on D18 [61]. The mouse pubic symphysis model shows a physiological process in which elastic fiber assembly, remod-eling, and homeostasis are associated with normal pregnancy, parturition and recovery in adult tissues. Thus, this model can be used in future studies to investigate the complex molecular mechanisms of elastic fiber formation and to understand risk factors that affect the biomechanical properties of the reproductive tract and its supportive structures, such as the pubic symphysis, thereby improving our understanding of pelvic disorders.

ACKNOWLEDGMENT

This work is part of a Master's dissertation submitted by S.R.C. to the Institute of Biology, State University of Campinas, in partial fulfillment of the requirements for the Master's degree. The authors would like to thank Dr. Hernandes F. Carvalho for his support during the real-time PCR analysis.

REFERENCES

1. Drewes PG, Yanagisawa H, Starcher B, Hornstra I, Csiszar K, Marinis SI, Keller P, Word RA. Pelvic organ prolapse in fibulin-5 knockout mice: pregnancy-induced changes in elastic fiber homeostasis in mouse vagina. Am J Pathol 2007; 170:578–589.
2. Liu X, Zhao Y, Gao J, Pawlyk B, Starcher B, Spencer JA, Yanagisawa H, Zuo J, Li T. Elastic fiber homeostasis requires lysyl oxidase-like 1 protein. Nat Genet 2004; 36:178–182.
3. Rahn DD, Acevedo JF, Roshanravan S, Keller PW, Davis EC, Marmorstein LY, Word RA. Failure of pelvic organ support in mice deficient in fibulin-3. Am J Pathol 2009; 174:206–215.
4. Yiou R, Delmas V, Carmeliet P, Gherardi RK, Barlovatz-Meimon G, Chopin DK, Abbou CC, Lefaucheur JP. The pathophysiology of pelvic floor disorders: evidence from a histomorphologic study of the perineum and a mouse model of rectal prolapse. J Anat 2001; 199:599–607.
5. Abramowitch SD, Feola A, Jallah Z, Moalli PA. Tissue mechanics, animal models, and pelvic organ prolapse: a review. Eur J Obstet Gynecol Reprod Biol 2009; 144(Suppl 1):S146–S158.
6. Lee UJ, Gustilo-Ashby AM, Daneshgari F, Kuang M, Vurbic D, Lin DL, Flask CA, Li T, Damaser MS. Lower urogenital tract anatomical and functional phenotype in lysyl oxidase like-1 knockout mice resembles female pelvic floor dysfunction in humans. Am J Physiol Renal Physiol 2008; 295:F545–F555.
7. Budatha M, Roshanravan S, Zheng Q, Weislander C, Chapman SL, Davis EC, Starcher B, Word RA, Yanagisawa H. Extracellular matrix proteases contribute to progression of pelvic organ prolapse in mice and humans. J Clin Invest 2011; 121:2048–2059.
8. Rundgren A. Physical properties of connective tissue as influenced by single and repeated pregnancies in the rat. Acta Physiol Scand Suppl 1974; 417:1–138.
9. Rahn DD, Ruff MD, Brown SA, Tibbals HF, Word RA. Biomechanical properties of the vaginal wall: effect of pregnancy, elastic fiber deficiency, and pelvic organ prolapse. Am J Obstet Gynecol 2008; 198: 590.e1–590.e6.
10. Word RA, Pathi S, Schaffer JI. Pathophysiology of pelvic organ prolapse. Obstet Gynecol Clin North Am 2009; 36:521–539.
11. Timmons B, Akins M, Mahendroo M. Cervical remodeling during pregnancy and parturition. Trends Endocrinol Metab 2010; 21:353–361.
12. Leppert PC, Yu SY. Three-dimensional structures of uterine elastic fibers: scanning electron microscopic studies. Connect Tissue Res 1991; 27: 15–31.
13. Starcher B, Percival S. Elastin turnover in the rat uterus. Connect Tissue Res 1985; 13:207–215.
14. Wagenseil JE, Mecham RP. New insights into elastic fiber assembly. Birth Defects Res C Embryo Today 2007; 81:229–240.
15. Ramirez F, Pereira L. The fibrillins. Int J Biochem Cell Biol 1999; 31: 255–259.
16. Shifren A, Mecham RP. The stumbling block in lung repair of emphysema: elastic fiber assembly. Proc Am Thorac Soc 2006; 3: 428–433.
17. Nakamura T, Lozano PR, Ikeda Y, Iwanaga Y, Hinek A, Minamisawa S, Cheng CF, Kobuke K, Dalton N, Takada Y, Tashiro K, Ross J Jr, et al. Fibulin-5/DANCE is essential for elastogenesis in vivo. Nature 2002; 415: 171–175.
18. Cenizo V, Andre V, Reymermier C, Sommer P, Damour O, Perrier E. LOXL as a target to increase the elastin content in adult skin: a dill extract induces the LOXL gene expression. Exp Dermatol 2006; 15:574–581.
19. Csiszar K. Lysyl oxidases: a novel multifunctional amine oxidase family. Prog Nucleic Acid Res Mol Biol 2001; 70:1–32.
20. Kielty CM, Stephan S, Sherratt MJ, Williamson M, Shuttleworth CA. Applying elastic fibre biology in vascular tissue engineering. Philos Trans R Soc Lond B Biol Sci 2007; 362:1293–1312.
21. Swee MH, Parks WC, Pierce RA. Developmental regulation of elastin production. Expression of tropoelastin pre-mRNA persists after down-regulation of steady-state mRNA levels. J Biol Chem 1995; 270: 14899–14906.
22. Weaver TD, Hublin JJ. Neandertal birth canal shape and the evolution of human childbirth. Proc Natl Acad Sci U S A 2009; 106:8151–8156.
23. da Rocha RC, Chopard RP. Nutrition pathways to the symphysis pubis. J Anat 2004; 204:209–215.
24. Ortega HH, Munoz-de-Toro MM, Luque EH, Montes GS. Morphological characteristics of the interpubic joint (Symphysis pubica) of rats, guinea pigs and mice in different physiological situations. A comparative study. Cells Tissues Organs 2003; 173:105–114.
25. Zhao L, Roche PJ, Gunnersen JM, Hammond VE, Tregear GW, Wintour EM, Beck F. Mice without a functional relaxin gene are unable to deliver milk to their pups. Endocrinology 1999; 140:445–453.
26. Zhao L, Samuel CS, Tregear GW, Beck F, Wintour EM. Collagen studies in late pregnant relaxin null mice. Biol Reprod 2000; 63:697–703.
27. Cunningham PM, Brennan D, O'Connell M, MacMahon P, O'Neill P, Eustace S. Patterns of bone and soft-tissue injury at the symphysis pubis in soccer players: observations at MRI. Am J Roentgenol 2007; 188: W291–W296.
28. Hall K. The effects of pregnancy and relaxin on the histology of

the pubic symphysis of the mouse. J Endocrinol 1947; 5:174–185.

29. Kroc RL, Steinetz BG, Beach VL. The effects of estrogens, progestagens, and relaxin in pregnant and nonpregnant laboratory rodents. Ann N Y Acad Sci 1959; 75:942–980.
30. Steinetz BG, Beach VL, Kroc RL. The influence of progesterone, relaxin and estrogen on some structural and functional changes in the pre-parturient mouse. Endocrinology 1957; 61:271–280.
31. Storey E. Relaxation in the pubic symphysis of the mouse during pregnancy and after relaxin administration, with special reference to the behavior of collagen. J Pathol Bacteriol 1957; 74:147–162.
32. Crelin ES, Newton EV. The pelvis of the free-tailed bat: sexual dimorphism and pregnancy changes. Anat Rec 1969; 164:349–357.
33. Becker I, Woodley SJ, Stringer MD. The adult human pubic symphysis: a systematic review. J Anat 2010; 217:475–487.
34. Crelin ES. The development of the bony pelvis and its changes during pregnancy and parturition. Trans NY Acad Sci 1969; 31:1049–1058.
35. Gamble JG, Simmons SC, Freedman M. The symphysis pubis. Anatomic and pathologic considerations. Clin Orthop Relat Res 1986; 203:261–272.
36. Sherwood OD. Relaxin. In: Knobil E, Neill JD (eds.), The Physiology of Reproduction. New York: Raven; 1994:861–1009.
37. Gardner WU. Sexual dimorphism of the pelvis of the mouse, the effect of estrogenic hormones upon the pelvis and upon the development of scrotal hernias. Am J Anat 1936; 59:459–483.
38. Albert H, Godskesen M, Westergaard JG, Chard T, Gunn L. Circulating levels of relaxin are normal in pregnant women with pelvic pain. Eur J Obstet Gynecol Reprod Biol 1997; 74:19–22.
39. Bjorklund K, Nordstrom ML, Bergstrom S. Sonographic assessment of symphyseal joint distention during pregnancy and post partum with special reference to pelvic pain. Acta Obstet Gynecol Scand 1999; 78:125–130.
40. Bjorklund K, Bergstrom S, Nordstrom ML, Ulmsten U. Symphyseal distention in relation to serum relaxin levels and pelvic pain in pregnancy. Acta Obstet Gynecol Scand 2000; 79:269–275.
41. Ronchetti I, Vleeming A, van Wingerden JP. Physical characteristics of

Anexo

DECLARAÇÃO

Declaro para os devidos fins que o conteúdo de minha **Tese de Doutorado** intitulada **"Estudos sobre os genes da família *Dapper*: origem, evolução e análise da expressão durante a ontogênese dos membros de galinha"**:

( ) não se enquadra no § 3º do Artigo 1º da Informação CCPG 01/08, referente a bioética e biossegurança.

Tem autorização da(s) seguinte(s) Comissão(ões):

( ) CIBio - Comissão Interna de Biossegurança , projeto nº _____, Instituição: _____.

(**X**) CEUA - Comissão de Ética no Uso de Animais , projeto nº 1362-1, Instituição: Universidade Estadua de Campinas – UNICAMP.

( ) CEP - Comissão de Ética em Pesquisa, protocolo nº _____, Instituição: _____.

* *Caso a Comissão seja externa ao IB/UNICAMP, anexar o comprovante de autorização dada ao trabalho. Se a autorização não tiver sido dada diretamente ao trabalho de tese ou dissertação, deverá ser anexado também um comprovante do vínculo do trabalho do aluno com o que constar no documento de autorização apresentado.*

Débora R. Sobreira
Alunoa: Débora Rodrigues Sobreira

Lúcia Elvira Alvares
Orientadora: Lúcia Elvira Alvares

Para uso da Comissão ou Comitê pertinente:
(X) Deferido ( ) Indeferido

Carimbo e assinatura

Profa. Dra. ANA MARIA APARECIDA GUARALDO
Presidente da CEUA/UNICAMP

Para uso da Comissão ou Comitê pertinente:
( ) Deferido ( ) Indeferido

_____
Carimbo e assinatura